Investigating the effects of FoxO transcriptional activity on metabolic homeostasis.

Lauren Rachel McDonagh

Doctor of Philosophy

Aston University

February 2022

Aston University

Investigating the effects of FoxO transcriptional activity on metabolic homeostasis.

Lauren Rachel McDonagh

Doctor of Philosophy

2022

THESIS SUMMARY

As with many other age-related pathologies, metabolic disorders entail lifelong treatment producing economic and social burdens in ageing populations. Therefore, improving the study of metabolic disorder and associated treatments is essential to healthy ageing.

FoxO transcription factors modulate the expression of key metabolic factors. Previous work focusses on FoxO targets that are controlled by FoxO binding directly to DNA. Recently, studies have highlighted the importance of recruiting FoxO to regulatory gene regions via protein-protein interactions. However, most interactions required FoxO binding to DNA to modulate gene expression. Therefore, there is still little information available regarding the interactions and effects of FoxO on gene expression independent of its DNA-binding abilities.

The overall aim of this thesis was to use *Drosophila melanogaster* as a model system to gain more in-depth knowledge of FoxO activity, particularly its DNA-binding independent activity, to allow for the identification of new and potentially more effective therapeutic targets for treating metabolic disorder. In this thesis, previously unpublished *Drosophila FoxO* mutants with a canonical DNA-binding domain mutation were verified for appropriate regulation and loss of DNA-binding ability. Phenotypic analysis of FoxO-dependent physiological responses in these mutants identified growth and starvation survival as potential DNA-binding independent processes. Subsequent RNA-sequencing identified genes that were also modulated in a DNA-binding independent manner. Transcription factor binding motif analysis of these differentially expressed genes identified Hp1b and Sin3a as potential co-modulators of these genes alongside FoxO. Analysis of publicly available RNA-sequencing and chromatin immunoprecipitation-sequencing datasets found significant overlaps between Hp1b and Sin3a regulated genes and genes that were modulated in a FoxO-dependent DNA-binding independent manner. Thus, Hp1b and Sin3a represent candidate co-factors for modulating metabolism-related genes in conjunction with FoxO.

Overall, key discoveries involving FoxO's DNA-binding independent activity including specific metabolism-related phenotypes, genes, and binding partners have been made. Ultimately, more in-depth research on the identified co-regulators will facilitate the identification of potential therapeutic targets for treating metabolic disorder without targeting FoxO directly, preventing severe side effects seen with FoxO-targeted treatments.

Keywords: *Drosophila*, metabolism, FoxO, binding, RNA-seq

ACKNOWLEDGEMENTS

I would like to express my sincere gratitude to my supervisor, Dr Cathy Slack for giving me such an amazing opportunity to work on such an interesting project. Without your support and guidance, my success in this project would not have been possible and I cannot begin to express my appreciation for everything you have done.

I would also like to thank my co-supervisor Dr James Brown for the belief in my work, as well as Dr Victor Bustos and Prof. Dame Linda Partridge at the Max Planck Institute for the Biology of Ageing for letting me continue such an interesting project.

Further thanks go to Dr Zita Balklava and Dr Mariaelena Repici, as well as all past and current members of the Fly/Worm/Cell group, for helping me to improve my presenting ability and provide indispensable advice and interesting insights on my work I wouldn't have thought of.

I am also grateful to Dr Abigail Otchere, Dr Cui Guan, and all other members of the Aston Fly lab for making the lab a great place to work, as well as providing support during such a trying period for everyone. Also, thanks to Dr Sarah Routledge for helping with the biochemical aspects of my project and answering the myriad of questions I had.

Special thanks to my family and friends who supported me and gave me their patience throughout.

CONTENTS

ABBREVIATIONS **9**

TABLE OF FIGURES **17**

TABLE OF TABLES **21**

1. INTRODUCTION **23**

1.1 METABOLIC HOMEOSTASIS AND ASSOCIATED DISORDERS 23

1.2 FOXO FAMILY OF TRANSCRIPTION FACTORS 24

1.2.1 FoxO structure and action 28

1.2.1.1 FoxO structure 28

1.2.1.2 FoxO post-translational modifications 30

1.2.1.2.1 FoxO phosphorylation 31

1.2.1.2.2 FoxO acetylation 33

1.2.1.2.3 FoxO methylation 34

1.2.1.2.4 FoxO ubiquitination 36

1.2.1.2.5 FoxO glycosylation 37

1.2.1.3 Other key FoxO structures 38

1.2.2 Roles of FoxO in metabolic homeostasis 39

1.2.2.1 FoxO and carbohydrate metabolism 40

1.2.2.2 FoxO and lipid metabolism 41

1.2.2.3 Other roles for FoxO in regulating metabolism 43

1.2.3 DNA-binding independent functions of FoxO 45

1.3. CONSERVATION OF FOXO FUNCTION BETWEEN ORGANISMS 52

1.3.1 *Drosophila* as a model organism 58

1.4 FOXO AS A THERAPEUTIC TARGET 60

1.5 AIMS AND OBJECTIVES 64

2. MATERIALS AND METHODS **66**

2.1 *DROSOPHILA* STOCKS AND MAINTENANCE 67

2.1.1 *FoxO* mutant *Drosophila* lines used in this study 67

2.1.2 *Drosophila* control strain 67

2.1.3 Fly husbandry 67

2.2 GENOMIC DNA PREPARATION AND POLYMERASE CHAIN REACTION (PCR) 68

2.2.1 Single fly genomic DNA preps 68

2.2.2 Polymerase Chain Reaction (PCR) 69

2.2.3 QIAquick PCR purification and analysis 70
2.3 VALIDATING *DROSOPHILA FOXO* MUTANT FUNCTION 71
2.3.1 Western blot analysis 71
2.3.2 Chromatin immunoprecipitation and quantitative PCR 73
2.3.2.1 Chromatin extraction from adult flies 73
2.3.2.2 Chromatin sample preparation and quantitative PCR 75
2.4 ASSESSING METABOLIC FUNCTION OF ADULT *DROSOPHILA* 77
2.4.1 Measurement of triglyceride (TAG) in adult flies 77
2.4.2 Quantification of free fatty acids (FFA) in adult flies 78
2.4.3 Measurement of glycogen and trehalose in adult flies 79
2.4.4 Haemolymph extractions and blood sugar measurements 79
2.4.5 Measurement of protein in adult flies 80
2.4.6 Quantification of lipid species in adult fly extracts by thin layer chromatography (TLC) 81
2.5 STRESS ASSAYS 82
2.5.1 Responses to starvation stress 82
2.5.2 Responses to oxidative stress 82
2.5.3 Responses to xenobiotic stress and metabolism 82
2.6 ASSESSING *DROSOPHILA* GROWTH 82
2.6.1 Measurement of adult body mass 83
2.6.2 Measurement of adult wing area 83
2.7 MEASUREMENT OF ADULT FEEDING BEHAVIOUR 83
2.7.1 Capillary Feeder (CAFE) assay 83
2.7.2 Proboscis extension (PE) and blue absorbance assay 84
2.8 MEASUREMENT OF LIFESPAN 84
2.9 MEASUREMENT OF FECUNDITY 85
2.10 TRANSCRIPTOMICS 85
2.10.1 RNA extraction 85
2.10.2 RNA-sequencing and analysis 86
2.10.3 Chromatin immunoprecipitation-sequencing and analysis 88
2.10.4 Quantitative reverse transcription PCR (qRT-PCR) 89
2.10.4.1 Complementary DNA synthesis 89
2.10.4.2 qRT-PCR 90
2.11 STATISTICAL ANALYSIS 93

3. *FOXO* MUTANT VERIFICATION AND PHENOTYPIC ASSESSMENT 96

3.1 INTRODUCTION 96
3.2 AIMS AND OBJECTIVES 99
3.3 RESULTS 101
3.3.1 *Drosophila FoxO* mutant validation 101
3.3.1.1 Verification of *FoxO* mutant stocks 101
3.3.1.2 Validating mutant FoxO activity 103
3.3.1.2.1 Verifying FoxO protein production 103
3.3.1.2.2 Verifying FoxO post-translational modification 105
3.3.1.2.3 Validation of disruption to DNA-binding activity in DBD mutants 107
3.3.2 Phenotypes associated with *Drosophila* FoxO activity 112
3.3.2.1 *Drosophila* FoxO DNA-binding dependent phenotypes 112
3.3.2.1.1 Lifespan and Fecundity 112
3.3.2.1.2 Feeding behaviour 117
3.3.2.1.3. Xenobiotic metabolism 121
3.3.2.1.4. Oxidative stress resistance 123
3.3.2.2 *Drosophila* FoxO DNA-binding independent activity 127
3.3.2.2.1 Growth 127
3.3.2.2.2 Starvation resistance 130
3.4 DISCUSSION 133
3.4.1 Verification of mutant stocks 133
3.4.2 *Drosophila* FoxO DNA-binding dependent phenotypes 134
3.4.3 *Drosophila* FoxO DNA-binding independent phenotypes 138

4. ASSESSMENT OF THE ASSOCIATION BETWEEN FOXO ACTIVITY AND METABOLIC PHENOTYPES IN *DROSOPHILA MELANOGASTER* 141

4.1 INTRODUCTION 141
4.2 AIMS AND OBJECTIVES 142
4.3 RESULTS 143
4.3.1 *Drosophila* FoxO in metabolic storage 143
4.3.2 Utilisation of metabolic stores during starvation 147
4.3.3 Modulation of circulating sugars 158
4.4 DISCUSSION 161
4.4.1 *Drosophila* FoxO in modulating metabolic phenotypes 161

5. TRANSCRIPTOMICS SHOWING THE EFFECTS OF DIFFERENT *FOXO* MUTATIONS 169

5.1 INTRODUCTION 169
5.2 AIMS AND OBJECTIVES 171
5.3 RESULTS 172
5.3.1 RNA-sequencing of *Drosophila FoxO* mutants 172
5.3.1.1 Quality control of the RNA-sequencing data 172
5.3.1.2 Mapping and alignment of the RNA-sequencing data 174
5.3.1.3 Analysis of differential gene expression 176
5.3.1.4 Verification of dFoxO-ΔV3 mutants 194
5.3.1.5 Verification of RNA-seq data and analysis 203
5.3.1.5.2 Quantitative reverse transcription PCR (qRT-PCR) verification of RNA-seq analysis 203
5.3.1.5.3 Comparisons of transcriptional responses to loss of dFoxO ... 213
5.4. DISCUSSION 217
5.4.1 RNA-sequencing of *Drosophila FoxO* mutants 217
5.4.1.1 Quality control of the RNA-sequencing data, mapping, and alignment 217
5.4.1.2 Verification of the RNA-seq results and analysis 218
5.4.1.3 Analysis of differential gene expression 224
5.4.1.3.1 Genes modulated in a dFoxO-independent manner 224
5.4.1.3.2 Genes modulated in a dFoxO-dependent DNA-binding dependent manner 227
5.4.1.3.3 Genes modulated in a dFoxO-dependent DNA-binding independent manner 232

6. ANALYSIS OF POTENTIAL FOXO BINDING PARTNERS 240

6.1 INTRODUCTION 241
6.2 AIMS AND OBJECTIVES 242
6.3 RESULTS 243
6.3.1 Transcription factor binding motif enrichment analysis 243
6.3.2 ChIP-sequencing analysis of transcription factors of interest 244
6.3.3 RNA-sequencing analysis for transcriptional regulation by Sin3a and Hp1b 252
6.4 DISCUSSION 262

6.4.1 Transcription factor binding motif enrichment analysis 262
6.4.2 ChIP-sequencing analysis of transcription factors of interest..... 267
6.4.3 RNA-sequencing analysis of transcription factors of interest 271

7. DISCUSSION AND CONCLUSIONS..... 274

7.1 DISCUSSION..... 275
7.1.1 *Drosophila FoxO* mutant verification and phenotyping..... 276
7.1.2 dFoxO-dependent DNA-binding dependent phenotypes 277
7.1.3 dFoxO-dependent DNA-binding independent phenotypes..... 282
7.1.3.1 dFoxO-independent activity in metabolic processes 282
7.1.3.2 dFoxO-dependent DNA-binding independent lipid mobilisation 285
7.1.3.3 dFoxO-dependent DNA-binding independent growth effects 291
7.1.4 Identification of dFoxO binding partners..... 292
7.2 SUMMARY OF DFOXO-DEPENDENT DNA-BINDING INDEPENDENT FINDINGS 296
7.3 CONCLUSION 299

REFERENCES..... 301

APPENDIX 1 353

ABBREVIATIONS

20E	20-hydroxyecdysone
A	Alanine
ACC	Acetyl-CoA carboxylase
AdipoR	Adiponectin receptor
Akh	Adipokinetic hormone
AMPK	Adenosine monophosphate-activated protein kinase
ANOVA	Analysis of variance
AQP	Aquaglyceroporin
ATGL	Adipose triglyceride lipase
BLAST	Basic local alignment search tool
bmm	*brummer*
BSA	Bovine serum albumin
CAFE	Capillary feeder
CBP	CREB- binding protein
CC	Corpora cardiaca
cDNA	complementary DNA
ChIP	Chromatin immunoprecipitation
ChIP-qPCR	ChIP-quantitative polymerase chain reaction
ChIP-seq	Chromatin immunoprecipitation sequencing
ChREBP	Carbohydrate response element binding protein
CREB	Calcium-response element-binding
Ct	Cycle threshold
DAG	Diacylglycerol

DAVID	Database for Annotation, Visualization and Integrated Discovery
DBD	DNA-binding domain
DBD-i	dFoxO-dependent DNA-binding independent
DBD1	dFoxO-DBD1-3xFLAG
DBD2	dFoxO-DBD2-3xFLAG
DBE	DAF-16 family member-binding element
DDT	Dichlorodiphenyltrichloroethane
DEG	Differentially expressed gene
dFoxO	*Drosophila* Forkhead Box O
DGAT	Diglyceride O- acyltransferase
dILP	*Drosophila* insulin-like peptide
dNTP	Deoxynucleoside triphosphate
dob	doppelganger von brummer
DRSC	*Drosophila* RNAi Screening Center
E1	Ubiquitin-activating enzyme
E2	(or UBC) Ubiquitin-conjugating enzyme
E3	Ubiquitin ligase
EASE	Expression Analysis Systematic Explorer
EcR	Ecdysone receptor
Eip74EF	Ecdysone-induced protein 74EF
EMC10	Endoplasmic reticulum membrane protein complex subunit 10
ER	Endoplasmic reticulum
ERK	Mitogen-activated extracellular signal-regulated kinase
FA	Fatty acid

FASN	Fatty acid synthase
FDR	False discovery rate
FFA	Free fatty acid
Fox	Forkhead box
FoxO	Forkhead Box O
FoxOA3	Constitutively active FoxO1
FTO	Fat mass and obesity associated
G6pc	Glucose-6-phosphatase catalytic subunit
GATOR2	GTPase-activating protein toward Rags 2
GCK	Glucokinase
gDNA	Genomic DNA
GFAT	Glucosamine-fructose-6-phosphate aminotransferase
GlcN6P	Glucosamine-6-phosphate
GLUT4	Glucose transporter type 4
GlyS	Glycogen synthase
GO	Gene ontology
GPAT4	Glycerol-3-phosphate acyltransferase 4
H	Histidine
H3	Histone 3
H4	Histone 4
HAT	Histone acetyltransferase
HBP	Hexosamine biosynthetic pathway
HDAC	Histone deacetylase
Hex-C	Hexokinase-C

HIF1	Hypoxia-induced factor 1
HNF-4	Hepatocyte nuclear factor 4
Hp1	Heterochromatin protein 1
HRP	Horse radish peroxidase
IC_{50}	Half-maximal inhibitory concentration
ICDR	Ionic compatibility detergent reagent
IGF-1	Insulin-like growth factor 1
IGFBP1	Insulin growth factor binding protein 1
IGV	Integrated genome viewer
IIS	Insulin/insulin-like growth factor signalling
ILP	Insulin-like peptide
InR	Insulin receptor
IP	Immunoprecipitation
IPC	Insulin-producing cells
IRE	Insulin-responsive element
IRS	Insulin receptor substrate
JH	Juvenile hormone
Jheh	Juvenile hormone epoxide hydrolase
JNK	Jun N-terminal kinase
K	Lysine
Kdm5	(aka LID) Lysine demethylase 5
KEGG	Kyoto Encyclopedia of Genes and Genomes
Kr-h1	Krüppel-like homologue-1
L-FoxO1	Liver-specific FoxO1 deletion

LD	Lipid droplet
LOCI	Laboratory for Optical and Computational Instrumentation
logFC	Log fold change
LPL	Lipoprotein lipase
MAG	Monoacylglycerol
Maml1	Mastermind-like 1
mdy	midway
mRNA	messenger RNA
mTOR	Mammalian target of rapamycin
mTORC1	Mammalian target of rapamycin complex 1
mTORC2	Mammalian target of rapamycin complex 2
NCBI	National Center for Biotechnology Information
NcoR	Nuclear corepressor
NES	Nuclear export sequence
NF-κB	Nuclear factor kappa B
NIH	National Institutes of Health
NLS	Nuclear localisation sequence
Npc1a	Niemann-Pick type C-1a
O-GlcNAc	β-linked N-acetylglucosamine
Obp	Odorant binding protein
PBS	Phosphate buffered saline
PCA	Principal component analysis
Pck1	Phosphoenolpyruvate carboxykinase
PCR	Polymerase chain reaction

PDK-1	Phosphoinositide-dependent kinase- 1
PDX-1	Pancreas/duodenum homeobox gene-1
PE	Proboscis extension
Pepck1	Phosphoenolpyruvate carboxykinase 1
PERK	Protein kinase RNA (PKR)-like ER kinase
PGC-1α	Peroxisome proliferator-activated receptor-**γ** coactivator 1-alpha
PGRA	Progesterone receptor A
PGRB	Progesterone receptor B
PI3K	Phosphoinositide 3-kinase
PIP_2	Phosphatidylinositol 4,5-bisphosphate
PIP_3	Phosphatidylinositol (3,4,5)-trisphosphate
polyQ	Polyglutamine
PP1	Protein phosphatase 1
PP2A	Protein phosphatase 2A
PPAR-α	Peroxisome proliferator-activated receptor-α
PPAR-γ	Peroxisome proliferator-activated receptor-γ
PRMT1	Protein arginine N-methyltransferase 1
PTEN	Phosphatase and tensin homolog
PTM	Post translational modification
QMR	Quantitative magnetic resonance
qPCR	quantitative polymerase chain reaction
qRT-PCR	quantitative reverse transcription polymerase chain reaction
R	Arginine
RNA-seq	RNA-sequencing

RNAi	RNA interference
ROS	Reactive oxygen species
S	Serine
SCA-3	Spinocerebellar ataxia type 3
sdr	Secreted decoy receptor
SDS	Sodium dodecyl sulfate
SDS-PAGE	SDS-polyacrylamide gel electrophoresis
SES	Signal extraction scaling
siRNA	small interfering RNA
Smrt	Silencing mediator for retinoid and thyroid hormone receptor
SOD	Superoxide dismutase
SREBP-1c	Sterol regulatory element-binding protein 1c
sug	sugarbabe
SYA	Sugar/yeast/agar
T	Threonine
TAD	Transactivation domain
TAE	Tris-acetate-EDTA
TAG	Triacylglycerol (or triglyceride)
TBS	Tris buffered saline
TBST	Tris buffered saline-Triton-x
TE	Tris-EDTA
TLC	Thin layer chromatography
TOR	Target of rapamycin
tps1	trehalose phosphate synthase 1

Tret1-1	Trehalose transporter 1-1
UAS	Upstream activation sequence
UDP-GlcNac	Uridine diphosphate N-acetylglucosamine
Upd2	Unpaired-2
UPR	Unfolded protein response
UTX-1	Ubiquitously transcribed TPR on X 1
V3	dFoxO-V3
V3F	dFoxO-V3-3xFLAG
w^{Dah}	*white Dahomey*
WT	Wild-type
ΔV3	dFoxO-ΔV3 (null)

TABLE OF FIGURES

Figure 1.1. Insulin/insulin-like growth factor (IIS) signalling pathway. 27

Figure 1.2. Schematic graph showing interactions between the mammalian FoxO1 DNA-binding domain (DBD) and consensus sequences within DNA. 29

Figure 1.3. Overview of FoxO protein structure and key post translational modifications. 31

Figure 1.4. Methods of FoxO-binding interactions to alter gene expression. 46

Figure 1.5. Evolutionary conservation of the insulin/insulin-like growth factor signalling (IIS) pathway. 53

Figure 1.6. Amino acid alignment of FoxO proteins from different species. 55

Figure 3.1. Schematic of the wild-type *Drosophila FoxO* (*dFoxO*) and mutant *dFoxO* gene locus. 98

Figure 3.2. Schematic of the *Drosophila FoxO* (*dFoxO*) gene locus and placement of primers. 101

Figure 3.3. Verification of *dFoxO*-mutant stock identity using PCR. 102

Figure 3.4. Western blot analysis of FLAG-dFoxO protein expression. 104

Figure 3.5. Western blot analysis of FLAG-dFoxO post-translational modification. 106

Figure 3.6. Optimisation of chromatin immunoprecipitation (ChIP) using w^{Dah} and an anti-RNA polymerase II antibody. 109

Figure 3.7. Chromatin immunoprecipitation (ChIP) of dFoxO DNA-binding domain mutants. 111

Figure 3.8. Comparing lifespan of various *dFoxO* mutant lines. 113

Figure 3.9. Assessment of fecundity of the different *dFoxO* mutants over 24 hours. 116

Figure 3.10.1. Measurement of food consumption of different *dFoxO* mutants over 96 hours. 118

Figure 3.10.2. Assessing short-term feeding behaviour of different *dFoxO* mutants. 120

Figure 3.11. Survival of *dFoxO* mutants in the presence of dichlorodiphenyltrichloroethane (DDT). 122

Figure 3.12. Survival of *dFoxO* mutants exposed to hydrogen peroxide (H_2O_2). ... 124

Figure 3.13. Survival of *dFoxO* mutants when exposed to paraquat. 126

Figure 3.14. Measurement of body mass and wing area of *dFoxO* mutants to evaluate the role of dFoxO in organismal growth. 129

Figure 3.15. Survival during starvation of *dFoxO* mutants. 131

Figure 4.1. Measurements of glycogen and trehalose within different *dFoxO* mutants under fully fed conditions. 144

Figure 4.2. Triglyceride (TAG) concentration and thin layer chromatography (TLC) assessment of various lipids in *dFoxO* mutants. 146

Figure 4.3. Measurements of trehalose stores within different *dFoxO* mutants under starvation conditions. 148

Figure 4.4. Measurements of glycogen stores within different *dFoxO* mutants under starvation conditions. 149

Figure 4.5. Triglyceride (TAG) concentration in different *dFoxO* mutants under starvation conditions. 152

Figure 4.6. Triglyceride (TAG) concentrations after prolonged starvation in *dFoxO* mutant females..... 155

Figure 4.7. Free fatty acid (FFA) concentrations after prolonged starvation in *dFoxO* mutants. 157

Figure 4.8. Measurement of circulating haemolymph sugars in *dFoxO* mutants. .. 159

Figure 5.1. Basic raw sequence quality control for *dFoxO* mutants. 173

Figure 5.2. Quality assessment of the mapping of paired-end reads for *dFoxO* mutants. 175

Figure 5.3. Principal component analysis (PCA) for all *dFoxO* mutants in both the fed and the starved state. 178

Figure 5.4. Visualisation of differentially expressed genes for each *dFoxO* mutant under different nutritional conditions. 180

Figure 5.5. Comparisons of the differentially expressed genes of the *dFoxO* mutants during starvation.....182

Figure 5.6. Differentially expressed genes modulated during starvation in only dFoxO-DBD2 mutants.....186

Figure 5.7. Differential expression of genes modulated during starvation in *dFoxO* mutants. 188

Figure 5.8. Differential expression of genes modulated during starvation in V3F and DBD2 mutants.....192

Figure 5.9. Identification of an appropriate reference gene for qRT-PCR.....196

Figure 5.10. Analysis of the expression of *dFoxO* by qRT-PCR. 198

Figure 5.11. Analysis of *dFoxO* gene expression in the dFoxO-V3F and -ΔV3 mutants using the Integrated Genomics Viewer (IGV).....200

Figure 5.12. Analysis of *dFoxO* gene expression in the dFoxO-ΔV3 mutant.....201

Figure 5.13. Western blot for the dFoxO protein in the dFoxO-ΔV3 mutant. 202

Figure 5.14. Analysis of the expression of *bmm* by qRT-PCR. 204

Figure 5.15. Analysis of the expression of *tps1* by qRT-PCR. 206

Figure 5.16. Analysis of the expression of *bigmax* by qRT-PCR. 208

Figure 5.17. Analysis of the expression of *dILP3* by qRT-PCR. 210

Figure 5.18. Analysis of *dFoxO* expression in the male dFoxO-ΔV3 mutant.....212

Figure 5.19. Visualisation of differentially expressed genes comparing the fully fed V3F and ΔV3 mutants.....214

Figure 5.20. Comparison of differentially expressed genes identified in the dFoxO-ΔV3 mutant with differentially expressed genes characterised in an additional *dFoxO* null allele.....215

Figure 6.1. Correlation heatmaps and signal strength fingerprints for Sin3a and Hp1b *Drosophila* ChIP-seq analysis. 245

Figure 6.2. Comparisons of genes identified as direct targets of Hp1b and Sin3a by chromatin immunoprecipitation (ChIP)-sequencing with the dFoxO-dependent DNA-binding independent differentially expressed genes. 247

Figure 6.3. Principal component analysis (PCA) for differential gene expression in response to loss of Sin3a and Hp1b expression. 253

Figure 6.4. Visualisation of differentially expressed genes in response to loss of *Sin3a* and *Hp1b* expression. 255

Figure 6.5. Comparisons of genes identified as targets of Hp1b and Sin3a by RNA-sequencing with the starvation induced dFoxO-dependent DNA-binding independent differentially expressed genes. 259

Figure 6.6. Differential expression of genes modulated by Hp1b or Sin3a as well as in a dFoxO-dependent DNA-binding independent manner. 261

Figure 7.1. Graphical representation of dFoxO's hypothesised DNA-binding independent modulation of metabolism. 297

TABLE OF TABLES

Table 1.1. FoxO target genes and their function. 40

Table 1.2. FoxO transcription factor binding partners. 47

Table 1.3. Drugs that target FoxO function and activity. 60

Table 2.1. Primer list used during stock verification. 70

Table 2.2. Accession numbers for the raw sequence files for previously published RNA-sequencing and chromatin immunoprecipitation-sequencing data. 89

Table 2.3. Primers used for reference gene identification in quantitative reverse transcriptase PCR (qRT-PCR). 91

Table 2.4. Primers used in the verification of RNA-sequencing (RNA-seq) results using quantitative reverse transcriptase PCR (qRT-PCR). 92

Table 2.5. Primers used in chromatin immunoprecipitation (ChIP)- quantitative PCR (qPCR). 93

Table 5.1. Gene ontology (GO) analysis of the genes differentially expressed only in one mutant. 184

Table 5.2. Differential expression of genes modulated during starvation only in V3F mutants. 190

Table 5.3. Enriched gene ontology (GO) terms for the genes potentially modulated in a dFoxO-dependent DNA-binding independent manner. 194

Table 5.4. Comparisons of the differential expression of the *dFoxO* gene between *dFoxO* mutants under fully fed conditions. 195

Table 6.1. Enriched transcription factors for the genes potentially modulated in a dFoxO-dependent DNA-binding independent manner. 243

Table 6.2. Genes bound by Hp1b or Sin3a as well as modulated in a dFoxO-dependent DNA-binding independent manner. 249

Table 6.3. Enriched gene ontology (GO) terms for the genes potentially modulated in a dFoxO-dependent DNA-binding independent manner by Hp1b and/or Sin3a. 251

Table 6.4. Enriched gene ontology (GO) terms for the genes potentially modulated by either Hp1b or Sin3a.x 257

Chapter 1

Introduction

1. INTRODUCTION

1.1 METABOLIC HOMEOSTASIS AND ASSOCIATED DISORDERS

For a number of years, incidences of obesity have been drastically increasing across the world, where based on current data it is estimated that 60% of men and 50% of women will be obese by 2050 in England alone (Agha & Agha, 2017).

As a consequence, there is an increase in associated metabolic disorders such as diabetes mellitus (hereafter diabetes). Diabetes has various forms, with the two most well-known being type I and type II. Type I diabetes is an autoimmune disorder caused by T-cells of the immune system, targeting and removing insulin-producing pancreatic β-cells, leading to disorder in insulin biosynthesis and release, and the subsequent inability to control blood glucose (DiMeglio *et al.* 2018). However, the majority (~90%) of diabetic patients are diagnosed type II, often associated with older age the key characteristic of this form is insulin resistance (i.e., a loss of response to insulin and β-cell dysfunction) leading to hyperglycaemia and associated complications (Whicher *et al.* 2020; Chatterjee *et al.* 2017).

Projections approximate that there will be 693 million patients living with diabetes globally by 2045 (Cho *et al.* 2018; Ragab *et al.* 2014), and even now, the UK is in a position where approximately 7% of the population is living with some form of diabetes with diagnoses being made every 2 minutes and diabetes-related amputations every hour (Whicher *et al.* 2020). Furthermore, in 2017 there was an estimated 5 million deaths and an overall global healthcare expenditure of $850 billion due to diabetes (Cho *et al.* 2018), with the National Health Service bill in the UK alone already surpassing the billions of pounds mark (calculated at approximately £19,000 a minute or 10% of the current budget) where 1 in every 20 GP prescriptions is issued for diabetes treatments (Stedman *et al.* 2019; Whicher *et al.* 2020). Although often treatable, a diagnosis of a metabolic disorder, such as diabetes, begins a lifetime of treatment and an increased risk of the fatal or life-changing complications that frequently arise including retinopathy, nephropathy, dysfunction of the immune system, loss of musculoskeletal integrity, and cardiovascular disease which is the most common cause of mortality in type II diabetic patients (Maiese, 2015).

A key type II diabetes treatment is a drug called metformin (dimethylbiguanide), which has its roots in the French lilac plant that was used as an anti-diabetic in mediaeval medicine (Bailey *et al.* 1996). This drug improves insulin sensitivity by decreasing

hepatic glucose release and increasing glucose uptake in the periphery, potentially through the suppression of gluconeogenic mitochondrial glycerol-3-phosphate dehydrogenase by the adenosine monophosphate-activated protein kinase (AMPK) signalling pathway (Bailey *et al.* 1996; Hawley *et al.* 2002; Wang *et al.* 2019).

However, as well as drug treatments, there must be lifestyle changes including dietary requirements and increased physical activity, which are reportedly difficult to maintain (Bailey *et al.* 1996). This then leads to adverse conditions in other aspects of life, including mental well-being, where psychological struggles and overwhelming feelings due to the demands of the disorder have been reported by 70% of diabetics (Whicher *et al.* 2020).

Together, these sobering statistics help to highlight the importance of researching metabolic diseases and their treatments, and the urgence at which this needs to occur. Not only to improve quality of life but also to reduce the overwhelming burden on healthcare systems (Maiese, 2015). Therefore, to better understand the complexities of metabolic disorders and identify potential avenues of treatment, in-depth research into the mechanisms that underpin these disorders is key.

1.2 FoxO family of transcription factors

For a number of decades, since the discovery of the *forkhead* gene in *Drosophila melanogaster* (hereafter, *Drosophila*), the Forkhead Box (Fox) family of proteins has been widely researched (Shimeld *et al.* 2010; Weigel *et al.* 1989). This grouping of proteins comes via the shared 100-residue DNA-binding, winged-helix 'forkhead' domain, and consists of over 2000 proteins (of which there are 18 in *Drosophila*) divided into subgroups A to S with high conservation across species (Benayoun *et al.* 2011; Shimeld *et al.* 2010). Additional FoxX and FoxY subgroups exist as further subclassifications for Fox proteins in sea urchins, as they do not fit unequivocally into existing groups (Hannenhalli & Kaestner, 2009). These Fox proteins have key roles within an organism, for example FoxA and FoxP proteins are essential during development (e.g., FoxA is important during formation of the notochord, a backbone precursor essential in nervous system development), with FoxP additionally acting as an important tumour suppressor (Friedman & Kaestner, 2006; Kim *et al.* 2019). However, one critical group to consider when researching metabolism and its associated disorders is the Fox group O (FoxO) transcription factors.

In mammals there are four FoxO paralogues namely FoxO1, FoxO3a, FoxO4, and FoxO6 (FoxO2 was found to be identical to FoxO3a and FoxO5 is the counterpart of FoxO3a in fish) (Link, 2019). FoxO1, FoxO3a, and FoxO4 are ubiquitously expressed in mammals and can localise to both the nucleus and the cytoplasm, whereas FoxO6 (the least well-researched of the four mammalian FoxOs) is confined to the tissues of the nervous system and is only present in the nucleus (Link, 2019). Despite small differences in their locality however, it is well known that they all show overlap and redundancy in function in various processes (including, glucose metabolism and diet responses) due to possessing almost identical 'butterfly-like' winged DNA-binding domains (Li *et al*. 2017; Obsil & Obsilova, 2011; Schmitt-Ney, 2020). Therefore, although there are tissue-specific targets for different FoxO proteins, there is a core set of target genes involved in processes such as metabolism and stress resistance that do not change between them.

FoxO proteins are well known for their roles in regulating homeostasis and various biological processes, including the cell cycle, apoptosis, resistance to oxidative stress, lifespan, and metabolism (Lu & Huang, 2011). Their dysfunction can lead to the pathogenesis and key phenotypes observed in metabolic disorders such as diabetes and its associated complications, as well as some cancers (Lee & Dong, 2017; Ragab *et al*. 2014).

Most importantly in regulating metabolism and for an organism to be able to adapt to nutritient availability, these factors respond to environmental cues by being negatively regulated by insulin (*Figure 1.1*) (Eijkelenboom & Burgering, 2013). In the insulin/insulin-like growth factor signalling (IIS) pathway, insulin released in response to high blood glucose binds to a receptor of the tyrosine kinase family, known as the insulin receptor (InR). This receptor is found on surface membranes of target tissues as a dimer, which when ligand bound induces a conformational change leading to autophosphorylation and the activation of further tyrosine kinase activity (Sparks & Dong, 2009).

Consequently, InR phosphorylation of the insulin receptor substrates (IRS) is increased due to elevated recruitment of the IRS to the phosphorylated InR via the pleckstrin homology, phosphotyrosine binding, and kinase regulatory loop binding

domains of the IRS (Mardilovich *et al.* 2009). Of the four mammalian IRS proteins in mammals, IRS-1 and IRS-2 are the main adaptor proteins in regulating insulin responses and are found in the cytoplasm exhibiting no studied intrinsic enzymatic activity (Mardilovich *et al.* 2009). Instead, these proteins act as key scaffold proteins in the formation of fundamental complexes that when disrupted can cause growth defects, insulin resistance, and pancreatic β-cell dysfunction in mice (Mardilovich *et al.* 2009; Tamemoto *et al.* 1994).

The phosphorylation of the IRS by the InR then allows for the activation of phosphoinositide 3-kinase (PI3K), as the IRS brings PI3K into close proximity to the activated receptor for phosphorylation. This results in active PI3K producing PIP_3 (phosphatidylinositol (1,4,5)-triphosphate) from PIP_2 (phosphatidylinositol (4,5)-bisphosphate) at the plasma membrane. PIP_3 is able to then recruit both Akt and phosphoinositide-dependent kinase- 1 (PDK-1), via their pleckstrin homology domains to allow the latter to phosphorylate and activate Akt using PIP_3 (Murillo-Maldonado & Riesgo-Escovar, 2017).

This activation allows a proportion of the Akt present in the cell to enter the nucleus and phosphorylate FoxO at 3 amino acid residues (e.g., human FoxO1 threonine (T) 24, serine (S) 256, and S319) (Zhang *et al.* 2011; Bridge *et al.* 2010). After which, FoxO is excluded from the nucleus causing FoxO's transcriptional activity to be greatly reduced, a state that is maintained through interactions with the regulatory protein, 14-3-3 (Ni *et al*. 2007). 14-3-3 is a phospho-binding protein involved in the regulation of key biological processes, including the cell cycle, apoptosis, glucose metabolism, and autophagy, and has for the most part been studied in nutrient-deficient environments (Pennington *et al.* 2018). These proteins enact this hold on FoxO by causing conformational changes in the nuclear localisation sequence (NLS) of FoxO and masking the DNA-binding domain (Kodani & Nakae, 2020). Once removed from the nucleus FoxO is often degraded via the ubiquitin proteasome pathway (Zhang *et al.* 2011). However, this does not always occur and FoxO can be dephosphorylated by protein phosphatase 2 (PP2A), allowing for re-entry into the nucleus and resumption of the direct regulation of its target genes (Singh *et al*. 2010; Zhang *et al.* 2011).

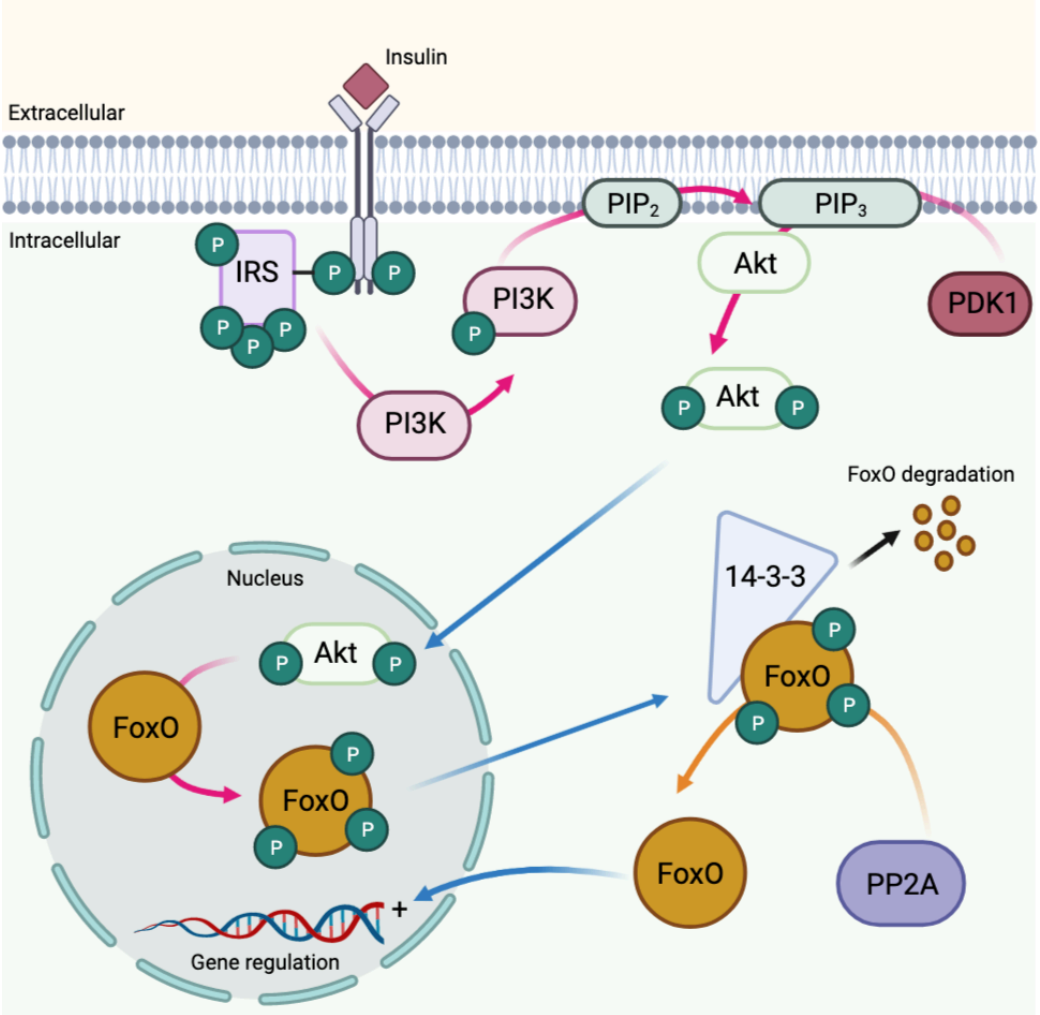

Figure 1.1. **Insulin/insulin-like growth factor (IIS) signalling pathway.**
Diagram of the insulin/insulin-like growth factor signalling pathway (IIS) and the regulation of FoxO transcription factors. Pink arrows denote phosphorylation events and orange dephosphorylation events. Blue arrows indicate movement and black degradation. Regulation of FoxO is caused by insulin binding to the insulin receptor's extracellular domain initiating the downstream activation of the intracellular PI3K/Akt signalling pathway. This ultimately leads to FoxO exclusion from the nucleus and subsequent degradation, causing decreased transcription of FoxO's target genes. (Adapted from Sparks & Dong, (2009). Created in Biorender).

1.2.1 FoxO structure and action

1.2.1.1 FoxO structure

The DNA-binding forkhead domain of FoxO proteins makes up ~25% of the overall protein structure, with the remaining 75% of the protein being so-called 'intrinsically disordered' regions comprised of a nuclear localisation sequence, a nuclear export sequence and a transactivation domain (Obsil & Obsilova, 2011; Wang *et al.* 2009a).

As transcription factors, it is unsurprising that FoxO's main method of action is to bind to DNA. This binding occurs at a consensus recognition motif, 5'-(A/C)AA(C/T)A-3', leading to modulation of target gene expression (Obsil & Obsilova, 2011). This motif is present in two sequences that FoxO is able to bind to, the insulin-responsive element (IRE) and the DAF-16 family binding element (DBE), which have the sequences 5'-(C/A)(A/C)AAA(C/T)AA-3' and 5'-GTAAA(T/C)AA-3', respectively (Brent *et al.* 2008a).

The forkhead domains are comprised of three major α-helices (mostly responsible for DNA-binding through hydrogen bonds), three β-sheets, and two 'winged' loops towards the C-terminus, which fold around the helices to form the unique butterfly-like structure; however, amongst the Fox family members the FoxO subfamily has a unique forkhead box domain, due to the presence of a GDSNS amino acid sequence just before the major helix 3 structure (Calissi *et al.* 2020).

Several important amino acids, namely human asparagine (N) 211 and histidine (H) 215 (*Drosophila* N146, H150) exist within the FoxO DNA-binding domain (DBD) facilitating the binding to the DNA through direct base specific contacts and water-mediated interactions (*Figure 1.2*) (Brent *et al.* 2008a). These amino acids are considered essential as they are found within FoxO's α-helix 3, which docks perpendicular into the major DNA groove allowing for the production of the major base contacts (Li *et al.* 2021). In addition to these interactions with the DNA's major groove, the junction between α-helices 2 and 3 and the 2 wings also form key interactions with bases situated within the DNA's minor groove (Benayoun *et al.* 2011).

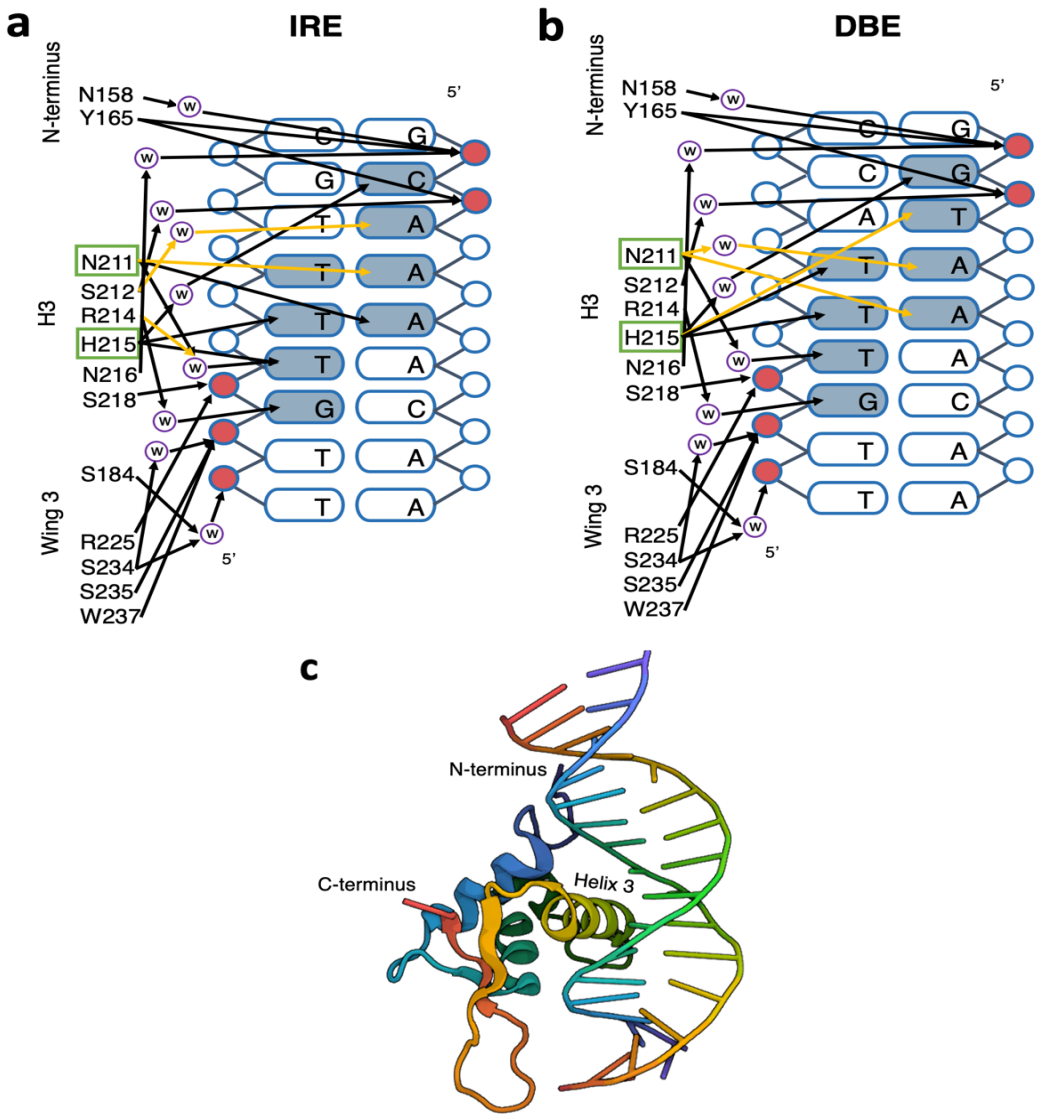

Figure 1.2. **Schematic graph showing interactions between the mammalian FoxO1 DNA-binding domain (DBD) and consensus sequences within DNA.** Schematic of residues present in mammalian (human) FoxO1 DBD and their binding to bases within the (a) insulin-responsive element (IRE) and (b) DAF-16 family binding element (DBE) sequences within DNA. Grey shaded bases and red phosphates represent those that are contacted directly or through water-mediated interactions (w). Yellow arrows indicate the differences in hydrogen bonds between IRE and DBE sequences. Green boxes indicate amino acids N211 and H215, which are instrumental in FoxO DNA binding. (c) Structural visualisation of FoxO1 binding to the DBE DNA sequence (Adapted from Brent *et al.* (2008a) and protein data bank (PDB) ID: 3CO7 Brent *et al.* (2008b). Created in Biorender).

1.2.1.2 FoxO post-translational modifications

There are many post-translational modifications that FoxO is able to undergo so that it can serve its far-reaching purposes, these include phosphorylation, acetylation, methylation, ubiquitination, and glycosylation (*Figure 1.3*) (Eijkelenboom & Burgering, 2013). In conjunction with the vast number of types of post-translational modifications that can occur, there is also a further ability to 'layer' these modifications which enables FoxO to elicit the appropriate response within so many different processes (Eijkelenboom & Burgering, 2013; Calnan & Brunet, 2008).

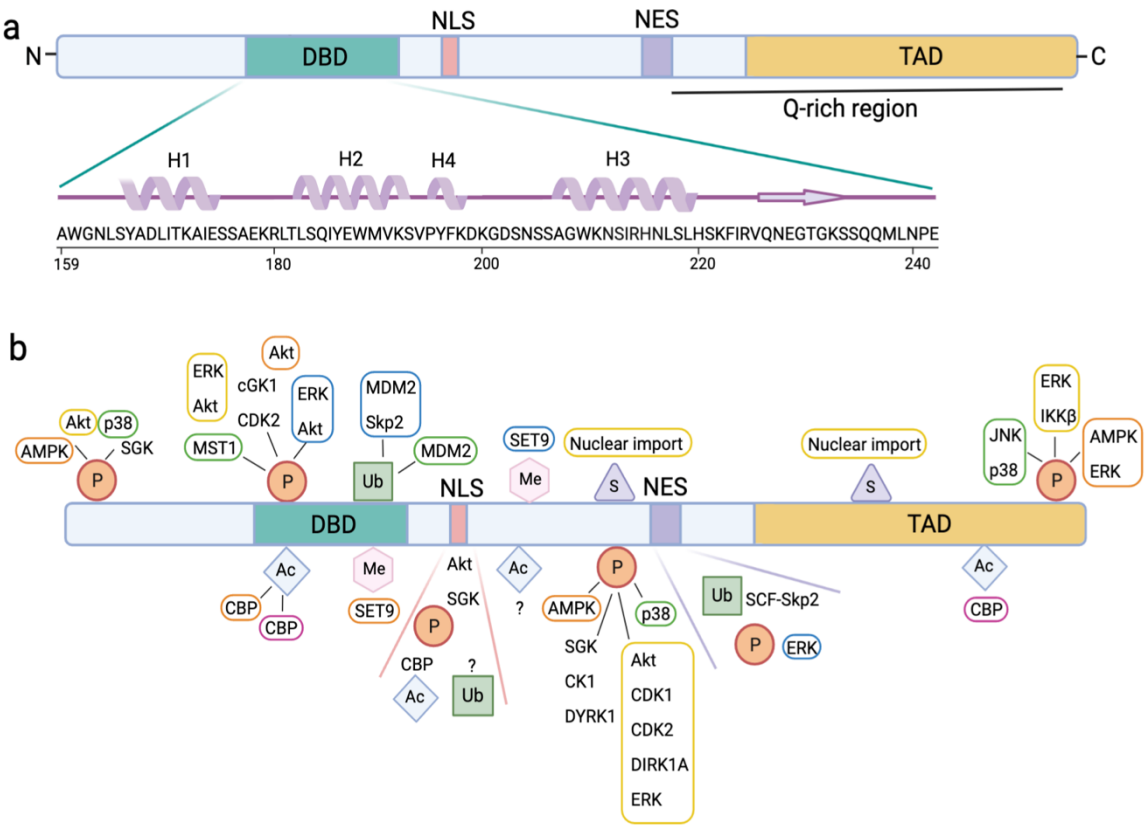

Figure 1.3. **Overview of FoxO protein structure and key post translational modifications.**

Graphical representation of (a) a general mammalian FoxO protein showing the four key domains within the protein structure: DNA-binding domain (DBD), nuclear localisation sequence (NLS), nuclear export sequence (NES), and transactivation domain (TAD), as well as further exposition of the DBD structure including an approximation of the Q-rich region. (b) an overview of the key post-translational modifications of various residues within the FoxO protein including phosphorylation, acetylation, and ubiquitination, and the proteins responsible. P: phosphate; Ac: acetyl group; Me: methyl group; Ub: ubiquitin; S: intermolecular disulfide bonds. Coloured boxes represent the processes these modifications are associated with if known. Yellow: nuclear export; green: nuclear import; pink: nuclear factor interactions; blue: degradation; orange: transcription. (Adapted from Li *et al.* 2021; Calissi *et al.* 2020; van der Horst & Burgerring, 2007. Created in Biorender).

1.2.1.2.1 FoxO phosphorylation

As described above, one of the most widely characterised and important post-translational modifications that FoxO can undergo is phosphorylation by Akt during insulin signalling. However, FoxO is also able to undergo phosphorylation via other kinases. For example, FoxO can be phosphorylated by the protein kinase R-like

endoplasmic reticulum kinase (PERK) at serine residues not targeted by Akt, which leads to an opposing increase in FoxO activity (Wang *et al*. 2016b). PERK is an important pathway component for mediating endoplasmic reticulum (ER) stress, a process often associated with obesity and metabolic disturbance due to FoxO upregulation causing increasing insulin-resistance within cell populations, therefore this modification has a potential role in the onset of type II diabetes (Zhang *et al*. 2013).

Other enzymes that give rise to FoxO phosphorylation are AMPK, the Jun N-terminal kinase (JNK), and the mitogen-activated extracellular signal-regulated kinase (ERK). These enzymes have varying effects on FoxO activity for example, like PERK, AMPK is able to phosphorylate FoxO at several residues and increase its activity (Wang *et al.* 2017). This activation is involved in processes such as redox regulation and autophagy via FoxO-dependent increases in the expression of genes that encode proteins which are key regulators in these processes, such as the redox regulator superoxide dismutase (SOD), and the autophagy inducer, ATG12 (Jeon, 2016). This AMPK-mediated FoxO activation has also been shown to be involved with dietary restriction-associated lifespan extension and stress resistance in *Caenorhabditis elegans*, a process that could potentially be replicated in mammals using the type II diabetes treatment, metformin (Greer *et al.* 2007). In addition to phosphorylation, AMPK can interfere with FoxO's other post-translational modifications as AMPK is able to phosphorylate histone deacetylases (HDACs) preventing deacetylation of FoxO proteins and continued repression of FoxO activity, reducing the expression of FoxO-dependently regulated gluconeogenic genes (Jeon, 2016).

This activation by phosphorylation is also carried out by JNK, increasing FoxO's transcriptional activity usually under oxidative stress, where JNK antagonises the IIS pathway by activating FoxO activity leading to an increase in redox-related genes (Essers *et al.* 2004; Wang *et al.* 2005). These JNK-FoxO interactions also seem to be evolutionarily conserved as they have also been identified in *Drosophila,* where in the fly eye *Drosophila* FoxO (dFoxO) has interactions with the *Drosophila* JNK, BSK, as well as the JNK-related serine/threonine protein kinase, Hep (Wang *et al.* 2005). Direct phosphorylation of FoxO is not the only way that JNK can regulate FoxO activation. It has also been shown that JNK can phosphorylate 14-3-3 proteins causing dissociation of FoxO from 14-3-3, preventing FoxO degradation and allowing FoxO to be imported back into the nucleus (Sunayama *et al.* 2005).

Unlike these kinases, however, ERK behaves more in line with Akt as it inhibits FoxO activity leading to a downregulation of its target genes via shuttling into the cytoplasm (Wang *et al.* 2017). As well as nuclear exclusion, this phosphorylation also engenders instability and degradation in the FoxO protein due to an increased association with the E3 ubiquitin ligase, MDM2 (Huang & Tindall, 2011; Xie *et al.* 2012a). This inhibition of FoxO activity has been implicated in the promotion of tumorigenesis, due to the alleviation of FoxO's tumour suppressor activity, and has even been targeted as a cancer therapy and a clinical marker for the efficacy of cancer drugs (such as, AZD6244) (Yang *et al.* 2008; Yang *et al.* 2010).

1.2.1.2.2 FoxO acetylation

Another important modification associated with FoxO regulation is acetylation, which allows for the regulation of *FoxO* gene transcription and related processes. Although, most evidence points towards acetylation having a repressive action on FoxO activity, there is seemingly contradictory evidence showing FoxO acetylation can lead to gene activation (Yang *et al.* 2009b; Zhou *et al.* 2020, Matsuzaki *et al.* 2005; Fukuoka *et al.* 2003; van der Horst *et al.* 2004). It seems however that these inconsistencies have been reconciled as being dependent on cell type and the specificity of FoxO to different target genes (van der Heide & Smidt, 2005).

Acetylation of FoxO involves the transfer of acetyl groups to lysine residues. Within human FoxO1, the most influential lysine residues seem to be lysine (K) 245 and K248, which when acetylated lead to a severe decline in DNA-binding activity (Xie *et al.* 2012a). An example of this type of modification involves the calcium-response element-binding (CREB) binding protein (CBP) and its partner, p300. CBP/p300 transfers acetyl groups to FoxO lysine residues altering their charge (i.e., so they are no longer positive), preventing their binding to DNA (Matsuzaki *et al.* 2005). In addition, the acetylation of FoxO also means that there is a higher likelihood for FoxO to localise to the cytoplasm from the nucleus, reducing its transcription (Xie *et al.* 2012a).

An interesting role for CBP/p300 acetylation is that of energy homeostasis. Where Zhou *et al.* (2020) show that by inhibiting these co-activators via the recently reported inhibitor A-485 (a compound shown to be 1000-fold more potent than previously researched inhibitors), both lipogenesis and glucose production can be reduced in

mouse hepatocytes. This reduction is due to reduced acetylation of FoxO, prompting key genes in these processes to be downregulated as a consequence of increased FoxO ubiquitination and subsequent degradation (Zhou *et al.* 2020). It should be noted that this is not the only CBP/p300-FoxO association, as this direct interaction between the two proteins also causes acetylation of chromosomal histone proteins allowing for recruitment of RNA polymerase II to the gene promoter region, and the subsequent activation of transcription (Kodani & Nakae, 2020).

The acetylation of FoxO is a reversible process with deacetylation of FoxO predominantly controlled by deacetylases from the sirtuin family. This family includes the class III HDACs NAD^+-dependent enzymes that regulate various biological processes in a cell-specific manner (such as, metabolic homeostasis and responses to oxidative stress) (Rajendran *et al.* 2011). The most well-researched is Sirt1 and is an essential regulator of FoxO activity, deacetylating the residues acetylated by CBP/p300 (Rajendran *et al.* 2011; Kodani & Nakae, 2020). Sirt1 has shown to be co-immunoprecipitated with various mammalian FoxO proteins (including, FoxO4 and FoxO3a), with this interaction leading to the deacetylation of FoxO and the regulation of GADD45 induction in response to oxidative stress, growth arrest, and DNA damage (Kobayashi *et al.* 2005).

As mentioned above, this interaction has also been connected to metabolism, and has been exploited in a model using diabetic rats and metformin, leading to the identification of the Sirt1-FoxO autophagy-related signalling pathway as the mechanism of protection by metformin on renal function during diabetic nephropathy, a microvascular complication associated with diabetes and end-stage renal disease (Xu *et al.* 2020).

1.2.1.2.3 FoxO methylation

As well as acetylation, methylation is also a common post-translational modification associated with the alteration of FoxO activity. Both arginine and lysine residues within the FoxO protein have the ability to be methylated via methyltransferases, however they have opposing actions on FoxO activity, namely nuclear-retention and activation, and DNA-binding inhibition respectively (Xie *et al.* 2012a).

Arginine methylation via protein arginine N-methyltransferase 1 (PRMT1) occurs on two residues in mouse FoxO1 proteins, arginine (R) 248 and R250 (Yamagata *et al.*

2008). Importantly, it has been shown that methylation of these residues is highly conserved, with evidence identifying the role of PRMT1 in methylation of the *C. elegans* FoxO homologue, DAF-16, leading to extensions in lifespan by increasing the expression of several key longevity and stress resistance genes (Takahashi *et al.* 2011).

The close proximity of the methylation and phosphorylation sites has been shown to allow for competition between the two events, where methylation of arginine residues blocks Akt phosphorylation of the closely situated S253 residue enabling continued transcription of FoxO target genes (Yamagata *et al.* 2008). Such genes are often those involved in oxidative stress-induced apoptosis (e.g., *Bim*), a process which is eradicated in the presence of PRMT1 small interfering RNA (siRNA) due to increased degradation via Akt phosphorylation (Yamagata *et al.* 2008).

With regards to lysine methylation, human FoxO3a has been shown to be methylated at K271 by the methyltransferase, Set9 (Calnan *et al.* 2012). This modification allows for the destabilisation of the FoxO protein causing a brief increase in FoxO activity in response to stress without inducing apoptosis (Xie *et al.* 2012b; Calnan *et al.* 2012). This residue is also known to be deacetylated by Sirt1 indicating a potential competitive nature between methylation and acetylation as well as phosphorylation in regulating FoxO activity (Calnan *et al.* 2012). Aside from methylation of K271 on FoxO3a, there has also been shown to be methylation events that occur on K270 via Set9 which has an opposing effect on FoxO activity by reducing FoxO-dependent transcription (Chae *et al.* 2019).

Although K270me and K271me are the only methylation events that have been shown to be possible on FoxO3a, human FoxO1 has also been shown to be methylated at K273 via the euchromatic histone lysine methyltransferase, EHMT2 (also known as, G9a) leading to elevated association with the FoxO degradation protein Skp2 during heightened insulin signalling (Chae *et al.* 2019).

As with most other post-translational modifications that occur on mammalian FoxO proteins, this methylation is also conserved in *Drosophila.* However, various databases indicate there is no specific *Drosophila* homologue for the *Set9* gene although various other lysine methyltransferases do exist such as, Set1, and Su(var)3-9, E(z), and Trx the proteins that give the Set domain its name (Larkin *et al.* 2021; Stelzer *et al.* 2016).

There are also demethylases that are associated with FoxO activity, however unlike the various other post-translational modifications that seem to have well-researched opposing actions (e.g., dephosphorylation via phosphatases and deacetylation via HDACs), information on the demethylation of FoxO is relatively lacking. For instance, one of the key histone demethylases, lysine demethylase 5 (Kdm5), is known to regulate *Drosophila* FoxO activity, particularly in responses to oxidative stress like the other methylation events, however this influence on FoxO, and the subsequent increase in FoxO DNA-binding seems to be exerted via HDAC4 and an increase in deacetylation activity rather than via the removal of methyl groups (Liu *et al.* 2014).

1.2.1.2.4 FoxO ubiquitination

An important mechanism for regulating the activity of a transcription factor is its degradation, as this maintains a tight control over target gene expression. For FoxO, degradation is mediated by ubiquitination. The transferal of ubiquitin is carried out by 3 crucial enzymes, ubiquitin-activating enzyme (E1), ubiquitin-conjugating enzyme (UBC also known as, E2), and ubiquitin ligase (E3) (Kodani & Nakae, 2020). The critical ubiquitin ligase in FoxO ubiquitination is Skp2, a component of the Skp1/cullin-1/F-box protein ubiquitin complex, which combines with human FoxO1 when the S256 residue within the FoxO amino acid chain is phosphorylated (Wang *et al.* 2016b).

Interestingly, ubiquitination is also connected to other modifications of FoxO. For example, deacetylation of FoxO by Sirt1 or Sirt2 promotes polyubiquitination of the FoxO proteins by enhancing Skp2 binding ultimately initiating FoxO degradation (Wang *et al.* 2012a).

However, FoxO proteins are also able to undergo monoubiquitination, which in contrast to the degradation caused by polyubiquitination, enhances FoxO transcriptional activity (Wang *et al.* 2016b). Intriguingly MDM2, mentioned above, influences both. Fu *et al.* (2009a) showed that by activating p53, MDM2 activity is also enhanced leading to polyubiquitination and degradation of both FoxO1 and FoxO3a. However, MDM2 is also able to govern the monoubiquitination of FoxO4 via direct binding; a process reversed by the ubiquitin-specific protease, USP7, allowing for nuclear import and increase in FoxO target gene expression particularly during moments of elevated oxidative stress (Brenkman *et al.* 2008).

These forms of ubiquitination are also associated with metabolic control, where de-ubiquitination by USP7 on FoxO1 leads to a reduction in FoxO1 binding to its promoter regions particularly on genes associated with gluconeogenesis (Hall *et al.* 2014). Furthermore, FoxO ubiquitination also leads to increased FoxO activity with regards to muscle atrophy however, this increase in FoxO activity is caused by an increased transfer of polyubiquitin chains onto K63 residues, identifying not all polyubiquitination leads to FoxO protein degradation (Li *et al.* 2007). This regulation is interesting as muscle atrophy has an important role in energy homeostasis, as it produces energy during fasting. This unconventional ubiquitination is controlled by the muscle-specific E3, atrogin-1, which interestingly is also a FoxO target gene causing positive feedback onto its own expression in a FoxO-dependent manner (Wang *et al.* 2016b).

1.2.1.2.5 FoxO GLYCOSYLATION

Those above are not the only post-translational modifications associated with metabolism or metabolic disorder. FoxO activity can also be increased via O-glycosylation, a nutrient sensing process where O-linked β-N-acetylglucosamine (O-GlcNAc) transferase transfers O-GlcNAc to specific FoxO serine/threonine residues (Mattila & Hietakangas, 2017; Housley *et al*. 2008). The activity of O-GlcNAc transferase is dependent on the concentration of the amino sugar, uridine diphosphate (UDP)-GlcNAc, which is produced via the hexosamine biosynthetic pathway (HBP) from glucose using the enzyme glutamine-fructose-6-phosphate amidotransferase (GFAT) (Kim *et al*. 2018; Wells *et al*. 2003).

Excess glucose uptake into the cell stimulates the HBP causing over-activation of GFAT, this increases intracellular levels of UDP-GlcNAc, subsequently allowing for both the development of ER stress as well as increased O-glycosylation of FoxO increasing its target processes such as gluconeogenesis (Marshall *et al*. 1991; Copeland *et al*. 2008). Ultimately, this increases glucose levels leading to hyperglycaemia, insulin resistance, and further stimulation of the HBP and elevation of FoxO activity (Housley *et al*. 2008; Buse, 2006; Slawson *et al*. 2010). This promotes the already existing hyperglycaemic state, pushing the organism further from homeostatic norms and producing the aberrant FoxO activity seen in the pathology of some metabolic disorders. This connection between an overactive HBP and metabolic disorder has been shown in previous study, where overexpression of the

O-GlcNAc transferase enzyme in the muscle or adipose tissue of transgenic mice led to the development of type II diabetes (McClain *et al*. 2002).

However, in human studies activation of the HBP does not affect insulin sensitivity, indicating the consequences of this aberrant modification may not be conserved in humans (Pouwels *et al*. 2001). However, elongated periods of aberrant activity are often key in the production of metabolic disorders and the associated complications, and glucosamine infusion (i.e., the method used to enhance O-glycosylation in this human study) was only carried out over a period of 5 hours, perhaps not fully representing the elevated glucosamine conditions in the long term (Pouwels *et al*. 2001).

1.2.1.3 Other key FoxO structures

In addition to regulating processes through DNA-binding dependent activity, FoxO also has the ability to produce protein-protein interactions. This is possible due to the presence of several different regions within the FoxO protein.

One such region is the LXXLL motif within the transactivation domain (where L is leucine and X any amino acid) (van der Vos & Coffer, 2008; Nakae *et al.* 2006; Calissi *et al.* 2020). These motifs are a signature motif of nuclear hormone receptors (to the point where they are also known as the 'nuclear receptor box') and have been shown to conciliate protein-protein interactions (Savkur & Burris, 2008). These nuclear receptors and their interactions with FoxO are particularly important in reproductive biology, where progesterone nuclear receptors (PGR) A and B in human endometrial cells were shown to cooperate directly with FoxO1 to synergistically influence the transcriptional activity of both proteins (Kim *et al.* 2005). Despite this interesting form of activity these LXXLL motifs are absent from the single *Drosophila* dFoxO and the *C. elegans* DAF-16 proteins (van der Vos & Coffer, 2008). Therefore, whilst these motifs are interesting and warrant further research they seemingly cannot be considered when working in non-mammalian model systems.

Another key region is the polyglutamine (polyQ) region, which is defined as a region that contains at least 8 glutamine repeats within a stretch of 10 amino acid residues (Schaefer *et al*. 2012; Totzeck *et al*. 2017; Gemayel *et al*. 2010). In dFoxO, this Q-

rich region is relatively large (approximately amino acids 314-569) covering most of the protein's transactivation domain (TAD) and contains two coiled-coil supersecondary structures (amino acids 429-449 and 543-578) (Kwon *et al.* 2018). As well as *Drosophila*, these tracts exist in many human proteins, however they are well known for their structural instability (Kwon *et al.* 2018; Totzeck *et al*. 2017). This is unsurprising given that most would recognise these regions from the study into various genetic diseases, including Huntington's disease and spinocerebellar ataxia type 3 (SCA-3), as they are characterised as disorders caused by atypical expansion of the relevant protein's polyQ regions (Totzeck *et al*. 2017; Kwon *et al.* 2018). Despite their ability to cause disorder, these polyQ proteins also carry out roles within normal physiology, including the mediation of protein-protein interactions via electrostatic interactions and hydrogen bonds and recruitment of other polyQ proteins (Schaefer *et al*. 2012; Atanesyan *et al*. 2012; Grigoryan & Keating, 2008).

1.2.2 Roles of FoxO in metabolic homeostasis

Regulating metabolism and ensuring the delicate balance of nutritional macromolecules within the blood via insulin is imperative for ensuring the health of an organism. Deregulation of FoxO is a common feature involved in the pathogenesis of both type I and type II diabetes, as well as being an influential component in the complications related to such disorders (Li *et al.* 2017, Altomonte *et al.* 2004). For example, hyperglycaemia perpetuated by FoxO dysfunction is a risk factor associated with cardiovascular disease development and dyslipidaemia, and alongside obesity is one of the main characterisations of metabolic syndrome (Owusu-Ansah & Perrimon, 2014).

Gene ontology analysis carried out by Shin *et al.* (2012) has identified that FoxO1 significantly affects the metabolic processes of carboxylic acids, fatty acids, steroids, and even vitamin A, with elevated serum levels of the latter being interestingly shown as a characteristic of type II diabetes (Rhee & Plutzky, 2012). FoxO is also implicated in regulating adipogenesis (Klotz *et al.* 2015), as well as myoblast differentiation and pancreatic β-cell growth, all of which are pivotal in the regulation of metabolic homeostasis (Puig & Tjian, 2005). The important role FoxO has in metabolism is potentially due to its high expression in insulin-sensitive tissues, which allows FoxO to have a diverse range of roles in a number of different organs (*Table 1.1*).

FoxO target gene	Change in expression	Process effected	Reference
G6pc	Increase	Glycogenolysis/Gluconeogenesis	Nakae *et al.* 2008
Pck1	Increase	Gluconeogenesis	Nakae *et al.* 2008
ApoC-III	Increase	Disrupting lipid metabolism	Sparks & Dong 2009
Atrogin-1	Increase	Muscle atrophy	Sandri *et al.* 2004
LPL	Increase	Lipolysis	Lu & Huang, 2011
ATGL	Increase	Lipolysis	Pan *et al.* 2017
NPY	Increase	Food intake	Ma *et al.* 2015
AgRP	Increase	Food intake	Ma *et al.* 2015
PDX-1	Decrease	Pancreatic β-cell differentiation/insulin sensitivity	Kousteni, 2012; van der Horst & Burgering, 2007
PDK-4	Increase	Carbohydrate-lipid switch	Lu & Huang, 2011
CD36	Increase	Carbohydrate-lipid switch	Cheng & White, 2011
MnSOD	Increase	Oxidative stress resistance	Huang & Tindall, 2007
Catalase	Increase	Oxidative stress resistance	Huang & Tindall, 2007
SREBP-1c	Decrease	Lipogenesis	Deng *et al.* 2012
NeuroD	Increase	Insulin biosynthesis	Buteau & Accili, 2007
MAFA	Increase	Insulin biosynthesis	Buteau & Accili, 2007
p21	Decrease	Adipocyte differentiation/cell survival	Xing *et al.* 2018; Peng *et al.* 2015

Table 1.1. **FoxO target genes and their function.**
FoxO has a variety of roles in ensuring metabolic homeostasis in a number of different tissues. FoxO has the ability to up- or down-regulate a variety of different genes that impact metabolism as shown here; however, this list is not exhaustive.

1.2.2.1 FoxO and carbohydrate metabolism

There are many examples of FoxO regulating carbohydrate homeostasis with many of these roles requiring FoxO's ability to bind to DNA. In the mammalian liver, FoxO is known to control the expression of a number of important factors, including G6pc and Pck1, two key gluconeogenic liver enzymes that catalyse the first few steps of the gluconeogenesis pathway (Lee & Dong, 2017; Lu & Huang, 2011). In conjunction, FoxO is also paramount in the synthesis and breakdown of the sugar, trehalose. A disaccharide of glucose, trehalose is a well-known energy source for insects such as *Drosophila,* as well as being an important stress protectant against conditions including heat, freezing, and deregulation of water homeostasis (Hibshman *et al.* 2017). Studies have shown that FoxO in a variety of organisms is able to not only directly regulate a number of trehalose synthesis genes, such as trehalose phosphate synthase-1 (*tps-1*) and trehalose phosphatase, but also trehalase, the enzyme

associated with trehalose catabolism (Hibshman *et al.* 2017; Matsushita & Nishimura, 2020).

In addition to affecting sugar synthesis and breakdown, transgenic FoxO overexpression in C2C12 mouse skeletal muscle cells has been shown to cause severe muscular atrophy by inducing expression of *atrogin-1* (Cheng & White, 2011). This reduces muscle mass and causes loss of glucose homeostasis by reducing the muscles capacity to respond to insulin as a major mammalian metabolic organ, including in humans (Kousteni, 2012; Kitamura & Kitamura, 2007; Nwadozi *et al*. 2016). Therefore, logically inhibiting this pathway would be an ideal scenario for treating hyperglycaemia and diabetes. However, given the tight balance needed to maintain normal homeostatic control, over-compensation in FoxO function in either direction has poor consequences. So, whilst overexpression of FoxO1 in mice leads to an increase in blood glucose during fasting due to elevated gluconeogenesis, knockout of FoxO1 produces fasting hypoglycaemia (Tikhanovich *et al*. 2013; Lu & Huang, 2011; Lee & Dong, 2017).

1.2.2.2 FoxO and lipid metabolism

In conjunction with the above, FoxO is also considered a key modulator of lipid metabolism via the integration of insulin signalling with circulating glucose and lipid concentrations (Vihervaara & Puig, 2008). Similarly to carbohydrate metabolism, many of these effects in lipid metabolism also require FoxO's DNA-binding activity. Triglycerides, the main form of fat storage in many organisms from insects to mammals, are known to have a FoxO-dependent control on their breakdown via the enhancement of the expression of various lipases, particularly lipase 4 and adipose triglyceride lipase (ATGL) (Vihervaara & Puig, 2008; Grönke *et al.* 2007; Kitamura & Kitamura, 2007). Both of which potentially have the ability to cause hypertriglyceridaemia when FoxO activity is aberrant. This dyslipidaemia can produce lipotoxicity, inflammation, and ER stress which can lead to insulin resistance, thereby reinforcing feedback on abnormal lipid levels and further moving concentrations away from a normal physiological balance (Li *et al.* 2014).

As well as these lipid stores, circulating lipids are also affected by FoxO, as FoxO regulates the production of the monooxygenase cytochrome P450, CYP8B1 (also known as, 12α-hydroxylase), which synthesises 12α-hydroxylated bile acids allowing

for activation of the bile acid receptor, Fxr, and lowering of TAG in the circulation (Haeusler *et al.* 2012). Therefore, inactivation of FoxO leads to a decrease in 12α-hydroxylated bile acids leading to less effective control on both TAG and cholesterol synthesis, as well as circulating and stored lipid concentrations, which have all been linked to the liver lipid abnormalities associated with type II diabetes (Haeusler *et al.* 2012).

FoxO also plays a role in hepatic lipid metabolism by suppressing expression of sterol regulatory element-binding protein-1c (SREBP-1c), an important insulin-induced factor in lipogenesis (Deng *et al.* 2012; Kitamura & Kitamura, 2007; Pan *et al.* 2017). Constitutively active FoxO1 in the liver is able to prevent induction of SREBP-1c expression pre- and post-feeding, by reducing its basal mRNA expression by as much as 60% (Deng *et al.* 2012).

In addition, FoxO is also able to supress lipogenesis by regulating steps within the interconnected process of glycolysis (Zhang *et al.* 2006). By downregulating various glycolytic enzymes such as glucokinase (GCK), FoxO prevents the induction of lipogenesis by inhibiting production of pyruvate from glucose, which subsequently arrests acetyl-coenzyme A formation and triglyceride production (Saponaro *et al.* 2015).

There is also evidence to suggest that FoxO1 may also be able to influence insulin resistance via effects on fat storage and adipokine secretion, both of which require successful differentiation and subsequent maintenance of mature adipocytes. This belief is due to FoxO1 interacting with and inhibiting the transcription factor peroxisome proliferator-activated receptor (PPAR)-γ, contributing to the development of insulin resistance via the inhibition of adipocyte differentiation and fat storage (Barthel *et al.* 2005; Cheng & White, 2011). This is also possible through FoxO's role in regulating the lipid droplet associated protein, FSP27, impacting autophagy and lipid droplet growth, another potential cause of increased adiposity during aberrant FoxO activity (Liu *et al.* 2016).

Affects on the adipose tissue also impacts the roles of various adipokines, with a key adipokine affected by FoxO activity being adiponectin. This adipokine is known to be

regulated by FoxO1 in the adipose tissue, through direct binding of FoxO to the DNA then subsequent formation of a complex with CCAAT/enhancer-binding protein alpha leading to adiponectin upregulation (Qiao & Shao, 2006). The importance of this adipokine cannot be understated, as not only is it the most abundantly produced adipokine, but loss of its action is often central to the onset of insulin resistance and type II diabetes via tight control on energy homeostasis and insulin sensitivity, and even cardiovascular disease due to its anti-inflammatory and anti-atherogenic effects (Achari & Jain, 2017).

Altogether, this disruption in lipid metabolism and homeostasis could potentially be one of the cardinal events in emerging insulin resistance, either by impairing insulin sensitivity due to fatty acid accumulation (Walther & Farese, 2012, Li *et al.* 2017), or by further promoting the secretion of adipokines, such as adipocyte lipid chaperone 2 that encourages gluconeogenesis and the development of insulin resistance if left unchecked (Morigny *et al.* 2016).

1.2.2.3 Other roles for FoxO in regulating metabolism

In addition to playing a key part in maintaining nutrient balance through the control of carbohydrate and lipid metabolism, FoxO also has roles in maintaining key metabolic organs (e.g., the cells of the pancreas), as well as feeding behaviour, and nutrient switching.

In the pancreas, FoxO regulates both the function and development of pancreatic β-cells (Kitamura & Kitamura, 2007; Hesp *et al*. 2015). This is important as pancreatic β-cells have major roles in sensing glucose within the blood, to allow for the production of post-prandial insulin and therefore the maintenance of appropriate blood glucose levels (Kousteni, 2012). This process occurs through the FoxO-dependent translocation of a crucial master transcription factor in the β-cell, the pancreas/duodenum homeobox gene-1 (PDX-1), where FoxO competes for its promoter region with the PDX-1 activator, FoxA2, preventing β-cell proliferation and function (Hesp *et al.* 2015; Barthel *et al.* 2005; Kitamura & Kitamura, 2007; Kitamura *et al.* 2002). This translocation ensures FoxO and PDX-1 have mutually opposed cellular localisations, which when maintained indefinitely in the case of aberrant FoxO activity can cause disorder. As not only is insulin release reduced preventing glucose uptake into cells, but the identity and function of the β-cells is also diminished leading

to an overall reduced cell number (Gao *et al.* 2014). This, coupled with the increased gluconeogenesis caused by overactive FoxO in the liver, can lead to chronic hyperglycaemia resulting in glucotoxicity and further damage to β-cells via oxidative stress (Gross *et al.* 2008). Despite this, the role of FoxO is not always deleterious, as it can promote the expression of *NeuroD* and *MAFA*, which encode transcription factors that upregulate expression of the insulin gene increasing insulin production (Buteau & Accili, 2007). In addition, FoxO can also increase production of antioxidant enzymes such as MnSOD and catalase, as well as cell cycle-inhibitory and DNA-repair genes (Gross *et al.* 2008; Kitamura & Kitamura, 2007; Huang & Tindall, 2007).

It has been widely recognised that this compensation in insulin secretion and oxidative protection is only possible in the short term, as during chronic hyperglycaemia caused by overactive FoxO, cellular stress (including ER stress) continues to increase to an overwhelming degree, leading to cell death (Fonseca *et al.* 2011). In conjunction to this cell death, due to their opposing localisation, PDX-1 activity is reduced preventing proliferation leading to a diminished overall pancreatic β-cell number severely reducing insulin biosynthesis and glycogenesis in the long term (Kawahito *et al*. 2009). Therefore, this failing mechanism supports the underlying issues and metabolic abnormalities causing diabetes as well as its associated complications, where it has been reported that this activity can cause systemic issues by exacerbating insulin resistance in the periphery, including in the muscle (Gross *et al*. 2008; Hesp *et al*. 2015; Cheng & White, 2011).

This is of importance as the muscle has a principal role in metabolic homeostasis, as skeletal muscle is involved in approximately 80% of glucose uptake in the body (Kousteni, 2012). Here, FoxO activity also underpins the carbohydrate-to-lipid switch during prolonged periods of fasting via upregulation of different effectors, including PDK-4 to prevent glucose metabolism, LPL to hydrolyse triglycerides into free fatty acids, and CD36 to facilitate free fatty acid uptake into the skeletal muscle (Cheng & White, 2011; Lu & Huang, 2011). Furthermore, FoxO also modulates the expression of adiponectin receptors, which when activated initiate energy-producing fatty acid oxidation in the muscle (Sanchez *et al.* 2014). All this ultimately reduces carbohydrate consumption in the majority of tissues ensuring adequate energy sources for obligate glucose utilisers.

Interestingly, FoxO's effect on other secreted factors can also regulate metabolic homeostasis through effects on feeding behaviour. This process is regulated in part by feedback signalling of the orexigenic NPY (*Drosophila* homologue sNPF), which leads to the deacetylation and activation of FoxO via the PKA-CREB pathway and Sirt1, allowing for FoxO to subsequently upregulate numerous genes, including sNPF itself (Hong *et al.* 2012). FoxO also regulates another orexigenic peptide, AgRP, which causes reductions in energy expenditure, increases food intake similar to NPY, and disrupts anorexigenic leptin activity (Ma *et al.* 2015). Therefore, a dysfunctional overactive FoxO in this instance can often lead to overstimulation of appetite, and the onset of obesity and its associated inflammation, causing further homeostatic dysregulation and insulin resistance (Rehman & Akash, 2016).

However, similarly to the copious roles in carbohydrate and lipid metabolism outlined above, these examples of FoxO activity in regulating these metabolic processes also depend on FoxO's ability to bind to DNA.

1.2.3 DNA-BINDING INDEPENDENT FUNCTIONS OF FOXO

As well as the wide variety of roles that FoxO has in a plethora of processes by binding directly to DNA to regulate its own target genes, there are now various examples of FoxO binding to other proteins, allowing it to exert its effects in a variety of different mechanisms including chromosomal translocations, co-factor recruitment or sequestration, and co-factor displacement (*Figure 1.4*) (van der Vos & Coffer, 2008).

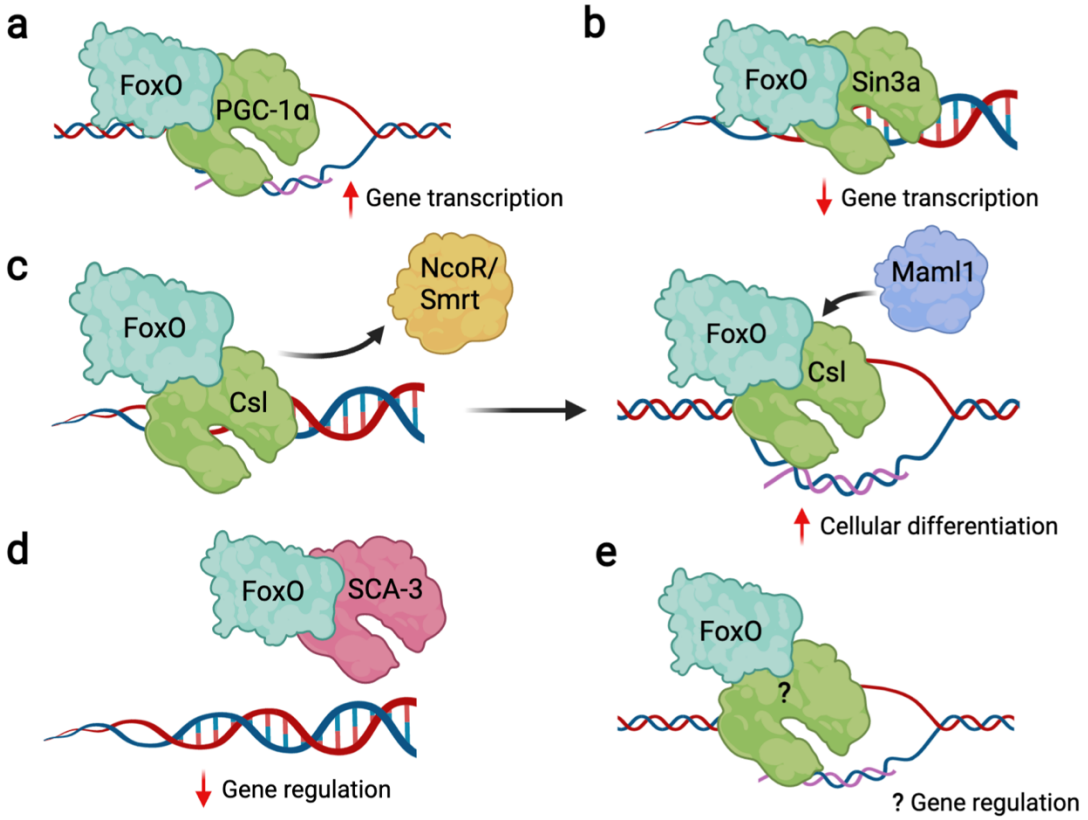

Figure 1.4. **Methods of FoxO-binding interactions to alter gene expression.** Various mechanisms of FoxO binding interactions that influence gene expression are shown. Here, (a) co-activation of gene regulation, (b) co-repression of gene regulation, (c) displacement, sequestration, and recruitment of transcription factor co-factors and other transcription factors by FoxO can enhance or suppress target gene transcription, (d) sequestration of active FoxO proteins by pathogenic (pink) polyQ proteins, and (e) the unknown potential for FoxO to regulate expression of another transcription factor's target genes without binding to DNA in relation to metabolic homeostasis. Proteins given as FoxO binding partners are examples for each consequence of FoxO interaction, the examples are not exhaustive (Adapted from van der Vos & Coffer (2008). Created in Biorender).

With this, there are now clearly several explicit examples of FoxO's ability to bind to other proteins, whether they are intermediary co-factors, receptors, or other transcription factors themselves (*Table 1.2*).

Binding partner	Function/process	Reference
Sin3a	Transcriptional co-repressor of glucokinase	Langlet *et al.* 2017
p53	FoxO co-factor mediating FoxO transcription	Rupp *et al.* 2017
PPAR-α	Antagonises FoxO in apoC-III expression	Qu *et al.* 2007
PPAR-γ	Represses PPAR-γ regulating adipocyte function	Fan *et al.* 2009; Dowell *et al.* 2003
HNF-4	Mediation of metabolic cascades	Hirota *et al.* 2003
Kr-h1	Downregulation of *bmm* gene expression	Kang *et al.* 2017
PGC-1α	Co-activation of gluconeogenic genes	Puigserver *et al.* 2003
β-catenin	Inhibition of β-catenin activity	Hoogeboom *et al.* 2008
PGR-A	Ligand-independent activity	Rudd *et al.* 2007
CBP/p300	FoxO co-factors mediating FoxO transcription	van der Heide & Smidt, 2005

Table 1.2. **FoxO transcription factor binding partners.**
Summary of FoxO's binding partners that allow for FoxO to indirectly influence the regulation of another transcription factor's target genes, however this list is not exhaustive, and some binding interactions still require FoxO's DNA binding ability to elicit the appropriate response.

One compelling development that has been done on this type of action by FoxO comes from a gene expression analysis of cultured human cells expressing a FoxO1 DNA-binding domain mutant (H215R), which identified that these mutants have the ability to regulate a disparate set of genes compared to cells expressing a constitutively active FoxO1 protein (Ramaswamy *et al*. 2002). Subsequent *in vivo* introduction of this DNA-binding domain mutant in mice was able to show that FoxO1 controlled glucose-related metabolism entirely as a transcription factor but alters lipid metabolism via both DNA-binding dependent and independent activity (Cook *et al*. 2015). However, despite these advances in analysing the DNA-binding independent roles exhibited by FoxO in metabolism, in-depth gene expression analysis into these DNA-binding independent roles of FoxO was lacking and research in this area has seemingly stalled as information delving deeper into FoxO's DNA-binding independent functions is scarce.

However, as mentioned above, there are different regions in the FoxO protein that facilitate these protein-protein interactions and influence metabolic homeostasis. For example, mammalian FoxO proteins use the LXXLL motif to mediate interactions with proteins such as CBP/p300 and Sirt1, as well as affect the transcription of the *insulin-like growth factor binding protein 1* (*IGFBP-1*) and *glucose-6-phosphatase c* (*G6pc*) (Nakae *et al.* 2006). Interestingly, a constitutively active FoxO1 DBD mutant (i.e., with a mutation of mammalian H215R; analogous to *Drosophila* H150) was able to both modulate the activity of the nuclear hormone receptors: PGR A and B, and oestrogen receptor-1, independent of DNA-binding, displaying a distinct functional role from a constitutively active FoxO1 non-DBD mutant in a monkey-derived COS-1 cell culture system (Rudd *et al.* 2007). However, despite these DBD-mutants still increasing the nuclear receptor activity, they were less potent in increasing the transcription of certain genes (such as, *IGFBP-1*) than the fully functional protein, potentially due to the lack of binding by FoxO to the IRS elements within the IGFBP-1 promoter (Rudd *et al.* 2007). Therefore, this indicates that the full of effect of these interactions on metabolic gene regulation still requires binding to DNA in some capacity.

FoxO also uses this motif to interact and form a complex with CBP/p300, a process conserved from *C. elegans* to mammals (Wang *et al.* 2009a). FoxO interacts with the kinase-inducible domain interacting domain of CBP/p300 upon FoxO's binding to DNA (Wang *et al.* 2009a). The formation of this FoxO-CBP complex allows for the acetylation of histones, allowing RNA polymerase II and other factors that make up the pre-initiation complex access to the DNA, leading to activation of target gene transcription (Kodani & Nakae, 2020). There is evidence to suggest that potentially this FoxO-CBP/p300 complex synergistically activates genes associated with the IGFBP-1 promoter and insulin signalling, leading to effects in metabolic homeostasis (Waddell *et al.* 2008). However, as before the effects of this interaction still require FoxO's ability to bind to DNA.

The other region of interest in the FoxO protein's TAD is the polyQ region, examples of FoxO using this structure to promote protein-protein interactions include those with the Kruppel-like homologue-1 (Kr-h1) to repress lipolysis during development via *brummer* (*bmm*) (the homologue to mammalian ATGL) lipase gene modulation in *Drosophila*, and those with mutated SCA-3 proteins to repress dFoxO activity through coiled-coil interactions in *Drosophila* class-4 sensory neurons to produce the dendrite

pathologies observed in the neurodegenerative SCA-3 disorder (Kang *et al.* 2017; Kwon *et al.* 2018). Although, both of these interactions have effects on dFoxO activity and not *vice versa*.

There are also other explicit examples of FoxO's ability to bind to other proteins. For example, FoxO can regulate key metabolic processes via protein-protein interactions with the PPARs, which are key players in regulating nutrient-sensing metabolism of carbohydrate and lipids (van der Vos & Coffer, 2008). The direct interaction between FoxO1 and PPAR-γ causes antagonism of PPAR-γ activity, an interaction that could be important for regulating adipogenesis, glucose homeostasis, and insulin sensitivity (Dowell *et al*. 2003). These effects are potentially due to FoxO-PPAR-γ antagonism leading to a downregulation of genes predominantly associated with adipocyte differentiation, effecting adipokine secretion, adipogenesis and glucose transporter type 4 (GLUT4) expression (Kodani & Nakae, 2020; van der Vos & Coffer, 2008). However, as with these other examples, it still seems that some of these affects still require FoxO's ability to bind to DNA (Fan *et al.* 2009). In addition, FoxO has also shown to interact with PPAR-α where PPAR-α antagonises FoxO activity, reducing apolipoprotein C-III production, preventing dysregulated triglyceride metabolism, onset of diabetic dyslipidaemia, and insulin resistance (Qu *et al.* 2007).

Co-immunoprecipitation assays also showed that FoxO can interact with the PPAR-γ coactivator 1-alpha (PGC-1α), with in-depth analysis showing this interaction leads to them being recruited to the same promoter regions within the DNA (Olmos *et al.* 2009). This interaction seems to influence FoxO activity as a co-activator, ultimately leading to the upregulation of oxidative stress related FoxO target genes (such as, MnSOD) (Olmos *et al.* 2009). This co-activation is also associated with upregulation of FoxO target genes involved in gluconeogenesis (Puigserver *et al.* 2003). However, similarly to the PPARs above this interaction effects the activity of FoxO target genes thereby still requiring FoxO to bind to DNA.

A further example comes via the hepatocyte nuclear factor 4 (HNF-4). This factor is essential in regulating PGC-1α-dependent gene expression with regard to gluconeogenesis (Rhee *et al.* 2003). However, its activity can also be affected by FoxO interactions, where direct binding of FoxO to HNF-4 can lead to the repression

of the glycolytic gene *GCK*, and the activation of the gluconeogenic gene *G6pc* (Hirota *et al.* 2003; Hirota *et al.* 2008). This is a seemingly insulin-independent process and requires FoxO binding to the DNA to occur, where DNA-binding allows FoxO to subsequently adjust the HNF-4 binding element within the DNA in a context-dependent manner to produce the desired output (Hirota *et al.* 2008).

Interestingly, FoxO can also regulate *GCK* expression through binding interactions with Sin3a, one of two mammalian Sin3 isoforms that shows high conservation with the *Drosophila Sin3a* gene (Barnes *et al.* 2018). Sin3a is considered a pleiotropic co-repressor and an essential gene within both *Drosophila* and mammalian cells, regulating key processes in development (such as, DNA damage), carbohydrate and lipid metabolism, and responses to oxidative stress (Liu & Pile, 2017; McDonel *et al.* 2012). Mammalian FoxO1 has been shown via reciprocal co-immunoprecipitations to be able to bind to Sin3a through its N-terminus, leading to the recruitment of Sin3a to the GCK promoter and the repression of *GCK* transcription (a process that is reversible by insulin action) (Langlet *et al.* 2017). This repression ensures tight homeostatic control on normal cellular glucose-6-phosphate levels, improved glucose handling, and prevention of the induction of lipogenesis by inhibiting production of pyruvate from glucose by arresting acetyl-coenzyme A formation and triglyceride production (Langlet *et al.* 2017). Again, however, these interactions are still reliant on the ability of the FoxO protein to also bind to DNA.

An interesting example of a FoxO interaction with another protein is that of the interaction with itself. This interaction is not independent of DNA-binding however, but research has now suggested that mammalian FoxO1 may not only act as a monomer when altering gene transcription (i.e., in binding the IRE and DBE), but may also act as a homodimer (Li *et al.* 2021). Research then identified the DIV2 sequence, a palindromic DNA motif formed of two forkhead motifs, that can be bound by a FoxO1 dimer that is stabilised via the FoxO1 wing 1 regions leading to mediation of transcriptional modulation potentially in a stronger manner than which occurs at a singular forkhead site (Li *et al.* 2021). Despite this interesting find, the genes regulated via this mechanism have not yet been touched upon and therefore it is unknown whether different genes are regulated or if it is more of a compensatory mechanism, which takes advantage of the higher binding affinity of FoxO1 to DIV2 sequences allowing for gene regulation even when expression of FoxO is low (Li *et al.* 2021).

In a similar vein to this, FoxO is also able to interact with other members of the Fox family. Interactions with FoxA1 and FoxA2 have been shown to lead to associations with and relaxing of the chromatin, leading to the subsequent upregulation of insulin-regulated genes (e.g., *G6pc*), however binding to DNA is still necessary for this to occur (Yalley *et al.* 2016; Schill *et al.* 2019). This supports previous studies that indicate that FoxO1 and FoxA2 binding (analysed using chromatin immunoprecipitation (ChIP)-sequencing) leads to co-activation of several genes related with glucose and lipid metabolism (namely, *Pck1* and *PDK-4*) in mouse liver (Shin *et al.* 2012).

Importantly, there is at least one example of FoxO affecting gene regulation that occurs seemingly independent of its need to bind to DNA. In the regulation of cellular differentiation FoxO was found to displace the Notch signalling corepressors, nuclear corepressor (NcoR) and silencing mediator for retinoid and thyroid hormone receptor (Smrt) and recruit the coactivator mastermind-like 1 (Maml1) to activate Csl activity leading to changes in gene expression (Kitamura *et al.* 2007). This effect was found in the presence of a constitutively active mouse FoxO1 and a constitutively active FoxO1 DNA-binding domain mutant (N208R and H212R) (Kitamura *et al.* 2007). However, this role seems to only effect FoxO activity in cellular differentiation and myogenesis and does not seem to be linked to FoxO's role in metabolic homeostasis in any great detail.

Together, these examples give evidence that whilst there is precedence in the structure of FoxO proteins and examples that show how FoxO can influence and is influenced by other proteins, many of these interactions still require the binding of FoxO to DNA in some form. Therefore, despite the initial findings using a FoxO DNA-binding domain mutant that showed there is DNA-binding independent modulation of metabolic processes, how FoxO uses this mechanism to carry out its affects is still relatively unknown. This highlights a promising area of research, as it is imperative to understanding FoxO function and consequently for identifying potential therapeutic targets for treating metabolic disorders, like diabetes, so FoxO does not have to be targeted directly reducing the severity or number of side effects produced.

1.3. CONSERVATION OF FOXO FUNCTION BETWEEN ORGANISMS

One of the most important pathways, with regards to metabolism, that is conserved across organisms is the IIS pathway.

Where even though the yeast, *Saccharomyces cerevisiae*, does not have an IIS pathway as we recognise it, there is still a precursor nutrient-sensing pathway that enables proper metabolic control through a signalling cascade involving an Akt homologue (Barbieri *et al.* 2003).

Due to evolving multicellularity, there comes an increased level of conservation where all the components of mammalian insulin signalling are present in *Drosophila,* including FoxO transcription factors (*Figure 1.5*) (Wang *et al*. 2011; Owusu-Ansah & Perrimon, 2014).

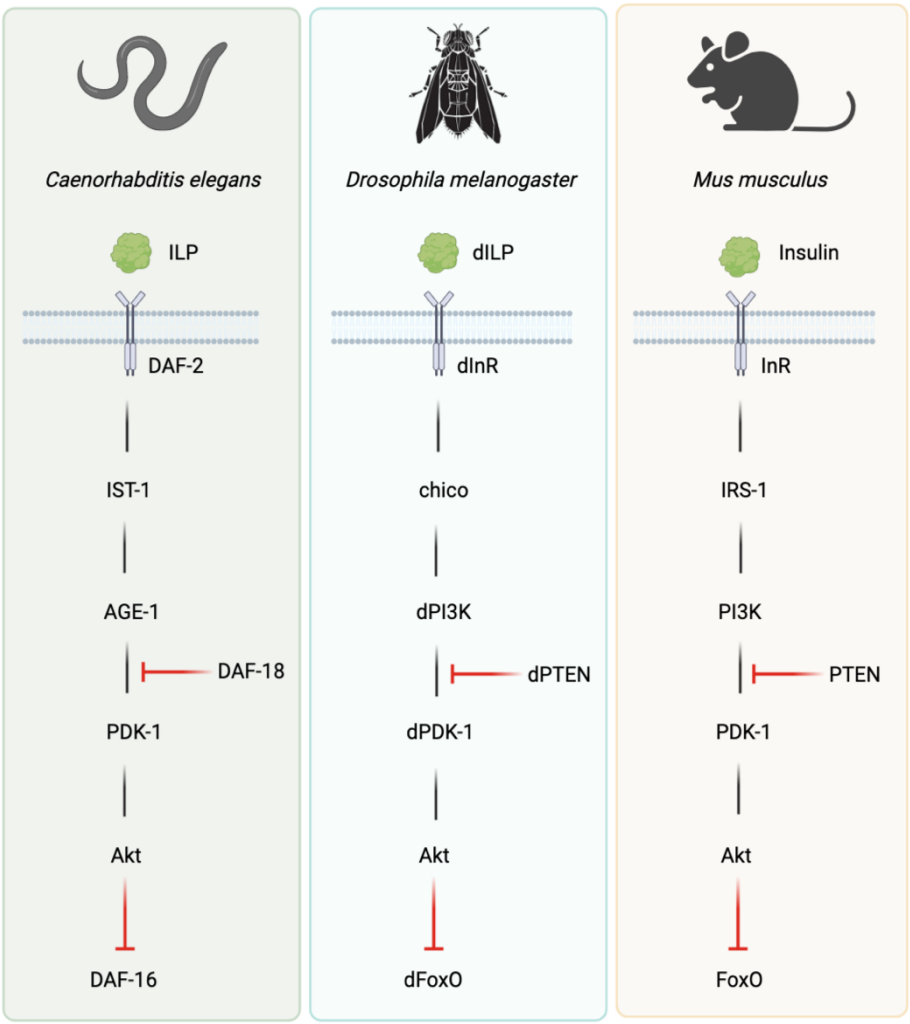

Figure 1.5. **Evolutionary conservation of the insulin/insulin-like growth factor signalling (IIS) pathway.**
Evolutionary conservation of the insulin-insulin like growth factor signalling (IIS) pathway in *Caenorhabditis elegans, Drosophila melanogaster,* and *Mus musculus*. The latter is also the signalling pathway in other mammals (including, humans). These reveal high levels of conservation in a principal metabolic pathway. All 3 possess insulin peptides that bind homologous receptors, initiating activation of the downstream PI3K/Akt signalling pathway, leading to the inhibition of homologous FoxO proteins (Adapted from Martins *et al.* (2016). Created in Biorender).

The conservation between organisms is such that it is evident even when comparing mammals and *C. elegans,* where DAF-16 is able to be partially replaced by mammalian FoxO3a (van der Heide & Smidt, 2005).

This conservation is possible due to the fact that Fox proteins, including FoxO, are essential genes (for example, FoxO1 knockouts are lethal) so there are evolutionary constraints (such as, genomic location or regulatory elements) that potentially prevent too much divergence in these proteins (Link, 2019; Hannenhalli & Kaestner, 2009).

The overlap of function between FoxOs of different species coupled with the conservation of both the DNA-binding domains and the binding sequences of FoxOs, (*Figure 1.6*), suggests that it is likely that the key metabolic functions of mammalian FoxOs are encompassed in the overall function of the single dFoxO (Jünger *et al*. 2003).

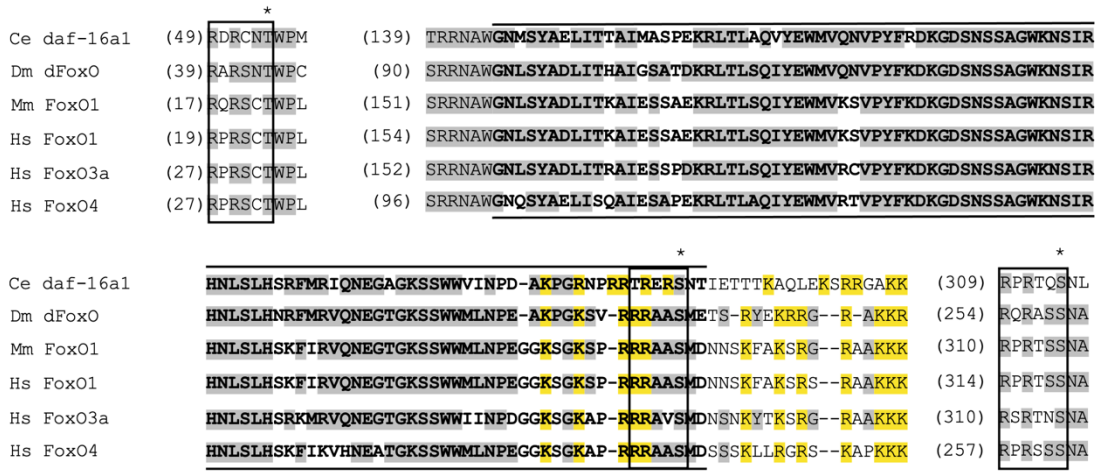

***Figure 1.6*. Amino acid alignment of FoxO proteins from different species.**
Schematic of FoxO amino acid sequence alignments from various species. Boxes enclose Akt phosphorylation motifs, with asterisks above phosphorylated residues. FoxO DNA-binding domains, also known as the 'forkhead' domain, are indicated by lines above and below the sequences. Yellow highlighting represents basic amino acids found in the nuclear localisation domain. Grey shading identifies amino acids in the sequence identical to those found in dFoxO. Ce: *Caenorhabitis elegans*, Dm: *Drosophila melanogaster*, Mm: *Mus musculus,* Hs: *Homo sapiens.* (Adapted from Bridge *et al*. (2010)).

However, it should be stated that of the four mammalian paralogues, FoxO1 is more prominently discussed in the literature with regards to metabolism and is described as the equivalent of dFoxO in these circumstances by many (Ni *et al*. 2007; Lee & Dong, 2017; Puig & Tjian, 2005). Regardless, this gives an advantage of using *Drosophila,* as only possessing one FoxO protein makes researching these complex mechanisms much simpler (Blice-Baum *et al*. 2019).

There are also structural similarities between the components of this pathway including the insulin receptors, the signalling blocks (e.g., IRS proteins), and even the insulin/insulin-like peptides that initiate the cascade (Pertseva & Shpakov, 2002).

Both mammalian and *Drosophila* insulin receptors contain two α and two β subunits, with one of the β subunits containing a cytoplasmic tyrosine kinase domain (Garofalo, 2002). The similarity between the two is so high that the *Drosophila* InR can even bind mammalian insulin with an impressive binding affinity (i.e., this interaction has an equilibrium dissociation constant of 15 nM, where a high binding affinity is often considered to be <100 nM)) (Garofalo, 2002).

As well as the structural and pathway similarities, there is also FoxO target gene conservation between organisms with *Drosophila* also possessing a number of genes homologous to those found in humans, including the major genes and gene families involved in mammalian metabolic processes, such as enzymes that co-ordinate membrane lipid biosynthesis as well as lipid, carbohydrate, amino acid, and sterol metabolism (Owusu-Ansah & Perrimon, 2014; Pandey & Nichols, 2011; Thanh *et al.* 2020; Peregrín-Alvarez *et al.* 2009). Alongside this highly conserved core group of metabolic enzymes, however, there are enzymes associated with this core that are more species-specific allowing for flexibility within pathways dependent on the species needs (Peregrín-Alvarez *et al.* 2009).

Between species, there are 121 genes linking dFoxO and DAF-16 that are bound by both factors in their respective organisms (Alic *et al.* 2011). Between *Drosophila* and mammals, Webb *et al.* (2016) observed using ChIP-seq and ChIP-chip data that

50.9% of genes bound by dFoxO are also bound by mammalian FoxO in mice, with the overlapping genes identified as those specifically involved in processes such as metabolism, growth factor signalling, proteostasis, and modulation of transcription.

Examples of conserved metabolically related genes include *mdy* the *Drosophila* homologue of diglyceride O- acyltransferase (DGAT), which converts diacylglycerol (DAG) into TAG, the lipase *bmm,* and *phosphoenolpyruvate carboxykinase 1* (*Pepck1*), the gluconeogenic FoxO target homologous to human Pck1 (Thanh *et al.* 2020; Grönke *et al.* 2005; Nakae *et al.* 2008). The conservation of these genes is such that when the *bmm* gene was shown by Grönke *et al.* (2005) to be involved with lipid metabolism in flies (i.e., loss of *bmm* led to fly obesity and over activation led to depleted fat stores), it was then posited that this would allow for flies to be used as both mechanical and therapeutic models of human obesity.

Due to this conservation in target genes, unsurprisingly the IIS pathway is also able to regulate some of the same processes such as, metabolism, fecundity, oxidative stress resistance, and lifespan, in all organisms from flies to humans (Barbieri *et al.* 2003). In addition, there is also conservation in responses to changes in nutrients in the environment where it has been shown that the organismal response to starvation is conserved from worms, to flies, to mammals (Hibshman *et al.* 2017). This conserved response was dependent on FoxO proteins and their ability to support the carbon flux of fatty acids to sugars and subsequent glycolysis via gluconeogenesis (Hibshman *et al.* 2017).

This evolutionary conservation in the processes that they regulate allows for important elucidations concerning metabolism and its associated disorders to be made using simpler model organisms, such as *Drosophila* (Owusu-Ansah & Perrimon, 2014). For example, the hallmark characteristics of type II diabetes, such as insulin resistance, fasting hyperglycaemia, and enhanced fat storage, have already been shown to be easily modelled in *Drosophila* by high-sugar feeding (Pendse *et al.* 2013; Thanh *et al.* 2020).

1.3.1 *Drosophila* as a model organism

Past research has overwhelmingly shown the advantages of using model organisms, such as *Drosophila,* to study the aetiology and complexities of numerous disorders. This is in part due to *Drosophila* having a short life cycle, high fecundity, and a high number of easily available, simple, validated tools for genetic modifications allowing for quick and cost-effective study (Wang *et al*. 2011; Pandey & Nichols, 2011).

As mentioned, *Drosophila* have been shown to be excellent models for studying metabolic function due to the high levels of conservation in the metabolic pathways and components between *Drosophila* and mammals and the ease of reproducing metabolic disorder in flies that shows the same (or similar) phenotypes to that in mammals. However, in addition to this, *Drosophila* also possess internal structures that function in a similar manner to mammalian organs, particularly in relation to metabolic functions (Pandey & Nichols, 2011). The main metabolic tissues in *Drosophila* are the fat body, the main storage site of triglycerides and the fly counterpart to both the mammalian liver and white adipose tissue, and the muscle where both oxidative and glycolytic muscles are represented in flies by the flight and leg muscles, respectively (Morris *et al*. 2012; Owusu-Ansah & Perrimon, 2014).

Whilst the fat body represents both the mammalian adipose tissue and liver, *Drosophila* also possess oenocytes, which also carry some hepatocellular-like functions by storing and mobilising lipids through a bidirectional communication with the fat body analogous to the mammalian adipose-liver axis (Gutierrez *et al*. 2007).

Other metabolically important components include the haemolymph, which allows for circulation of various hormones and nutrients, and the various neurosecretory cells such as the insulin-producing cells (IPCs) and corpora cardiaca (CC) (Baker & Thummel, 2007). These cells represent pancreatic β- and α-cells respectively, where IPCs produce *Drosophila* insulin-like peptides (dILPs) analogous to mammalian insulin, and CC cells produce the adipokinetic hormone (Akh), the *Drosophila* counterpart to mammalian glucagon (Owusu-Ansah & Perrimon, 2014). Despite being correlated with mammalian insulin, there are 8 known dILPs that are released in a highly regulated spatial-temporal manner during development and adulthood to assert various functions on the single InR (Nässel *et al.* 2013).

Moreover, the release of these hormones in response to nutrients occurs under similar mechanisms where Kréneisz *et al*. (2010) has shown that, similarly to mammalian pancreatic cells, IPCs respond to increased circulating glucose levels with Ca^{2+} influx and action potentials similar to those seen in mammalian β-cells.

Despite all these similarities, *Drosophila* does not contain a pancreatic organ. The IPCs are located within the neurosecretory centre of the insect brain called the pars intercebralis, a region of the fly brain often associated with the mammalian hypothalamic region as it mediates stress and metabolic responses (Subramanian *et al.* 2013).

Similarities are also seen with regards to inter-organ communication, a key aspect of an organism's ability to regulate metabolic homeostasis (Liu & Jin, 2017). Important secreted factors in regulating metabolism include the anorexigenic peptide leptin, which is known to modulate glucose metabolism, food intake, and overall energy homeostasis (Meek & Morton, 2012). Aberrations in leptin signalling can lead to the onset of oxidative stress, inflammation, obesity, and diabetes through altering insulin sensitivity and lipid accumulation (Meek & Morton, 2012; Marseglia *et al.* 2015). Some studies suggest Unpaired-2 (Upd2) as the *Drosophila* equivalent of mammalian leptin, as overexpression of human leptin in the fly fat body can rescue disorders that develop in Upd2 mutants (Mattila & Hietakanagas, 2017; Subramanian *et al*. 2013).

Despite the numerous advantages of using *Drosophila* as a model organism, there are limitations to consider when studying metabolism. These include the main circulating sugar in *Drosophila* being trehalose instead of glucose and that *Drosophila* models of diabetes have only been used to consolidate phenotypes already observed in mammalian models not to identify new ones (Graham & Pick, 2017; Owusu-Ansah & Perrimon, 2014). However, this has been used to argue that these models are now further validated in their usage for this line of research (Owusu-Ansah & Perrimon, 2014).

1.4 FoxO as a therapeutic target

FoxO proteins are well known for their implications in disorders such as diabetes, cancer formation, and endometriosis (Lu & Huang, 2011). This has led to FoxO becoming an attractive drug target, including through disruptions of FoxO phosphorylation and nuclear export (*Table 1.3*) (Lu & Huang, 2011).

Drug name	Function	Investigated in relation to [disorder]	Reference
Compound 8	Interferes with FoxO-Sin3a binding	Metabolic disorder	Langlet *et al.* 2017
AS1842856	FoxO inhibition	Obesity/metabolic disorder	Zou *et al.* 2014
Tanzawaic acid D	Binds FoxO DBD to stabilise DNA-binding	Metastatic lung cancer	Sun *et al.* 2017
Carbenoxolone	Targets FoxO3 DBD to repress DNA-binding	High stage neuroblastoma	Salcher *et al.* 2019
JY-2	FoxO inhibition	Metabolic disorder	Choi *et al.* 2021
AS1708727	FoxO inhibition	Metabolic disorder	Tanaka *et al.* 2010
ETP-45658	PI3K inhibition	Breast cancer	Hill *et al.* 2014
Torin-2	mTOR inhibitor	Skin cancer	Feehan & Shantz, 2016
AZD5363	Akt inhibitor	Breast cancer	Davies *et al.* 2012
Entacapone	FTO inhibition preventing FoxO1 expression	Obesity/metabolic disorder	Peng *et al.* 2019
STI571	Increases FoxO3 expression	Leukaemia and breast cancer	Essafi *et al.* 2005

***Table 1.3*. Drugs that target FoxO function and activity.**
Numerous therapeutics have been produced to target FoxO or factors involved in its activity in an attempt to treat the underlying causes of disturbed phenotypes caused by dysregulated FoxO activity. The names and roles of various therapeutics are shown here; however, this list is not exclusively metabolically related nor exhaustive.

There are a number of drugs that are used to treat a variety of disorders (including metabolic disorder and cancer), which do not target FoxO but the upstream effectors that target FoxO activity. For example, the PI3K inhibitor ETP-45658 is able to inhibit cell proliferation in a variety of human cancer cell lines in a FoxO-dependent manner (Hill *et al.* 2014). This allows for a small subset of FoxO target genes to be upregulated counteracting the action of the constitutively active PI3K, which is seen in some cancer cell lines, particularly those associated with breast cancer (Hill *et al.* 2014).

Another potential anti-cancer drug is Torin-2, this drug inhibits the mammalian target of rapamycin (mTOR) complex 2 (mTORC2) decreasing FoxO3a phosphorylation (via decreased Akt phosphorylation and activation) and increasing FoxO3a nuclear localisation and apoptosis in ultraviolet B irradiated cells which mimic non-melanoma skin cancer cells (Feehan & Shantz, 2016).

In metabolism, the *fat mass and obesity associated* (*FTO*) gene is associated with metabolic disorder, particularly obesity and diabetes (Freathy *et al.* 2008). FTO proteins are "master regulators" and members of the Fe (II)/α-ketoglutarate–dependent AlkB dioxygenase family, which regulate the demethylation of N6-adenosine–modified and N6,2′-O-dimethyladenosine–modified sites within the mRNA and N1-methyladenosine sites in transfer RNA (Zhang *et al.* 2019a).

This role in metabolic homeostasis identified a potential therapeutic target for diabetic treatments leading to the discovery of a drug called entacapone, which can inhibit FTO function preventing demethylation of FoxO1 mRNA reducing its translational efficiency and subsequent target gene transcription (Peng *et al.* 2019). The effect on this FTO-FoxO1 pathway was able to reduce body mass and circulating fasting glucose in obese mice by altering FoxO's role in adipocytes leading to a downregulation of genes involved with hepatic gluconeogenesis and upregulation of those involved with thermogenesis (e.g., those associated with the oxidative phosphorylation pathway such as complexes I-V of the electron transport chain) (Peng *et al.* 2019).

However, there are drugs that target FoxO directly, one such drug is the FoxO antagonist, AS1842856, that binds to the active form of mammalian FoxO1 (Zou *et al.* 2014). This was used to successfully study the pattern of FoxO activation during adipogenesis and its ability to suppress adipocyte differentiation, identifying this as a potential agent capable of preventing obesity (Zou *et al.* 2014). In addition, by inhibiting FoxO1 using this small molecule, pancreatic-islet differentiation related genes were upregulated, promoting the differentiation of human embryonic stem cells into insulin-producing cells, thereby elucidating a potential mechanism by which mature β-cells can be produced for uses in cell transplantation therapies in diabetic patients (Yu *et al.* 2018).

Another potentially interesting anti-diabetic agent is JY2, which targets FoxO1 (with an oral bioavailability of 98%) to reduce the expression of key genes involved with gluconeogenesis (namely, *G6pc* and *Pepck1*) and TAG accumulation, as well as to increase PDX-1 transcriptional activity and insulin biosynthesis in a rat insulinoma cell line (Choi *et al.* 2021).

Similar to this is the FoxO1 inhibitor, AS1708727, which was shown to have anti-hyperglycaemic and anti-triglyceridaemic effects in db/db mice (an obesity and diabetic mouse model) via changes in expression of FoxO target genes such as *G6pc* and *Pepck1*, as well as *apolipoprotein C-III*, a gene associated with preventing the uptake and clearance of triglycerides from the circulation (Tanaka *et al.* 2010).

An interesting development is the use of inhibitors that only interfere with specific functions of FoxO, allowing for the unaffected continuation of other processes whilst disordered phenotypes can be specifically targeted.

With the example of AS1842856, there is selectivity for the FoxO1 protein compared to either the FoxO3a or FoxO4 proteins indicated by significant increases in the half-maximal inhibitory concentration (IC_{50}) from an IC_{50} of 0.03 μM for FoxO1 to an IC_{50} of >1 μM for FoxO3a/FoxO4 (Peng *et al.* 2020). Therefore, selectively inhibiting FoxO1 over the other FoxO proteins allows for a more specific response.

There is also the ability to disrupt specific protein-protein interactions, such as those involving FoxO and either p53 or Sin3a (Calissi *et al.* 2020). Where in the former the FoxO-p53 interaction is able to be disrupted by the FoxO4-DRI, a FoxO4 peptide in the D-retro inverso conformation (i.e., reversal of the amino acid sequence and inversion of the chiral centre) to initiate p53 nuclear removal and subsequent apoptosis in senescent cells with a higher potency and tolerance compared to other treatments (Baar *et al.* 2017). This cell removal can help to restore tissue homeostasis by removing senescent cells that have a persistent pro-inflammatory phenotype, preventing the onset of the age-related diseases and accelerated ageing often associated with these cells in the long-term (Baar *et al.* 2017).

However, the pleiotropism, paradoxical nature, and the necessity to maintain a strict balance in activity of FoxO proteins, makes them too complex to be ideal targets for therapeautic treatment. As, whether they are targeted directly or through their upstream effectors, altering their activation can often lead to a vast number of unwanted and severe side effects (for example, induction of tumourigenesis through FoxO inhibition) (Hesp *et al*. 2015; Cheng & White, 2011, Lu & Huang, 2011).

With regards to metabolism, there is the issue that therapeutically reducing FoxO activity to combat hyperglycaemia can concurrently increase aberrant lipogenesis, potentially leading to the production of steatosis (Langlet *et al*. 2017). Therefore, to prevent these issues the manipulation would have to occur very specifically or locally, however diabetes is a systemic disorder so treatments using FoxO become complex and unlikely to succeed (Hesp *et al*. 2015).

As mentioned above, moves have been made recently to try to inhibit specific functions of FoxO activity or it's related pathways to try to account for this, such as the use of small-molecule inhibitors that reduce glucose production whilst preventing lipogenesis and the subsequent associated disorder in a FoxO1-dependent manner (Peng *et al.* 2020; Langet *et al.* 2017). However, this research has run into issues when trying to relate this to *in vivo* studies due to the troublesome pharmacokinetic properties of these drugs (Langlet *et al.* 2017).

This shows that as well as the biological consequences of targeting FoxO therapeutically, there are also issues with the physical dynamics involved in the drug-protein interactions. Where trying to interfere with the mechanisms of FoxO action is problematic as interactions involve surfaces that can either be flat or convex, as well as highly charged (i.e., DNA-binding surfaces), all of which are troublesome in drug design (Calissi *et al.* 2020).

These complications therefore highlight an area of study where other targets that are involved in FoxO-dependent signalling can be researched and potentially used for future treatments, particularly those downstream of FoxO activity.

1.5 Aims and objectives

The overall aim of this project was to use *Drosophila* as a model system to determine the mechanisms of FoxO activity in influencing metabolic phenotypes, particularly those that occur in a DNA-binding independent manner. Thereby identifying potential co-factors FoxO interacts with to regulate metabolic homeostasis, which could then be used as potential therapeutic targets for treating metabolic disorders, like diabetes, that do not target FoxO directly, thereby avoiding the severe side effects often seen during FoxO-targeted treatments.

The overall hypothesis was that there were metabolic phenotypes regulated independently of FoxO's ability to bind to DNA, which were affected by changes in gene expression caused by FoxO directly interacting with other proteins.

Therefore, the first aim was to verify the *dFoxO* mutants used in this study, as well as to characterise known dFoxO-regulated phenotypes for DNA-binding dependent or independent activity. The hypothesis was that there were DNA-binding independent roles in dFoxO's activity which impact on metabolic function, and that these novel mutants were fit for investigating this purpose. To do this, novel mutants of *dFoxO* which disrupt the canonical DNA-binding domain were used, allowing for investigation into the effects of inhibiting dFoxO transcriptional activity on metabolic regulation and other dFoxO-regulated processes using various molecular and phenotypic techniques.

Based on the results produced from this initial stage, the second aim was to identify differentially expressed genes in the DNA-binding domain mutants compared to controls to pinpoint changes in gene expression that could be affecting the assessed metabolic phenotypes. The hypothesis was that there was a difference in gene expression in these *dFoxO* mutants, leading to the observed differences in dFoxO activity. To do this, RNA-sequencing (RNA-seq) was used to identify genes which were differentially expressed in these *dFoxO* mutants and therefore, could potentially be affecting the metabolic processes dFoxO regulates in a DNA-binding independent manner.

To achieve the final goal of the stated aim (i.e., to identify FoxO co-factors that help regulate these FoxO-dependent DNA-binding independent metabolic processes) further bioinformatical approaches were used on the RNA-seq data to identify potential FoxO binding partners that could be associated with these changes in gene expression. The hypothesis was that the differential expression in the identified genes would lead to transcription factor enrichment, identifying co-factors with which dFoxO could be interacting with to directly impact on metabolism independent of DNA-binding. Using the previously differentially expressed genes allowed for the identification of co-factors associated with dFoxO's DNA-binding independent activity and the elucidation of the effects of the downstream mechanisms through which these interactions directly impact on metabolism.

Chapter 2

Materials and methods

2. MATERIALS AND METHODS

2.1 *DROSOPHILA* STOCKS AND MAINTENANCE

2.1.1 FOXO MUTANT *DROSOPHILA* LINES USED IN THIS STUDY

The *dFoxO* mutant *Drosophila* lines used in this study were generated by Dr Victor Bustos at the Max Planck Institute for the Biology of Ageing (MPI-AGE), Cologne, Germany. In brief, a parental knock-out line was established using ends-out homologous recombination to replace an ~3 kb region (arbitrarily named V3) of the *dFoxO* locus. This region contained exons 3-8 and encoded amino acids 146-613 of the dFoxO protein. The V3 region was replaced with an attP recombination site and a loxP site (Huang *et al*. 2009). This parental knock-out line was then used to generate control and DNA-binding domain mutant lines by reintroducing specific DNA sequences by ΦC31 integrase-mediated recombination. The following lines were used in this study: dFoxO-ΔV3 ((ΔV3) parental knock-out line, functions as a genetic null for dFoxO), dFoxO-V3 ((V3) reinsertion of the wild-type V3 sequence), dFoxO-V3-3xFLAG ((V3F) reinsertion of the wild-type V3 sequence plus 3x FLAG sequences), dFoxO-DBD1-3xFLAG ((DBD1) reinsertion of DNA-binding domain mutant (H150A) sequence plus 3x FLAG sequences) and dFoxO-DBD2-3xFLAG ((DBD2) reinsertion of DNA-binding domain mutant sequence (H150A and N146A) plus 3x FLAG sequences).

2.1.2 *DROSOPHILA* CONTROL STRAIN

The control *Drosophila* strain used in this study was *white*^{Dahomey} (*w*^{Dah}). *w*^{Dah} was originally created by backcrossing the *white*^{1118} (*w*^{1118}) mutation into the *Dahomey* background. *Dahomey* flies are an outbred wild-type strain, collected originally in Dahomey, West Africa (now known as Benin). Since their collection in 1970, they have been kept in large population cages at 25 °C with overlapping generations on a 12-hour light:12-hour dark cycle (Bass *et al.* 2007). All *dFoxO* alleles were backcrossed for six generations into the *w*^{Dah} background prior to experimental analysis.

2.1.3 FLY HUSBANDRY

All *Drosophila* stocks were maintained at 25 °C on a standard sugar/yeast/agar (SYA) medium consisting of 5% (w/v) granulated sugar (Tate & Lyle, London, UK), 10% (w/v)

brewer's yeast (MP Biomedicals, Eschwege, Germany), 1.5% (w/v) agar (Sigma-Aldrich, now Merck, Darmstadt, Germany), and preservatives 3% (v/v) nipagin (diluted from a 10% (w/v) stock solution of tegosept (Apex Bioresearch Products, California, United States) prepared in 95% ethanol (Fisher Scientific, Loughborough, UK)), and 0.3% (v/v) propionic acid (Fisher Scientific, Loughborough, UK) (Bass *et al*. 2007). Catalogue numbers and manufacturers for all reagents used in this project can be found in Appendx 1. All lines were maintained on a 12-hour light-12-hour dark cycle at constant humidity (Bass *et al*. 2007). All experiments were conducted at 25 °C.

All experimental flies (including controls) were reared from synchronised egg collections. Parental flies were transferred to collection cages and eggs were collected on grape juice-agar plates (produced using agar (Merck, Darmstadt, Germany), sugar (Tate & Lyle, London, UK), red grape juice (Ritchies, Deeside, UK), 10% (w/v) nipagin (as above) in a ratio of 2:2:10:3) with a small amount of yeast paste (produced using distilled water and active dried yeast (S.I. LeSaffre, Marcq, France)). Eggs were collected overnight and were then washed from the surface of the grape juice-agar plate using 1x phosphate buffered saline (PBS) (Fisher Scientific, Loughborough, UK). 20 µL of eggs were dispensed into bottles of fresh SYA food to maintain standard larval densities and incubated at 25 °C for 10 days until the adult flies emerged. Adult flies were transferred to fresh SYA food and allowed to mate for 24 hours, homozygous flies were then separated by sex using a Leica M80 zoom stereomicroscope (Leica Microsystems, Wetzlar, Germany) and CO_2 anaesthesia. Flies were housed as single sexes in experimental vials.

2.2 Genomic DNA preparation and Polymerase Chain Reaction (PCR)

Extraction of genomic DNA and subsequent polymerase chain reaction (PCR) and DNA-sequencing was carried out to verify the identity of the stocks received.

2.2.1 Single fly genomic DNA preps

To extract genomic DNA (gDNA) from female 7-day old adult flies, individual flies were homogenised in 150 µL 'squishing buffer', containing: 10 mM Tris-HCl pH 8.2 (Fisher Bioreagents, Loughborough, UK), 1 mM EDTA (Fisher Bioreagents, Loughborough, UK), 25 mM NaCl (Fisher Bioreagents, Loughborough, UK), and 200 µg/mL

Proteinase K (Fisher Scientific, Loughborough, UK) added fresh from a 20 mg/mL stock solution. The homogenate was transferred to a 0.2 mL PCR tube (Star Labs, Milton Keynes, UK) and incubated at 37 °C for 60 mins and then at 95 °C for 15 mins to allow for inactivation of Proteinase K. All incubations were performed in a 5PrimeG thermal cycler (model: PrimeG/02, Prime Techne, Stone, UK). The gDNA was then stored at -20 °C until used.

2.2.2 Polymerase Chain Reaction (PCR)

PCRs were performed in a final volume of 25 µL containing: 12.5 µL Platinum Hot Start PCR 2X Master Mix (Invitrogen, Loughborough, UK), 0.5 µL of each primer (*Table 2.1*) (Eurofins Genomics, Wolverhampton, UK) at a concentration of 10 µM, and 1 µL of template gDNA. Reactions were made up to the final volume using sterile distilled H_2O (dH_2O) (10.5 µL per reaction). Platinum Hot Start PCR 2X Master Mix (Invitrogen, Loughborough, UK) contains Platinum Taq DNA polymerase in an optimised PCR buffer alongside dNTPs, and Mg^{2+}.

PCRs were performed using a 5PrimeG thermal cycler (model: PrimeG/02, Prime Techne, Stone, UK) with PCR cycling parameters as follows: initial denaturation at 94 °C for 2 mins, then 35 repeating cycles of 94 °C for 30 s, appropriate annealing temperature for 30 s, and 72 °C for 1 min, followed by a final extension step at 72 °C for 10 mins.

PCR products were then analysed using 1% (w/v) agarose (Fisher Scientific, Loughborough, UK) gel electrophoresis with 5 µL Midori Green DNA stain (Geneflow, Lichfield, UK) in 1x Tris-Acetate-EDTA (TAE) buffer diluted in dH_2O from a stock solution (50x stock solution was produced as follows: 2 M Tris-base (Fisher Scientific, Loughborough, UK), 1 M acetic acid (Fisher Scientific, Loughborough, UK), and 50 mM EDTA (Fisher Scientific, Loughborough, UK) in dH_2O). Each sample was mixed with 5 µL Orange-G (Merck, Darmstadt, Germany) DNA-loading dye at a ratio of 5:1 (sample to dye) before being added to the wells alongside a 1 kb DNA hyperladder (Meridian Biosciences, Ohio, United States). Gels were run at 85 V for 45 minutes-1 hour then imaged using a G:Box Chemi HR 1.4 (Syngene, Cambridge, UK) gel imaging system.

Primer name	Sequence (5' – 3')	Melting Temperature (°C)	Identification
SOL792	GCATACATTATACGAAGTTATGG	55.3	dFoxO-null (ΔV3) (*Forward*)
SOL887	GACGAGGTCTGGTGAAGACA	59.4	dFoxO-null (ΔV3) (*Reverse*)
SOL669	TGCACAACCGCTTTATGAGGGT	60.3	WT (*Forward*)
SOL670	CAGTTGATAGTTACCTGTGGAG	58.4	WT (*Reverse*)
SOL725	ATTGCTTACAAATCGTTACATCAG	55.9	dFoxO-V3 reinsertions (*Forward*)
SOL726	GCAAAAACCGAAATATATTGAATG	54.2	dFoxO-V3 reinsertions (*Reverse*)
SOL883	GCAATGCGGCCGCTAGCATTTTGC	66.1	dFoxO-DBD (*Forward*)
SOL885	GTTGATAGTTACCTGTGGAGCGGA	62.7	dFoxO-DBD (*Reverse*)
dFoxO-V3F-F1	CAGCGTGGTGACCTCGCC	62.8	dFoxO-V3-3xFLAG (*Forward*)
dFoxO-V3F-R1	CAACAACGACGACTACCGGC	61.4	dFoxO-V3-3xFLAG (*Reverse*)

Table 2.1. **Primer list used during stock verification.**
These primers were used in PCRs during the verification of *dFoxO* mutant stocks. Annealing temperatures are calculated to be 5 °C below the lowest melting temperature of the primer pair.

2.2.3 QIAquick PCR purification and analysis

PCR products for sequencing were first purified using the QIAquick PCR purification Kit (Qiagen, Hilden, Germany) according to manufacturer's instructions. Buffer PB was added to the PCR sample at a ratio of 5:1 (buffer PB to PCR sample). This was then applied to a QIAquick column inserted in a 2 mL collection tube and centrifuged for 30 s to enable DNA binding to the column. All centrifugation steps were performed at 19,090 g using an Eppendorf 5415R refrigerated microcentrifuge (Eppendorf, Stevenage, UK). The flow-through was discarded and the column was washed with 750 µL of buffer PE. After centrifugation the flow-through was again discarded and the column dried by centrifugation as above for an additional 1 min. 50 µL of buffer EB were applied directly to the centre of the QIAquick column to elute bound DNA, this was then incubated at room temperature for 5 mins before being centrifuged for 1 min. To increase the DNA yield, the flow-through containing the eluted DNA was reapplied to the column and the above step repeated. DNA concentration was measured by UV spectrophotometry using a Nanodrop (Thermo Fisher Scientific,

Loughborough, UK). DNA sequencing was performed by Eurofins Genomics (Wolverhampton, UK) and sequence files were subsequently analysed using SerialCloner 2.6 software (version 2.6.1) (Serial Basics).

2.3 Validating *Drosophila FoxO* mutant function

2.3.1 Western blot analysis

Western blot analysis was carried out to verify the presence, or lack thereof, of the FLAG-tagged dFoxO protein in the appropriate *dFoxO* mutants and wild types. This analysis was also used to assess the appropriate post-translational modification of FLAG-tagged dFoxO proteins in the fully fed and starved state.

Protein extracts were produced by homogenising 5 7-day old adult male or female flies in 100 µL of Laemmli Sodium Dodecyl Sulfate (SDS) sample buffer (Alfa Aesar, Loughborough, UK) containing 0.1 M dithiothreitol (DTT) (Thermo Fisher Scientific, Loughborough, UK). Flies were homogenised in a 1.5 mL tube (Fisher Scientific, Loughborough, UK) using a clean microtube pestle, after which the homogenate was incubated at 85 °C for 10 mins and then centrifuged at 4 °C for 5 mins using an Eppendorf 5415R refrigerated microcentrifuge (Eppendorf, Stevenage, UK).

Protein concentration was measured using the Pierce™ 660 nm Protein Assay Reagent (Thermo Fisher Scientific, Loughborough, UK) containing ionic compatibility detergent reagent (ICDR) (Thermo Fisher Scientific, Loughborough, UK) as per the manufacturer's instructions. Standards of Pierce™ bovine serum albumin protein standard (Thermo Fisher Scientific, Loughborough, UK) from 0-1 µg/µL were also prepared in Laemmli SDS sample buffer (Alfa Aesar, Loughborough, UK) containing 0.1 M DTT (Thermo Fisher Scientific, Loughborough, UK). Protein samples were diluted 1:10 in sterile dH_2O and then 5 µL of the standards or diluted samples were added in duplicate to 150 µL of Pierce™ 660nm Protein Assay Reagent (Thermo Fisher Scientific, Loughborough, UK) containing ICDR (Thermo Fisher Scientific, Loughborough, UK) in a clear flat-bottomed 96-well plate (Corning, Massachusetts, United States). The plate was then incubated for 5 mins at room temperature before absorbances were read using a Multiskan GO (Thermo Fisher Scientific, Loughborough, UK) plate reader at λ660 nm. Protein samples were then frozen in liquid nitrogen and stored at -80 °C.

Proteins were resolved on 8% acrylamide:bis-acrylamide (33.5:0.3) (Fisher Scientific, Loughborough, UK) gels in 1x SDS-PAGE running buffer pH 8.3 (produced as follows: 0.25 M Tris-base (Fisher Scientific, Loughborough, UK), 1.91 M glycine (Fisher Scientific, Loughborough, UK), and 0.03 M SDS (Fisher Scientific, Loughborough, UK)) at 80 V up to the resolving gel, then 120 V to end. 25 µg of protein were loaded into each well alongside 5 µL PageRuler™ Plus Prestained Protein Ladder (Thermo Scientific, Loughborough, UK).

In preparation for blotting, the gels were rinsed in sterile dH_2O before being left in Towbin buffer (produced as follows: 25 mM Tris-base (Fisher Scientific, Loughborough, UK), 192 mM glycine (Fisher Scientific, Loughborough, UK), and 20% (v/v) methanol (Fisher Scientific, Loughborough, UK)) for 15 mins to equilibrate. Amersham™ Protran™ premium 0.45 µM nitrocellulose membrane (Cytiva, Chalfont St Giles, UK) and 2 pieces of heavy-duty blotting paper (BioRad, Watford, UK) were also soaked in Towbin buffer.

Blots were then assembled onto the electrode of a semi-dry transfer cell (TransBlot® Turbo transfer system (BioRad, Watford, UK)) as follows: heavy duty blotting paper, membrane, gel, heavy duty blotting paper. After removal of air bubbles, the cell was then run at a constant 25 V for 30 mins.

Once transferred, membranes were rinsed 2x in tris buffered saline (TBS) (produced as follows: 0.15 M Tris-HCl (Fisher Scientific, Loughborough, UK), 0.05 M Tris-base (Fisher Scientific, Loughborough, UK), and 1.5 M NaCl (Fisher Bioreagents, Loughborough, UK)) containing 0.1% (v/v) Tween-20 (Fisher Bioreagents, Loughborough, UK) pH 7.6 (TBST), before being incubated in blocking solution (5% (w/v) skimmed milk (Merck, Darmstadt, Germany) in TBST (as above)) for at least 1 hour. All washes and incubations are carried out on a rocking platform.

Blots were then incubated overnight at 4 °C in either rabbit anti-tubulin (diluted 1:5000, Cell Signalling Technologies, London, UK), mouse anti-FLAG (diluted 1:2500, Merck, Darmstadt, Germany), or rabbit anti-dFoxO (diluted 1:1000, Giannakou *et al.* 2007; received as a gift from Prof. Dame Linda Partridge) antibodies. Antibodies were diluted in in 5% (w/v) skimmed milk (Merck, Darmstadt, Germany) in TBST (produced as above).

After incubation, blots were rinsed 2x in TBST (as above) and then washed 5x in TBST for 5 mins (25 mins total). Subsequently, blots were incubated in TBST for

1 hour at room temperature with either goat anti-mouse (Abcam, Cambridge, UK) antibodies for FLAG blots, or goat anti-rabbit (Abcam, Cambridge, UK) antibodies for dFoxO and tubulin blots, where both antibodies were diluted 1:10,000 in 5% (w/v) skimmed milk (Merck, Darmstadt, Germany).

A further 2x rinses and 5x 5 min washes in TBST were repeated after incubation with the secondary antibody. The blots were then incubated in Luminata Forte Western HRP substrate (Millipore, Croxley Park, UK) for 5 mins at room temperature. Excess substrate was blotted from the back of the membrane which was then inserted into a plastic wallet. Visualisation of blots was carried out using a G:Box Chemi HR 1.4 (Syngene, Cambridge, UK) imaging system.

2.3.2 Chromatin immunoprecipitation and quantitative PCR

Chromatin immunoprecipitation and subsequent quantitative PCR (qPCR) was carried out to verify the DNA-binding activity, or lack thereof, of the various *dFoxO* mutants. This was to ensure any DBD-independent phenotypes observed in the DBD mutants were not caused by residual DNA-binding activity.

2.3.2.1 Chromatin extraction from adult flies

Chromatin was extracted from 100 fully fed 7-day old adult female flies per replicate for the V3F, DBD1, and DBD2 genotypes. All buffers and sample tubes were kept on ice as much as possible throughout to ensure optimum chromatin extraction. Glass beads (Merck, Darmstadt, Germany) were added to a 2 mL screw cap tube (Fisher Scientific, Loughborough, UK) to the 100 µL graduation marking. Flies were first homogenised at 6 m/s for 40 s using the FastPrep-24 5G homogeniser (MP Biomedicals, Eschwege, Germany) in 400 µL PBS (Fisher Scientific, Loughborough, UK) containing Pierce protease and phosphatase inhibitor (EDTA-free) (Fisher Scientific, Loughborough, UK) made to manufacturer's instructions (100x solution) and used as a 1x working solution. A further 600 µL PBS (Fisher Scientific, Loughborough, UK)-Pierce protease and phosphatase inhibitor (EDTA-free) (Fisher Scientific, Loughborough, UK) solution were added and homogenised again using the same parameters.

After homogenisation, extra PBS (Fisher Scientific, Loughborough, UK)-Pierce protease and phosphatase inhibitor (EDTA-free) (Fisher Scientific, Loughborough,

UK) solution was added dropwise until the level of the liquid reached the 1.5 mL graduation marking on the tube (~500 µL).
47 µL of 16% formaldehyde (Thermo Fisher Scientific, Loughborough, UK) (final concentration 0.5%) were added and mixed thoroughly via nutation for exactly 10 mins at room temperature. To stop cross-linking, 300 µL of 2.5 M glycine (Fisher Scientific, Loughborough, UK) were then added and tubes nutated for another 20 mins at room temperature.

The sample was then transferred to a fresh 2 mL tube (Fisher Scientific, Loughborough, UK) and centrifuged at 13,362 g for 20 mins at 4 ºC. All centrifugation steps were carried out using an Eppendorf 5415R refrigerated microcentrifuge (Eppendorf, Stevenage, UK). The supernatant was discarded along with any floating debris within the fly homogenate and the pellet was washed twice using 2 mL of a FA-SDS-1 mM PMSF (Melford, Ipswich, UK) solution. The base FA-SDS buffer was produced as follows: 50 nM HEPES (Fisher Scientific, Loughborough, UK)-KOH (Melford, Ipswich, UK) pH 7.5, 150 nM NaCl (Fisher Bioreagents, Loughborough, UK), 1 mM EDTA (Fisher Bioreagents, Loughborough, UK), 0.1% (v/v) Na deoxycholate (Fisher Scientific, Loughborough, UK), 0.1% (v/v) SDS (Fisher Bioreagents, Loughborough, UK), and 1% (v/v) Triton-x100 (Merck, Darmstadt, Germany)). PMSF (Melford, Ipswich, UK) was added from a 200 mM stock solution prepared in isopropanol (Fisher Scientific, Loughborough, UK) on the day of the experiment to give a final working concentration of 1 mM.

After washing, the pellet was then resuspended using 600 µL of the FA-SDS-PMSF buffer and a clean glass rod, ensuring the white top layer was resuspended first. When the pellet had been resuspended, 1 mL of the FA-SDS-PMSF solution was added and the tubes nutated for 1 hour at 4 ºC. The samples were then centrifuged at 13,362 g for 20 mins at 4 ºC. The supernatant was discarded, and the pellet was again resuspended using 240 µL of the FA-SDS-PMSF solution with an extra 400 µL subsequently added when the pellet had resuspended.
The chromatin was then fragmented by sonication on ice using a Bandelin Sonopuls HD 2200 (Bandelin, Berlin, Germany) for 2, 3, or 4 mins using a pulse of 15 s on / 45 s off at an amplitude of 50, 75 or 100%. Final parameters used after optimisation were 3 mins of 15 s on / 45 s off at 100% amplitude. Subsequently, at a ratio of 1:4 (FA-SDS-PMSF solution to chromatin) more of the FA-SDS-PMSF solution was

added. Tubes were nutated for 30 mins at 4 ºC and centrifuged at 13,362 g for 20 mins at 4 ºC.

The supernatant containing the chromatin was collected and separated into a 600 µL and a 200 µL aliquot before being frozen in liquid nitrogen and stored at -80 ºC.

2.3.2.2 Chromatin sample preparation and quantitative PCR

For each sample used in chromatin immunoprecipitation (ChIP), 50 µL of Dynabeads (Invitrogen, Loughborough, UK) were added into a 2 mL tube (Fisher Scientific, Loughborough, UK) and washed twice using 2 mL of ice-cold PBS (Fisher Scientific, Loughborough, UK)-0.5% (w/v) BSA (Fisher Scientific, Loughborough, UK) solution. BSA solution was made using sterile dH_2O.

The Dynabeads (Invitrogen, Loughborough, UK) were then resuspended in 350 µL PBS (Fisher Scientific, Loughborough, UK)-0.5% (w/v) BSA (Fisher Scientific, Loughborough, UK). For the antibody IP (i.e., the pulldown of DNA associated with the protein of interest), 1 µL of mouse anti-FLAG primary antibody (Merck, Darmstadt, Germany) or mouse anti-RNA polymerase II antibody (Merck, Darmstadt, Germany) was added to each tube. Mock IPs (i.e., pulldown of DNA associated with no antibody) were also produced in the same manner without the introduction of any antibody. All tubes were left to incubate on a rocking platform overnight at 4 ºC.

The supernatant was removed from the Dynabeads (Invitrogen, Loughborough, UK), and the beads were washed twice as above. The Dynabeads (Invitrogen, Loughborough, UK) were then resuspended in 30 µL PBS (Fisher Scientific, Loughborough, UK)-0.5% (w/v) BSA (Fisher Scientific, Loughborough, UK). Subsequently, 25 µL of 2% (w/v) BSA (Fisher Scientific, Loughborough, UK) produced in PBS (Fisher Scientific, Loughborough, UK) were added. In conjunction, chromatin samples were thawed on ice and centrifuged at 19,090 g for 15 mins at 4 ºC using an Eppendorf 5415R refrigerated microcentrifuge (Eppendorf, Stevenage, UK).

100 µL of chromatin sample were kept aside on ice as the input sample (i.e., all DNA retrieved via sonication used as a positive control). The remaining chromatin was divided in 2 so equal volumes of the chromatin sample were added to the tubes containing the washed beads (i.e., 50% in the mock and 50% in the antibody IP).

All samples containing beads were then incubated at room temperature on a rocking platform for 2 hours, after which the supernatant was discarded. Dynabeads (Invitrogen, Loughborough, UK) were washed using 2x 700 µL of FA-SDS (produced as above) allowing for transfer into a 2 mL tube (Fisher Scientific, Loughborough, UK). These tubes were then rocked at room temperature for 5 mins.

Multiple wash steps were then carried out as follows: 3x washes with 1.4 mL FA-SDS-500 mM NaCl (Fisher Bioreagents, Loughborough, UK) (the FA-SDS was made as above but subsequent addition of NaCl produced a final concentration of 500 mM instead of 150 mM), 1x wash with 1.4 mL wash buffer (10 mM Tris-HCl pH 8 (Fisher Bioreagents, Loughborough, UK), 250 mM LiCl (Melford, Ipswich, UK), 1 mM EDTA (Fisher Bioreagents, Loughborough, UK), 1% (v/v) Nonidet-P40 (Melford, Ipswich, UK), and 0.5% (v/v) Na deoxycholate (Fisher Bioreagents, Loughborough, UK)), and 1x wash with 1.4 mL TE buffer (10 mM Tris-HCl pH 8 (Fisher Bioreagents, Loughborough, UK) and 1 mM EDTA pH 8 (Fisher Bioreagents, Loughborough, UK)). After washing, 125 µL of 1x pronase buffer (diluted from 5x pronase buffer produced with 125 mM Tris-HCl pH 8 (Fisher Bioreagents, Loughborough, UK), 25 mM EDTA pH 8 (Fisher Bioreagents, Loughborough, UK), and 2.5% SDS (Fisher Bioreagents, Loughborough, UK)) were added to the beads and then incubated at 65 ºC for 20 mins. The supernatant was used as the ChIP sample (i.e., the DNA pulled down via protein of interest). 25 µL of 5x pronase buffer were then added to the input sample previously set aside. A further 6.25 µL (12,800 units) 1x pronase E from *Streptomyces griseus* (Merck, Darmstadt, Germany) were added to all samples, which were then incubated at 37 ºC for 1 hour and then 65 ºC overnight.

To each sample, 3.3 µL of 1 mg/mL RNase A (Thermo Fisher Scientific, Loughborough, UK) in PBS (Fisher Scientific, Loughborough, UK) were added and then samples were incubated at 37 ºC for 1 hour.

DNA was then purified using the QIAgen gel extraction kit (Qiagen, Hilden, Germany) as follows: equal volumes of QG buffer and isopropanol (Fisher Bioreagents, Loughborough, UK) were added to each sample. Samples were then applied to a spin column in a collection tube. This was then centrifuged, and the flowthrough discarded. All centrifugation steps were carried out at 15,682 g for 1 min using an Eppendorf 5415R refrigerated microcentrifuge (Eppendorf, Stevenage, UK). The spin column was placed back in the collection tube and an additional 500 µL QG buffer added. This was then centrifuged, and the resulting flowthrough discarded. 750 µL PE buffer

were then added to the spin column and centrifuged, after which the flowthrough was discarded, and the centrifugation step repeated to remove any residual buffer. The spin column was then placed into a fresh 1.5 mL tube (Fisher Scientific, Loughborough, UK). 30 µL EB buffer were added to the centre of the membrane in the column and left to stand for 5 mins at room temperature, before centrifuging. The eluate was reapplied onto the column membrane, incubated for a further 5 mins at room temperature and centrifuged for 1 min.

Chromatin was visualised on 1.5% (w/v) agarose (Fisher Scientific, Loughborough, UK) gel electrophoresis with 5 µL Midori Green DNA stain (Geneflow, Lichfield, UK) in Tris-Acetate-EDTA (TAE) buffer (produced as follows: 2 M Tris-base (Fisher Scientific, Loughborough, UK), 1 M acetic acid (Fisher Scientific, Loughborough, UK), and 50 mM EDTA (Fisher Scientific, Loughborough, UK)). 10 µL of each sample were mixed with 5 µL Orange-G (Merck, Darmstadt, Germany) DNA-loading dye before being added to the wells alongside a 1 kb DNA hyperladder (Meridian Biosciences, Ohio, United States). Gels were run at 85 V for 45 mins-1 hour then imaged using a G:Box Chemi HR 1.4 (Syngene, Cambridge, UK) gel imaging system.

Chromatin was also quantified using a Nanodrop (Thermo Fisher Scientific, Loughborough, UK). Samples were then used for qPCR at a dilution of 1 in 50 and 1 in 5 for the input and ChIP samples respectively. Genes were chosen based on previous research by Alic *et al.* (2011), which identified *GATAd* and *phl* (also known as, *Raf*) as dFoxO-bound dFoxO targets, as well as the peaks associated with these genes. Primers were designed using peak sequence information obtained using Flybase (dos Santos *et al.* 2015), and the National Center for Biotechnology Information (NCBI) primer BLAST tool (Ye *et al.* 2012). Details of the primers used for qPCR can be found below in Section 2.10.3 (*Table 2.3*).

2.4 Assessing metabolic function of adult *Drosophila*

The measurement of metabolic stores in adult *Drosophila* to assess the affects of *dFoxO* mutation on metabolic phenotypes was carried out using protocols adapted from Tennessen *et al*. (2014).

2.4.1 Measurement of triglyceride (TAG) in adult flies

TAG levels were measured in whole 7-day old adult fully fed male and female *Drosophila* or those that had been starved for 0, 2, 4, 6, or 8 days as appropriate. 5

flies per replicate sample were homogenised in 150 µL 0.05% (v/v) Tween-20 (Fisher Bioreagents, Loughborough, UK) in dH_2O in a Thermo Electron FastPrep FP120A cell homogeniser (Thermo Electron Corporation, Loughborough, UK) at level 6.0 for 30 s. Glycerol standards at concentrations ranging from 0-20 µg/µL were prepared by serial dilution of a 2.5 mg/mL stock solution (Merck, Darmstadt, Germany) in 0.05% (v/v) Tween-20 (Fisher Bioreagents, Loughborough, UK) in dH_2O. Standards and samples were incubated at 70 °C for 5 mins and then centrifuged at 2,320 g for 1 min using an Eppendorf 5415R refrigerated microcentrifuge (Eppendorf, Stevenage, UK). Samples were diluted 1:4 in 0.05% (v/v) Tween-20 (Fisher Bioreagents, Loughborough, UK) in dH_2O in fresh 1.5 mL microcentrifuge tubes (Fisher Scientific, Loughborough, UK). 5 µL of each standard or sample were then added to 150 µL of Infinity™ Triglycerides reagent (Thermo Fisher Scientific, Loughborough, UK) (linear range: up to 10 mmol/L) in the wells of a clear flat-bottomed 96-well plate (Corning, Massachusetts, United States). Plates were incubated for 5 mins at 37 °C, then centrifuged at 164 g for 1 min using an Eppendorf 5804R centrifuge (Eppendorf, Stevenage, UK). Absorbance was read using a Multiskan GO (Thermo Fisher Scientific, Loughborough, UK) plate reader at λ574 nm.

Protein concentration was also measured for all samples as found in Section 2.4.5.

2.4.2 Quantification of free fatty acids (FFA) in adult flies

The same fly homogenates prepared for TAG concentration measurements (as described in Section 2.4.1) were also used to quantify free fatty acids using the Free Fatty Acid Assay Kit (Abcam, Cambridge, UK) (sensitivity: > 2 µM) according to the manufacturer's instructions. Standards of concentrations 0-10 nmol/well were produced using palmitic acid. Samples were diluted 1:5 in the free fatty acid assay buffer. Subsequently 50 µL of standards or diluted samples were added to a clear flat-bottomed 96-well plate (Corning, Massachusetts, United States). 2 µL of the ACS reagent were added to each well and mixed thoroughly. The plate was then incubated at 37 °C for 30 mins. After incubation, 50 µL of the Reaction Mixture containing: fatty acid assay buffer, fatty acid probe, enzyme mix, and enhancer in a ratio of 22:1:1:1, were added to each well. The plate was then incubated for a further 30 mins at 37 °C protected from light. Absorbances were then measured using a Multiskan GO (Thermo Fisher Scientific, Loughborough, UK) plate reader at λ570 nm immediately afterward.

2.4.3 Measurement of glycogen and trehalose in adult flies

Glycogen and trehalose concentrations were measured in whole 7-day old adult fully fed male and female *Drosophila* or those that had been starved for 0, 2, 4, or 6 days as appropriate. 5 flies per replicate sample were homogenised in 50 µL 0.2 M Na_2CO_3 in a Thermo Electron FastPrep FP120A cell homogeniser (Thermo Electron Corporation, Loughborough, UK) at level 6.0 for 30 s, before being centrifuged at 93 g for 1 min. All centrifugation steps were carried out using an Eppendorf 5415R refrigerated microcentrifuge (Eppendorf, Stevenage, UK). 2 µL of the homogenate were set aside in 18 µL of 0.2 M Na_2CO_3 for the measurement of protein concentration in the homogenates. Glycogen standards were prepared in 0.2 M Na_2CO_3 at concentrations of 0-2 µg/µL using glycogen from oyster (Merck, Darmstadt, Germany). Trehalose standards were prepared in 0.2 M Na_2CO_3 at concentrations of 0-2 µg/µL using D-(+)-trehalose dihydrate (Merck, Darmstadt, Germany). Standards and samples were incubated at 95 °C for 2 hours and then placed on ice for 2 mins before centrifugation at 93 g for 1 min.

30 µL 1 M acetic acid (Fisher Bioreagents, Loughborough, UK) and 120 µL 0.2 M Na-acetate (pH 5.2) were added to each tube. For glycogen standards and samples, 0.0096 units of amyloglucosidase from *Aspergillus niger* (Merck, Darmstadt, Germany) were added to 50 µL of standard or homogenate and incubated at 57 °C overnight. For trehalose standards and samples, 4.2 units of trehalase (Megazyme, Bray, Ireland) were added to 50 µL of standard or homogenate and incubated at 37 °C overnight. Liberated glucose was then measured by adding 5 µL of each standard or sample to 150 µL of Infinity™ Glucose reagent (Thermo Fisher Scientific, Loughborough, UK) (linear range: 0 – 45 mmol/L) in a clear flat-bottomed 96-well plate (Corning, Massachusetts, United States). Plates were then incubated at room temperature for 15 mins and absorbances read using a Multiskan GO (Thermo Fisher Scientific, Loughborough, UK) plate reader at λ340 nm.

Protein concentration was also measured for all samples as found in Section 2.4.5.

2.4.4 Haemolymph extractions and blood sugar measurements

To collect haemolymph from adult flies, 20 7-day old adult female flies per replicate sample were beheaded and then placed in a 0.6 mL microcentrifuge tube (Fisher Scientific, Loughborough, UK) with a hole pierced in the bottom by a 25-gauge needle (BD, Vaud, Switzerland). Flies were 7-day old fully fed or starved for 48 hours. The

0.6 mL tube (Fisher Scientific, Loughborough, UK) was then placed inside a 1.5 mL microcentrifuge tube (Fisher Scientific, Loughborough, UK) with the inner lid closed. Tubes were centrifuged at 2,320 g for 5 mins to collect the haemolymph using a MiniSpin plus centrifuge (Eppendorf, Stevenage, UK). Haemolymph was immediately frozen in liquid nitrogen to prevent evaporation or coagulation and subsequently stored at -80 °C.

Glucose standards were prepared from D-(+)-glucose anhydrous (Fisher Bioreagents, Loughborough, UK) at concentrations from 0-40 mM. Trehalose standards were prepared from D-(+)-trehalose dihydrate (Merck, Darmstadt, Germany) at concentrations from 0-80 mM. The haemolymph was then thawed on ice before being centrifuged at 19,090 g for 5 mins at 4 °C using an Eppendorf 5415R refrigerated microcentrifuge (Eppendorf, Stevenage, UK). To measure liberated glucose, 1 µL of standards or haemolymph was added to 200 µL Infinity™ Glucose reagent (Thermo Fisher Scientific, Loughborough, UK) (linear range: 0 – 45 mmol/L) in a clear flat-bottomed 96-well plate (Corning, Massachusetts, United States). Plates were incubated at room temperature for 15 mins and absorbances were measured at λ340 nm using a Multiskan GO (Thermo Fisher Scientific, Loughborough, UK) plate reader.

To subsequently measure trehalose concentration in the same haemolymph sample, 4.2 units of trehalase suspension (Megazyme, Bray, Ireland) were added to each well of the trehalose standards and samples. The plate was then sealed and incubated overnight at 37 °C. Absorbance was then measured as before at λ340 nm.

2.4.5 Measurement of protein in adult flies

Protein concentration was measured in fly homogenates (produced above in Sections 2.3.1, 2.4.1, and 2.4.3) using the Pierce™ 660 nm Protein Assay Reagent (Thermo Fisher Scientific, Loughborough, UK). 150 µL Pierce™ Assay Reagent were added to a clear flat-bottomed 96-well plate (Corning, Massachusetts, United States) with 5 µL Pierce™ bovine serum albumin protein standard (Thermo Fisher Scientific, Loughborough, UK) (at concentrations ranging from 0-2 µg/µL) or 5 µL sample (diluted 1:5 in appropriate homogenate buffer). Plates were incubated at room temperature for 5 mins and centrifuged at 164 g for 1 min using an Eppendorf 5804R centrifuge (Eppendorf, Stevenage, UK). Absorbance was read using a Multiskan GO (Thermo Fisher Scientific, Loughborough, UK) plate reader at λ660 nm.

2.4.6 Quantification of lipid species in adult fly extracts by thin layer chromatography (TLC)

Thin layer chromatography (TLC) was carried out according to Reiff *et al.* (2015) and Baumbach *et al.* (2014). 5 7-day old fully fed adult female flies per replicate sample were homogenised in 285 µL of 10:5:4 methanol (Fisher Scientific, Loughborough, UK), chloroform (Fisher Scientific, Loughborough, UK), and sterile dH_2O using Thermo Electron FastPrep FP120A cell homogeniser (Thermo Electron Corporation, Loughborough, UK) at level 6.0 for 30 s. The fly homogenate was then incubated at 37 °C for 1 hour, after which 75 µL chloroform (Fisher Scientific, Loughborough, UK) and 75 µL 1 mol/L KCl (Fisher Bioreagents, Loughborough, UK) were added. Phase separation was achieved via centrifugation at 1,000 g for 2 mins using an Eppendorf 5415R refrigerated microcentrifuge (Eppendorf, Stevenage, UK). The chloroform phase was transferred to a new tube and the solvent was evaporated using nitrogen gas forming a desiccated lipid pellet.

Desiccated lipids were resuspended in 100 µL of 1:1 (v/v) methanol (Fisher Scientific, Loughborough, UK) and chloroform (Fisher Scientific, Loughborough, UK). 20 µL of the lipid suspension were applied to a cut to size polymeric silica gel 60 matrix thin layer chromatography aluminium sheet (Merck, Darmstadt, Germany). Alongside experimental samples, standard lipids were also applied to TLC plates. These include: 4 µg trioleoylglycerol (Merck, Darmstadt, Germany) and 4 µg oleic acid (Merck, Darmstadt, Germany). For the mobile phase, plates were then submerged in ~1 cm 70:30:1 (v/v) hexane (Fisher Scientific, Loughborough, UK), diethyl ether (Fisher Scientific, Loughborough, UK), and acetic acid (Fisher Scientific, Loughborough, UK) before briefly air drying. Plates were then dipped in 8% (w/v) H_3PO_4-containing 10% (w/v) copper (II) sulphate pentahydrate (all reagents: Fisher Bioreagents, Loughborough, UK) before being developed at 180 °C for 5 mins. Plates were imaged using a G:Box Chemi HR 1.4 (Syngene, Cambridge, UK) imaging system and lipid content was analysed using photodensitometry tools in ImageJ software (National Institutes of Health (NIH) and the Laboratory for Optical and Computational Instrumentation (LOCI)) (Schneider *et al.* 2012).

2.5 Stress assays

Various stress assays were carried out to assess responses to types of stress known to be modulated by dFoxO activity to determine the method of dFoxO activity in these phenotypes.

2.5.1 Responses to starvation stress

Adult flies of both sexes were separately maintained on standard SYA medium for 7 days, at which point they were transferred to 1% (w/v) agar (Merck, Darmstadt, Germany). Deaths were scored at regularly timed intervals (every 4 hours for 12 hours with a 12-hour break overnight) until all flies were dead.

2.5.2 Responses to oxidative stress

Adult flies of both sexes were separately maintained on standard SYA medium for 7 days, at which point they were transferred to sucrose-agar media consisting of 60 g/L sucrose (Tate & Lyle, London, UK), 18 g/L agar (Merck, Darmstadt, Germany)) containing 6% (v/v) hydrogen peroxide (H_2O_2) (Fisher Scientific, Loughborough, UK) or standard SYA media containing 20 mM methyl viologen dichloride hydrate (also known as, paraquat) (Merck, Darmstadt, Germany). Deaths were scored at regularly timed intervals (every 4 hours for 12 hours with a 12-hour break overnight) until all flies were dead.

2.5.3 Responses to xenobiotic stress and metabolism

Adult flies of both sexes were separately maintained on standard SYA medium for 7 days, at which point they were transferred to SYA medium containing 0.03% (w/v) dichlorodiphenyltrichloroethane (DDT) (Merck, Darmstadt, Germany). Deaths were scored at regularly timed intervals (every 4 hours for 12 hours with a 12-hour break overnight) until all flies were dead.

2.6 Assessing *Drosophila* growth

Two phenotypes associated with *Drosophila* growth and dFoxO activity were assesed to determine the method used by dFoxO to modulate these phenotypes.

2.6.1 Measurement of adult body mass

Adult flies of both sexes were separately maintained on standard SYA medium for 10 days, at which point they were then flash-frozen in liquid nitrogen and stored at -80 °C. Individual flies were weighed using an analytic balance MH-124 (FB73651, Fisher Scientific, Loughborough, UK) to measure body mass. After weighing, individual flies were placed in numbered 1.5 mL tubes (Fisher Scientific, Loughborough, UK) for wing dissection (see Section 2.6.2).

2.6.2 Measurement of adult wing area

To measure wing area, fly wings of the 10 flies per genotype used to measure body mass (see Section 2.6.1) were dissected and placed on a microscope slide with 50% (v/v) glycerol (Merck, Darmstadt, Germany) in ethanol (Fisher Scientific, Loughborough, UK). The same wing was taken from each fly. Wings were then imaged using an MZ10F stereo microscope (Leica Microsystems, Wetzlar, Germany) and area between standardised points measured using ImageJ software tools (Schneider *et al.* 2012).

2.7 Measurement of adult feeding behaviour

Two phenotypes associated with *Drosophila* feeding behaviour and dFoxO activity were assesed to determine the method used by dFoxO to modulate these phenotypes.

2.7.1 Capillary Feeder (CAFE) assay

To measure the volume of fly food media consumed in real time over a period of days, individual adult 7-day old flies of both sexes were transferred to a 7 mL Sterilin™ bijou (Sterilin, Newport, Wales) containing approximately 1 mL of 1% (w/v) agar (Merck, Darmstadt, Germany). The top of each bijou was sealed with Parafilm® (Merck, Darmstadt, Germany). The Parafilm® was then pierced to create air holes and allow for the insertion of a p200 pipette tip with the tip cut down to allow for the insertion of a capillary. Ringcaps® graduated capillaries (Hirschmann Laborgerate, Eberstadt, Germany) were filled with liquid fly food media (produced as follows: 5% (w/v) sucrose (Tate & Lyle, London, UK), 2% (w/v) autolysed yeast (MP Biomedicals, Eschwege, Germany), and Brilliant Blue dye (Fiorio Colori, Milan, Italy) at a ratio of 1:2000 (dye to media)). A drop of mineral oil was added to the top of the capillary to prevent

evaporation. The level of food within the capillary was marked and the capillary inserted into the pipette tips in the bijoux.

Every 24 hours for 96 hours, a ruler was used to measure the distance between the mark placed previously and where the media was now situated. Capillaries were changed between each time point. Measurements were converted to µL from mm (each measurement was divided by the distance between 2 markings (15 mm), representing 1 µL on the graduated capillary).

2.7.2 Proboscis extension (PE) and blue absorbance assay

For proboscis extension assays, 7-day old adult flies of both sexes were tipped into vials containing standard SYA media with 25 g/L Brilliant Blue (Fiorio Colori, Milan, Italy) at a density of 5 flies per vial. To reduce observer influence, vials were randomised and numbered blind. Vials were lined up and left for 5 minutes for flies to settle, the number of feeding events were noted by observing the number of flies extending their proboscis into the food over the course of 1.5- or 3-min intervals over a total of 30- or 60- mins for males and females respectively.

After monitoring proboscis extension, flies were immediately frozen in liquid nitrogen and then homogenised in 250 µL of dH_2O using glass beads (Merck, Darmstadt, Germany) and a FastPrep FP120A cell homogeniser (Thermo Electron Corporation, Loughborough, UK) at level 4.0 for 30 s. Samples were then centrifuged at 19,090 g for 5 mins using an Eppendorf 5415R refrigerated microcentrifuge (Eppendorf, Stevenage, UK). 50 µL of the homogenate were transferred to a clear flat-bottomed 96-well plate (Corning, Massachusetts, United States) and absorbance was read using a Multiskan GO (Thermo Fisher Scientific, Loughborough, UK) plate reader at λ629 nm.

2.8 Measurement of lifespan

Assessment of lifespan was carried out to determine the method used by dFoxO to modulate a phenotype known to be regulated by dFoxO activity.

For lifespan assays, newly eclosed male and female flies were sorted by sex into vials after 24 hours at a density of 15 flies per vial and 10 vials per genotype. Flies were transferred, without CO_2 anaesthesia, onto fresh SYA media 3 times per week. During transfer any deaths or censors were recorded, flies are censored when the death is considered unnatural (e.g., stuck to food or squashing) or flies have escaped.

2.9 Measurement of fecundity

Assessment of *Drosophila* fecundity was carried out to determine the method used by dFoxO to modulate a phenotype known to be regulated by dFoxO activity.

For measurements of female fecundity, fully fed 7-day old adult flies used in the measurement of lifespan were transferred to fresh SYA vials. After 24 hours, the flies were removed and the number of eggs laid on the surface of the food over the 24-hour period were counted.

2.10 Transcriptomics

2.10.1 RNA extraction

RNA was isolated from 7-day old whole adult flies of both sexes of the ΔV3, V3F, DBD2, and w^{Dah} genotypes in both the fed (i.e., frozen straight from SYA medium) and the starved (i.e., frozen after 72 hours on starvation medium) state. At 72 hours starvation, 100% of female flies of all genotypes were still alive and 100% of male flies of all genotypes were still alive, excepting the ΔV3 male flies of which only 95% were still alive. However, this is the starting time point at which ΔV3 females begin to die.

15 female or 30 male flies were added to a 2 mL screw cap tube containing glass beads and 0.5 mL TRIzol™ (Fisher Scientific, Loughborough, UK) on ice. Flies were then homogenised using a Thermo Electron FastPrep FP120A cell homogeniser (Thermo Electron Corporation, Loughborough, UK) at speed 4.0 for 30 s.

Samples were then incubated at room temperature for 5 mins, before 100 µL of chloroform (Fisher Scientific, Loughborough, UK) were added. Tubes were vortexed for 15 s and incubated at room temperature for 2 mins. After incubation, tubes were centrifuged at 19,090 g for 5 mins at 4 °C. All centrifugation steps were carried out using an Eppendorf 5415R refrigerated microcentrifuge (Eppendorf, Stevenage, UK). Subsequently, 250 µL of the upper colourless phase containing the RNA were transferred into a new 1.5 mL tube (Fisher Scientific, Loughborough, UK) and 250 µL of 100% ethanol (Fisher Scientific, Loughborough, UK) were added. After mixing, all of the sample (500 µL) was placed into a RNeasy spin column (RNeasy Kit, Qiagen, Hilden, Germany) within a 2 mL collection tube. All centrifugation steps were carried out at 9,279 g at room temperature. Columns were centrifuged for 30 s, after which

the flow through was discarded. 350 µL of Buffer RW1 were then added to the column and centrifuged for 15 s after which flow through was again discarded.

For on-column DNase-I digestions of gDNA, 10 µL of DNase-I stock solution (Qiagen, Hilden, Germany) were added to 70 µL of Buffer RDD (Qiagen, Hilden, Germany) and gently mixed by inverting the tube. 80 µL of this solution were then added directly to the centre of the membrane of each spin column. This was then incubated at room temperature for 15 mins.

350 µL of Buffer RW1 were again added to the spin column, centrifuged for 15 s, and the flow through discarded. 500 µL of Buffer RPE were added to the column, centrifuged for 30 s, and the flow through discarded. This step was repeated with a 2 min centrifugation. The column was centrifuged for an additional 1 min to dry. The column was then transferred to a new 1.5 mL Axygen™ MaxyClear Snaplock microtube (Corning, Massachusetts, United States) and 30 µL of RNase-free water (RNeasy Kit, Qiagen, Hilden Germany) were added directly to the column membrane to elute the RNA.

Columns were incubated at room temperature for 5 mins, before centrifugation for 1 min. The eluate was reapplied onto the column membrane, incubated for a further 5 mins at room temperature and centrifuged for 1 min.

RNA concentration and purity was assessed by UV absorbance using a Nanodrop (Thermo Fisher Scientific, Loughborough, UK).

2.10.2 RNA-SEQUENCING AND ANALYSIS

RNA-sequencing analysis was carried out to identify changes in gene expression in the different *dFoxO* mutants, in an attempt to elucidate the changes at the gene level that could be affecting the assayed phenotypes.

Total RNA was prepared as described above. Library preparations and paired-end (75 bp) RNA sequencing were performed by Novogene Co. Ltd UK (Cambridge, UK) using 4 biological replicates per genotype (V3F, ΔV3, DBD2) and condition (fed or starved).

Raw data files were uploaded to Galaxy Europe (usegalaxy.eu) (Afgan *et al.* 2018) and analysed using the online software. Paired-end reads were first assessed for quality using the FastQC (Andrews, 2010) and MultiQC (Ewels *et al.* 2016) tools. The quality of sequences was ensured by using the Cutadapt tool (Martin, 2011) to filter and trim the poorer quality ends from the sequences to allow for more accurate downstream analysis and prevent bias. Cutadapt parameters filtered sequences less

than 20bp and/or with a lower quality Phred score of 20 (i.e., when the precision of the base call is less than 99% accurate). These analyses were carried on forward and reverse reads simultaneously, to ensure pairs were removed and not just single reads.

Subsequently reads were aligned to the Berkeley *Drosophila* Genome Project assembly release 6, dm6 (dos Santos *et al.* 2015) using RNA STAR (Dobin *et al.* 2012). The length of the genomic sequence around annotated junctions was 149bp (the length of the reads minus 1). Quality of the mapping was then examined using MutliQC (Ewels *et al.* 2016) as above, and the Integrated Genome Viewer (IGV) (Robinson *et al.* 2011).

Further quality determination was carried out using MarkDuplicates from the Picard suite (Broad Institute, n.d.) to analyse duplication levels, Samtools idxstats from the SAMtools suite (Li *et al.* 2009) to review the number of reads mapped to each chromosome, Gene Body Coverage from the RSeQC tool suite (Wang *et al.* 2012b) to ensure even coverage and no 5' or 3' end bias, and Read Distribution also from the RSeQC tool suite (Wang *et al.* 2012b) to identify the position of the reads on gene features to ensure no DNA contamination.

Strandedness of the library was determined using the Infer Experiment tool from the RSeQC tool suite (Wang *et al.* 2012b). Subsequently, the number of reads per gene were counted using featureCounts (Liao *et al.* 2014) and the mapped.bam file outputs from RNA STAR. Parameters set for featurecounts ensured that reads did not contribute to multiple features and that the minimum mapping quality score per read (i.e., the probability that a read is misplaced) was 10 (i.e., when the precision of the read placement is less than 90% accurate).

Differential expression was then analysed using a generalised linear model in the DESeq2 tool (Love *et al.* 2014), allowing for normalisation in library composition. Fold-changes in expression were calculated by the internal DESeq2 functions.

Differentially expressed genes were extracted and annotated with the parameters p-adjusted value < 0.05. There were no extra normalisation steps taken as DESeq2 provides its own internal normalisation (median of ratios), which is ideal for differential expression analysis. Transcript size bias correction was not necessary as counts were compared between samples for the same genes.

Differentially expressed genes were visualised using the Volcano Plot (Intergalactic Utilities Commission, n.d.a) and the heatmap2 (Intergalactic Utilities Commission, n.d.b) tools. The overlap between the differentially expressed gene lists of different conditions were visualised using proportional Venn diagrams using BioVenn (Hulsen *et al.* 2008) and analysed using hypergeometric analysis in Excel (version 16.61) (Microsoft Corporation, Washington, United States) based on a modified Fisher Exact p-value test called the Expression Analysis Systematic Explorer (EASE) from Database for Annotation, Visualization and Integrated Discovery (DAVID) bioinformatics resources. Heatmaps were produced in Excel (version 16.61) (Microsoft Corporation, Washington, United States).

Gene ontology (GO) analysis and Kyoto Encyclopedia of Genes and Genomes (KEGG) pathway analysis were carried out using the goseq tool (version 1.44.0) (Young *et al.* 2010). Supplementary GO analysis was also carried out using ShinyGO (version 0.66) (Ge *et al.* 2020).

Transcription factor enrichment analysis on the differentially expressed gene lists was carried out using i-cisTarget (Herrmann *et al.* 2012; Imrichová *et al.* 2015), a web-based genomics tools to predict regulatory and cis-regulatory features and modules.

To find supporting evidence to the assertion that Hp1b and Sin3a are potential FoxO binding partners, this process was repeated for previously published data for *Hp1b* mutant 3rd instar larvae produced via imprecise excision (Mills *et al.* 2018), and *Sin3a* knockdown *Drosophila* S2 cells produced via interference RNA (RNAi) (Gajan *et al.* 2016). NCBI accession numbers are found in *Table 2.2.*

2.10.3 Chromatin immunoprecipitation-sequencing and analysis

As well as analysing previously published RNA-seq datasets, chromatin immunoprecipitation-sequencing analysis was carried out to find supporting evidence to the assertion that Hp1b and Sin3a are potential FoxO binding partners and could possibly co-regulate metabolic phenotypes.

Data from previously published datasets (Hp1b: Schoelz *et al.* (2021), Sin3a: Das *et al.* (2012)) was imported into Galaxy Europe (usegalaxy.eu) (Afgan *et al.* 2018) and analysed using the online software. Quality control was carried out as above for the RNA-sequencing data. Subsequently reads were mapped to the dm6 reference genome used above using the Map with BWA tool (Li & Durbin, 2010) and post-processed using the Filter SAM or BAM files (Li *et al.* 2009) removing any non-

uniquely mapped reads. ChIP quality was then assessed, firstly by checking sample correlation using the multiBamSummary and plotCorrelation tools (Ramírez *et al.* 2016), and then subsequently by assessing signal strength using signal extraction scaling (SES) and the plotFingerprint tool (Ramírez *et al.* 2016).

To call ChIP peaks genome-wide, the MACS2 predictd tool (Zhang *et al.* 2008; Feng *et al.* 2012) was first used to find optimal parameters for running the subsequent MACS2 callpeak tool (Zhang *et al.* 2008; Feng *et al.* 2012). Sequence motifs present within these called peaks were identified by first converting underlying sequences using the MEME-ChIP tool (Machanick & Bailey, 2011). Conserved motifs in the ChIP peaks were also identified with the MACS2 output BED file using i-cisTarget (Herrmann *et al.* 2012; Imrichová *et al.* 2015) as above. The list of genes associated with Hp1b or Sin3a binding was produced using ChIPseeker (Yu *et al.* 2015). Accession numbers and reference material are shown (*Table 2.2*).

Factor name	Accession number	Sequencing	*Drosophila* stage or cell type	Source
Hp1b	GSE120841	RNA	3rd instar larvae	Mills *et al.* 2018
Hp1b	GSE47243	ChIP	3rd instar larvae	Schoelz *et al.* 2021
Sin3a	GSE68775	RNA	Embryo	Gajan *et al.* 2016
Sin3a	GSE23122	ChIP	S2 cells	Das *et al.* 2012

***Table 2.2*. Accession numbers for the raw sequence files for previously published RNA-sequencing and chromatin immunoprecipitation-sequencing data.**

Accession numbers for the raw sequence files for both previously published Hp1b and Sin3a RNA-sequencing and chromatin immunoprecipitation (ChIP)-sequencing data are shown.

2.10.4 Quantitative reverse transcription PCR (qRT-PCR)

Quantitative reverse transcription PCR (qRT-PCR) was carried out to verify the results found in the RNA-sequencing analysis. This was to ensure any statements made based on the RNA-sequencing were accurate.

2.10.4.1 Complementary DNA synthesis

Complementary DNA (cDNA) for quantitative reverse transcription PCR (qRT-PCR) was synthesised in a RNase-free environment as follows: 2 µg of total RNA taken

from the same extracts used for RNA-seq (prepared as described above in Section 2.10.1) were mixed with 1 µL of oligo(dT) at concentration of 0.5 µg/µL (Invitrogen, Loughborough, UK), and 1 µL of 10 mM dNTP mix (Invitrogen, Loughborough, UK), dH_2O was also added to make a total reaction volume of 12 µL.
Samples were incubated at 65 °C for 5 mins and then immediately placed on ice for 5 mins. All incubation steps were carried out using a 5PrimeG Thermal Cycler (model: PrimeG/02, Prime Techne, Stone, UK). Subsequently, 4 µL of 5x first-strand buffer (Invitrogen, Loughborough, UK), 2 µL 0.1 M DTT (Invitrogen, Loughborough, UK), and 1 µL RNase-OUT RNase inhibitor (Invitrogen, Loughborough, UK) were added. Samples were then mixed and centrifuged briefly. Samples were incubated at 42 °C for 1 min, before 1 µL of Superscript-II RT enzyme (Invitrogen, Loughborough, UK) was added whilst keeping the tubes at 42 °C as much as possible. A further 50-minute incubation at 42 °C was carried out. The reaction was then inactivated by incubating at 70 °C for 15 mins. Samples were subsequently stored at -20 °C.

2.10.4.2 qRT-PCR

qRT-PCR was carried out using the LightCycler® 480 instrument II (Roche Life Science, Penzberg, Germany) with bright-white real-time PCR 96-well plates (Primer Design, Eastleigh, UK) sealed using StarSeal Advanced Polyolefin film (Star Lab, Milton Keynes, UK).

Each 20 µL reaction contained: 10 µL 2x PrecisionPLUS qPCR Master Mix with SYBRgreen (containing 2x reaction buffer, 0.025 U/µL Taq Polymerase, 5 mM $MgCl_2$, 100 µM dNTP mix (containing 200 µM of each dNTP)) (Primer Design, Eastleigh, UK), 1 µL of each forward and reverse primer (diluted from a 6 µM stock to give a final concentration of 300 nM) (Eurofins Genomics, Wolverhampton, UK), 6 µL of sterile dH_2O, and 2 µL of template. For RNA-seq verification cDNA (diluted 1:10 in sterile dH_2O) produced using the same extracts used for RNA-seq was added. For ChIP-qPCR either input DNA (diluted 1:50 in sterile dH_2O) or IP DNA (dilute 1:5 in sterile dH_2O) was added. All reactions were performed in duplicate. A negative control was also run for each primer set, where sterile dH_2O was used instead of the template.

For RNA-seq verification, relative quantities of transcripts were determined using a relative standard curve made from a pool of cDNA generated from RNA isolated from w^{Dah} flies. Standards were also used to check for non-specific amplification and the

presence of primer-dimers. Relative expression of genes of interest were calculated relative to the expression of the reference gene, *endoplasmic reticulum membrane protein complex subunit 10* (*EMC10).* This gene was identified via analysis of reference gene stability using Normfinder in R (Andersen *et al.* 2004).

Reference gene primer sequences (*Table 2.3*), RNA-seq gene verification primer sequences (*Table 2.4*), and ChIP-qPCR primer sequences (*Table 2.5*) are shown.

Primer name	Sequence (5' – 3')	Identification for [gene]	Source
EMC10-F	AATGTGACGATTCCCAGTCTCA	*EMC10*	DRSC/TRiP Functional Genomics Resources
EMC10-R	CAGTTTCTTCAGCAAGTCCAGAT	*EMC10*	DRSC/TRiP Functional Genomics Resources
Cog-6-F	CTCGACGCAGGAAAAACCG	*Cog6*	DRSC/TRiP Functional Genomics Resources
Cog-6-R	TCCAATGTGTCCTTGTCCGAC	*Cog6*	DRSC/TRiP Functional Genomics Resources
gzl-F	GGTTTACCGGAAAGCAACCAG	*gzl*	DRSC/TRiP Functional Genomics Resources
gzl-R	GGCAGATTGGGACCGAATTGA	*gzl*	DRSC/TRiP Functional Genomics Resources

***Table 2.3*. Primers used for reference gene identification in quantitative reverse transcriptase PCR (qRT-PCR).**
Primer sets for candidate housekeeping genes for validation of previous RNA-sequencing (RNA-seq) analysis results are shown. Non-significant ($p > 0.05$) genes were chosen from the RNA-seq analysis with primers identified via the *Drosophila* RNAi Screening Center (DRSC) FlyPrimerbank (Hu *et al.* 2013).

Primer name	Sequence (5' – 3')	Identification for [gene]	Source
FoxO-Fwd1	TCTCGCCGAACTCAGTAAC	*FoxO*	Molaei *et al.* 2019
FoxO-Rev1	CCTCCAGGCATTGTCCTATC	*FoxO*	Molaei *et al.* 2019
tps1-Fwd1	CGTGTGACATCGTCGGATATT	*tps1*	Miyamoto & Amrein, 2019
tps1-Rev1	AGTGTCGTTCCACCCATTTC	*tps1*	Miyamoto & Amrein, 2019
Rel-Fwd1	CATCAGGAGACAGAGCGTGA	*Relish*	Molaei *et al.* 2019
Rel-Rev1	CCGACTTGCGGTTATTGATT	*Relish*	Molaei *et al.* 2019
bigmax-PP25294F	CTCGGCGCACAATTCAGAC	*bigmax*	DRSC/TRiP Functional Genomics Resources
bigmax-PP25294R	CGCTCCTTGTAACTCAGCGT	*bigmax*	DRSC/TRiP Functional Genomics Resources
bmm-PP22244F	GTCTCCTCTGCGATTTGCCAT	*bmm*	DRSC/TRiP Functional Genomics Resources
bmm-PP22244R	CTGAAGGGACCCAGGGAGTA	*bmm*	DRSC/TRiP Functional Genomics Resources
dILP3-F	AGAGAACTTTGGACCCCGTGA	*dILP3*	Hur *et al.* 2013
dILP3-R	TGAACCGAACTATCACTCAACAGTCT	*dILP3*	Hur *et al.* 2013
FoxO-PP34853-F	CATGGGGAAATCTATCCTATGCG	*FoxO*	DRSC/TRiP Functional Genomics Resources
FoxO-PP34853-R	ACTCAGTGTCAATCGTTTGTCG	*FoxO*	DRSC/TRiP Functional Genomics Resources

***Table 2.4*. Primers used in the verification of RNA-sequencing (RNA-seq) results using quantitative reverse transcriptase PCR (qRT-PCR).**
Primers were used in verification of RNA-sequencing (RNA-seq) analysis results. Genes were chosen based on their log fold change (logFC), their roles in metabolism, and their previous associations with dFoxO in the literature. Primers were produced either from previous studies as indicated or via the *Drosophila* RNAi Screening Center (DRSC) FlyPrimerbank (Hu *et al.* 2013).

Primer name	Sequence (5' – 3')	Identification for [gene]	Source
GATAd-F1	AGGAACTGCATATGTGGGTGT	*GATAd*	NCBI primer BLAST
GATAd-R1	ACAAAACATCGGAGAGCCCG	*GATAd*	NCBI primer BLAST
phl-F3	GATTCCCCGACTGGAATGTG	*phl* (aka *Raf*)	NCBI primer BLAST
phl-R3	CCCAGTTGGTCAAGTCTTCC	*phl* (aka *Raf*)	NCBI primer BLAST

***Table 2.5*. Primers used in chromatin immunoprecipitation (ChIP)- quantitative PCR (qPCR).**
Primers were used in chromatin immunoprecipitation (ChIP)-quantitative PCR (qPCR) to verify loss of DNA-binding in the *dFoxO* DNA-binding domain (DBD) mutants compared to the V3-3xFLAG control. Genes were chosen based on previous research (Alic *et al.* 2011), which identified *GATAd* and *phl* (also known as, *Raf*) as dFoxO-bound dFoxO targets, as well as the peaks associated with these genes. Primers were designed using peak sequence information obtained using Flybase (dos Santos *et al.* 2015) and the National Center for Biotechnology Information (NCBI) primer BLAST tool (Ye *et al.* 2012).

2.11 Statistical analysis

Statistical analysis was carried out on the results obtained using R (version 1.4.1103) (RStudio, Massachusetts, United States), JMP 14 (JMP Statistical Discovery LLC, Washington, United States), GraphPad (version 9.3.0) (GraphPad Software, California, United States), and Excel (version 16.61) (Microsoft Corporation, Washington, United States). Tests for normalcy (Q-Q plots and Shapiro-Wilk), variance (F-test for equality of variances), and outliers (Grubbs) were performed on various datasets using R, Excel, and GraphPad respectively.

On normal data, one-way analysis of variance (ANOVA) or general linear models were carried out using R depending on the number of treatment variables. Where significance was observed, Welch's t-tests were used in Excel for *post-hoc* analysis on datasets showing unequal variance. When equal variance was observed standard t-tests were carried out in Excel.

For non-normal data, Mood's median tests in Excel or generalised linear models in R were carried out depending on the number of treatment variables. Where significance was observed individual Mood's median tests were carried out in Excel.

Where significance was not observed but expected based on data visualisation or other data, power analysis in Excel was carried out.

All survival data was analysed using a Log Rank test in Excel.

Chapter 3

FoxO mutant verification and phenotypic assessment

3. FoxO mutant verification and phenotypic assessment

3.1 Introduction

As a transcription factor, FoxO is able to interact with consensus sequences within the DNA via a specific DNA-binding domain known as the winged-helix or 'forkhead' domain (Wang *et al.* 2014). These interactions result in the ability of FoxO to regulate target gene expression. FoxO proteins also contain polyglutamine, or 'polyQ', regions within their transactivation domain (Gemayel *et al.* 2010). These regions are strings of glutamine repeats that are well known for their structural instability as atypical, expanded regions are observed in a variety of genetic diseases (Totzeck *et al.* 2017). However, they also carry out roles within normal physiology, including the mediation of protein-protein interactions, and recruitment of other proteins containing these polyQ regions (Schaefer *et al.* 2012; Atanesyan *et al.* 2012).

Recent evidence has suggested that several of the transcriptional changes initiated by FoxO activity may occur indirectly through FoxO's interactions with other proteins. For example, gene expression profiling of cultured cells expressing a mammalian FoxO1 DNA-binding domain mutant identified differential expression of a separate set of genes compared to cells expressing the native protein (Ramaswamy *et al.* 2002; Rudd *et al.* 2007). Furthermore, introduction of this mutation into mice showed that FoxO1 controls glucose metabolism solely as a DNA-bound transcription factor but can alter lipid metabolism via both DNA-binding dependent and independent activities (Cook *et al.* 2015).

To investigate the role of dFoxO activity on metabolic homeostasis, the use of several *dFoxO* mutants produced via genomic engineering were employed in this project. Genomic engineering produced a knock-out founder line with a dFoxO-null mutant phenotype (dFoxO-ΔV3) by removing a 3 kb region arbitrarily named 'V3', which codes for amino acids 146-613 and overlaps with a portion of the forkhead domain. This knock-out was then used to generate distinct mutant alleles by reinsertion of modified sequences. These include reinsertion of the unmodified V3 region (dFoxO-V3), reinsertion of the unmodified V3 region including FLAG epitopes (dFoxO-V3-3xFLAG) for use in localisation and precipitation assays, and two DNA-binding domain mutants (dFoxO-V3-DBD1-3xFLAG and dFoxO-V3-DBD2-3xFLAG).
These DNA-binding domain mutants, hereafter dFoxO-DBD1 and dFoxO-DBD2, have alterations in amino acid residues within the DNA-binding domain. Both mutants

share the same point mutation that changes the histidine (H) amino acid residue in position 150 to an alanine (A) residue (H150A), however dFoxO-DBD2 has an additional point mutation converting the asparagine (N) residue in position 146 to an alanine residue (N146A) (*Drosophila* residues H150 and N146 are analogous to human H215 and N211) (*Figure 3.1*).

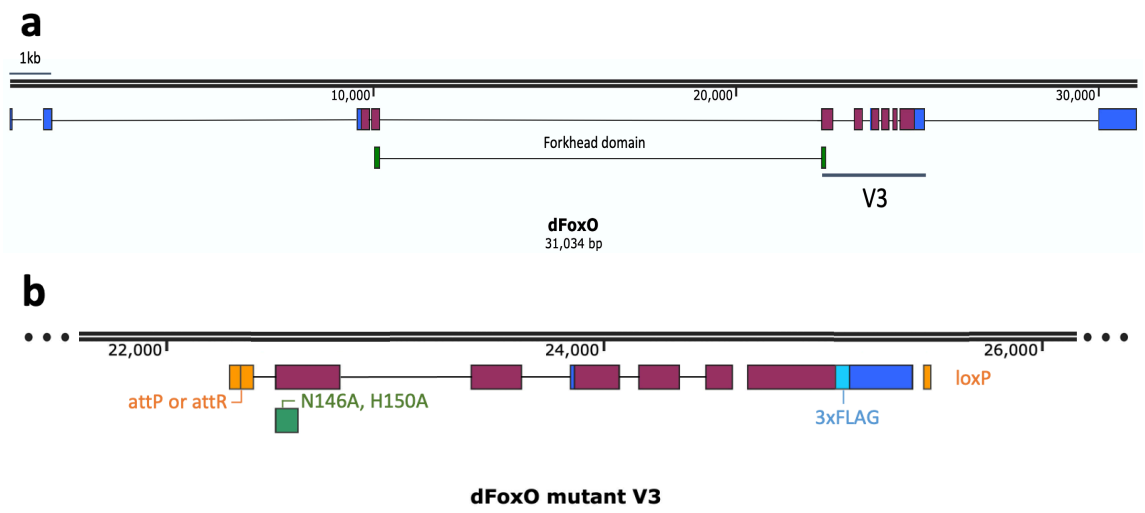

Figure 3.1. **Schematic of the wild-type *Drosophila FoxO* (*dFoxO*) and mutant *dFoxO* gene locus.**

Schematic of the *Drosophila FoxO* (*dFoxO*) gene locus for (a) wild-type (WT), and (b) null-mutant (ΔV3) and reinsertion lines. Untranslated regions, coding sequences, and genomic engineering artefacts are represented by dark blue, burgundy, and orange boxes respectively. Green boxes represent amino acids 97-145, and 146-179 that make up part of the forkhead DNA-binding domain (amino acids 95-201 total), with the mutated amino acids N146A and H150A highlighted. 3xFLAG tag sequence is represented by an aqua box. Schematic created using SnapGene and sequence information from Flybase.

These residues were altered to create the DBD mutants are major residues that come into direct contact with the DNA, forming bonds and water-mediated interactions. Therefore, mutating these residues and changing their polarity inhibited the production of these interactions, meaning these mutants no longer bound to DNA. This confered loss of the classic transcription factor activity of FoxO but retained the ability to act as a co-activator or repressor. The alteration of these specific amino acids has already been shown by previous studies to significantly alter mammalian FoxO activity, by causing the loss of transcriptional activity but maintaining its DNA-independent interactions and effects (Ramaswamy *et al*. 2002; Tang *et al*. 1999). For example, a mammalian study comparing an over-active FoxO1 protein with complete functionality (FoxOA3) to an over-active DBD mutant FoxO1 protein with a H215 mutation, showed that the FoxOA3 protein had some functional activities similar to and others distinct from those of the DBD mutant (Rudd *et al.* 2007).

3.2 Aims and objectives

In this section, the main aim was to verify aspects of each *dFoxO* mutant line, including identity, DNA-binding acitivty, and post-translational modification, and then assess their effects on different dFoxO-associated physiological functions in *Drosophila*.

Firstly, the hypothesis stated that the novel *dFoxO* mutants used were the appropriate genotype, lacked DNA-binding activity where appropriate, and correctly underwent post-translational modification particularly during starvation. Secondly, the hypothesis stated that some dFoxO-dependent phenotypes showed DNA-binding independent roles for dFoxO's activity.

To achieve this, PCR and subsequent sequencing was used to molecularly verify insertions or deletions within the V3 region, western blotting allowed for the determination of protein expression and post-translational modifications, and whole fly chromatin immunoprecipitation (ChIP) followed by qPCR was used to determine the effects of mutating the DNA-binding domain and the ability of the dFoxO proteins to bind to DNA. After verification was carried out, these mutants were then used to study the effects of these different mutations on phenotypes already known to require dFoxO activity.

This would help to fulfil the overall aim of the project by ensuring the mutants used are fit for purpose and allow for the identification of specific dFoxO-dependent DNA-binding independent phenotypes.

3.3 RESULTS

3.3.1 *DROSOPHILA FOXO* MUTANT VALIDATION

3.3.1.1 VERIFICATION OF FOXO MUTANT STOCKS

To verify the different *dFoxO* mutant lines procured for this study, PCR was used to amplify the appropriate regions within the various mutants to allow for their individual identification using primers specific to that reinsertion (*Figure 3.2*). Additional DNA sequencing of both DBD-mutants was carried out to accurately identify each mutant.

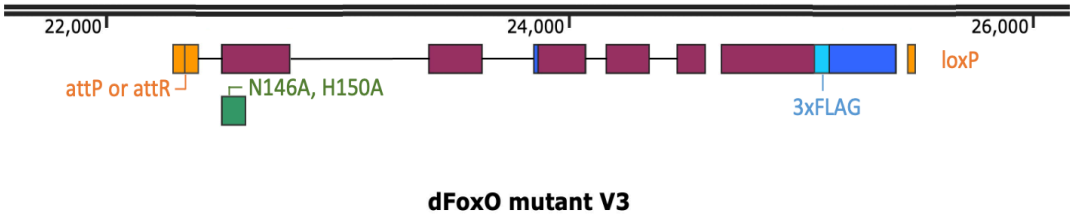

Figure 3.2. **Schematic of the *Drosophila FoxO* (*dFoxO*) gene locus and placement of primers.**
Schematic of the V3 region of the *Drosophila FoxO* (*dFoxO*) mutant gene locus for null-mutant (ΔV3) and reinsertion lines. Untranslated regions, coding sequences, and genomic engineering artefacts are represented by dark blue, burgundy, and orange boxes respectively. The green box represents amino acids 146-179 that make up part of the forkhead DNA-binding domain (amino acids 95-201 total), with the mutated amino acids N146A and H150A highlighted. The 3xFLAG tag sequence is represented by an aqua box. Primer placement is labelled in purple and coloured dots represent primer pairs. Primers SOL669-670 identify a wild-type, SOL792-887 the null, SOL725-726 and SOL883-885 any reinsertion, and V3F-F1-V3F-R1 the mutants with a 3xFLAG tag. Schematic created using SnapGene and sequence information from Flybase.

The results for this verification process are shown below (*Figure 3.3*).

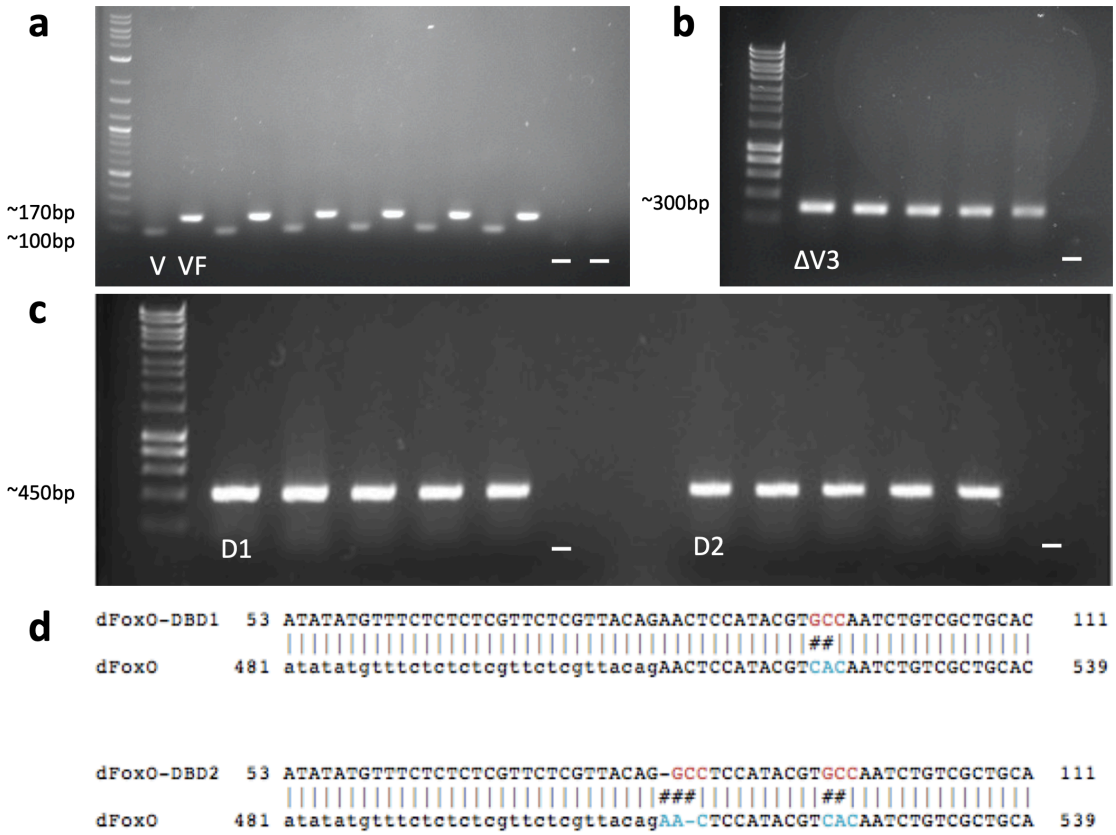

Figure 3.3. **Verification of *dFoxO*-mutant stock identity using PCR.**
Agarose gel electrophoresis of PCR products amplified from genomic DNA isolated from the indicated fly stocks using the primers described in Figure 3.2. Each gel shows mutant samples of the indicated genotypes and (-) negative controls. Gels include: (a) dFoxO-V3 (V3) and dFoxO-V3-3xFLAG (VF), (b) dFoxO-ΔV3 (ΔV3), and (c) dFoxO-DBD1-3xFLAG (D1) and dFoxO-DBD2-3xFLAG (D2) (n = 5 or 6 PCRs of single fly genomic DNA preps). As products for DBD-mutants cannot be differentiated based on PCR alone, DNA sequencing of the PCR products was carried out and the sequences compared to the wild-type *dFoxO* gene sequence to identify mutations in the DNA sequences (d).

All PCR produced bands of the expected sizes for the particular deletions or reinsertions for each of the single fly genomic DNA preparations produced. These results were able to verify the identity of the stocks received, therefore any phenotypic differences observed between these different lines were accurately ascribed to the differences in the FoxO protein expressed.

3.3.1.2 Validating mutant FoxO activity

3.3.1.2.1 Verifying FoxO protein production

Altering the amino acid sequence of the dFoxO protein may not only affect its ability to bind to DNA, but also its overall stability. In addition, these mutants have had 3x FLAG tags (DYKDDDDK) introduced in to the dFoxO protein sequence that may also affect stability of the resulting protein.

Therefore, western blotting using an antibody that specifically recognises the FLAG epitope was used to confirm expression of FLAG-tagged dFoxO proteins in the dFoxO-V3-3xFLAG (hereafter, V3F), DBD1 and DBD2 mutants (*Figure 3.4*).

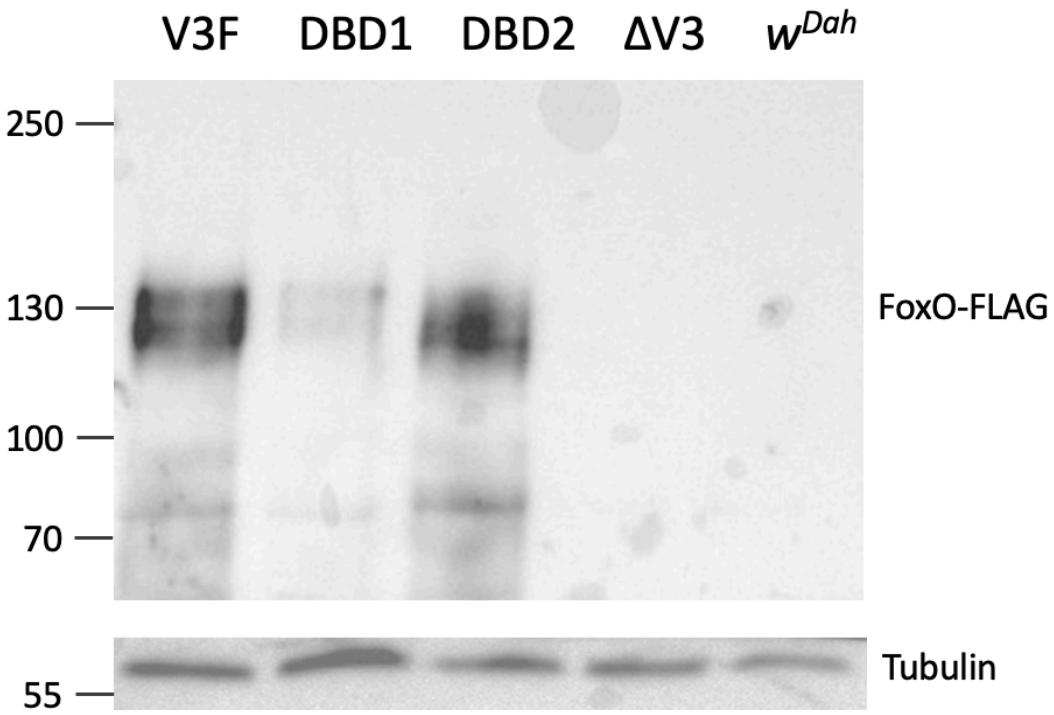

Figure 3.4. **Western blot analysis of FLAG-dFoxO protein expression.**
Analysis of protein extracts from whole 7-day old adult female *Drosophila* of the indicated genotypes to enable detection of FLAG-dFoxO protein expression. Blots were probed with an anti-FLAG antibody to identify FLAG-dFoxO protein expression, as well as an anti-tubulin antibody as a loading control. Image shown is representative of 3 individual western blots. Numbers represent where a protein of an approximate molecular weight (kDa) would lie to aid in identification of proteins found within the sample.

As expected, two bands were observed in the V3F and both DBD mutants representing proteins of ~130 kDa in size, which is expected for FLAG-dFoxO proteins. There were also bands present in these three mutants at lower molecular weights (~100 and 70 kDa), indicating the presence of non-specific binding when using this antibody.

The presence of two bands is characteristic for dFoxO, which is heavily modified by post translational modifications (PTM). No corresponding bands were observed in protein extracts from w^{Dah} or dFoxO nulls, which do not express tagged or dFoxO proteins respectively.

Therefore, these results confirm the expression of FLAG-tagged proteins of the corresponding size for FLAG-dFoxO in the different genotypes indicating mutations do not seemingly affect protein structure or stability.

3.3.1.2.2 VERIFYING FOXO POST-TRANSLATIONAL MODIFICATION

In the creation of the mutants there are several modifications that could affect PTM in response to a physiological change (such as, starvation). These modifications include the alteration of the amino acid sequence of the dFoxO DBD mutant proteins, the introduction of 3x FLAG tags (DYKDDDDK), as well as the presence of remnant sequences, namely loxP and attR, that are left within the genome during sequence reinsertion. These modifications could affect protein modification by masking Akt phosphorylation sites.

During feeding, Akt deactivates the dFoxO protein through phosphorylation of three highly conserved serine/threonine residues (namely, T44, S190, and S259) (Bridge *et al.* 2010). However, under starvation conditions these residues are dephosphorylated due to loss of insulin dependent Akt activation. Such changes in Akt activity have previously been shown to induce a FoxO band-shift on western blots (Yu *et al.* 2014). Therefore, it would also be expected that during starvation a band shift would be observable in the dFoxO protein extracted from the *dFoxO* mutants.
To assess the ability of each of the FLAG-tagged *dFoxO* mutants to undergo PTM and subsequent removal in response to dFoxO activation, protein PTM was observed using western blotting after flies were starved for 24 hours (i.e., a loss of dFoxO phosphorylation) (*Figure 3.5*).

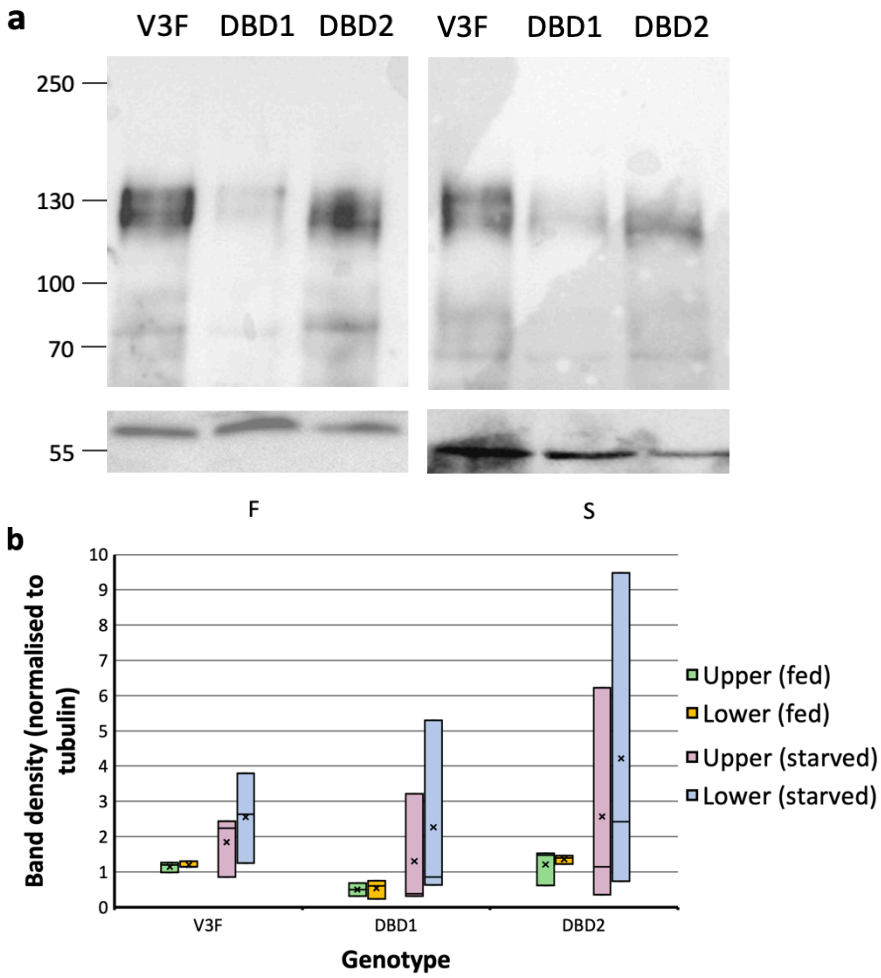

c

Genotype	Average difference between upper and lower band density	
	Fed	Starved
V3F	0.05	0.72
DBD1	0.04	0.96
DBD2	0.15	1.64

Figure 3.5. **Western blot analysis of FLAG-dFoxO post-translational modification.**

(a) Representative image of 3 individual western blots made using protein extracts taken from whole 7-day old adult female *Drosophila* of the indicated genotypes that were either fully fed (F) or starved for 24 hrs (S). Blots were probed with anti-FLAG antibody to detect FLAG-tagged dFoxO proteins and anti-tubulin antibody as a loading control. Numbers represent where a protein of an approximate molecular weight (kDa) would lie to aid in identification of proteins found within the sample.

(b) Quantification of FoxO band density normalised to tubulin for both upper and lower bands for both fed and starved flies of the various *dFoxO* mutants. (c) Average (mean) difference in the band density of the upper and lower bands for each genotype (n = 3 protein extracts using 5 flies per replicate; two-way ANOVA with *post-hoc* Welch's t-test).

Two bands were observed at the expected size of ~130 kDa for the FLAG-dFoxO proteins expressed within the V3F and two DBD mutant lines in both fully fed and starved conditions.

In the starved state there were no differences observed in the densities of the two bands between the genotypes. However, the DBD1 mutant showed a significantly lower ($p = 0.0001$ between the DBD1 and V3F, and $p = 0.001$ between the DBD1 and DBD2) band density than both the V3F and the DBD2 mutants in the fed state, indicating less overall dFoxO protein present in these extracts.

Statistical analysis showed there was a significant effect ($p = 0.02$) of starvation but not genotype on band density shift. There was also no significant interaction effect (i.e., the effect of one variable did not depend on the value of the other).
In the fully fed state, the average difference in density between the upper and lower bands was close to 0 for all genotypes (i.e., there was little difference between the density of the upper and lower bands) (0.05 +/- 0.2 for the V3F, 0.04 +/- 0.1 for the DBD1, and 0.15 +/- 0.4 for the DBD2).
However, after 24 hours of starvation a band-shift was observed showing a significant increase ($p = 0.02$) in the average difference between the density of the lower molecular weight band compared to the higher molecular weight band for all genotypes (0.72 +/- 0.6 for the V3F, 0.96 +/- 1 for the DBD1, and 1.64 +/- 1.5 for the DBD2). However, *post-hoc* analysis showed individually these differences did not reach statistical significance. Although, power analysis indicated sample sizes of 9, 12, and 11 would likely reach significance for the V3F, DBD1, and DBD2 respectively.

Overall, these results are indicative of a loss of dFoxO PTM during starvation and appropriate dFoxO activation for all genotypes.

3.3.1.2.3 Validation of disruption to DNA-binding activity in DBD mutants

The mutations introduced into the DNA-binding domain of the *dFoxO* gene in the DBD1 and DBD2 mutants are predicted to disrupt the binding of the resulting proteins to the DNA.

Chromatin immunoprecipitation followed by quantitative PCR (ChIP-qPCR) at well-characterised dFoxO genomic binding sites was therefore performed to confirm the loss of DNA-binding activity of these dFoxO DBD-mutants.

To ensure that ChIP-qPCR technical procedures were appropriate optimisation was carried out using wild type w^{Dah} flies and an anti-RNA polymerase II antibody (*Figure 3.6*). It was expected that DNA sequences for the chosen genes would increase when immunoprecipitated alongside RNA polymerase II, as they are known to be regulated by this enzyme.

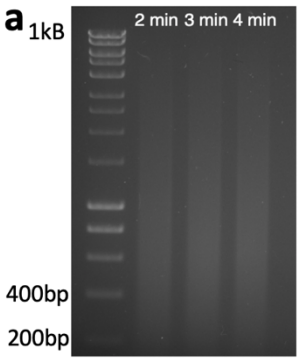

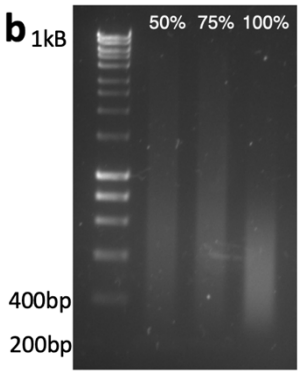

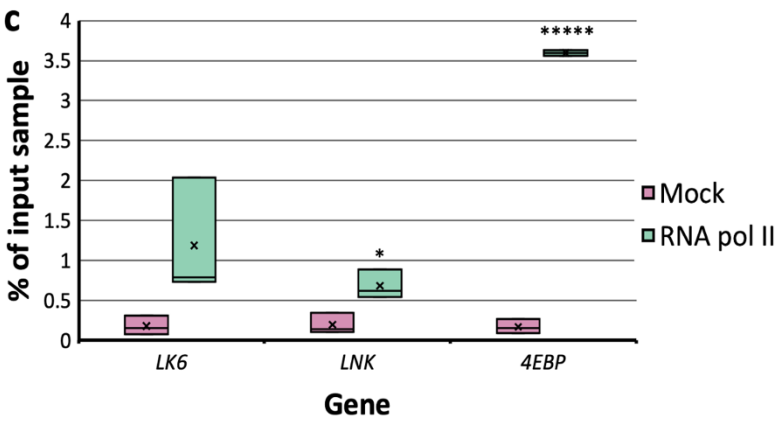

d

Gene	Fold enrichment over mock
LK6	8.69
LNK	4.80
4EBP	26.81

Figure 3.6. **Optimisation of chromatin immunoprecipitation (ChIP) using *w*^{Dah} and an anti-RNA polymerase II antibody.**
1.5% (w/v) agarose gel with 1 kb DNA ladder to visualise sheered chromatin from 2-day old whole adult female *w*^{Dah} after (a) different sonication durations (2 minutes, 3 minutes, and 4 minutes) at 50% amplitude, and (b) different sonication amplitudes (50%, 75% and 100%) for a duration of 3 minutes. (c) Quantification of the abundance of DNA associated with the *Lk6*, *Lnk*, and *4EBP* genes in the immunoprecipitated material as a percentage of input comparing a ChIP using an anti-RNA polymerase II antibody and a mock IP (i.e., no antibody IP) control. Box and whisker plots show the minimum and maximum value (bars), upper and lower quartiles (box), median (line within box), and mean (x). (d) the fold enrichment for each gene over a mock IP (n = 3 *w*^{Dah} chromatin extracts using 100 female flies each, $p < 0.05$ *, $p < 0.00001$ *****, Welch's t-test).

Sonication to sheer the chromatin was performed for different times and amplitudes, to ensure that the chromatin produced was of an appropriate size (200-1000 bp) for subsequent immunoprecipitation.

Sonication time showed no effect on chromatin fragment size when sheered chromatin was analysed by agarose gel electrophoresis. However, sonication amplitude showed that at 100% amplitude most chromatin fragments were between 200-1000 bp.

Therefore, ideal sonication conditions of 3 minutes and 100% amplitude were chosen for future experiments.

qPCR was then performed against genomic regions of the *Lk6*, *Lnk*, and *4EBP* gene loci to determine the abundance of these DNA sequences after immunoprecipitation using an antibody against RNA polymerase II. These gene loci were used as they are already known to be regulated by RNA polymerase II and have verified primer sequences for ChIP-qPCR (Slack *et al.* 2010). This was carried out to confirm that the chromatin extracts prepared using these ideal conditions were suitable for ChIP-qPCR.

qPCR for the *Lnk* ($p = 0.02$) and *4EBP* ($p = 0.00001$) genomic regions showed a significant enrichment for these DNA sequences after ChIP using an anti-RNA polymerase II antibody compared to mock ChIP controls, with fold-change increases of 4.8 and 26.8, respectively. The qPCR for the *Lk6* genomic region did not show a significant enrichment after ChIP, however a fold change increase of 8.7 was observed indicating a high level of enrichment that power analysis showed would reach significance with a sample size of 9.

Therefore, ChIP-qPCR using chromatin prepared by this method was able to detect enriched genomic sequences after immunoprecipitation.

Chromatin was therefore extracted from V3F and both DBD mutant flies using the optimised sonication conditions determined above. This was used to assess the DNA-binding activity or lack thereof of these different mutants, where it was expected that the quantity of DNA associated with the DBD mutant ChIP experiments would be decreased from the V3F control. After chromatin was prepared, ChIP was performed using an anti-FLAG antibody to immunoprecipitate dFoxO proteins and their associated genomic DNA sequences (*Figure 3.7*).

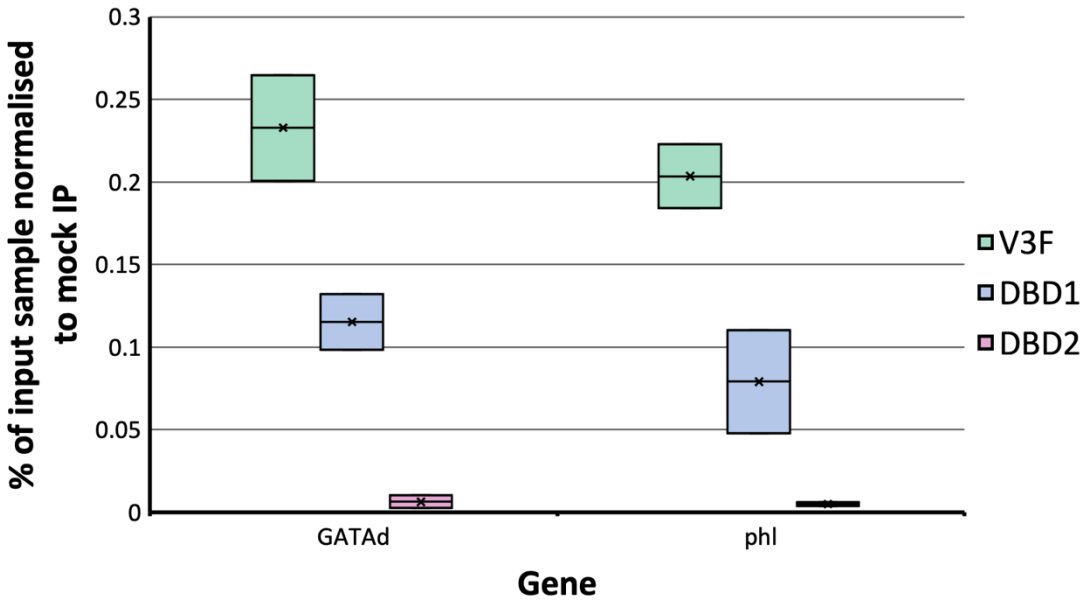

***Figure 3.7*. Chromatin immunoprecipitation (ChIP) of dFoxO DNA-binding domain mutants.**
ChIP-qPCR data for genes immunoprecipitated with an anti-FLAG antibody from extracts of 7-day old adult female dFoxO-V3-3xFLAG (V3F), dFoxO-V3-DBD1 (DBD1), and dFoxO-V3-DBD2 (DBD2) mutant *Drosophila*. Data shows quantification for the abundance of DNA of known dFoxO target genes, *GATAd* and *phl* associated with the immunoprecipitated material as a % of input chromatin isolated after ChIP normalised to a mock IP (i.e., no antibody IP) control. Box and whisker plots show the minimum and maximum value (bars), upper and lower quartiles (box), median (line within box), and mean (x) (n = 2 chromatin extracts per genotype using 100 flies each, ANOVA with *post-hoc* Welch's t-test).

Analysis of variance showed quantification of the chromatin immunoprecipitations for the V3F, DBD1, and DBD2 showed a significant effect of genotype on the abundance of *GATAd* ($p = 0.01$) and *phl* ($p = 0.02$) DNA.
Decreases were observed in both the DBD mutants compared to the V3F, with the DBD2 mutant showing a greater decrease for both the *GATAd* (DBD1: - 50% compared to V3F, DBD2: -97% compared to V3F) and *phl* (DBD1: -61% compared to V3F, DBD2: - 98% compared to V3F) genes.

However, *post-hoc* analysis showed these decreases did not reach statistical significance, but power analysis indicated sample sizes of 7 for the DBD1 and 6 for the DBD2 would likely reach significance.

Taken together, these data show that the dFoxO V3F and DBD mutants express stable proteins. It also shows the DBD mutants show similar band-shifts to the wild-type dFoxO protein, indicative of appropriate changes in PTMs in response to starvation. In addition, the DBD mutants also show loss of DNA-binding at known dFoxO loci, however the DBD1 mutants do not show as great a loss in associated DNA as the DBD2 mutants.

3.3.2 Phenotypes associated with *Drosophila* FoxO activity

After molecular verification of the mutant strains and confirmation that the DBD mutants express stable proteins, the effects of mutating the dFoxO DBD on protein function were assessed by phenotypic analysis, concentrating on phenotypic outputs that have already been associated with dFoxO activity.

For all experiments, wild-type w^{Dah} flies were included as controls to ensure that in the dFoxO-V3 (V3) and dFoxO-V3-3xFLAG (V3F) lines the expressed dFoxO proteins reconstituted the wild-type phenotype.
For each of these experiments, as these phenotypes seem to be dFoxO-dependent processes, no changes for the V3 and V3F and significant decreases for the null dFoxO-ΔV3 (ΔV3) would be expected compared to the w^{Dah} control. However, effects of the DBD mutations on any of these phenotypes was unknown.

3.3.2.1 *Drosophila* FoxO DNA-binding dependent phenotypes

3.3.2.1.1 Lifespan and Fecundity

Adult lifespan is widely known to be regulated by dFoxO with other dFoxO-null mutants showing a significant reduction in *Drosophila* lifespan compared with controls (Slack *et al.* 2011; Martins *et al.* 2016). Lifespan was therefore assayed for the different *dFoxO* mutant strains (*Figure 3.8*).

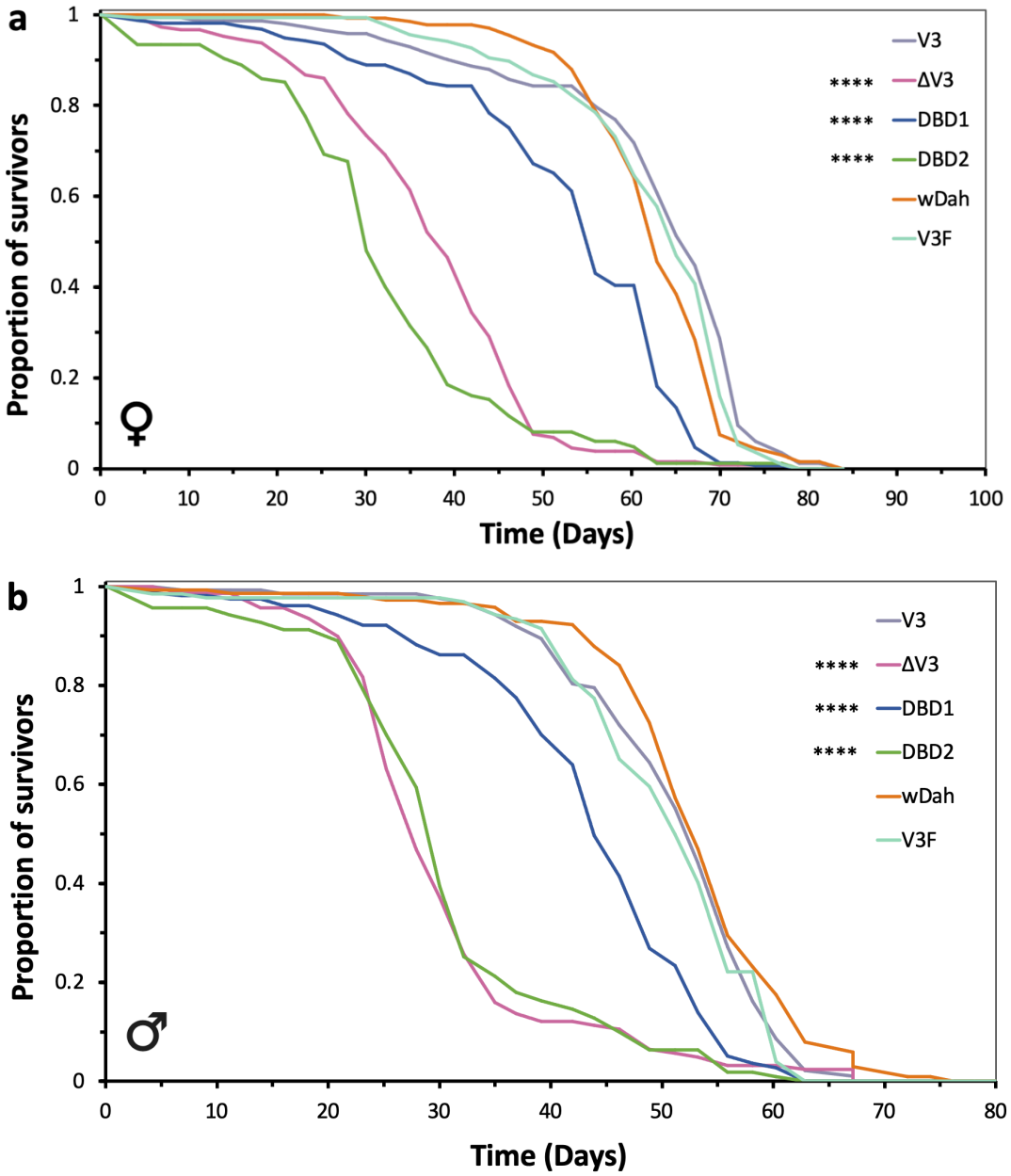

Figure 3.8. **Comparing lifespan of various *dFoxO* mutant lines.**
Survival analysis of (a) female and (b) male flies of the indicated genotypes. Results are plotted as proportion of survivors as a function of time (in days). Median survival times of female flies were: 66 days for V3 (n=149), 38 days for ΔV3 (n=149), 55 days for DBD1 (n=156), 29 days for DBD2 (n=136), 62 days for w^{Dah} (n=134) and 64 days for V3F (n=141). Median survival times for male flies were: 52 days for V3 (n=132), 27 days for ΔV3 (n=141), 43 days for DBD1 (n=158), 30 days for DBD2 (n=138), 52 days for w^{Dah} (n=146) and 50 days for V3F (n=131) ($p < 0.0001$ ****, Log rank test compared to V3F for females and V3 for males).

For females, no significant difference in lifespan was observed between the w^{Dah} and V3F flies, but the V3 mutants were slightly longer lived than w^{Dah} controls (+7% median lifespan, p = 0.01).
For males, no significant difference in lifespan was observed between the w^{Dah} and V3 flies, but V3F mutants were slightly shorter lived than w^{Dah} controls (-4% median lifespan, p = 0.02).
There were no significant differences between the V3 and V3F flies for either males or females.

Together, this shows that reinsertion of the endogenous V3 region with or without the FLAG tag epitope in to the *dFoxO* locus during genomic engineering does not drastically impact lifespan in either males or females.
However, as some significant differences were observed in relation to the w^{Dah} for the V3 and V3F, the mutant which was not significantly different from the w^{Dah} was used as a control for comparisons with the null and DBD mutants (i.e., V3F for females and V3 for males).

A significant reduction in lifespan was observed for the ΔV3 mutants when compared to the V3F controls for female (-41% median lifespan, p = 3.86E-41) and V3 controls for male (-48% median lifespan, p = 1.76E-27) flies.

Similarly, both DBD1 and DBD2 mutants showed a significant reduction in lifespan when compared to the V3F controls for female (DBD1: -14% median lifespan, p = 6.30E-13; DBD2: -54% median lifespan, p = 3.91E-43) and the V3 controls for male (DBD1: -17% median lifespan, p = 6.67E-10; DBD2: -44% median lifespan, p = 3.66E-31) flies.
Interestingly, DBD1 mutants did not show as great a reduction in lifespan as ΔV3 mutants for either females (+31% median lifespan for DBD1, p = 3.19E-24) or males (+37% median lifespan for DBD1, p = 7.17E-16). And in female flies, the DBD2 mutants were even shorter-lived than the ΔV3 mutants (-24% for the DBD2, p = 0.001).

Together, these data suggest that the presence of a functional DNA-binding domain in dFoxO is necessary for normal *Drosophila* lifespan.

Female egg-laying as a measure of fecundity has also been shown to be significantly affected by *dFoxO* mutation (Slack *et al.* 2011) and so egg-laying in the different *dFoxO* mutant strains was therefore examined (*Figure 3.9)*.

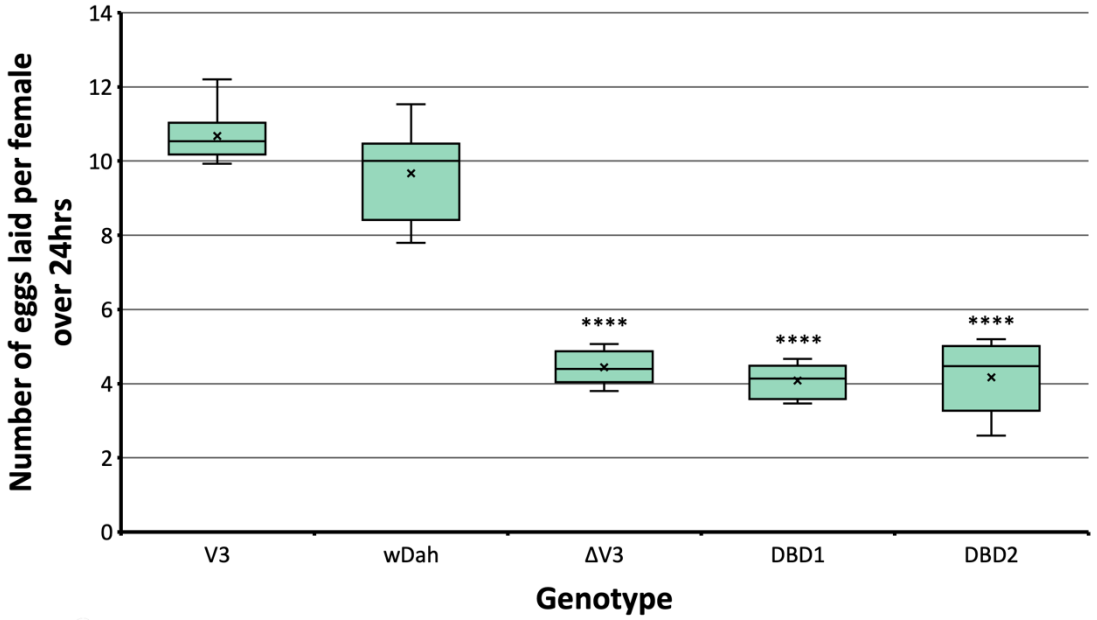

Figure 3.9. **Assessment of fecundity of the different *dFoxO* mutants over 24 hours.**
The fecundity of 7-day old adult female *Drosophila* of varying genotypes kept under standard conditions on SYA was assessed. Results are shown as number of eggs laid per female over 24 hours. Box and whisker plots show the minimum and maximum value (bars), upper and lower quartiles (box), median (line within box), and mean (x) (n = 15 vials of 15 flies per vial $p < 0.0001$ ****, ANOVA with *post-hoc* Welch's t-test).

No significant differences were observed in the number of eggs laid per female over 24 hours between the V3 and w^{Dah} lines, indicating that reinsertion of the V3 region during genomic engineering does not negatively impact female fecundity. Therefore, the V3 mutants were used for comparisons to other mutants.

Compared to the V3 controls, there were similar significant reductions in egg-laying observed for the ΔV3 (p = 2.80E-14), DBD1 (p = 1.30E-14), and DBD2 (p = 4.80E-12) mutants, with no apparent differences observed between these three mutants.

This indicates that the modulation of normal female fecundity is not only dependent on dFoxO but also the presence of a functional DNA-binding domain.

3.3.2.1.2 FEEDING BEHAVIOUR

Previously, it has been shown that FoxO activity is required for normal feeding behaviour (Hong *et al.* 2012; Ma *et al.* 2015). As normal food intake would be imperative to maintain metabolic homeostasis, feeding behaviour was examined in the different *dFoxO* mutant strains.

Two methods for assessing this phenotype were used: the capillary feeder (CAFE) assay that measures food consumption over time (*Figure 3.10.1*), and the proboscis extension (PE) assay, which measures food consumption alongside feeding behaviour (*Figure 3.10.2*).

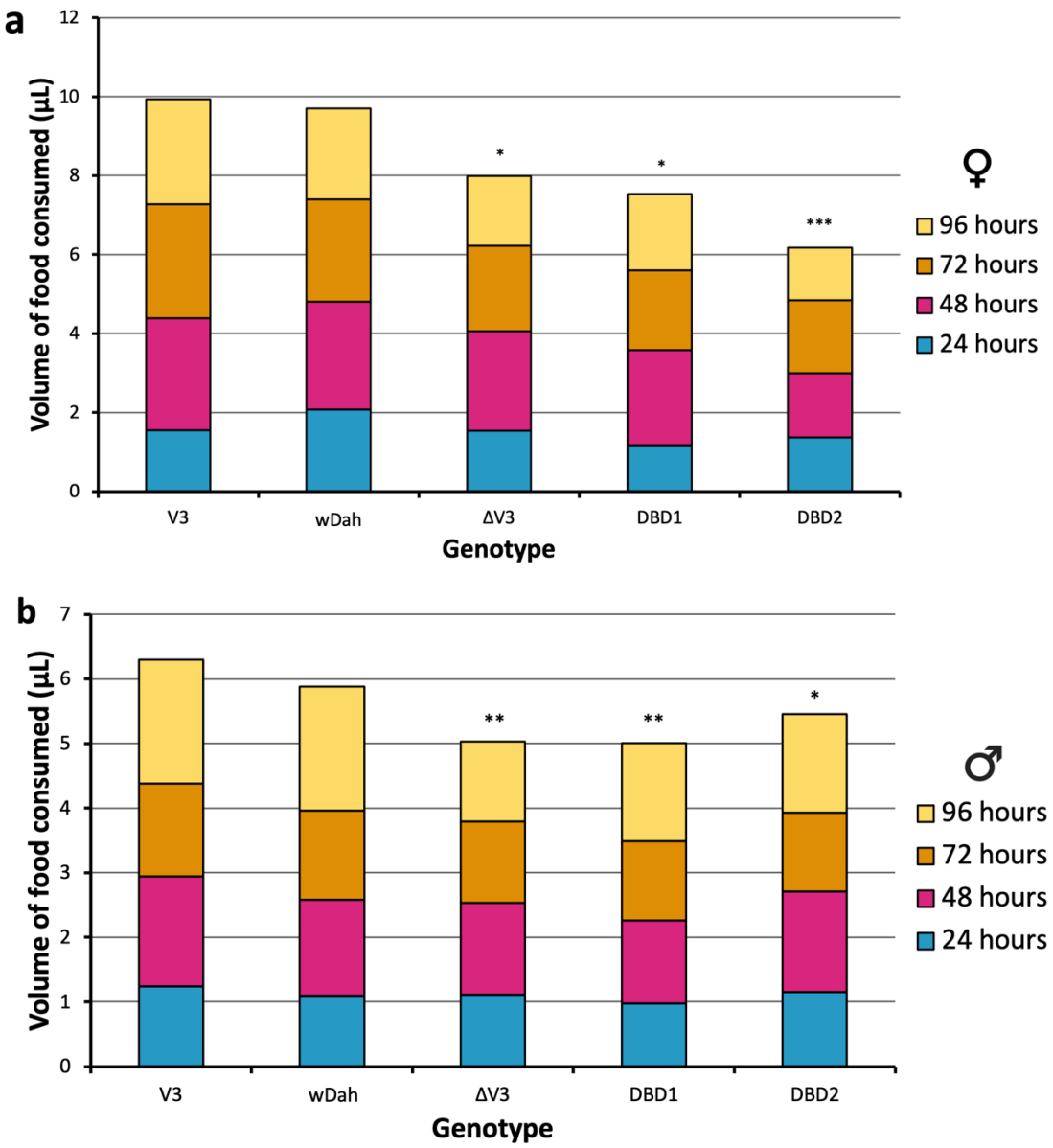

Figure 3.10.1. **Measurement of food consumption of different *dFoxO* mutants over 96 hours.**

Food consumption in 7-day old adult female (a) and male (b) *Drosophila* of the indicated genotypes was assessed using the capillary feeder (CAFE) assay. Results are shown as total volume of liquid fly food consumed over 96 hours (n = 10 individually housed flies per genotype $p < 0.05$ * $p < 0.01$ ** $p < 0.001$ ***, generalised linear model with *post-hoc* Mood's median test).

Statistical analysis showed that there was a significant effect of genotype (p = 2.17E-4 for females and p = 0.02 for males) and time (p = 3.50E-4 for females, and p = 4.23E-4 for males) on the volume of food consumed during the CAFE assay. However, there was also no significant interaction effect (i.e., the effect of one variable did not depend on the value of the other).

Post-hoc analysis showed no significant differences in the total volume of food consumed over 96 hours were observed between the V3 or w^{Dah} flies for either male or female flies, indicating that the V3 flies behave as wild-type flies with regards to their feeding behaviour. Therefore, the V3 mutants were used for comparisons to other mutants.

No significant differences were observed between any of the genotypes after 24 hours of capillary feeding. However, significant reduction in the volume of food consumed over the total 96 hours was observed for ΔV3 mutants when compared to the V3 controls ($p = 0.03$ for females and $p = 0.004$ for males). Similarly, both DBD1 and DBD2 mutants consumed significantly less food over the same period than V3 flies (DBD1: $p = 0.02$ for females and $p = 0.002$ for males, DBD2: $p = 7.97E\text{-}5$ for females and $p = 0.02$ for males) but showed no significant differences when compared to the ΔV3 mutants.

At the 24, 48, and 72-hour time points there was no significant difference observed between genotypes, suggesting a cumulative effect on feeding behaviour that only becomes observable after several days.

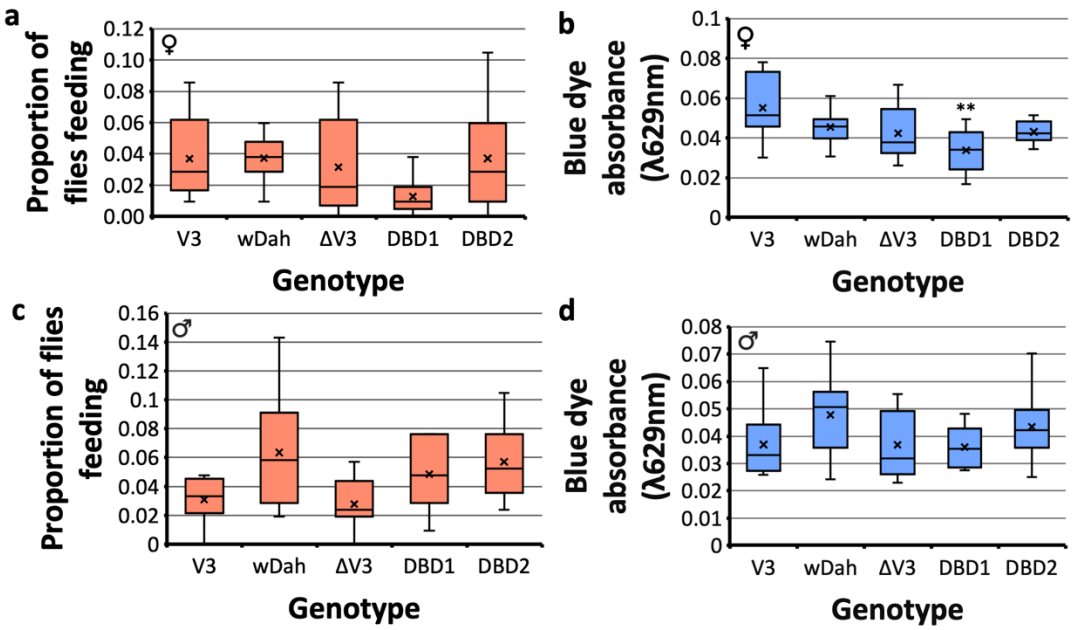

***Figure 3.10.2*. Assessing short-term feeding behaviour of different *dFoxO* mutants.**
Food intake and meal frequency using 7-day old adult *Drosophila* were assessed using measures of proportion of flies feeding at a specific time for (a) female and (c) male *Drosophila* of the indicated genotypes, and blue dye absorbance for (b) female and (d) male *Drosophila* of the indicated genotypes. Box and whisker plots show the minimum and maximum value (bars), upper and lower quartiles (box), median (line within box), and mean (x) (n = 4 or 5 flies per replicate with 10 replicates per genotype $p < 0.01$ **, one-way ANOVA with *post-hoc* Welch's t-test).

The PE assay determines food consumption measured via the absorbance of a blue dye and the proportion of time the flies spent feeding, to assay differences in meal size and frequency.

There was no significant difference between genotypes for either sex for either measurement, except for blue dye absorbance in the DBD1 females which showed significantly ($p = 0.002$) lower blue dye absorbance compared to all other genotypes except the ΔV3 flies.

Taken together, these results indicated that loss of dFoxO activity had no effect on the size and frequency of meals on solid food when measured over a short-term assay.
The difference in the DBD1 blue dye absorbance is unlikely to be caused by the DBD1 mutation itself, as it is not significantly different from the ΔV3 flies, which are not

significantly different from the other genotypes. Therefore, this variation is likely caused by variations within the assay itself. However, over a longer-term assay the presence of dFoxO with a functional DNA-binding domain seems necessary to maintain liquid food consumption.

3.3.2.1.3. XENOBIOTIC METABOLISM

FoxO proteins are also known 'xenosensors', responding to xenobiotic factors to mediate downstream responses to allow for xenobiotic excretion thereby avoiding deleterious effects to the organism (Klotz & Steinbrenner, 2017). Previous research has indicated a requirement for dFoxO in regulating xenobiotic stress and that removal of dFoxO makes flies more sensitive to xenobiotic challenge (Slack *et al.* 2011).

To examine the response to xenobiotic stress, the survival of flies in the presence of the xenobiotic toxin dichlorodiphenyltrichloroethane (DDT) was measured (*Figure 3.11*).

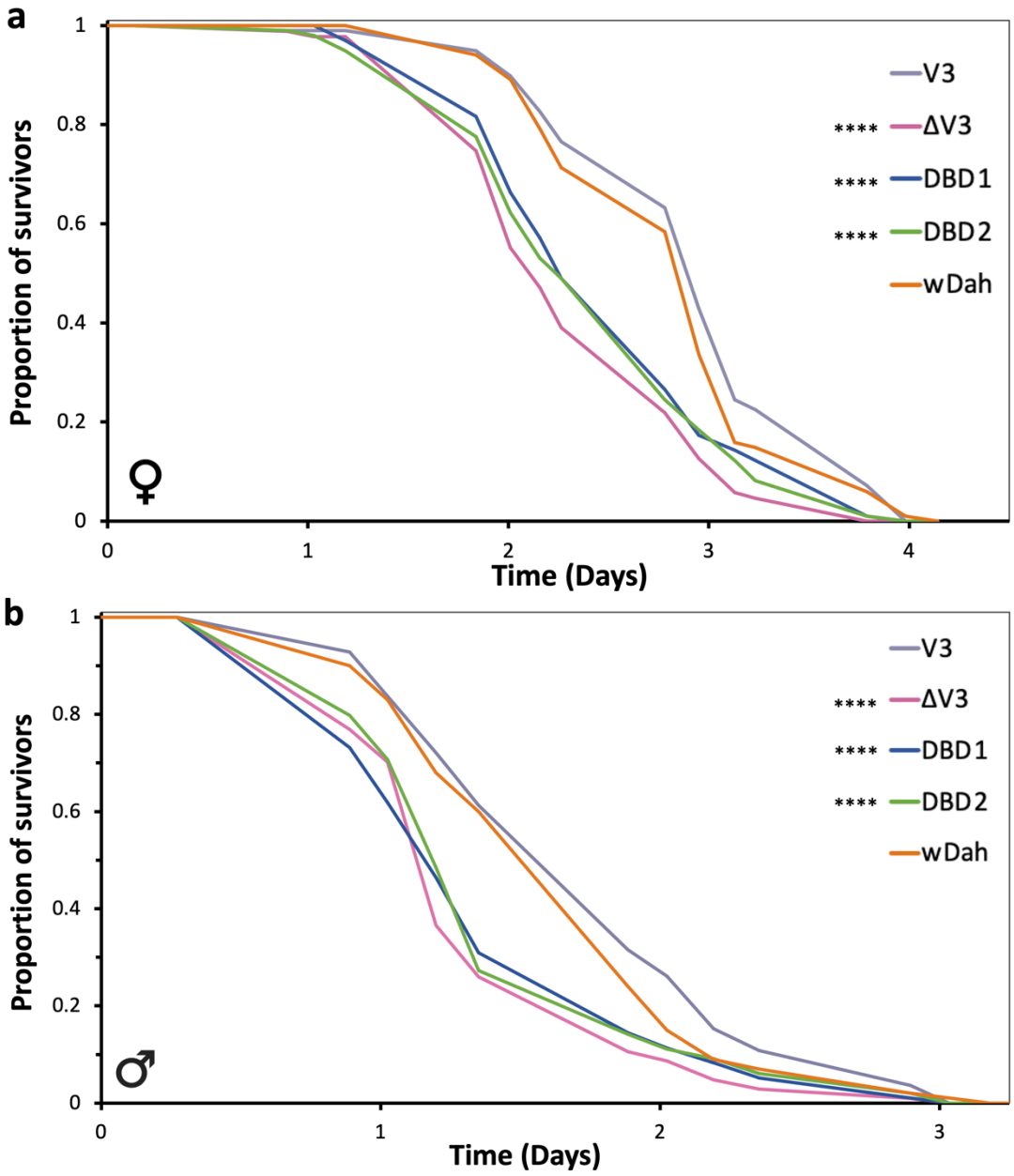

Figure 3.11. **Survival of *dFoxO* mutants in the presence of dichlorodiphenyltrichloroethane (DDT).**
The survival of 7-day old adult (a) female and (b) male *Drosophila* was assessed in the presence of 0.03% (w/v) DDT. Results are plotted as proportion of survivors as a function of time (in days). Median survival times of female flies were: 2.87 days for V3 (n=98) and w^{Dah} (n=101), 2.08 days for ΔV3 (n=87), and 2.21 days for both DBD1 (n=98) and DBD2 (n=98). Median survival times of male flies were: 1.62 days for V3 (n=112) and w^{Dah} (n=101), 1.11 days for ΔV3 (n=104), DBD1 (n=97), and DBD2 (n=99) mutants ($p < 0.0001$ ****, Log rank test compared to V3 flies).

No significant differences in survival were observed between V3 and w^{Dah} flies for either females or males, indicating that the V3 flies behaved as wild-type flies with regards to their response to DDT toxicity. Therefore, V3 flies were used as controls for comparisons with other mutants.

A significant reduction in survival was observed for ΔV3 mutants compared to V3 controls for both females (-28% median lifespan, p = 5.94E-10) and males (-31% median lifespan, p = 2.92E-7).

Further, both DBD1 and DBD2 mutants showed a significant reduction in lifespan when compared to the V3 controls for both female (DBD1: -23% median lifespan, p = 9.23E-6; DBD2: -23% median lifespan, p = 9.75E-7) and male (DBD1: -31% median lifespan, p = 2.61E-5; DBD2: -31% median lifespan, p = 6.98E-5) flies.

However, no significant differences in survival were observed between the DBD mutants and ΔV3 flies for either sex.

All together these data indicate that survival in response to xenobiotic challenge by DTT was not only dependent on dFoxO but also the presence of a functional DNA-binding domain.

3.3.2.1.4. Oxidative stress resistance

Survival under oxidative stress conditions is also a known phenotype that is regulated by FoxO activity, and loss of dFoxO has been shown to impact on fly survival in the presence of oxidative stressors, such as hydrogen peroxide and paraquat, an herbicide and neurotoxicant (Kops *et al.* 2002). Therefore, survival was monitored for all mutant lines when exposed to either hydrogen peroxide (H_2O_2) (*Figure 3.12*) or paraquat (*Figure 3.13*).

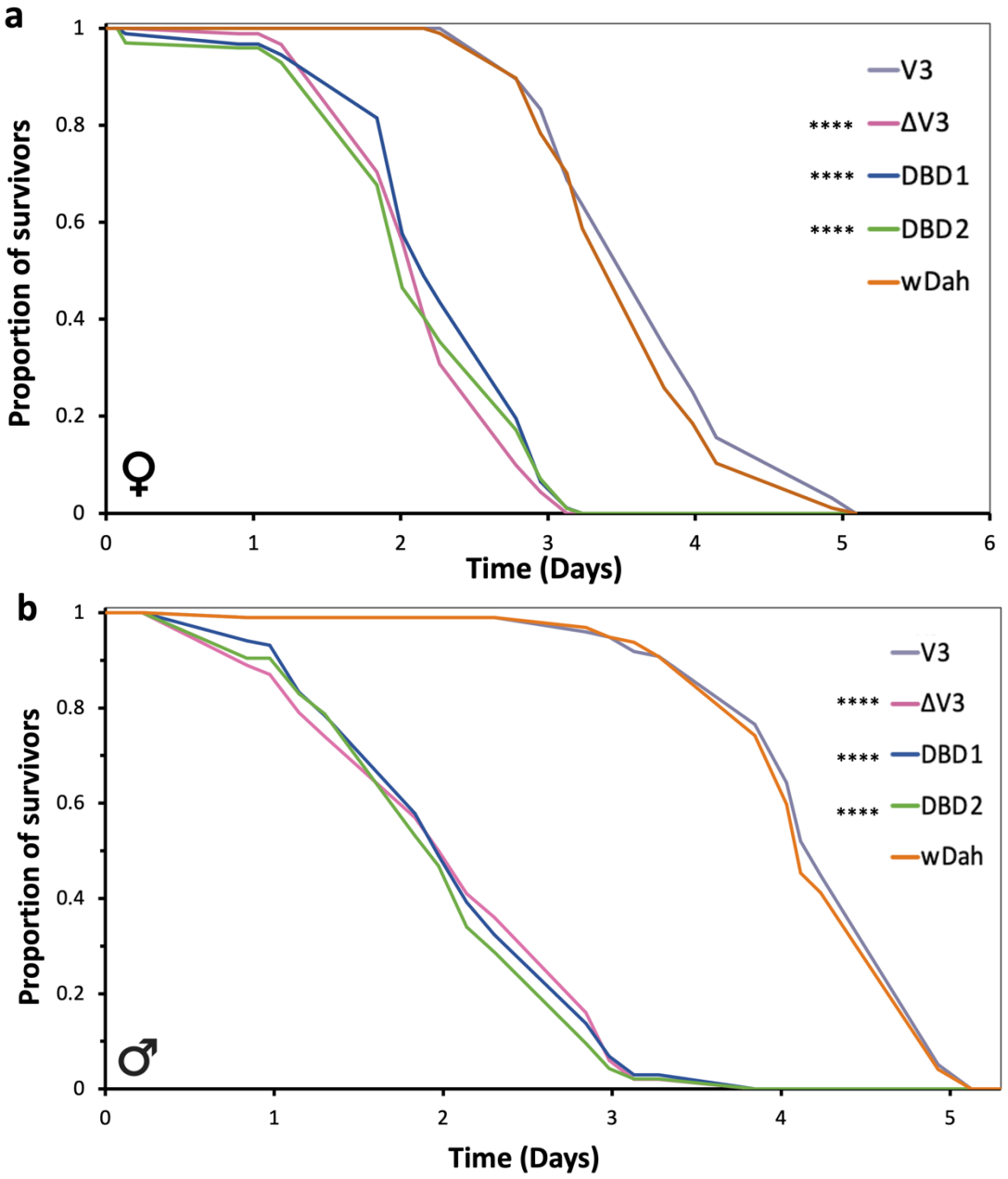

Figure 3.12*. Survival of *dFoxO* mutants exposed to hydrogen peroxide (H_2O_2).** Survival of (a) female and (b) male 7-day old adult *Drosophila* of the indicated genotypes when exposed to 6% (v/v) H_2O_2 was assessed. Results are plotted as proportion of survivors as a function of time (in days). Median survival times of female flies were: 3.51 days for V3 (n=96) and w^{Dah} (n=97), 2.08 days for ΔV3 (n=91) and DBD1 (n=92), and 1.92 days for DBD2 (n=99). Median survival times of male flies were: 4.17 days for V3 (n=98), 1.97 days for ΔV3 (n=100), 1.90 days for DBD1 (n=102) and DBD2 (n=94), and 4.07 days for w^{Dah} (n=97) mutants ($p < 0.0001$ *, Log rank test compared to V3 flies).

No significant differences in survival were observed between V3 and w^{Dah} flies when exposed to hydrogen peroxide for either females or males, indicating that the V3 flies behaved as wild-type flies with regards to their response to oxidative stress induced by hydrogen peroxide. Therefore, V3 flies were used as controls for comparisons with other mutants.

A significant reduction in survival was observed for ΔV3 mutants compared to V3 controls for both females (-41% median lifespan, p = 1.99E-39) and males (-53% median lifespan, p = 2.77E-45).

Both DBD1 and DBD2 mutants showed a significant reduction in lifespan when compared to the V3 controls for both female (DBD1: -41% median lifespan, p = 2.23E-45; DBD2: -45% median lifespan, p = 3.11E-45) and male (DBD1: -54% median lifespan, p = 2.23E-45; DBD2: -54% median lifespan, p = 3.11E-45) flies.

However, no significant differences in survival were observed between the DBD mutants and ΔV3 flies for either male or female flies.

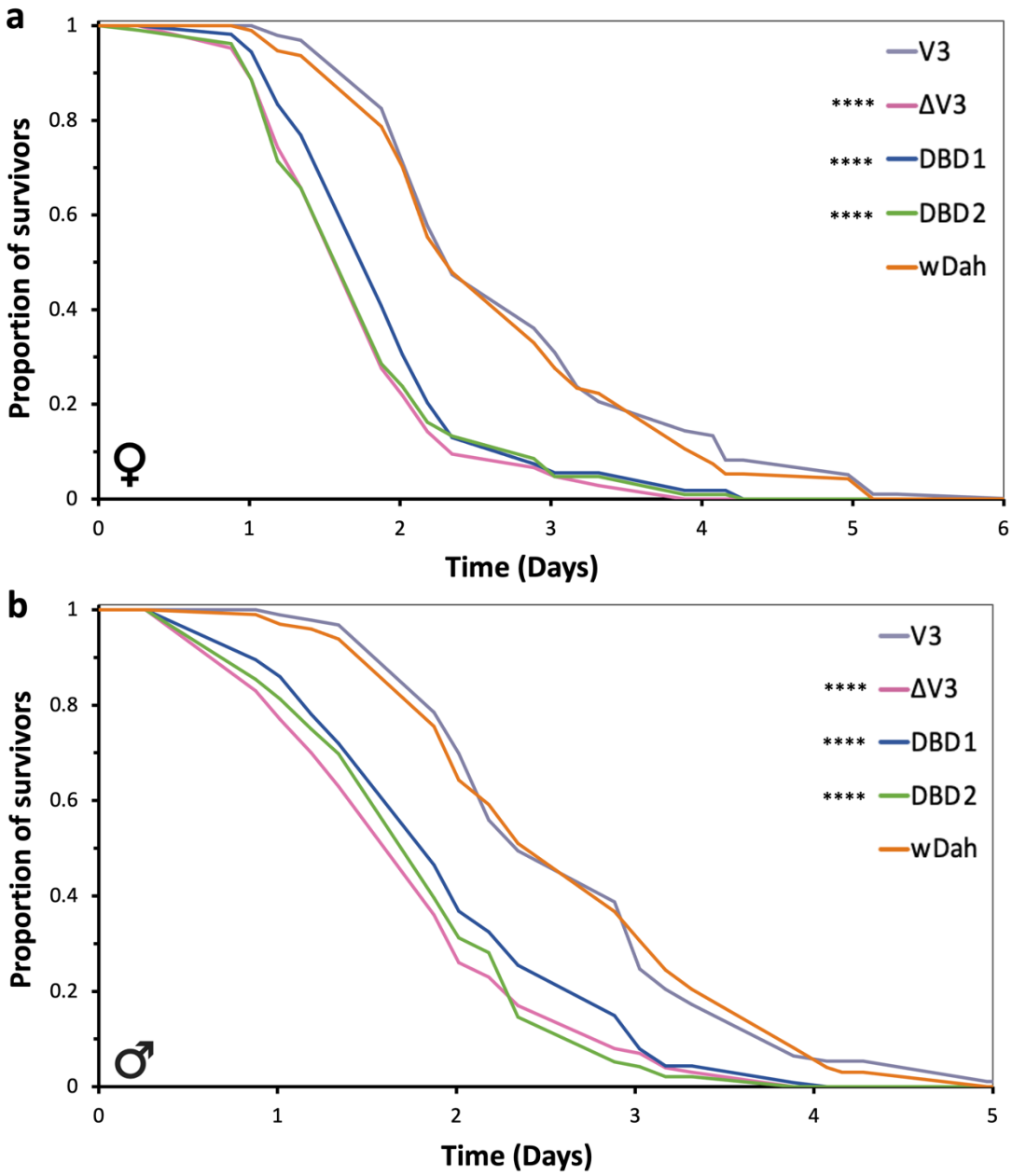

***Figure 3.13*. Survival of *dFoxO* mutants when exposed to paraquat.**
Survival of (a) female and (b) male 7-day old adult *Drosophila* of the indicated genotypes when exposed to 20 mM paraquat was assessed. Results are plotted as proportion of survivors as a function of time (in days). Median survival times of female flies were: 2.26 days for V3 (n=97) and w^{Dah} (n=94), and 1.61 days for ΔV3 (n=108), DBD1 (n=105), and DBD2 (n=105). Median survival times of male flies were: 2.26 days for V3 (n=93), 1.61 days for ΔV3 (n=100), DBD1 (n=114) and DBD2 (n=96), and 2.61 days for w^{Dah} (n=98) mutants ($p < 0.0001$ ****, Log rank test compared to V3 flies).

Again, no significant differences in survival were observed between V3 and w^{Dah} flies when exposed to 20 mM paraquat, indicating that the V3 flies behaved as wild-type flies with regards to their response to oxidative stress induced by paraquat. Therefore, V3 flies were used as controls for comparisons with other mutants.

A significant reduction in survival was observed for ΔV3 mutants compared to V3 controls for both females (-29% median lifespan, p = 1.99E-15) and males (-29% median lifespan, p = 8.39E-11).

Similarly, both DBD1 and DBD2 mutants showed a significant reduction in lifespan when compared to the V3 controls for both female (DBD1: -29% median lifespan, p = 6.6E-13; DBD2: -29% median lifespan, p = 3.34E-13) and male (DBD1: -29% median lifespan, p = 2.70E-7; DBD2: -29% median lifespan, p 7.48E-11) flies.

However, no significant differences in survival were observed between the DBD mutants and ΔV3 flies for either sex.

Together, this indicated that survival in response to oxidative stress induced by hydrogen peroxide or paraquat was not only dependent on dFoxO, but also on the presence of a functional DNA-binding domain.

3.3.2.2 *Drosophila* FoxO DNA-binding independent activity

3.3.2.2.1 Growth

Organismal growth during development is regulated by metabolism, in particular through the IIS pathway due to its effects in regulating both cell size and number, and its roles in assessing loss of nutrients and metabolic stores during development (Kramer *et al.* 2003).

This is especially important for *Drosophila*, as the adult body size is directly influenced by developmental growth and metabolism. For example, it has been demonstrated that the insulin receptor, and therefore insulin signalling, is critical in determining final adult body size during the stages of 'critical size' (i.e., the point at which larvae commit to metamorphosis and no longer feed) to pupariation (Shingleton *et al.* 2005). This

effect of insulin receptor activity and insulin signalling on cell size and cell number is also reflected in wing size (Shingleton *et al.* 2005).

To determine if mutation of the dFoxO DBD was associated with effects on growth during development, body mass and wing area of individual adult flies of the different *dFoxO* mutants were measured as a read-out for developmental growth (*Figure 3.14*).

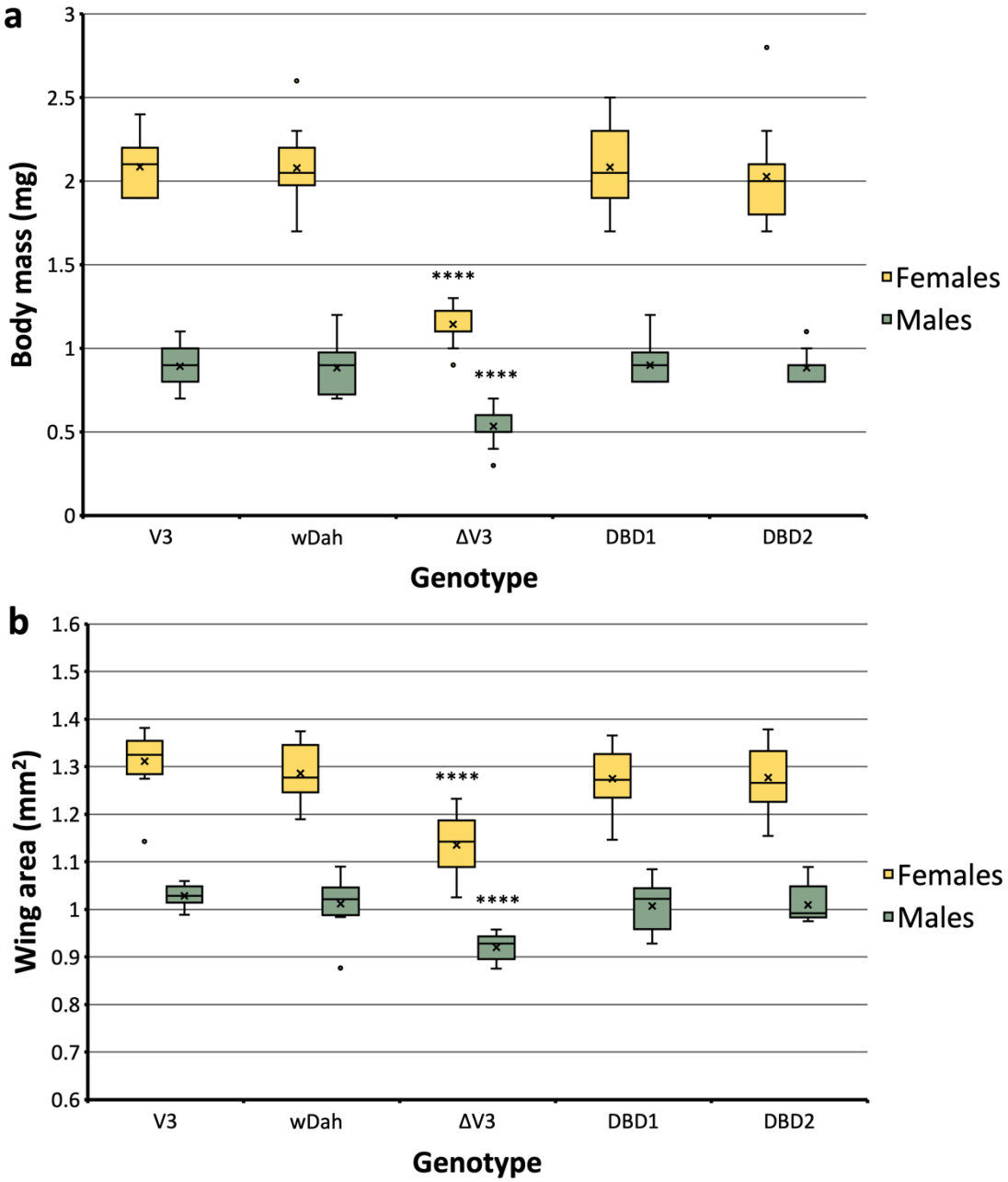

Figure 3.14. **Measurement of body mass and wing area of *dFoxO* mutants to evaluate the role of dFoxO in organismal growth.**
Measurements of (a) body mass and (b) wing area for 10-day old adult female and male *Drosophila* of the indicated genotypes. Box and whisker plots show the minimum and maximum value (bars), upper and lower quartiles (box), median (line within box), and mean (x) (n = 10 individual flies $p < 0.0001$ ****, ANOVA with *post-hoc* Welch's t-test).

No significant differences were observed in either body mass or wing area between V3 and w^{Dah} lines for males or females, indicating that the dFoxO-V3 lines show a

consistent wild-type growth phenotype. Therefore, V3 flies were used as controls for comparisons with other mutants.

Significant differences were observed for both males and females between the ΔV3 flies and V3 control mutants for both body mass ($p = 1.6E-15$ for females and $p = 2.5E-7$) and wing area ($p = 4.1E-6$ for females and $p = 3.1E-8$ for males).

Interestingly, both DBD1 and DBD2 mutants showed no significant differences in either body mass or wing area when compared to V3 control mutants.

These data suggest that the modulation of normal growth during development occurs in a dFoxO-dependent manner but does not require a functional DNA-binding domain.

3.3.2.2.2 Starvation resistance

Survival under starvation is controlled by several different factors, including developmental timing, sleep, and importantly metabolic regulation (Brown *et al.* 2019). Previous studies have shown that dFoxO is activated in response to starvation (Mattila *et al.* 2009; Hwangbo *et al.* 2004) and that dFoxO activity is required for normal survival responses to starvation (Mattila *et al.* 2009; Kramer *et al.* 2008; Slack *et al.* 2011). Therefore, survival during starvation was measured for the different *dFoxO* mutant lines (*Figure 3.15*).

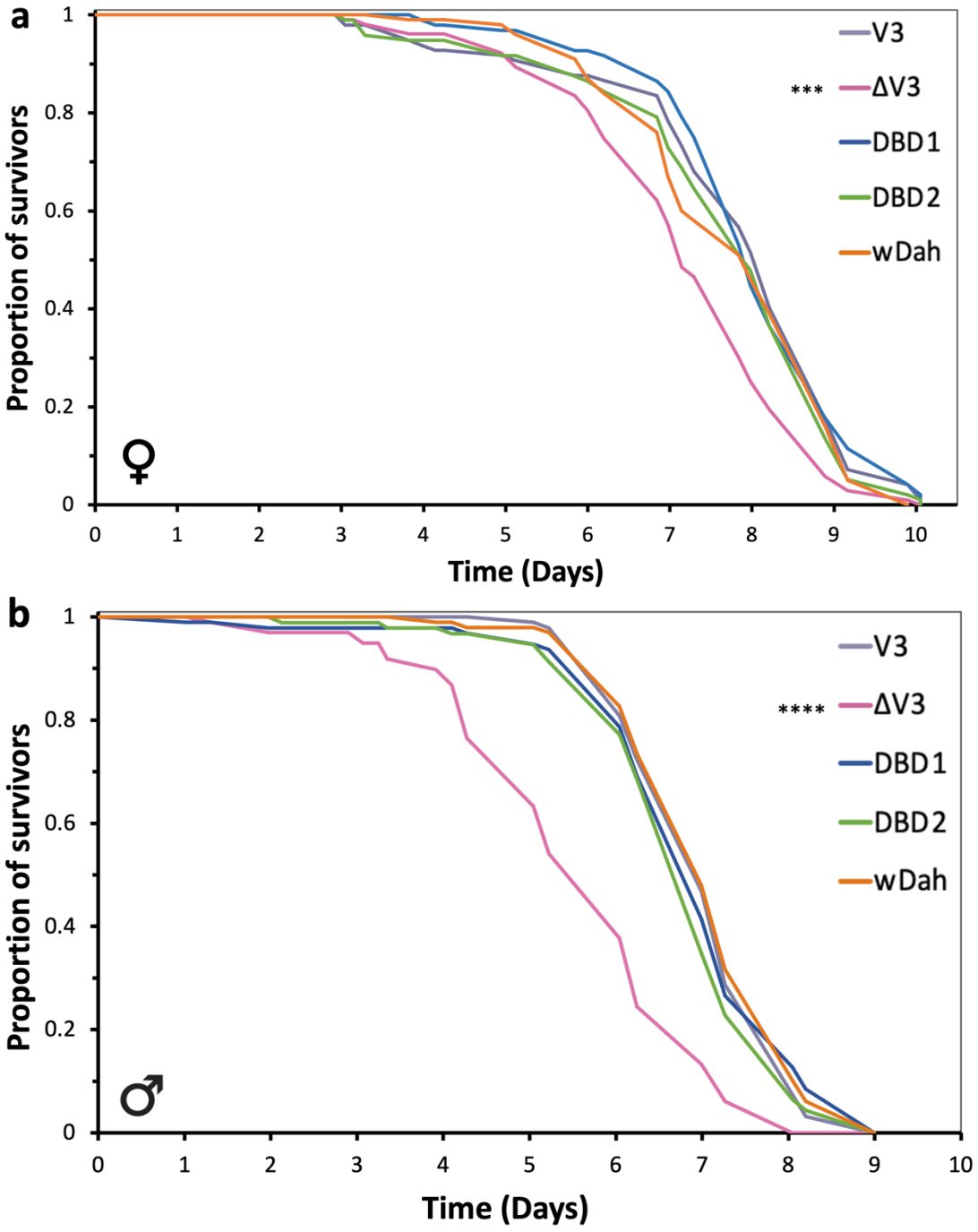

Figure 3.15. **Survival during starvation of *dFoxO* mutants.**
Survival of 7-day old adult (a) female and (b) male *Drosophila* of the indicated genotypes under starvation. Results are plotted as proportion of survivors as a function of time (in days). Median survival times of female flies were: 8.10 days for V3 (n=97), 7.06 days for ΔV3 (n=103), 7.91 days for both DBD1 (n=96) and DBD2 (n=96), and 7.91 days for w^{Dah} (n=100). Median survival times of male flies were: 6.62 days for V3 (n=94) and w^{Dah} (n=98), 5.63 days for ΔV3 (n=98), and 6.62 days for both DBD1 (n=95) and DBD2 (n=92) mutants ($p < 0.001$ ***, $p < 0.0001$ ****, Log rank test compared to V3 flies).

No significant differences in survival under starvation were observed between the V3 and w^{Dah} controls for females or males, indicating that the V3 flies behave as wild-type flies in their response to starvation. Therefore, V3 flies were used as controls for comparisons with other mutants.

A significant reduction in survival was observed for ΔV3 mutants compared to V3 controls for both females (-13% median lifespan, p = 0.0001) and males (-15% median lifespan, p = 3.3E-13).

However, no significant differences for either sex were observed for both DBD1 and DBD2 mutants when compared to the V3 control mutants.

Therefore, this suggests that although normal survival under starvation was dFoxO-dependent it did not require the presence of a functional DNA-binding domain.

3.4 Discussion

The main aim of this chapter was to validate genomically engineered *dFoxO* mutant lines to ensure their identity and function, as well as assess their different physiological functions in *Drosophila*. In this way, the precise role of dFoxO transcriptional activity, and the requirement of the DNA-binding domain (DBD), on various phenotypes associated with dFoxO activity could be determined.

The hypothesis stated that the novel *dFoxO* mutants used were the appropriate genotype, lacked DNA-binding activity where appropriate, correctly underwent post-translational modification particularly during starvation, and could be used to characterise a range of dFoxO-dependent phenotypes and identify DNA-binding independent roles for dFoxO's activity.

3.4.1 Verification of mutant stocks

Using a variety of molecular techniques, results have confirmed the appropriate identity, modification, and localisation of the proteins produced by these novel *dFoxO* mutants. Western blot analysis showed the presence of FLAG-dFoxO proteins in all genotypes, bar the null mutants, indicating that they all expressed a protein of the predicted size. An appropriate shift in protein size, indicative of changes in post-translational modification, was also observed after starvation. The lack of effect of the FLAG tags on these phenotypes was expected as the sequence of the 3x FLAG tag epitopes are already short (i.e., 8 amino acid residues, DYKDDDDK, or 24 bp) and they are inserted at the end of the coding sequence ensuring they are near to the surface and do not interfere with protein folding after translation (Zhao *et al.* 2013).

Chromatin immunoprecipitation (ChIP) qPCR also showed a loss in the abundance of DNA of known dFoxO target genes, *GATAd* and *phl*, in both DBD mutants compared to the V3F. This observation supports the need for direct DNA binding by dFoxO to regulate the expression of these genes, both of which were identified as being bound by dFoxO in previous research (Alic *et al.* 2011). Interestingly, the DBD2 mutant showed a much larger decrease in the abundance of DNA compared to the V3F for both genes tested, compared to the DBD1. Therefore, indicating that the DBD1 may still have some residual DNA-binding activity.

Taken together, these data demonstrate that the introduction of the FLAG epitope and mutation of the DNA-binding domain did not affect expression or stability of the encoded proteins or their ability to undergo appropriate post-translational

modification. However, the introduction of mutations into the DBD did disrupt association of the dFoxO proteins with specific target sequences in the DNA.

3.4.2 *Drosophila* FoxO DNA-binding dependent phenotypes

Subsequent research then focussed on examining the effects of these different *dFoxO* mutants on several of dFoxO's known physiological roles, including lifespan, fecundity, survival under xenobiotic challenge and oxidative stress, feeding behaviour, growth, and starvation survival.

Initial comparisons focused on the phenotypic responses of the dFoxO-V3 flies compared to w^{Dah} controls. Genomic engineering introduces exogenous sequences that could impact on gene expression from that locus. However, no significant differences were observed between the V3 and w^{Dah} flies in any of the phenotypic assays undertaken indicating that the dFoxO protein produced by the V3 behaves similarly to that produced in a wild-type fly in these contexts. This is most likely because the use of minimal attP (attP-50), attB (attB-53), and loxP sites during the genomic engineering process prevents the resulting sequences from being unnecessarily long, thereby reducing its potential to influence or interrupt gene expression of the final allele (Huang *et al.* 2009; Bouabe & Okkenhaug, 2013).

Normal lifespan, female fertility, xenobiotic metabolism, oxidative stress resistance, and feeding behaviour were all found to be dFoxO-dependent phenotypes that were also dependent on the presence of a functional DBD. This, therefore, implies that dFoxO is directly regulating the expression of target genes that encode for proteins, which directly modulate these processes.

The reduction in overall lifespan that is present in both the dFoxO-null and DBD-mutants, when compared to wild-type phenotypes, is not unexpected. The role of FoxO in this process has been well studied, whereby regulating DNA repair, apoptosis, gluconeogenesis, reactive oxygen species (ROS) breakdown, stem cell homeostasis, and immune system modulation, mammalian FoxOs are able to protect against age-related disorders including type II diabetes, cancer, and cardiovascular diseases to confer longevity (Morris *et al.* 2015). Specifically in *Drosophila,* it has been shown that insulin/insulin-like growth factor (IGF)-1 signalling (IIS) inhibition, and therefore FoxO activation, is able to extend lifespan (Martins *et al.* 2016; Fontana *et*

al. 2010). Furthermore, deletion of dFoxO also decreased the expression of factors involved in gene repression, such as CCCTC-binding factor, introducing the idea that dFoxO is critical in the maintenance of chromatin states (Alic *et al.* 2011), a process which dominates the functional decline associated with old age (Booth & Brunet, 2016).

In addition, ChIP-seq analysis of female *Drosophila* has shown that during normal ageing the number of dFoxO-bound genes drastically decreases by ~90%, possibly due to splice variant composition changes as dFoxO expression does not decrease, altering the expression of genes such as the lipase *bmm,* a kinase involved with neuronal differentiation *dlg1,* and a transcription factor involved with dendrite morphogenesis *jim* (Birnbaum *et al.* 2019). This indicates that increasing dFoxO activity later in life may ensure longevity by maintaining advantageous gene transcription, and therefore by removing dFoxO transcriptional activity this longevity control is removed leading to a reduction in lifespan.

There were differences in lifespan, however, that were observed between the DBD mutants and ΔV3 flies, where the reduction in lifespan seen in the DBD1 mutants was not as pronounced compared to the ΔV3 and the DBD2 counterpart. This could be due to residual DNA-binding of this mutant as possibly identified in the ChIP-qPCR verification, which affects lifespan but may not affect genes that regulate other phenotypes. This is even more likely as the genes used in the ChIP-qPCR, *GATAd* and *phl*, have functions related to the regulation of *Drosophila* lifespan.

Furthermore, there were small differences observed in the lifespan of the three control lines in both males and females. As well as a small difference in the lifespan of the ΔV3 and DBD2 female flies. This is possibly due to the genetic background affecting the genotype, as these flies were at least 15 generations post-backcrossing, which could lead to natural deviations in the genetic background that occur from generation to generation and then have knock-on effects in highly sensitive survival phenotypes (such as, lifespan) (Mackay, 2010; Burnett *et al.* 2011). However, it is important to note that these differences, whilst significant, are drastically smaller statistically than between the genotypes where differences were expected, and in every other assay performed the control lines behaved identically as did the ΔV3 and DBD2 flies where similar phenotypes were observed. This is possibly due to lifespan being a quantitative trait (i.e., variation in natural populations can be attributed to a number of different loci) affected by multiple trait loci (Mackay, 2002), making mutations in trait-specifc loci that affect the overall phenotype more likely. Therefore, it is unlikely that

genetic background is playing any decisive role in these phenotypes and lifespan is just a phenotype that is more sensitive to the differences between even similar genotypes.

Reductions in egg production as the result of the effects of a dFoxO-null have previously been shown by Slack *et al.* (2011), where $dFoxO^{\Delta 94}$ null mutants laid significantly fewer eggs compared to w^{Dah} controls. This indicates a role for dFoxO in maintaining normal fecundity. Little direct information regarding the role of dFoxO in maintaining normal *Drosophila* fecundity, or the mechanisms involved in egg production, was found. However, FoxO1 in mice prevents anovulation by repressing the expression of the luteinising hormone β-subunit, a subunit of the glycoprotein luteinising hormone that is responsible for regulating steroidogenesis and ovulation (Arriola *et al.* 2012). Whilst FoxO1 was found not to bind to the gene promoter, a functional DNA-binding domain was necessary for this regulation (Arriola *et al.* 2012). This is important to note as there is some conservation with the hormones involved with mammalian reproduction in *Drosophila*. For example, there are *Drosophila* homologues for the luteinising hormone-activated G protein-coupled receptor, LGR1, as well as a glycoprotein hormone that can activate this receptor (Sellami *et al.* 2011; Eriksen *et al.* 2000). This potential conservation and regulation could help to explain why reduced fecundity is also exhibited in the DBD mutants.

For feeding behaviour, the significant reduction in volume of food consumed over time for the dFoxO-null and DBD-mutants may represent defects in the ability of FoxO signalling to regulate many genes involved with the modulation of feeding behaviour (Hong *et al.* 2012; Ma *et al.* 2015). The fact that altered dFoxO activity is seemingly affecting feeding over time could possibly be caused by both a loss of dFoxO-induced orexigenic peptide expression reducing food intake, as well as a loss of inhibition by FoxO on leptin signalling (Yang *et al.* 2009a). This loss of inhibition will therefore increase the effects of leptin (*Drosophila* homologue *unpaired1*), which has shown through intracerebroventricular leptin treatment to reduce food intake cumulatively in rats (Kanoski *et al.* 2014). An improvement on the analysis of feeding behaviour would be to utilise the flyPAD (fly Proboscis and Activity Detector) system as a more accurate, reliable, and quantitave analysis on feeding (Itskov *et al.* 2014). This would potentially improve reproducibility for this phenotype, as the assays used in this project could be less accurate (i.e., the ruler measurements from a graduated capillary

in the CAFE assay) or more subjective (i.e., the observations of feeding events in the PE assay). However, as the results here are quite drastic and the 24-hour CAFE assay results reconcile with the PE assay, for the purposes of this project the assays used were adequate.

Data here shows that the dFoxO-null and DBD-mutant flies were also sensitive to both oxidative and xenobiotic stress. This is in line with other research as for instance, mammalian FoxO has shown to have an important role in regulating oxidative stress through upregulation of antioxidant enzymes, such as MnSOD and catalase, by binding directly to the promoter regions of these genes (Huang & Tindall, 2007; Kops *et al.* 2002). The presence of the *Drosophila* homologues *Sod2* and *Cat* identify a possible conservation of this protection, particularly as it has been found that there is an increase in expression of both dFoxO target genes *Sod2* and *Cat* upon exposure to H_2O_2, as well as a significant reduction in lifespan under normal conditions in *Sod2* mutants due to the inability to convert ROS, such as H_2O_2, to oxygen and H_2O for excretion (Subedi *et al.* 2017; Celotto *et al.* 2012). Therefore, due to the nature of these two genes as dFoxO targets, it would be expected that the increased expression and therefore protection afforded by these genes in the presence of H_2O_2 would be abolished, or at least diminished, in dFoxO-null and DBD-mutants explaining the sensitivity to oxidative stress in these mutants.

The role of FoxO in efficient biotransformation, particularly in detoxifying xenobiotics, has also been previously identified. By using IIS mutants that increased FoxO activity, xenobiotic metabolism was increased by causing the direct upregulation of antioxidants such as glutathione, where conjugation of this tripeptide to xenobiotics enhances their ability to be excreted and diminishes their susceptibility to this form of stress (Piper *et al.* 2008; Wang *et al.* 2014; Sipes *et al.* 1986). Therefore, by removing dFoxO activity either completely as with the nulls or by removing a functional DBD, these genes will not be upregulated during these types of stress leading to sensitivity and a reduction in survival time.

By comparing this data to that found in the literature, it is not surprising that without a functional dFoxO protein or DBD that these phenotypes occur.

3.4.3 *Drosophila* FoxO DNA-binding independent phenotypes

Interestingly, growth and survival under starvation, while dependent on dFoxO, did not require a functional DBD, potentially identifying DNA-binding independent roles for dFoxO in these processes.

Previous studies have shown that dFoxO is required for normal growth in *Drosophila* (Slack *et al.* 2011), and the data presented here shows that this function of dFoxO is not dependent on the DBD.

The size of the adult fly is determined during the developmental stages. During pupation, metabolic cues allow for the mobilisation of nutrients to developing cells to initiate normal growth. However, in the absence of dFoxO this is unable to occur leading to a reduced size of the resulting adults (Shingleton *et al.* 2005). Further research into the IIS pathway during growth using a temperature sensitive mutation for the insulin receptor (InR) has shown that the critical period for the influence of insulin signalling on growth is during mid-pupation (Shingleton *et al.* 2005).

Previous studies have also shown the various roles for FoxO in preventing starvation sensitivity and subsequent death (Tettweiler *et al.* 2005; Yuan Tang *et al.* 2011). It is well-reported that increasing metabolic stores, particularly lipids, and ensuring their mobilisation when needed increases starvation resistance (Brown *et al.* 2019). Sirt1 has also been identified as a possible target for these alterations that confer starvation resistance, as mutations here often lead to dysregulated lipid storage, abnormal lipid droplet size, starvation resistance, and insulin sensitivity (Hardy *et al.* 2018). This is interesting as FoxO is known to be closely associated with Sirt1 activity, where not only is Sirt1 able to activate FoxO via deacetylation, but FoxO is able to alleviate p53 suppression on Sirt1 via direct FoxO-p53 interactions (Wang *et al.* 2011; Zhang *et al.* 2011). Therefore, this latter process could possibly give an explanation why these effects on starvation resistance are independent of FoxO's ability to bind to DNA.

That these two phenotypes show similar responses is not out of line with previous research, as it is known that the same genes regulate growth and metabolism in *Drosophila* (however, this is not conserved into mammals) (Nayak & Mishra, 2021).

Overall, it is clear from the data presented that several dFoxO-associated phenotypes such as lifespan, fecundity, oxidative and xenobiotic stress survival, and feeding behaviour were not only reliant on dFoxO activity but also its ability to bind to DNA.

Removal of dFoxO completely conferred both sensitivity to starvation and inhibition of normal growth, asserting that these phenotypes are also dependent on dFoxO activity. However, the differential effects of dFoxO null mutation and mutation of the DBD on these phenotypes suggest that the presence of a functional DNA-binding domain for their normal regulation is dispensable. As both starvation survival and growth are highly energy dependent processes with a tight association to metabolism, further analysis into specific metabolic phenotypes were explored to shed more light on the underlying metabolic perturbations affecting these phenotypes.

Chapter 4

Assessment of the association between FoxO activity and metabolic phenotypes in Drosophila melanogaster

4. Assessment of the association between FoxO activity and metabolic phenotypes in *Drosophila melanogaster*

4.1 Introduction

The role of FoxO in regulating metabolic processes is well-known, where FoxO modulates a wide variety of actions in various metabolic organs to maintain appropriate metabolic homeostasis (Lu & Huang, 2011). This is possible due to the nutrient-dependent nature of FoxO regulation through the insulin signalling pathway (IIS), where FoxO activity is repressed in the presence of insulin during the post-prandial state (Eijkelenboom & Burgering, 2013).

For example, FoxO is already known to directly regulate the expression of gluconeogenic genes such as *phosphoenolpyruvate carboxykinase* (*Pepck*) and *glucose-6-phosphatase* (*G6pc*), as well as the atrophic muscle-specific *atrogin-1* which leads to muscle breakdown for the production of energy (Tanaka *et al.* 2010; Wang *et al.* 2016b). In addition, FoxO is also known as a regulator of pathways associated with lipid metabolism, where FoxO can modulate the expression of the adipokine adiponectin by binding directly to its promoter leading to reduction of lipid accumulation and fatty acid oxidation (Qiao & Shao, 2006; Yanai & Yoshida, 2019). Interestingly, FoxO also maintains the size and number of lipid storage vesicles called lipid droplets (LD) in adipocytes via the regulation of the autophagic fat-specific protein 27 effecting adipocyte differentiation and growth (Bielka & Przezak, 2021). Furthermore, FoxO is key in the maintenance and differentiation of pancreatic β cells, where loss of FoxO is often associated with increased oxidative stress and de-differentiation of β cells (Bielka & Przezak, 2021). Therefore, there are many ways in which metabolic phenotypes can be affected by aberrant FoxO activity.

The use of *Drosophila* to study these metabolic phenotypes is ideal as there are many similarities between *Drosophila* and other organisms, particularly when discussing metabolism. For example, as with mammals, carbohydrates are used as the primary energy source in *Drosophila* (Klepsatel *et al.* 2016). Therefore, dietary carbohydrates must be stored for utilisation during periods of stress or fasting. These dietary carbohydrates are broken down and transferred to the fat body where they are either converted into and stored as the branched polysaccharide, glycogen, or transformed into the disaccharide of glucose, trehalose, which is then released into the haemolymph for rapid deployment in various tissues (particularly flight muscles) (Hibshman *et al.* 2017; Chatterjee & Perrimon, 2021). Then, once carbohydrate stores are low, energy utilisation is switched to the most calorie dense form of metabolite

storage, the lipid triglyceride (TAG) enabling reservation of carbohydrate energy for obligate glucose utilisers (Cheng & White, 2011; Mergenthaler *et al.* 2013). Therefore, due to the intricate balance needed to maintain energy homeostasis and the critical nature of maintaining appropriate energy stores for different tissues, metabolic dysregulation can have a variety of unwanted effects in other phenotypes including growth and starvation survival.

4.2 Aims and objectives

In this section, the main aim was to assess the different metabolic functions of adult *Drosophila* to determine the method of *Drosophila* FoxO (dFoxO) transcriptional activity on various metabolic phenotypes, to elucidate whether the DNA-binding independent phenotypes observed could be caused by affects in the metabolism. The hypothesis was that there would be dFoxO-dependent DNA-binding independent effects in the modulation of metabolism, which could help explain the DNA-binding independent phenotypes observed earlier in the project.

To achieve this, coupled colorimetric metabolic assays and thin layer chromatography (TLC) were used to quantify the effects of dFoxO activity, or lack thereof, on the production or mobilisation and utilisation of key metabolic stores, namely glycogen, trehalose, and TAG.

This set of experiments helps to fulfil the overall aim of the project by determining the potential affects of dFoxO in metabolism and whether those effects can adequately explain the dFoxO-dependent DNA-binding independent processes observed in the previous chapter.

4.3 RESULTS

4.3.1 *DROSOPHILA FOXO* IN METABOLIC STORAGE

Metabolic dysregulation could potentially have knock-on effects in various other processes, particularly those known to be extremely energy demanding (for example, development). This metabolic dysregulation could manifest as differences in the ability to produce or maintain metabolic stores within the fly, or as differences in the ability of the fly to mobilise these stored nutrients appropriately and efficiently when required (Harshman & Schmid, 1997).

Quantitative measurements of metabolic storage molecules were therefore performed for the different *dFoxO* mutants to identify whether perturbations in dFoxO activity could lead to metabolic dysregulation and the ability to produce or mobilise the three core metabolic stores found in *Drosophila*: glycogen, trehalose, and TAG.

Carbohydrate storage was assessed by measuring the total amounts of glycogen and trehalose stores using simple coupled colorimetric assays (*Figure 4.1*).

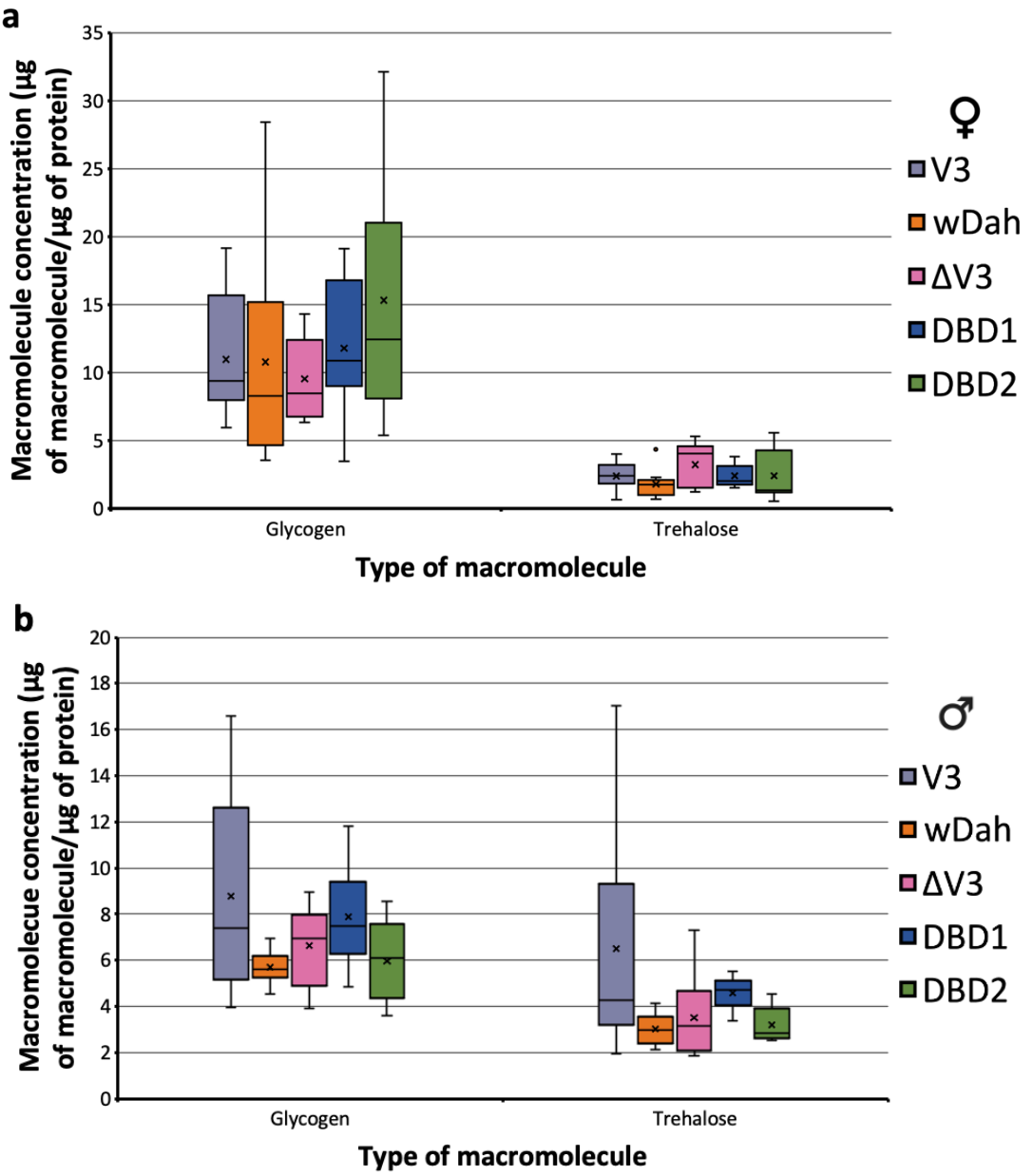

***Figure 4.1*. Measurements of glycogen and trehalose within different *dFoxO* mutants under fully fed conditions.**

Fully fed 10-day old adult (a) female and (b) male *Drosophila* of the indicated genotypes were homogenised, and the concentrations of different macromolecules were assessed. The results are shown as µg glycogen or trehalose per µg of protein for each genotype. Box and whisker plots show the minimum and maximum value (bars), upper and lower quartiles (box), median (line within box), and mean (x) (n = 10 replicates per genotype of 5 pooled flies each, glycogen data: Mood's Median and trehalose data: ANOVA with *post-hoc* Welch's t-test).

No significant differences were observed in the amounts of stored glycogen between any of the *dFoxO* mutant lines compared to control flies under fully fed conditions for either males or females.

No significant differences in the amounts of stored trehalose were observed between *dFoxO* mutants for female flies.

A significant difference in trehalose was observed ($p = 0.01$) between genotypes of male flies. However, *post-hoc* analysis showed that when considering unequal variance there were no significant differences in trehalose concentration compared to the V3 control for any of the other genotypes.

Therefore, this suggests that the storage of both glycogen and trehalose is independent of dFoxO activity, or can be rescued by other pathways, as even the null mutants were unaffected.

Similar to other organisms, including mammals, *Drosophila* store their lipids in the form of TAG. Previous research has shown that the presence of eye pigments, which were present in the *dFoxO* mutants but not w^{Dah} controls, may interfere with absorbance readings in the simple coupled colorimetric assays (Tennessen *et al.* 2014; Al-Anzi & Zinn, 2010). However, these simple coupled colorimetric assays are made more robust and reliable in quantifying *Drosophila* metabolic TAG stores when used in comparison and conjunction with TLC (Hildebrandt *et al*. 2011). Therefore, TLC was also carried out as a secondary assessment of lipid storage presence in the *dFoxO* mutants.

To assess how dFoxO activity affects lipid storage, total TAG levels were measured using simple coupled colorimetric assays and TLC (*Figure 4.2*). Oleic acid was also measured using the TLC method as it is a free unsaturated fatty acid that can produce a triglyceride called triolein after esterification with glycerol (Dolatabadi & Omidi, 2016). As such, as a component of a type of TAG, differences in oleic acid should be observed alongside differences in TAG giving another point of verification.

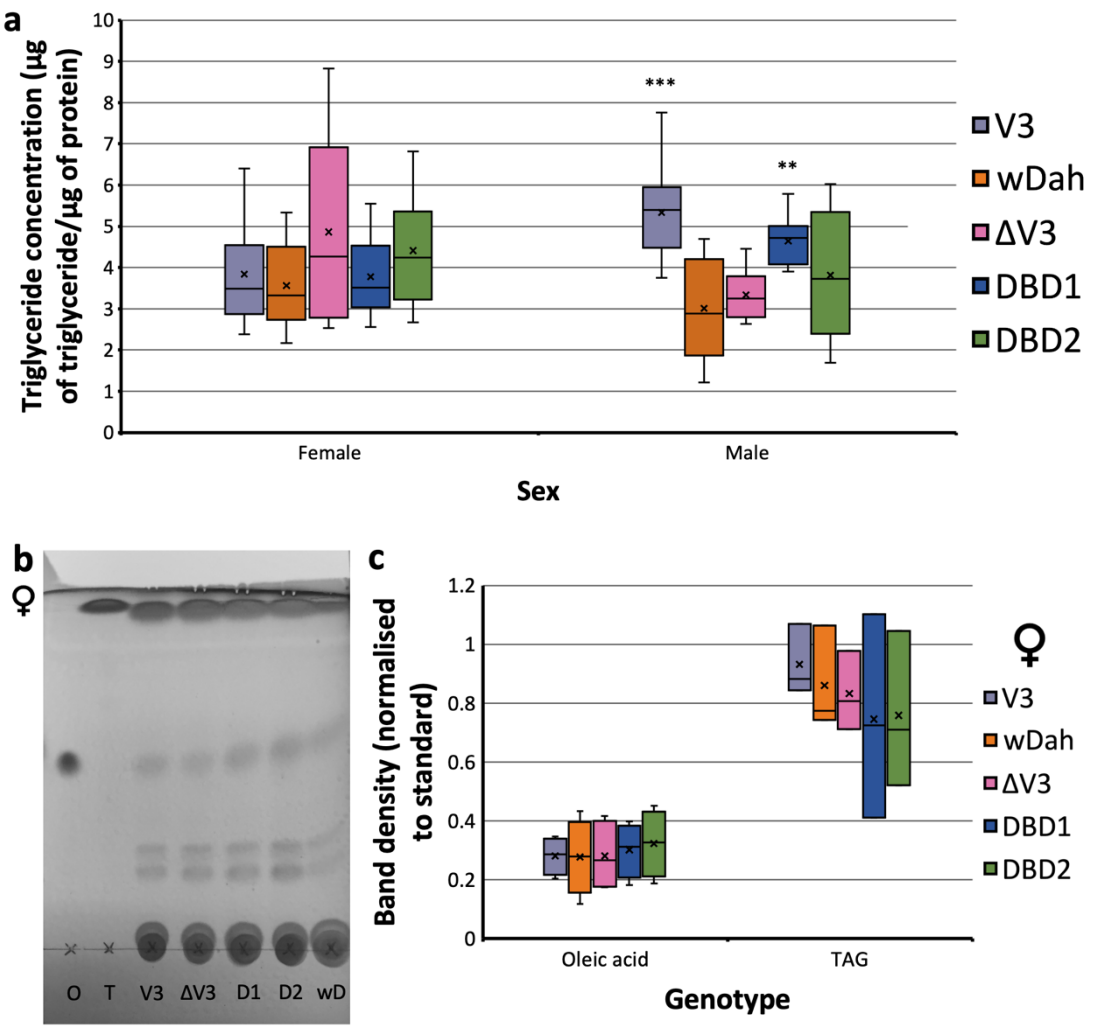

Figure 4.2. **Triglyceride (TAG) concentration and thin layer chromatography (TLC) assessment of various lipids in *dFoxO* mutants.**

(a) Fully fed 10-day old adult female and male *Drosophila* of the indicated genotypes were homogenised, and the TAG concentrations measured by coupled colorimetric assay. Concentration of TAG in the homogenate is expressed as µg TAG per µg of protein (n =10 replicates of 5 pooled flies each, $p < 0.01$ **, $p < 0.001$ ***, ANOVA and *post-hoc* Welch's t-test compared to w^{Dah}). (b) Representative image of a thin layer chromatography (TLC) plate with oleic acid (O) and TAG (T) standards, alongside extracted lipids from fully fed 10-day old adult female *Drosophila*. (c) quantification of identified lipid species in TLC using densitometry. Box and whisker plots show the minimum and maximum value (bars), upper and lower quartiles (box), median (line within box), and mean (x) (n = 4 replicates per genotype of 5 pooled flies except n = 3 replicates per genotype of 5 pooled flies for TAG in TLC), one-way ANOVA with *post-hoc* Welch's t-test).

No significant differences were observed in the amounts of stored TAG between any of the different *dFoxO* mutants under fully fed conditions for females using simple coupled colorimetric assays.

A significant difference was observed in the TAG concentration for male flies ($p = 0.001$). *Post-hoc* analysis showed the V3 and DBD1 flies compared to the w^{Dah} male flies in the fully fed state ($p = 0.0003$ for the V3 and $p = 0.002$ for the DBD1). However, there was no significant difference between the ΔV3 and DBD2 mutants compared to the w^{Dah}.

In the TLC analysis of the female flies, the same bands were present for each genotype indicating the presence of the same lipid species. No significant differences were observed in the amounts of TAG or oleic acid in any of the *dFoxO* mutants.

Taken together, these data indicate that the storage of TAG is independent of dFoxO activity, or can be rescued by other pathways, as even the null mutants were unaffected when using two different methodologies.

4.3.2 Utilisation of metabolic stores during starvation

Due to being unable to identify significant differences in the formation of the metabolic stores caused by the different *dFoxO* mutants under fully fed conditions, the next step was to assess macromolecule mobilisation and efficiency of utilisation during metabolic challenge.

Therefore, quantities of these same macromolecules were assessed in fly homogenates at different time points during starvation. Flies were collected after 0, 2, and 4 days of starvation for males with an additional 6-day time point for females. Trehalose (*Figure 4.3*) and glycogen (*Figure 4.4*) stores were then measured as before.

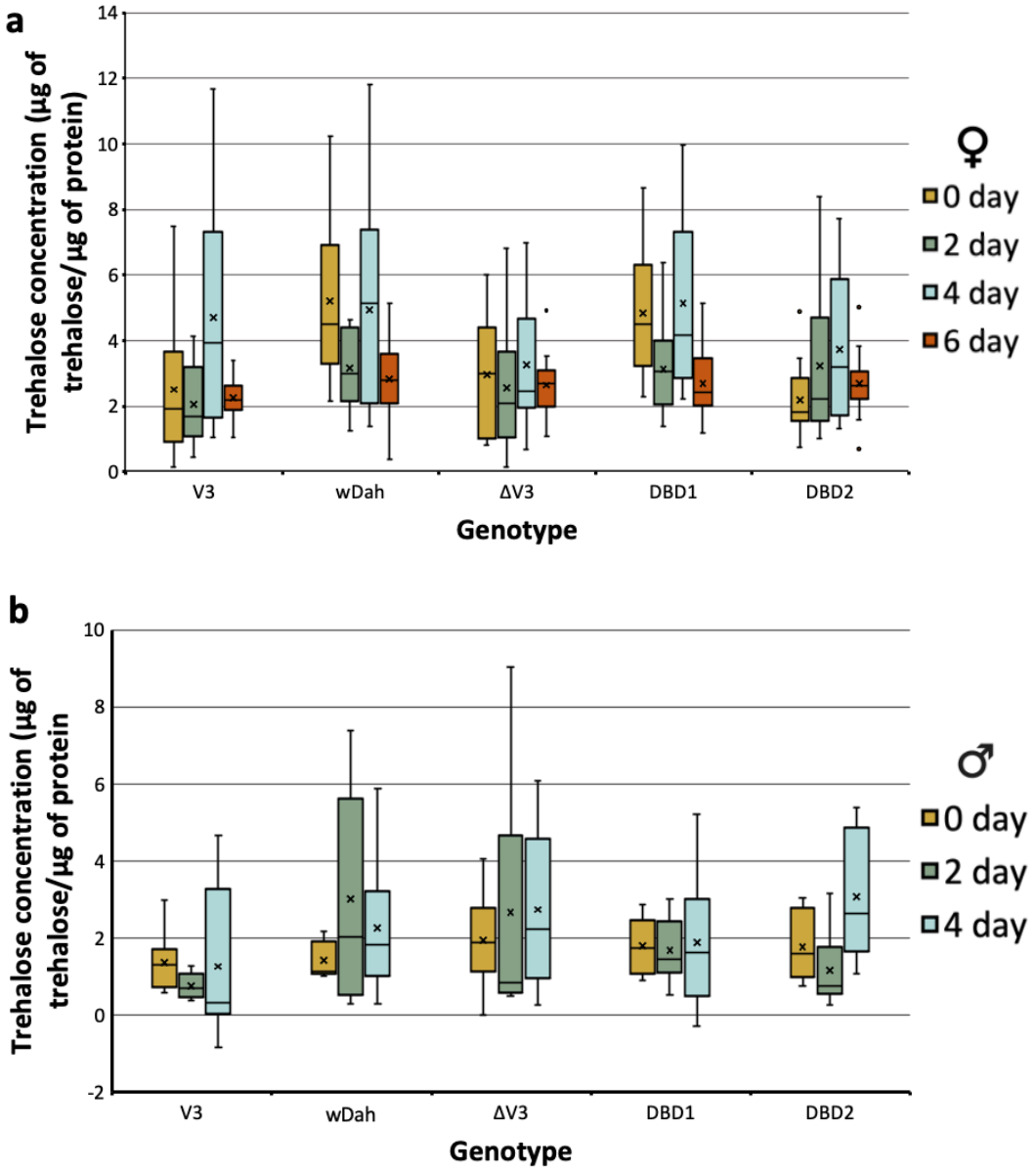

Figure 4.3. **Measurements of trehalose stores within different *dFoxO* mutants under starvation conditions.**

The trehalose stores of 7-day old adult (a) female and (b) male *Drosophila* of the indicated genotypes were measured. Flies were collected at 0, 2, and 4 days after starvation, with an additional 6-day time point for the females. Results are shown as µg trehalose per µg of protein for each genotype. Box and whisker plots show the minimum and maximum value (bars), upper and lower quartiles (box), median (line within box), and mean (x) (n = 10 replicates per genotype of 5 pooled flies each, generalised linear model).

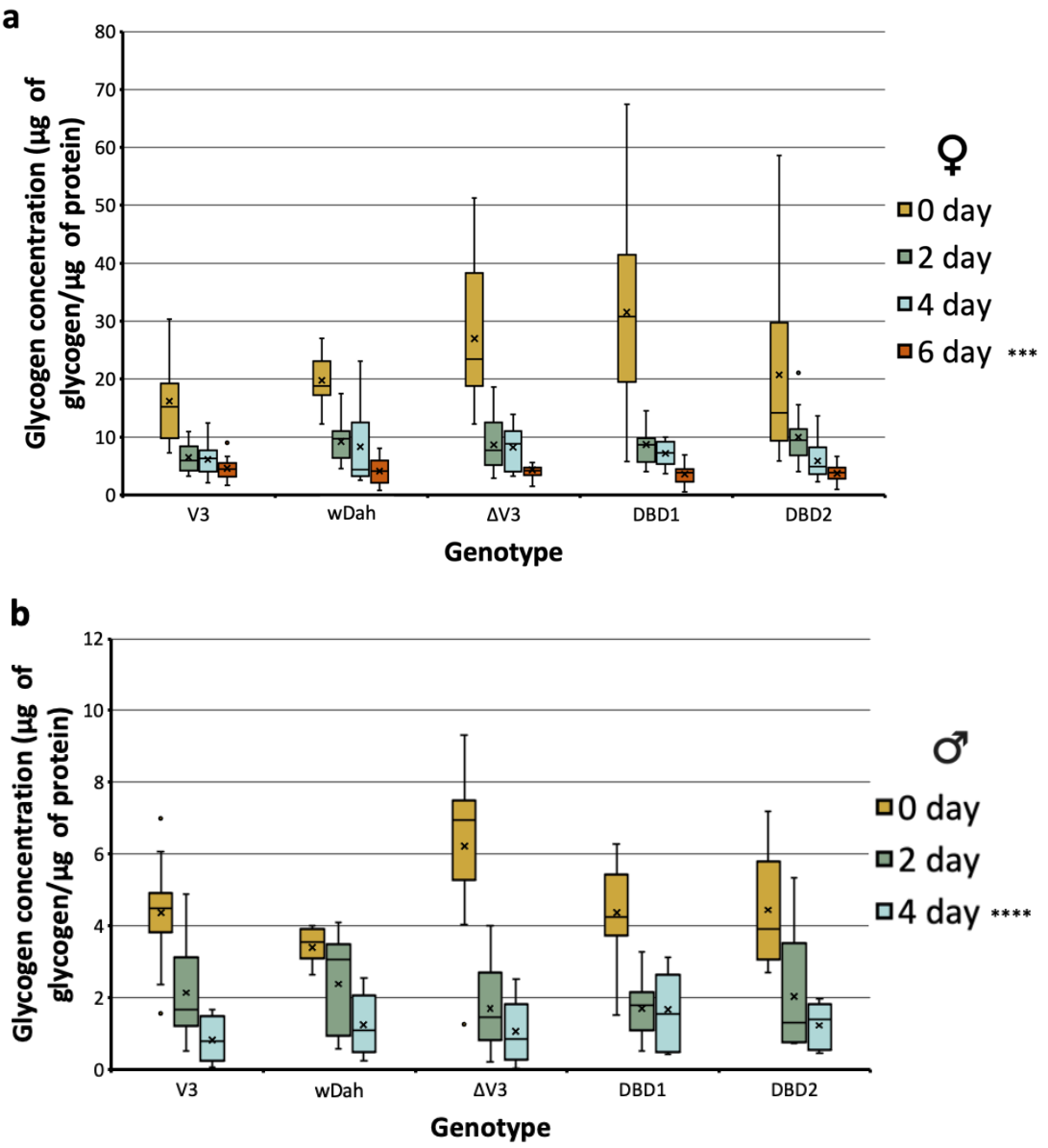

Figure 4.4. **Measurements of glycogen stores within different *dFoxO* mutants under starvation conditions.**

The glycogen stores of 7-day old adult (a) female and (b) male *Drosophila* of the indicated genotypes were measured. Flies were collected at 0, 2, and 4 days after starvation, with an additional 6-day time point for the females. The results are shown as µg glycogen per µg of protein for each genotype. Box and whisker plots show the minimum and maximum value (bars), upper and lower quartiles (box), median (line within box), and mean (x) (n = 10 replicates per genotype of 5 pooled flies each $p < 0.001$ *** for females, $p < 0.0001$ **** for males, general linear model with *post-hoc* ANOVA and Welch's t-test).

Trehalose stores showed a similar decrease across all genotypes over the course of the starvation period in both males and females. Statistical analysis showed no significant effect of genotype or time for females or males. There was also no

significant interaction effect (i.e., the effect of one variable did not depend on the value of the other) for either males or females.
With average differences between the 0-day and 6-day time points of -0.16 µg/µL +/- cumulative standard deviation 1.5, 2.2 µg/µL +/- 2.8, 0.71 µg/µL +/- 2.5, 1.6 µg/µL +/- 2.5, and -0.65 µg/µL +/- 6.3 for the V3, w^{Dah}, ΔV3, DBD1, and DBD2 female flies respectively. There were also average differences between the 0-day and 4-day time points of 0.74 µg/µL +/- 1.4, -0.59 µg/µL +/- 1.4, -0.35 µg/µL +/- 1.5, 0.11 µg/µL +/- 1.3, and -1.02 µg/µL +/- 1.4 for the V3, w^{Dah}, ΔV3, DBD1, and DBD2 male flies respectively.

Glycogen stores also showed a similar decrease across all genotypes in response to starvation with a significant effect of starvation time (females: p = 4.52E-5; males: p = 1.2E-4) but no effect of genotype. There was also no significant interaction effect (i.e., the effect of one variable did not depend on the value of the other) for either males or females.
With average differences between the 0-day and 6-day time points of 10.76 µg/µL +/- 7.6, 16.5 µg/µL +/- 19.6, 19.14 µg/µL +/- 13.56, 27.22 µg/µL +/- 18.6, and 10.4 µg/µL +/- 13.8 for the V3, w^{Dah}, ΔV3, DBD1, and DBD2 female flies respectively. There were also average differences between the 0-day and 4-day time points of 3.72 µg/µL +/- 2.2, 2.44 µg/µL +/- 1.3, 6.18 µg/µL +/- 3.6, 2.68 µg/µL +/- 1.8, and 2.91 µg/µL +/- 2.2 for the V3, w^{Dah}, ΔV3, DBD1, and DBD2 male flies respectively.
Due to the appearance of the data, separate statistical analysis of the fully fed glycogen concentration was carried out. It was found unlike in previous experiments carried out in this project, male ΔV3 mutant flies showed significantly higher levels of glycogen than other genotypes when fully fed (i.e., at the 0-day starvation time point) (p = 0.01).

Taken together, these data suggest that during starvation, glycogen but not trehalose stores are mobilised for energy usage in both female and male flies. Therefore, these actions on trehalose and glycogen mobilisation are not dependent on dFoxO activity or can be rescued by other pathways.

Over longer periods of stress or fasting, organisms switch from carbohydrate usage to lipid stores as a source of energy to allow for the remaining glucose stores to be used by obligate glucose utilisers (Mergenthaler *et al.* 2013).

Therefore, to determine whether dFoxO activity is required for that later mobilisation of TAG stores for energy usage, TAG concentration was measured during starvation (*Figure 4.5*).

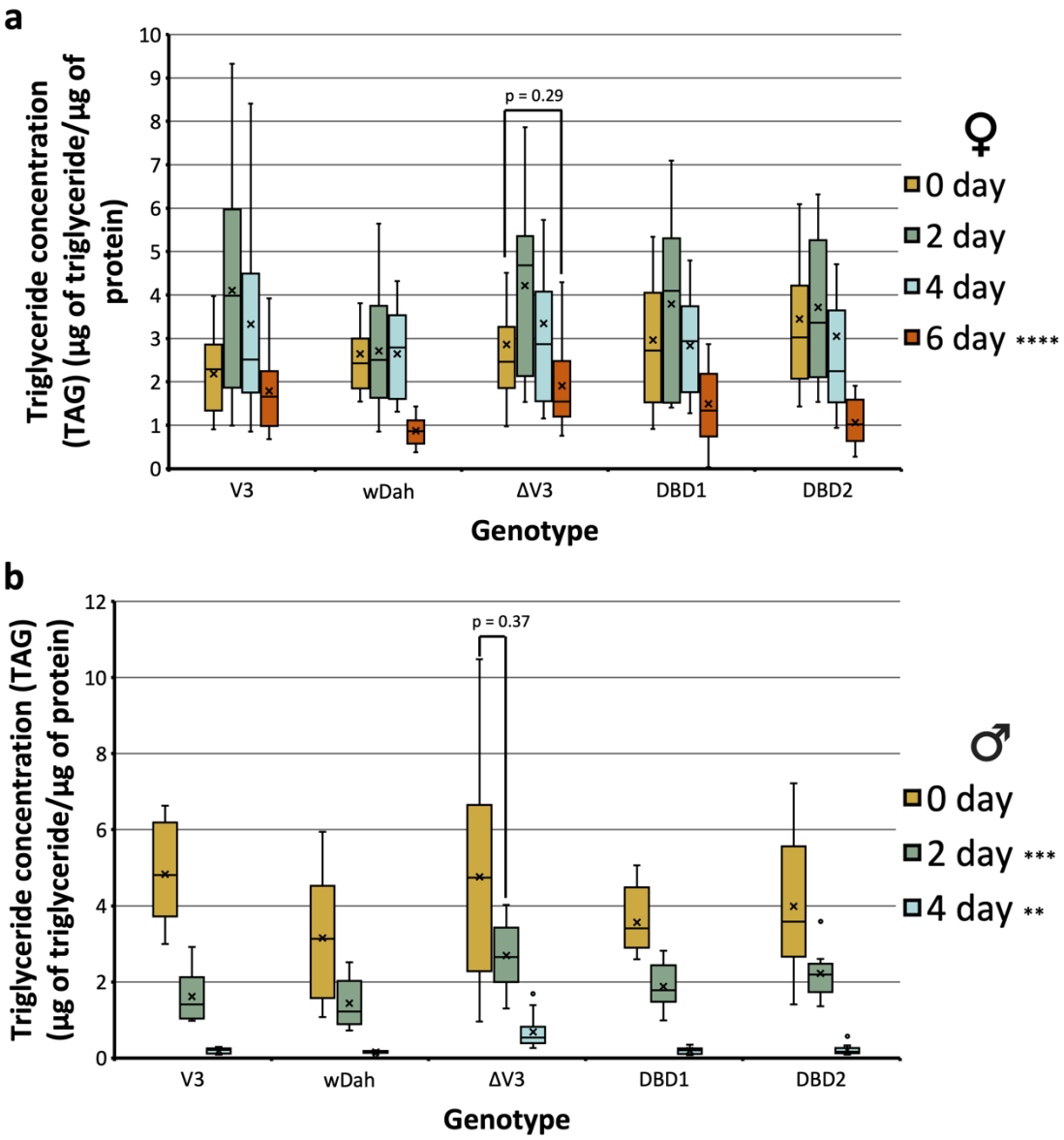

***Figure 4.5*. Triglyceride (TAG) concentration in different *dFoxO* mutants under starvation conditions.**

Triglyceride (TAG) concentration of 7-day old adult (a) female and (b) male *Drosophila* of the indicated genotypes were measured. Flies were collected at 0, 2, 4, and 6 days during starvation. Results are shown as µg TAG per µg of protein for each genotype. Box and whisker plots show the minimum and maximum value (bars), upper and lower quartiles (box), median (line within box), and mean (x) (n = 10 replicates per genotype of 5 pooled flies each $p < 0.01$ **, $p < 0.001$ ***, $p < 0.0001$ ****, generalised linear model with *post-hoc* Mood's median test).

For female flies, starvation time was found to be significant (p = 9.7E-9), as was observed with carbohydrate stores. In contrast however, for TAG concentration genotype was also significant (p = 0.02). However, there was no significant interaction effect (i.e., the effect of one variable did not seem to depend on the value of the other).

Post-hoc analysis showed that there was a significant decrease in TAG concentration between day 0 and day 6 times points for all genotypes (average difference between time points of 1.0 µg/µL +/- 0.8 (p = 0.005) for the V3, average difference between time points of 1.6 µg/µL +/- 1.1 (p = 1.3E-4) for the w^{Dah}, average difference between time points of 1.4 µg/µL +/- 1.3 (p = 0.01) for the DBD1, and an average difference between time points of 1.9 µg/µL +/- 1.2 (p = 5.4E-5) for the DBD2), expect the ΔV3 that was not significant (average difference between time points of 0.85 µg/µL +/- 1.1 (p = 0.29)).

For male flies, both starvation time (p = 2.2E-16) and genotype (p = 0.0003) had significant effects on TAG concentrations during starvation. However, there was no significant interaction effect (i.e., the effect of one variable did not depend on the value of the other).

Post-hoc analysis showed significant decreases at both time points for the V3 (after 2 days p = 7.7E-6 (average difference between time points of 3.4 µg/µL +/- 1.9); after 4 days p = 7.7E-6 (average difference between time points of 1.2 µg/µL +/- 0.9)), w^{Dah} (after 2 days p = 0.04 (average difference between time points of 2.3 µg/µL +/- 1.5); after 4 days p = 1.3E-5 (average difference between time points of 1.0 µg/µL +/- 0.8)), DBD1 (after 2 days p = 0.0003 (average difference between time points of 1.6 µg/µL +/- 1.2); after 4 days p = 7.7E-6 (average difference between time points of 1.6 µg/µL +/- 0.9)), and DBD2 (after 2 days p = 0.01 (average difference between time points of 1.4 µg/µL +/- 1.6); after 4 days p = 7.7E-6 (average difference between time points of 2.0 µg/µL +/- 1.1)) genotypes. However, for the ΔV3 mutants, there was no significant difference between the 0- and 2-day time points (average difference between time points of 2.1 µg/µL +/- 2.3 (p = 0.37)), but a significant effect after 4 days starvation p = 0.0003 (average difference between time points of 2.1 µg/µL +/- 1.2)).

Moreover, ΔV3 male mutants showed significantly higher TAG levels after 2- and 4 days of starvation compared to all other genotypes (after 2 days of starvation: p = 0.04; after 4 days of starvation: p = 0.004).

As the male ΔV3 flies showed an eventual significant reduction in TAG, the females were investigated further by exposing them to an even more prolonged starvation of

8 days, to see if this same eventual significant reduction in TAG was observed or if TAG stores remained the same throughout starvation (*Figure 4.6*).

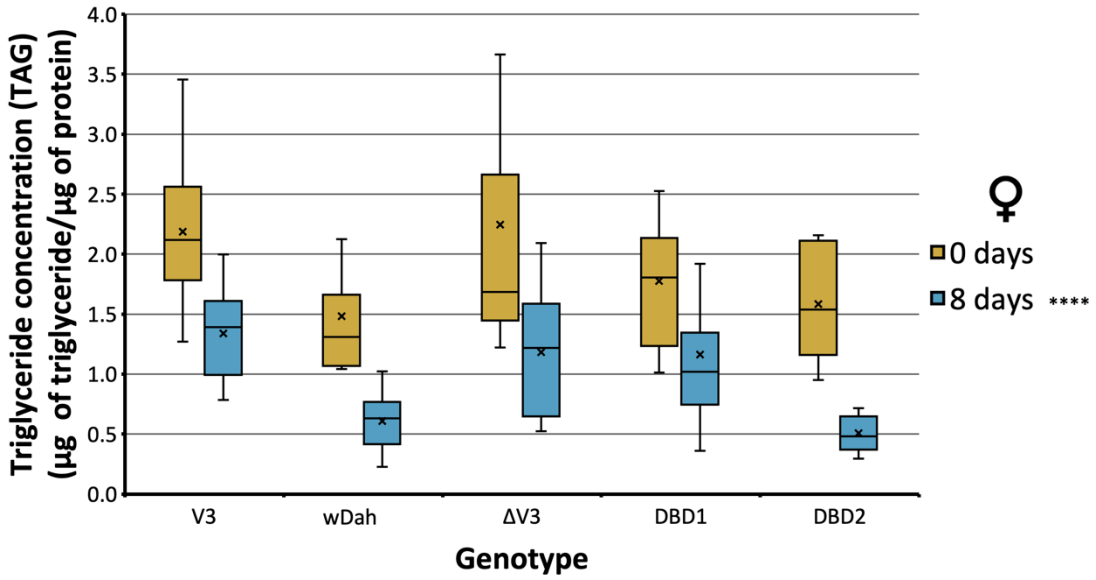

***Figure 4.6*. Triglyceride (TAG) concentrations after prolonged starvation in *dFoxO* mutant females.**
Triglyceride (TAG) concentration of 7-day old adult female *Drosophila* of the indicated genotypes was measured. Flies were collected after 0- and 8-days of starvation, where 0 days reflects the fully fed condition. The results are shown as µg TAG per µg of protein. Box and whisker plots show the minimum and maximum value (bars), upper and lower quartiles (box), median (line within box), and mean (x) (n = 10 replicates per genotype of 5 pooled flies each, $p < 0.0001$ ****, generalised linear model with *post-hoc* Mood's median tests).

Statistical analysis showed a significant effect of time (p = 3.8E-12) but not genotype for TAG concentration during long term starvation in female flies. There was also no significant interaction effect (i.e., the effect of one variable did not depend on the value of the other).

There was even a significant decrease in TAG levels in ΔV3 female mutants after this longer-term starvation (p = 0.01).
With average differences between the 0-day and 8-day time points of 0.73 µg/µL +/- 0.7, 0.74 µg/µL +/- 0.6, 0.49 µg/µL +/- 0.7, 0.87 µg/µL +/- 0.6, and 0.97 µg/µL +/- 0.6 for the V3, w^{Dah}, ΔV3, DBD1, and DBD2 female flies respectively.

Free fatty acid (FFA) quantification was also observed using these simple coupled colorimetric assays as another way of assessing TAG mobilisation, as during TAG

breakdown FFA are liberated and therefore a change in TAG concentration should also show a concomitant change in FFA concentration (*Figure 4.7*).

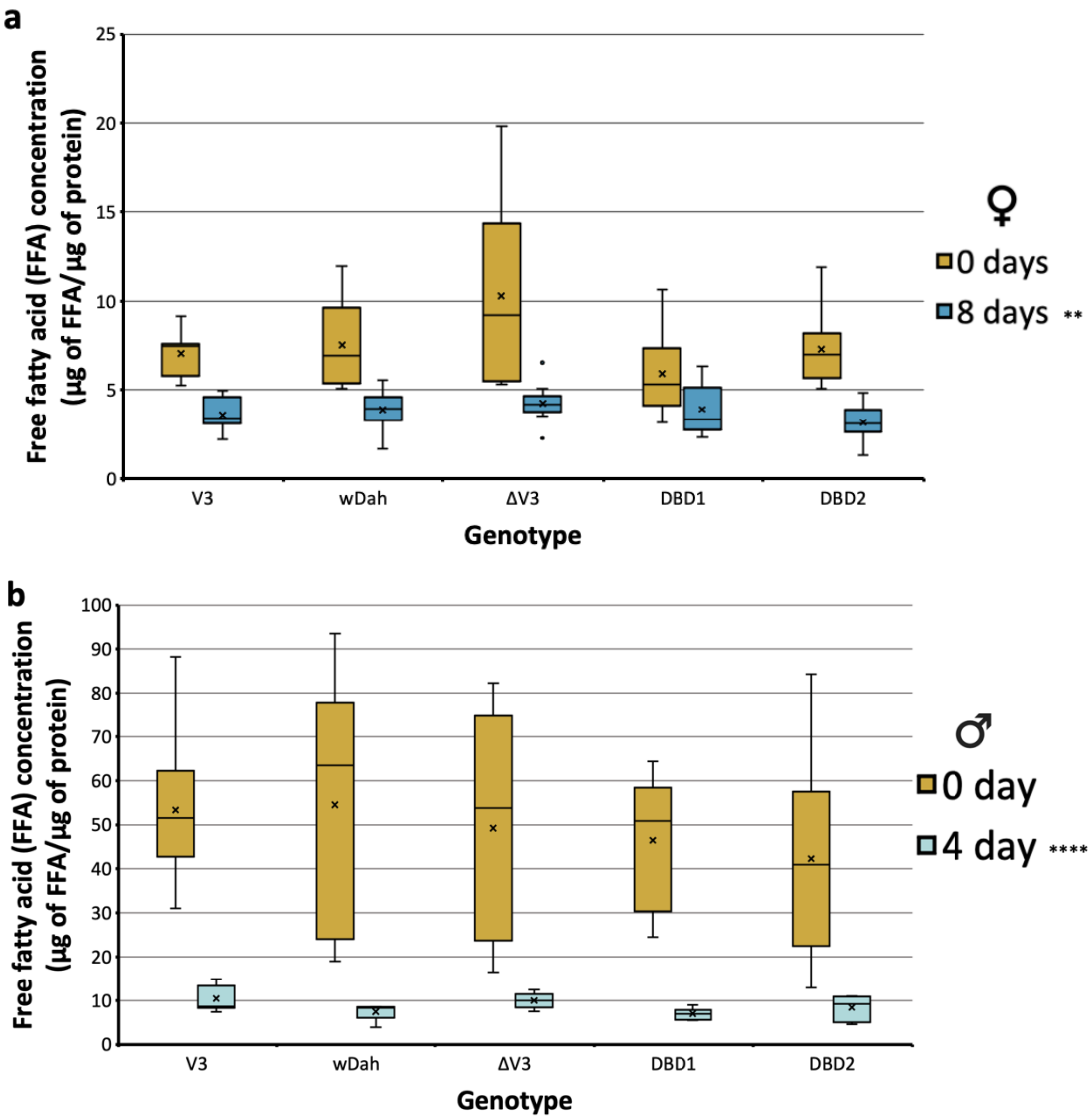

***Figure 4.7*. Free fatty acid (FFA) concentrations after prolonged starvation in *dFoxO* mutants.**

Free fatty acid (FFA) concentrations of 7-day old adult (a) female and (b) male *Drosophila* of the indicated genotypes were measured. Flies were collected at 0- and 8-days post-starvation for the females and 0- and 4-days post-starvation for the males. 0 days starvation reflects the fully fed condition. The results are shown as µg FFA per µg of protein for each genotype. Box and whisker plots show the minimum and maximum value (bars), upper and lower quartiles (box), median (line within box), and mean (x) (n = 10 replicates per genotype of 5 pooled flies each $p < 0.01$ **, $p < 0.0001$ ****, general linear model).

For females, statistical analysis showed there was a significant effect of 8-day starvation time ($p = 0.004$) but not genotype on FFA concentration as was observed with for TAG concentration under longer term starvation conditions. There was also

no significant interaction effect (i.e., the effect of one variable did not depend on the value of the other).
With average differences between the 0-day and 8-day time points of 4.07 µg/µL +/- 2.1, 3 µg/µL +/- 2.6, 5.05 µg/µL +/- 4.7, 2.49 µg/µL +/- 2.1, and 3.72 µg/µL +/- 2.6 for the V3, w^{Dah}, ΔV3, DBD1, and DBD2 female flies respectively.

Similarly, for males, a significant effect (p = 4.1E-5) was observed for time but not genotype. There was also no significant interaction effect (i.e., the effect of one variable did not depend on the value of the other).
There were also average differences between the 0-day and 4-day time points of 43.48 µg/µL +/- 30.9, 55.07 µg/µL +/- 31.3, 43.78 µg/µL +/- 27.9, 43.92 µg/µL +/- 22.8, and 31.79 µg/µL +/- 24 for the V3, w^{Dah}, ΔV3, DBD1, and DBD2 male flies respectively.

Taken together, these results suggest that there was a significant reduction in the breakdown of TAG stores within all mutants except the ΔV3 flies, at least during the first 2 or 6 days of starvation for males and females respectively. However, TAG concentration in the ΔV3 flies does eventually significantly decrease by days 4 and 8 of starvation for males and females respectively. Interestingly, a similar effect of delay in TAG mobilisation was not observed in the DBD mutants.

4.3.3 Modulation of circulating sugars

Drosophila contain two forms of circulating sugars within their haemolymph, glucose similarly to mammals, but also trehalose, the non-reducing sugar made up of two glucose monomers (Graham & Pick, 2017). These sugars, in conjunction with the above metabolic stores, are important in ensuring normal metabolic regulation, stress protection, and overall organism homeostasis.

In addition to the importance of these sugars during normal conditions, circulating sugars have also been implicated in the ability to survive starvation and ensure normal growth, and that the process of maintaining these sugars during metabolic challenge is dependent on DAF-16 (FoxO homologue in *Caenorhabditis elegans*)/FoxO activity (Hibshman *et al*. 2017; Matsushita & Nishimura, 2020). Due to this, and the lack of response seen on trehalose concentration using whole fly extracts, the concentrations

of these two blood sugars were therefore compared across the different *dFoxO* mutants in both fully fed and starved conditions (*Figure 4.8*).

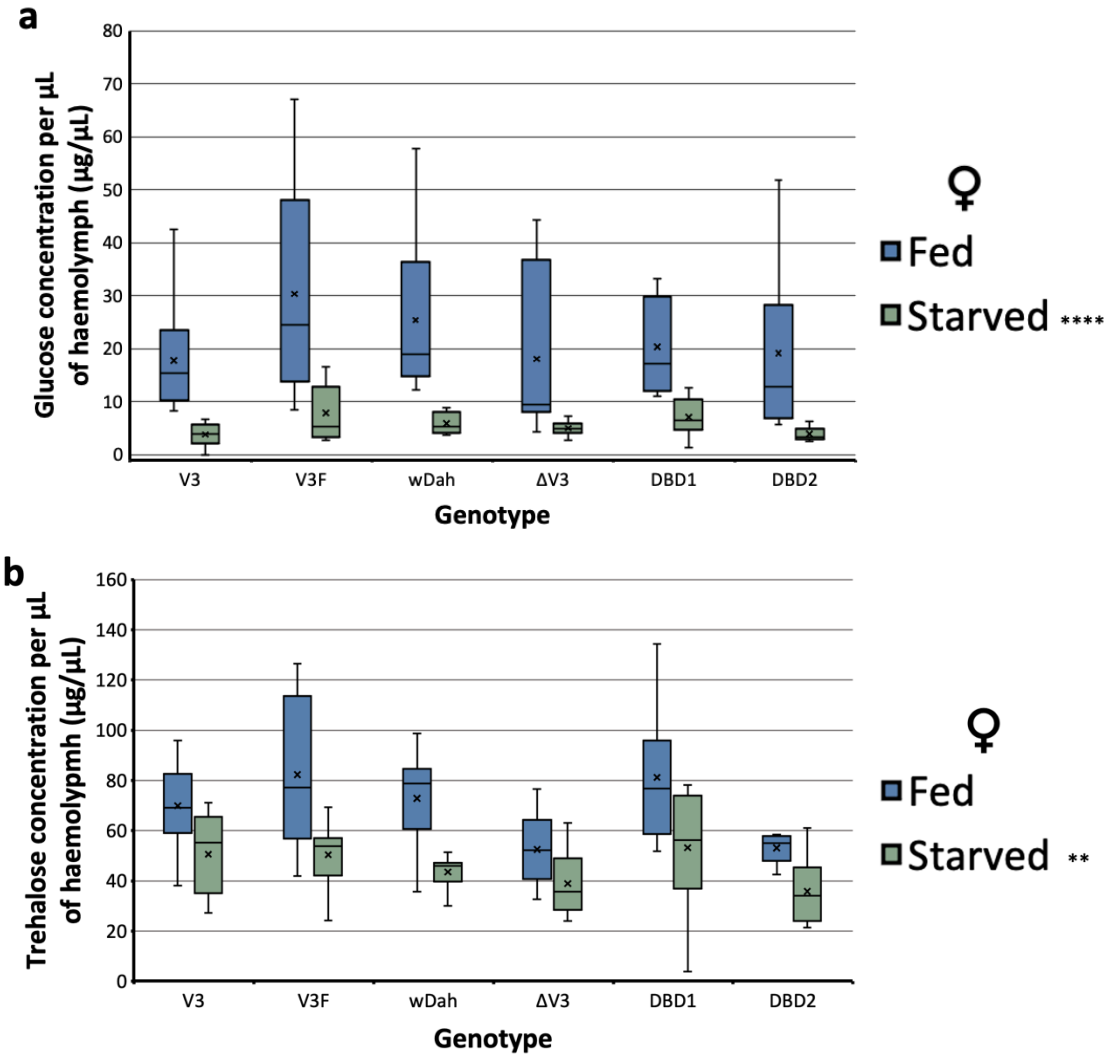

Figure 4.8. **Measurement of circulating haemolymph sugars in *dFoxO* mutants.** The circulating sugars of 7-day old fully fed or starved (using a 48-hour starvation period) adult female *Drosophila* were analysed. Results are shown as (a) µg of glucose or (b) trehalose per µL of haemolymph for each genotype and feeding condition. Box and whisker plots show the minimum and maximum value (bars), upper and lower quartiles (box), median (line within box), and mean (x) (n = 10 replicates per genotype of 20 beheaded flies each $p < 0.01$ **, $p < 0.0001$ ****, general linear model).

Statistcal analysis showed a significant effect of time (p = 1.0E-4) but not genotype on circulating haemolymph glucose for female flies. There was also no significant interaction effect (i.e., the effect of one variable did not depend on the value of the other) for either males or females.
With average differences between the time points of 19.81 µg/µL +/- 23.2, 23.22 µg/µL +/- 28.1, 34.32 µg/µL +/- 67.4 16.56 µg/µL +/- 15, 20.49 µg/µL +/- 28.6, and 22.42 µg/µL +/- 31.2 for the V3, V3F, w^{Dah}, ΔV3, DBD1, and DBD2 female flies respectively.

Statistcal analysis showed a significant effect of time (p = 0.004) but not genotype on circulating haemolymph trehalose for female flies. There was also no significant interaction effect (i.e., the effect of one variable did not depend on the value of the other) for either males or females.
There were also average differences between the time points of 9.03 µg/µL +/- 7.2, 19.13 µg/µL +/- 18.8, 13.6 µg/µL +/- 14.8, 4.37 µg/µL +/- 12.91, 10.59 µg/µL +/- 9.3, and 9.66 µg/µL +/- 14.1 for the V3, V3F, w^{Dah}, ΔV3, DBD1, and DBD2 male flies respectively.

This data suggests that there is no effect of dFoxO activity on haemolymph glucose or trehalose concentration in either the fully fed or starved state, indicating this process can be regulated independently of dFoxO.

4.4 Discussion

The main aim of this chapter was to assess specific metabolic phenotypes that could determine specific functions of dFoxO activity in regulating the storage of key metabolic macromolecules and/or the subsequent mobilisation and utilisation of those energy stores, and the requirement of the dFoxO DNA-binding domain (DBD) in modulating these various phenotypes associated with metabolism. The hypothesis stated that there would be dFoxO-dependent DNA-binding independent effects in the modulation of metabolism, which would explain the DNA-binding independent phenotypes observed earlier in the project.

4.4.1 *Drosophila* FoxO in modulating metabolic phenotypes

Some of the results found here were relatively unsurprising, for example there was seemingly no effect of dFoxO on glycogen production. This is unsurprising as this is a process that takes place during the fed or post-prandial state when FoxO is already inactivated by increased insulin signalling. For example, glycogen synthesis mostly occurs through regulation of *protein phosphorylase-1* (*PP1*) independent of FoxO, where insulin initiates its activation allowing for the subsequent dephosphorylation and activation of glycogen synthase, and the production of glycogen stores (Berg *et al.* 2002). Furthermore, the transcription factor, Mef2, is also a significant element to glycogen synthesis in the *Drosophila* adult, as it is able to upregulate key glycogenic genes, such as fat body *Hexokinase-C* (*Hex-C*), *Glycogen Synthase* (*GlyS*), and *Tret1-1*, a sugar transporter found in the fat body (Clark *et al.* 2013). A point of note however, is during the glycogen utilisation assay the 0-hour (i.e., fully fed) time point showed the ΔV3 males as having significantly more glycogen than other mutants, however as this was not observed previously and when all 20 fully fed replicates (i.e., from the separate fully fed and 0-hour time lapse analysis) are analysed together there is no significant difference observed. Furthermore, the Pierce™ 660nm Protein Assay reagent shows a realtively high level of protein-to-protein variation of 37% when compared to asays such as the bicinchoninic acid (BCA)-based protein assays that have a variation of 14.7% (Thermo Scientific, 2010). Therefore, this variability seen in the metabolic data is more likely due to variance within the protein assay or to a lesser extent in the fly population and is likely not caused by the mutation.

However, glycogen mobilisation was also seemingly regulated independently of dFoxO and as glycogenolysis is a catabolic process associated with the fasted state, it should logically be influenced in some way by FoxO activity. In fact, FoxO is well known to directly bind to and modulate expression of *G6pc*, which encodes the enzyme responsible for catalysing the terminal step in glycogen breakdown into glucose (Salih & Brunet, 2008). But there was seemingly no effect of loss of dFoxO activity on glycogen mobilisation during starvation, possibly due to the fact that other factors are able to compensate. For example, glycogenolysis is also regulated by the presence of glucagon and the subsequent initiation of cAMP/PKA signalling leading to the inactivation of PP1 increasing the rate of glycogen breakdown, including through the regulation of the *G6pc* gene, all of which occurs independently of FoxO (Janah *et al.* 2019; Wu *et al.* 2018).

Trehalose homeostasis and metabolism is important for regulating starvation survival and growth due to its protective nature and potential as an energy source (Hibshman *et al.* 2017; Matsushita & Nishimura, 2020). FoxO is known to modulate the expression of trehalose synthesis genes, *tps-1* and *trehalose phosphatase* (*CG5177*), as well as *trehalase*, the enzyme responsible for trehalose breakdown (Hibshman *et al.* 2017). Therefore, differences in the *dFoxO* mutants with regards to trehalose production and breakdown would be expected. However, the results shown here reveal this not to be the case. Initially, no change in trehalose concentration was observed for any dFoxO mutants however, by using whole fly extracts for the trehalose assay when most trehalose is found in the haemolymph, smaller changes that are likely to occur with this macromolecule may be masked or altered. This “masking” was also observed when circulating sugar levels were analysed in whole body extracts from *Akh* mutant *Drosophila*, but alterations were more easily captured when only haemolymph was used (Gáliková *et al.* 2015). Therefore, a subsequent haemolymph blood sugar assay was conducted, ultimately showing a significant decrease in blood glucose and trehalose during starvation but no difference between genotypes.

As with the other metabolic processes, there is also the possibility that trehalose metabolism is in part modulated independently of FoxO explaining the phenotypes observed here. For example, hormones such as, the juvenile hormone (JH) and 20-hydroxyecdysone (20E) have been implicated in the control of trehalose metabolic genes, particularly during development (Shukla *et al.* 2015). In addition, JH has been

implicated in regulating trehalase to maintain proper starvation survival in the red flour beetle, *Tribolium castaneum*, where reducing JH decreases trehalase in the fat body, decreasing carbohydrate metabolism and increasing starvation resistance (Xu *et al.* 2013).

That blood glucose concentrations significantly change regardless of genotype is not unsurprising as there are many ways in which glucose can be utilised and decreasing blood glucose during starvation is well documented (Berg *et al.* 2002; Watford, 2015). During the fed state, glucose is removed from the haemolymph due to insulin action upregulating the insulin-responsive glucose transporter GLUT4 expression (independently of FoxO due to its inactivation) leading to some glucose being removed from the circulation and either stored or utilised in the tissues for energy (Soeters *et al.* 2012). This process continues even in the starved state, where despite being drastically reduced at around 44%-50% of what is seen during the fed state, there is still glucose uptake that occurs from the circulation during starvation through remaining GLUT4 transporters that are not sequestered in storage vesicles (Soeters *et al.* 2012; Leto & Saltiel, 2012). However, the amount of GLUT4 proteins that are lost during starvation is controversial, from some studies finding no difference even after 72 hrs starvation to studies that show a loss of up to 50% (Vendelbo *et al.* 2012; Leto & Saltiel, 2012). Regardless, as GLUT4 expression is regulated independently of FoxO activity, this could therefore explain why all genotypes show the same response here.

Results of the lipid assays show that there are seemingly no differences in lipid storage between the different genotypes for female flies, but a significant difference between various genotypes for the males. This could either be a sexually dimorphic response or, as the ΔV3 and w^{Dah} are not significantly different from each other and the V3, DBD1, and DBD2 are not significantly different from each other could be due to the leftover reinsertion sequences that the ΔV3 and w^{Dah} do not possess. However, these are both unlikely as the DBD2 is also not significantly different from the ΔV3 or w^{Dah} indicating that the artefact sequences are likely not having an effect, and because this strange variety in significance level was not observed in the later TAG mobilisation assay. Where, similarly to glycogen above, when analysing all 20 fully fed replicates (i.e., from the separate fully fed and 0-hour time lapse analysis) together there is no significant difference observed, therefore this variability is likely due to variance within the assay or fly population and is not caused by the mutation.

Under normal conditions, FoxO has a role in modulating lipogenesis by disrupting the formation of transcriptional complexes to inhibit the actions of the sterol regulatory element-binding proteins 1c (SREBP1c), which are known to upregulate lipogenic genes such as *fatty acid synthase (FASN)* (Deng *et al.* 2012; Sekiya *et al.* 2007). Consequently, it could be assumed that a loss of FoxO could possibly lead to increased storage of lipids, something that is not replicated in the results shown here. However, insulin signalling is not the only pathway implicated in modulating lipogenesis. The Mondo-Mlx signalling pathway, a key glucose-sensing pathway, can also induce lipogenesis and TAG storage in *Drosophila* through the activation of the transcription factor Sugarbabe*,* which in turn activates the genes *FASN* and *Acetyl-CoA Carboxylase* (*ACC*)*,* both key drivers of lipogenesis (Mattila *et al.* 2015). In support of this, it has been shown in liver-specific knock outs of FoxO1 (L-FoxO1) and FoxO1-DBD in mice that there is no change in *ACC* transcription levels compared to controls (Cook *et al.* 2015). Furthermore, the glycogenic transcription factor Mef2 (mentioned above) also has lipogenic capabilities, wherein it can regulate both *FASN* and *ACC*, as well as the diacylglycerol transferase, *midway* (*mdy*) (Clark *et al.* 2013). Therefore, it is likely that these pathways are able to rescue any aberrations in FoxO/insulin signalling, allowing for the normal production of lipid stores observed here.

Results also show that for both males and females there is a possible delay during starvation in the mobilisation of lipids within the ΔV3 mutants that does not occur in the DBD mutants. This delay in TAG mobilisation in the ΔV3 mutants (observed at day 2 for the males and 6 for the females) seemed to correct itself by day 4 or day 8 of the starvation time-course for males and females respectively. However, by this time-point in the starvation assay ~80% of the null flies are already dead. Therefore, maintaining efficient macromolecule utilisation during the later stages of starvation may be most critical in ensuring normal starvation survival.

However, that lipids are mobilised at all during starvation in the ΔV3 is slightly unexpected as it is well known that FoxO is a main promoter of the carbohydrate-to-lipid switch and lipolysis. Therefore, it would be anticipated that flies lacking dFoxO activity would be unable to make this switch and subsequently lipid stores would remain unused during starvation (Cheng & White 2011).

FoxO is a major modulator of lipolysis and the release of insulin-mediated suppression on FoxO enables fat mobilisation (Vihervaara & Puig, 2008; Kühnlein,

2012). This FoxO-dependent modulation results in the upregulation of several lipases including *brummer* (*bmm*) (the *Drosophila* homologue to mammalian adipose triglyceride lipase (ATGL)) and *dLip4* (Vihervaara & Puig, 2008; Chakrabarti & Kandror, 2009; Kang *et al.* 2017). FoxO-dependent upregulation of *bmm*, one of the major lipases involved in lipid storage mobilisation, is dependent on DNA-binding due to the presence of FoxO-binding sites within the *bmm* gene promoter (Chakrabarti & Kandror, 2009). As such, it would be expected that flies without either dFoxO in its entirety or just its functional DBD, would be unable to catabolise TAG for energy. However, similarly to the other processes, lipolysis can also be influenced by other pathways. For example, other transcription factors can modulate key *Drosophila* lipolytic genes. One such transcription factor is Ci, initiated by the Hedgehog signalling pathway in the *Drosophila* fat body, Ci binds directly to and promotes the upregulation of the *bmm* gene, initiating lipolysis independently of dFoxO (Zhang *et al.* 2020b). This rescuing of or the presence of more essential long term metabolic modulators controlling DBD-dependent facets of this lipid mobilisation process therefore could explain why lipid mobilisation can eventually occur even in the ΔV3 mutants.

Interestingly, this is also shown by Cook *et al.* (2015) who describe how chow-reared FoxO1 DNA-binding deficient mice are able to modulate hepatic lipid metabolism on multiple levels, including through gene transcription or as a DBD-independent co-regulator. Where, similar to results shown here, during the fasted state liver TAG of the L-FoxO1 (liver-null) mice was higher and showed a smaller decrease between the fed and fasted state compared to the FoxO1-DBD, however this was not statistically significant due to interindividual variation (Cook *et al.* 2015). Despite the lack of statistical significance, this could support the identification of the initial stages of TAG mobilisation as a possible area of DBD-independent modulation and as results reconcile with those found here, it also provides a good indication that the effects in lipid mobilisation seen in this project with *Drosophila* could be evolutionarily conserved. However, the mechanism of the modulation of DBD-independent TAG mobilisation in *Drosophila* or mammals has yet to be elucidated.

Altogether, this previous research highlights both DBD-dependent and DBD-independent modulation for TAG mobilisation by FoxO. Therefore, it could be that whilst the DBD-dependent portions of this process can be rescued by other pathways, the DBD-independent initial stages of TAG mobilisation cannot with dFoxO seemingly essential for proper modulation of this area of metabolism.

An important note is that this response is seen for both males and females, however it does seem to be more easily observed using these assays in the male mutant flies. This may be due to females having a more complicated lipid biology than the males as reproduction (i.e., egg production and laying) would need to be considered. For instance, the nutritional status of *Drosophila* females (such as the onset of starvation) effects the development of the egg chamber leading to apoptosis and the reabsorption of macromolecules, like lipids, from the lipid droplets within these egg chambers into other tissues for use as energy (Terashima & Bownes, 2006; Welte, 2015).
Furthermore, there is the potential for the sex peptide (a seminal fluid protein key for regulating female fecundity that is present within mated females) to alter their lipid metabolism by altering gene expression (e.g., upregulation of the *bmm* gene) to ensure the metabolic demands of reproduction are met, or by increasing reproduction altogether (White *et al.* 2021).
A way of correcting for this could possibly be to use either virgin females or females reared under a controlled-mated environment. The ideal scenario would be to use more robust techniques, such as mass spectrometry to identify exact species and quantities of lipids present or, as in Mills *et al.* (2018), use quantitative magnetic resonance (QMR) to estimate fat and lean body mass. However, as whether the potential differences in these lipids was unknown when the experimental design was produced, it made more economical sense in both time and money to use a simpler technique for the preliminary findings and then employ these techniques if more in-depth analysis is required.

To ensure a robust analysis with regards to lipid metabolism, TLC was carried out in conjunction with simple coupled colorimetric assays. TLC was used as a secondary assessment of the presence and quantity of various lipid species in these *dFoxO* mutants. Previous research has shown that the presence of eye pigments, which are present in the *dFoxO* mutants but not w^{Dah}, may interfere with absorbance readings, with pigments potentially accounting for up to half of recorded absorbance measurements (Tennessen *et al.* 2014; Al-Anzi & Zinn, 2010). Therefore, the coupled colorimetric assays are made more robust and reliable in quantifying *Drosophila* metabolic stores when used in comparison and conjunction with the TLC method (Hildebrandt *et al*. 2011).

Despite these advantages, there were bands present within the TLC that remained unidentified due to lack of lipid standards and information regarding the Rf values of *Drosophila* lipids. However, other examples of TLC in various organisms (such as, green microalgae, bacteria (e.g., *Rhodococcus* and *Williamsia*), and *Drosophila*) identify these lower bands as the TAG precursor diacylglycerol (DAG) in one or both of its possible forms (1,2 DAG or 1,3 DAG), or DAG in conjunction with either monoacylglycerols (MAG) or sterols (Pal-Nath *et al.* 2017; Baumbach *et al.* 2014; Nahar *et al.* 2020). Based on the TLC plates produced using extracted *Drosophila* lipids and how close together these two bands appear, it is highly likely these smaller unidentified bands are the two forms of DAG (Baumbach *et al.* 2014).

Overall, it is clear from the data presented that the role of dFoxO in metabolism, or lack thereof, was varied. dFoxO activity was not associated with the production of carbohydrate or lipid stores and while the mobilisation and usage of carbohydrate stores was comparable between *dFoxO* mutants and controls, possibly indicating that for these processes there was a potential rescuing of these phenotypes in a dFoxO-independent manner or that FoxO is not an essential short-term metabolic modulator. However, differences were observed in ΔV3 mutants in the mobilisation of lipid stores indicating a possible effect of dFoxO-dependent DNA-binding independent modulation in this area of metabolism. Any differential phenotypic effects between the ΔV3 and the DBD-binding mutants are likely to represent differences in the activation of gene expression. Therefore, further analysis of gene expression within these mutants may reveal the underlying mechanisms causing these effects on TAG mobilisation.

Chapter 5

Transcriptomics showing the effects of different dFoxO mutations

5. TRANSCRIPTOMICS SHOWING THE EFFECTS OF DIFFERENT *FOXO* MUTATIONS

5.1 INTRODUCTION

The ability for FoxO to bind to other co-factors and use this activity to modulate various processes has been identified and reviewed in several studies (van der Vos & Coffer, 2008; Cook *et al.* 2015; Huang & Tindall, 2007; Rudd *et al.* 2007). However, more in-depth analysis into how these interactions affect gene expression and the knock-on effects these changes in gene expression cause phenotypically (particularly in metabolism) are few and far between.

Some clear examples have been put forward in recent years, such as the usage of FoxO's polyQ domain to produce coiled-coil to coiled-coil interactions with the spinocerebellar ataxia type 3 protein (SCA-3) to regulate gene expression (Kwon *et al.* 2018). This interaction allows for SCA-3 proteins with an expanded polyQ region to localise to the nucleus of *Drosophila* neurons and create abnormal dendritic phenotypes often associated with neurodegeneration, such as terminal dendrite defects and poor locomotion (Kwon *et al.* 2018).

Regarding metabolism, activity caused by FoxO protein-protein interactions has been reported alongside the juvenile hormone (JH) signalling pathway transcription factor, Krüppel-like homologue-1 (Kr-h1) (Kang *et al.* 2017). This interaction showed evidence of crosstalk between JH signalling and insulin signalling, where Kr-h1 binds to the transactivation domain (TAD) of the FoxO protein causing a downregulation of the FoxO target *bmm* (Kang *et al.* 2017). This interaction allows for lipolysis to be tightly regulated during development by the juvenile hormone (JH) signalling pathway.

Furthermore, Cook *et al.* (2015) used a previously defined mammalian FoxO1 DNA-binding domain (DBD) mutant (i.e., N208A, H212R) with an additional mutation (K219R) in mice to identify whether the modulation of carbohydrate and lipid metabolism occurred independently of FoxO's ability to bind to DNA. As has been shown previously with the *FoxO* mutants used in this project, these mutants were unable to drive luciferase activity in connection with the insulin responsive element (Cook *et al.* 2015). Subsequently, these mutants were used to identify that many processes were required DNA-binding activity such as glucose production, where an approximate 30% decrease in both basal and cAMP/dex-stimulated glucose production was observed in the FoxO1-DBD and FoxO1-null compared to controls with associated decreases in gluconeogenic genes, such as *Gpc* and *Pck1* which showed reduction of >80% and ~40% respectively (Cook *et al.* 2015). Another DNA-

binding dependent process identified was the inhibition of lipogenesis which ultimately led to hepatic steatosis and an almost 50% increase in liver triglyceride (TAG) levels potentially due to increases in the mRNA of lipogenic regulators *Fasn*, *Gck*, and *Scd1* (Cook *et al.* 2015). Alongisde these DBD-dependent discoveries however, one of the key findings of this study showed TAG liver content could potentially be modulated via FoxO-dependent DNA-binding independent processes, where after fasting liver specific FoxO1-null mice do not show as great a decrease in liver TAG levels compared to their fed state as the FoxO1-DBD or control mice (Cook *et al.* 2015). However, unfortunately there was no gene expression analysis carried out that could explain this phenotype or the mechanisms by which it is controlled by FoxO-protein binding interactions.

These examples, therefore, whilst interesting, still leave gaps within the literature as these either identify FoxO as the protein being affected rather than the effector, or do not provide in-depth analysis regarding FoxO's DNA-binding independent functions in metabolism. Therefore, considering the future applications of identifying the targets of FoxO to treat metabolic disorder, it is important to realise and analyse the different aspects of this form of FoxO modulation.

One way of assessing dFoxO transcriptional activity in an in-depth manner is to use RNA-sequencing (RNA-seq). The transcriptome consists of all of the gene transcripts in a cell or organism and the quantity of the transcripts that are present at any given point (Wang *et al.* 2009b). RNA-seq technology takes extracted RNA and converts it to its complementary DNA (cDNA), which is subsequently sequenced using a high throughput process from both ends in a process called paired-end sequencing creating forward and reverse reads (i.e., small sequence fragments) of around 30-400bp (Wang *et al.* 2009b). Paired-end sequencing offers advantages over single-end sequencing, as it more likely ensures accurate mapping to a reference genome (Risca & Greenleaf, 2015). These reads are then aligned and mapped to a reference genome (in this case, *Drosophila* dm6) from which counts of each read can be produced allowing for the analysis of differential gene expression between variables. The use of RNA-seq in this project opposed to other methods is key, as due to low levels of FoxO proteins within the cell and the extremely transient interactions they produce, a suitably sensitive method is needed (Perkins *et al.* 2010). Therefore, more common sequencing techniques may not be able to achieve this high level of

sensitivity, as techniques such as microarrays have more stringent limits on quantification levels where the dynamic range in which transcripts can be identified can be up to 100-fold smaller than for RNA-seq (Wang *et al.* 2009b). Another key advantage of this technique over microarrays is the lack of background signal that may be produced, as all reads are mapped to unique sequences within the genome making RNA-seq data highly reproducible across replicates (Wang *et al.* 2009b).

5.2 Aims and objectives

In this chapter, the main aim was to assess the effects of the different *dFoxO* mutants on gene expression under both fully fed and starved conditions. This would determine if the genes found to be differentially expressed between conditions could be used to identify potential mechanisms for how FoxO modulates these metabolic processes. The hypothesis was that there was a difference in gene expression in these *dFoxO* mutants during starvation, that could be leading to the observed differences in dFoxO activity, particularly with regard to metabolic phenotypes.

To achieve this, RNA was extracted from 7-day old adult female *dFoxO* homozygous mutant flies that were either fully fed or subjected to starvation conditions for 72 hours. The mutants chosen were the phenotypically wild-type dFoxO-V3-3xFLAG (V3F), the dFoxO-null dFoxO-ΔV3 (ΔV3), and the DBD mutant with two amino acid alterations dFoxO-DBD2-3xFLAG (DBD2). Females were chosen as standard to allow for comparisons between other datasets, which also used female flies. RNA-seq was then performed to analyse differences in gene expression. Quantitative reverse transcription polymerase chain reaction (qRT-PCR) and comparisons to previously published microarray data were also used to validate the gene expression changes identified by RNA-seq analysis.

This set of experiments helps to fulfil the overall aim of the project by determining potential mechanisms for dFoxO in modulating metabolic phenotypes.

5.3 Results

5.3.1 RNA-sequencing of *Drosophila FoxO* mutants

RNA-seq of the different *dFoxO* mutants was carried out to investigate the changes in gene expression that occur during starvation and classify those changes in relation to dFoxO's transcriptional activity.

Of the *dFoxO* mutant lines the V3F was chosen over the dFoxO-V3 as the DBD mutants also contain 3x FLAG tags therefore, using the wild-type *dFoxO* mutant with the FLAG tags ensures any effects of the FLAG tag on gene expression (however unlikely) are accounted for. Of the two DBD mutants the DBD2 was chosen as although there was unlikely to be much of a difference between the two, the DBD2 has 2 amino-acid alterations in its DBD making it a more robust choice in the event that the DBD1 possesses some residual DNA-binding, which seemed to be the case during the ChIP assay.

Adult female flies of the indicated genotypes were either fully fed or subjected to 72-hours under starvation conditions. Previous research has suggested that for *Drosophila* 12 hours starvation would be considered a 'short-term' starvation period at the gene level and over 36 hours a 'long-term' starvation period (Sudhakar *et al.* 2020). Therefore, by using a 'long-term' starvation period this will more likely encompass any changes in lipid metabolism that could be affecting the metabolic phenotypes observed previously.

5.3.1.1 Quality control of the RNA-sequencing data

The first step for analysing the RNA-seq data produced from the various adult female *dFoxO* mutants under different nutritional conditions was quality control. Carrying out quality control checks on the raw data allows for any errors introduced during sequencing (i.e., calling of incorrect nucleotides) to be identified, avoiding misinterpretation and bias that could arise due to misalignment or loss of reads.

Quality control provides a simple overview of the quality of the raw sequence data and was carried out for all the mutants in either the fed or the starved state (*Figure 5.1*).

a

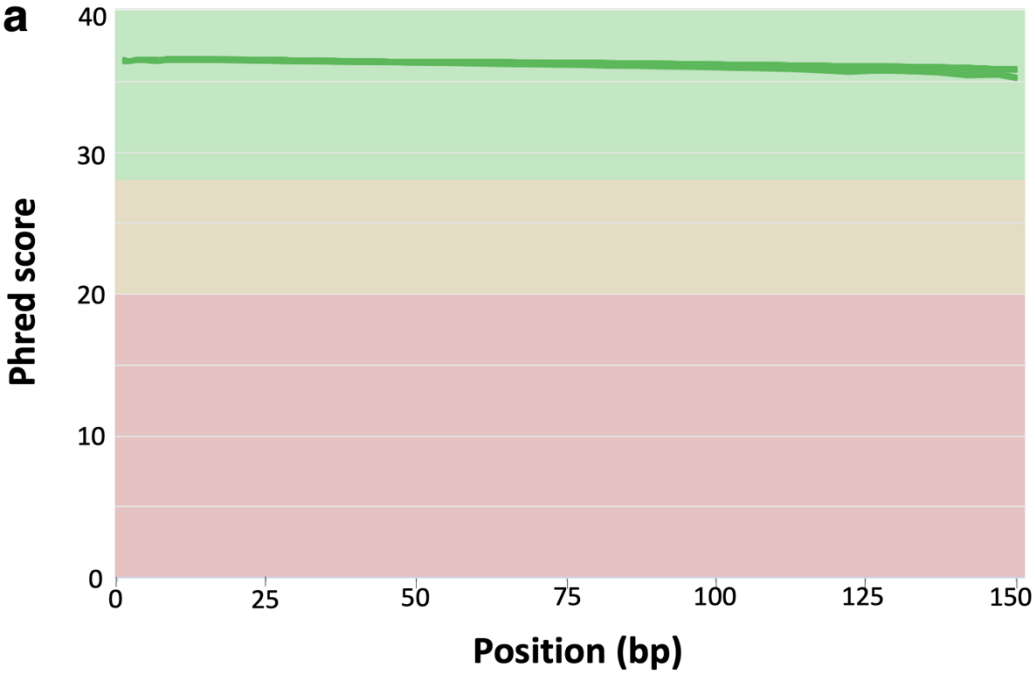

b

Condition	%GC content	% Dups	M Seqs
V3F_fed_forward	51%	62.05%	23.4
V3F_fed_reverse	51%	62.85%	23.4
V3F_starved_forward	50.75%	62.43%	23.6
V3F_starved_reverse	50.75%	61.55%	23.6
ΔV3_fed_forward	51%	64.65%	25.0
ΔV3_fed_reverse	51%	63.95%	25.0
ΔV3_starved_forward	50%	62.78%	22.4
ΔV3_starved_reverse	50%	61.93%	22.4
DBD2_fed_forward	51%	63.75%	23.4
DBD2_fed_reverse	51%	62.85%	23.4
DBD2_starved_forward	51%	62.43%	23.6
DBD2_starved_reverse	51%	61.55%	23.6

Figure 5.1. **Basic raw sequence quality control for *dFoxO* mutants.**
Mean quality sequence scores (a) and overall sequence statistics (b) for all *dFoxO* mutant raw sequencing data in both the fed and the starved states. Mean quality scores show Phred scores across the sequence length, where green areas indicate sequence quality reaches the 'pass' threshold and yellow/red indicate different levels of 'failure'. Overall sequence data shows the average duplication levels, GC content, and total amount of sequences (millions) for each condition.

Mean quality scores showed that all sequences were above the quality threshold score of 28. The Phred score measures the quality of the identification of the

nucleobases at each position. All sequences also maintained a consistent high Phred score between 35.06 and 36.57 across the sequence length. Together, this indicated that the raw RNA-seq reads were of good quality along their entire length.

Overall, sample data showed on average approximately 61-65% duplication of sequences, which is somewhat expected for RNA-seq data due to the presence of high abundance transcripts.
GC content was also consistent across the sequences with an average of 50-51% GC, indicating a relatively normal distribution of the sequences GC content suggesting there was likely no contamination or unwanted bias in the library.
Finally, M Seqs data showed that there were on average approximately 22-25 million sequences present for each condition, indicating a representatively sized data set that has not seemingly been affected by degradation of the RNA, allowing for a representative and more accurate downstream analysis.

Taken together, quality control shows seemingly no contamination, bias, or degradation in the library and overall high-quality reads. Therefore, analysis could continue without concerns as to the accuracy or representativity of the downstream analysis.

5.3.1.2 Mapping and alignment of the RNA-sequencing data

After the quality of the sequencing data was assessed, the sequences were mapped and aligned to the *Drosophila* reference genome, using the *Drosophila melanogaster* Release 6, dm6, produced by the Berkeley *Drosophila* Genome Project in 2014 (dos Santos *et al.* 2015) and the RNA Star tool (Dobin *et al.* 2012).

The quality of the mapping was subsequently assessed by analysing gene body coverage to show the gene regions to which the reads were aligned and read distribution, which shows the distribution of reads across the chromosomes. This was carried out for all mutants as above (*Figures 5.2*).

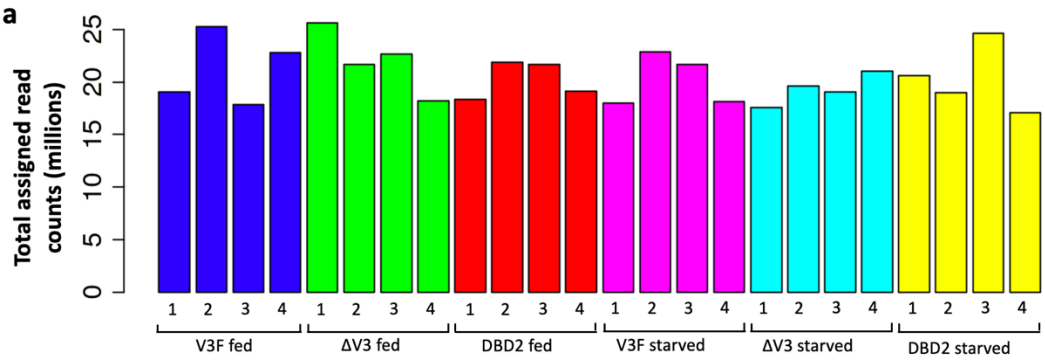

b

Condition	% uniquely mapped genes	% mapped to CDS of exons
V3F fed	95.7%	79.3%
V3F starved	95.3%	78.7%
ΔV3 fed	95.8%	79.5%
ΔV3 starved	95.2%	76.7%
DBD2 fed	94.3%	78.9%
DBD2 starved	94.1%	78.35%

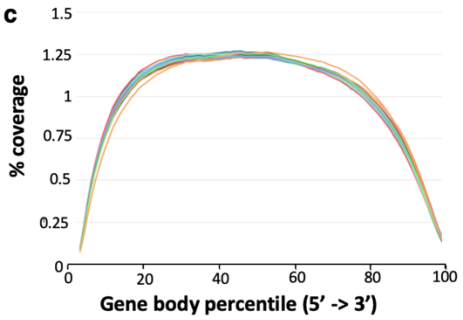

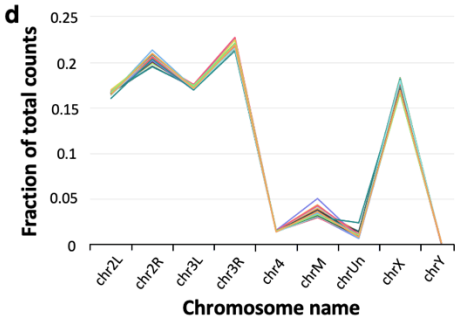

e

Condition	Total number of genes in samples	Number of genes with at least 1 read count in all replicates	Number of genes with at least 1 read count in all fed replicates	Number of genes with at least 1 read count in all starved replicates
V3F fed & starved	17,559	12,589	12,198	12,425
ΔV3 fed & starved	17,559	12,943	12,386	12,684
DBD2 fed & starved	17,559	12,816	12,556	12,534

Figure 5.2. **Quality assessment of the mapping of paired-end reads for *dFoxO* mutants.**
Assessment of the mapping for all *dFoxO* mutants in both fed and starved conditions showing (a) the total number of reads successfully assigned to genes in each replicate for each condition, (b) the overall average alignment statistics showing % of uniquely mapped genes and % of reads aligned to the coding DNA sequence (CDS) of exons, (c) the coverage of the reads across the gene body, (d) the number of reads that are mapped to each chromosome as a fraction of the total read count, and (e) the total number of genes found in all samples, as well as the number of genes with at least 1 assigned read in all, fed only, and starved only replicates.

All replicates of every condition showed a high number of assigned read counts. This included 19,017,712, 25,252,191, 17,868,318, and 22,767,349 assigned reads for the V3F fed replicates and 18,018,030, 22,876,904, 21,684,774, and 18,140,682 assigned reads for the V3F starved replicates.

There were also 25,605,127, 21,635,100, 22,656,850, 18,229,425 assigned reads for the ΔV3 fed replicates, 21,044,697, 17,588,551, 19,624,682, and 19,045,712 assigned reads for the ΔV3 starved replicates.

Mapping also assigned 18,320,563, 21,905,456, 21,674,264, and 19,103,682 assigned reads for the DBD2 fed replicates, and 20,630,312, 18,997,020, 24,655,460, and 17,064,585 assigned reads for the DBD2 starved replicates.

STAR alignment scores for all samples showed that 94-96% of reads were uniquely mapped, with the remaining ~4-6% unmapped due to length or mapped to multiple loci. Of the uniquely mapped reads, between ~78-80% were mapped to coding DNA sequence (CDS) exons with the remaining mapped to untranslated regions, or introns and other intergenic regions.

Gene body coverage assessed the location of the mapped reads across genes and for all samples and conditions showed an even coverage of reads across the length of the gene with no bias.

Most of the reads were mapped on to the 2nd, 3rd, and X chromosomes. No transcripts were mapped to the Y chromosome, as the RNA was isolated from female flies. ChrUn represents 'unknown' sequences not yet mapped to one of the existing chromosomes.

Taken together, this analysis indicates mapping was successful with high levels of uniquely mapped genes to CDS exons across the gene length. Therefore, as with assessment of quality control, analysis could continue without concerns as to the accuracy or representativity of the downstream analysis.

5.3.1.3 Analysis of differential gene expression

Changes in gene expression between conditions were analysed using read counts for each gene normalised using the tool DESeq2. DESeq2 has a strong statistical power, due to its high sensitivity, precision, and ability to correct any variability within the measurements to give a better estimate of significance between the different conditions (Love *et al.* 2014).

Principal component analysis (PCA) of transformed RNA-seq count data was performed (*Figure 5.3*).

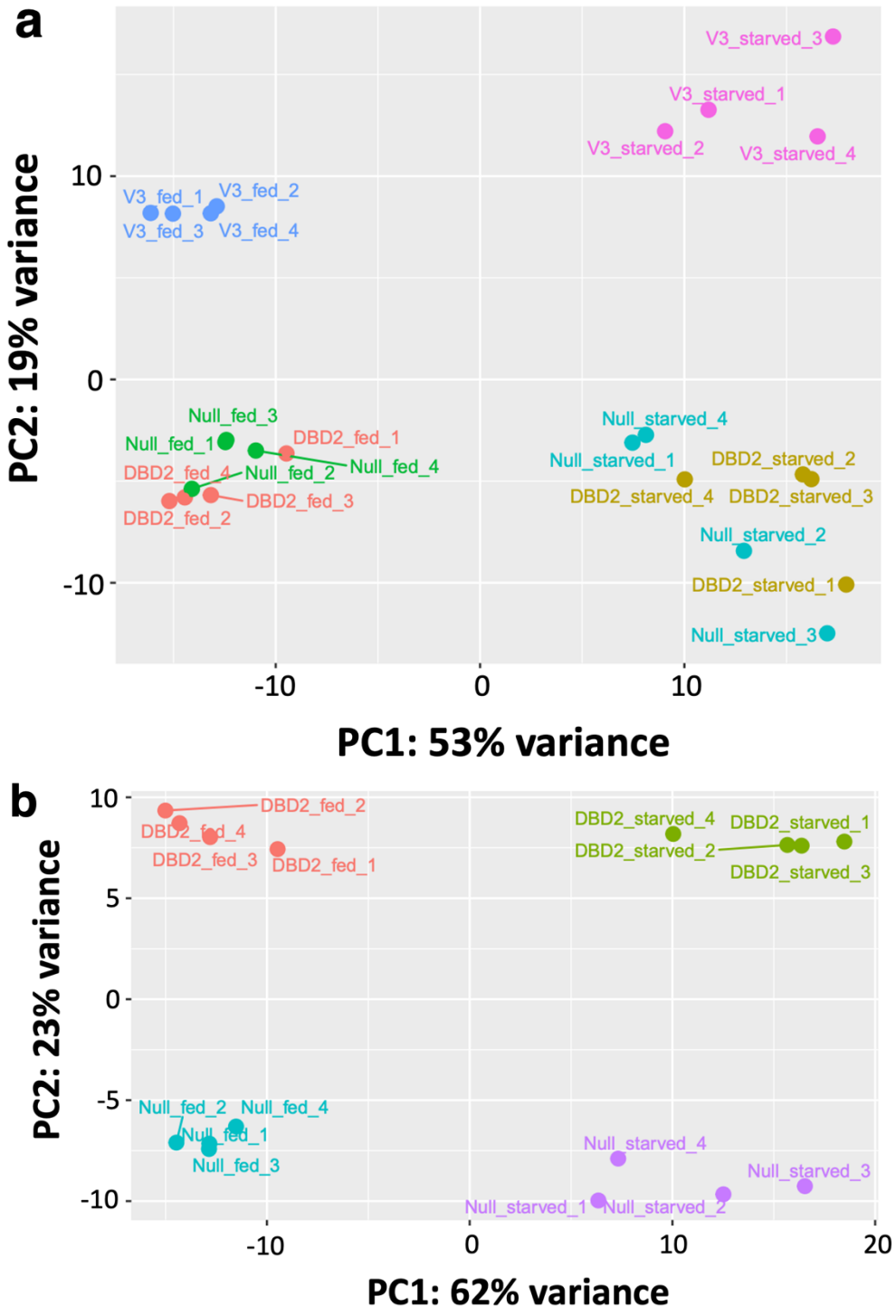

Figure 5.3. **Principal component analysis (PCA) for all *dFoxO* mutants in both the fed and the starved state.**

Scatter plot of Principal component analysis (PCA) of transformed count data from DESeq2 of (a) all mutants and (b) the ΔV3 and DBD2 mutants. Samples are clustered according to their nutritional state (fed or starved) (PC1) and genotype (PC2) (n = 4 independent biological replicates).

PCA revealed that 72% of the total variance amongst the 6 groups was represented by two principal components. Samples were separated along the first principal component showing 53% of the variation between samples was explained by their nutritional state. Samples were also separated along the second principal component, with 19% of the variation between samples being caused by their genotype.
In particular, the V3F samples were more distinguished from the other two genotypes, with the ΔV3 and DBD2 samples showing more similarity. Although, when only comparing the ΔV3 and DBD2 samples separation was also observed with a variation of 23%, indicating these datasets do have some observable differences.

For each genotype, genes that showed significant differential expression between fed and starved conditions were identified alongside their fold change in expression (*Figure 5.4*).

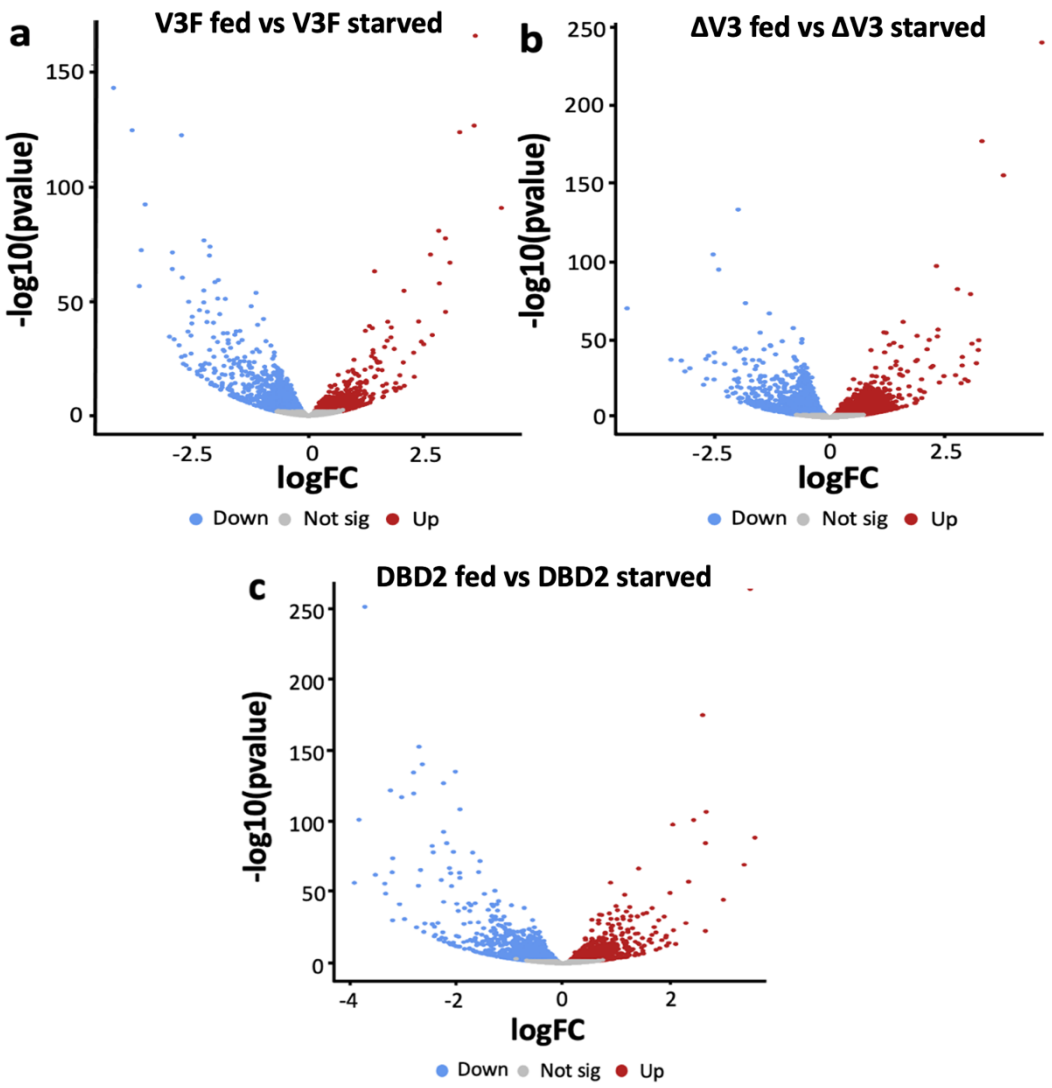

Figure 5.4. **Visualisation of differentially expressed genes for each *dFoxO* mutant under different nutritional conditions.**
Volcano plots comparing the (a) V3F fed and starved, (b) ΔV3 fed and starved, and (c) DBD2 fed and starved RNA-seq data sets. Plots show the -log10(pvalue) for each gene plotted against log2 fold change (logFC). Significantly upregulated genes (logFC > 0) are highlighted in red and downregulated genes (logFC < 0) in blue ($p < 0.05$). Genes that show no significant differences in expression are in grey.

A large number of genes were significantly ($p < 0.05$) differentially regulated in all *dFoxO* mutants when comparing the fed and the starved state, where a similar number of genes were differentially expressed during starvation for all mutants with 2,934, 3,886, and 3,376 genes present in the V3F, ΔV3, and DBD2 respectively. This reflects the preliminary analysis carried out by Novogene, who found 2894, 3869, and 3332 differentially expressed genes during starvation for the V3F, ΔV3, and DBD2 respectively.

Of these genes, similar numbers of genes were also up- and down-regulated for all mutants. With 1,288 upregulated and 1,646 downregulated in the V3F, 1,884 and upregulated and 2,002 downregulated in the ΔV3, and 1,558 upregulated and 1,818 downregulated in the DBD2.

To identify genes that respond differently to starvation in the DBD mutants compared to the ΔV3 mutants, and those that could therefore possibly be modulated in a dFoxO-dependent DNA-binding independent manner, the differentially expressed gene (DEG) lists produced from the analysis comparing the fed and starved states of each genotype were then compared and visualised using a Venn diagram (*Figure 5.5*).

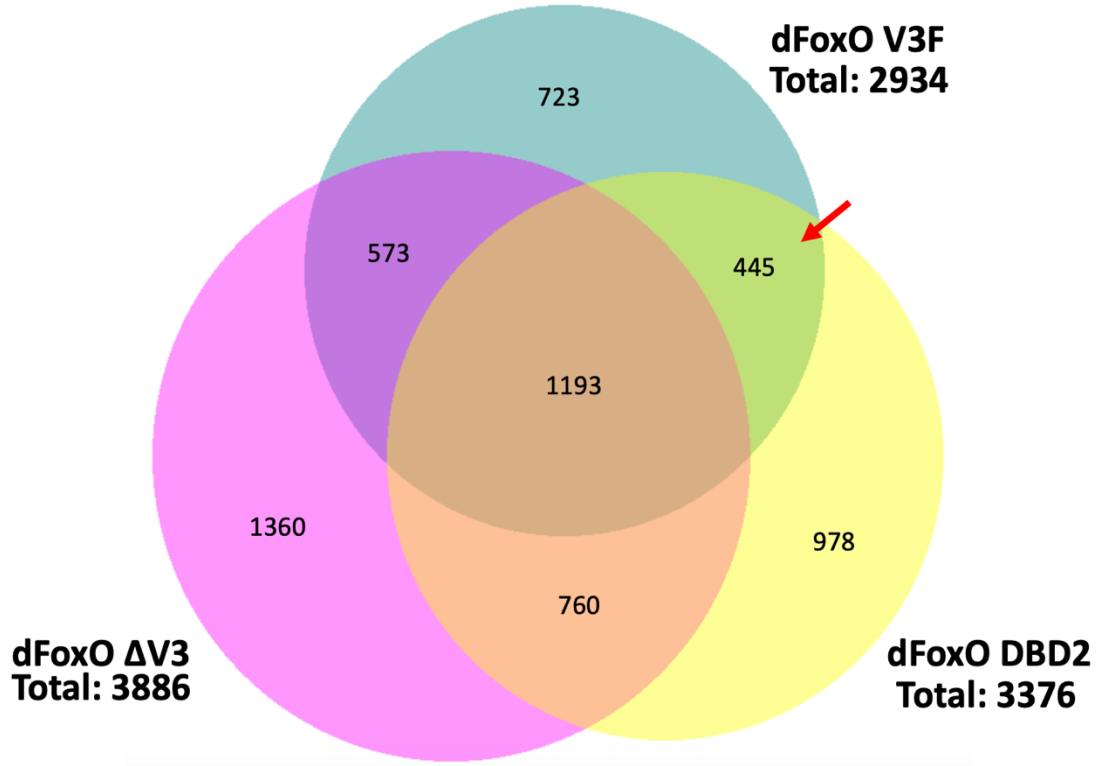

Figure 5.5. **Comparisons of the differentially expressed genes of the *dFoxO* mutants during starvation.**
Proportional Venn diagram comparing the differentially expressed gene lists of the different *dFoxO* mutants when comparing the difference between fully fed and starved conditions. Overlaps indicate the genes were represented in both or all datasets, where numbers indicate the number of genes in each section of the diagram and the red arrow represents the dataset corresponding to the genes modulated in dFoxO-dependent DNA-binding independent manner during starvation.

An overlap of approximately one third of all three datasets (1193 genes) was observed, indicating that a large number of genes were differentially expressed in response to starvation conditions but were regulated independently of dFoxO activity.

There were also 723 genes that only showed differential expression in the V3F during starvation, indicating 24.6% of genes in this DEG list were possibly modulated in a dFoxO-dependent DNA-binding dependent manner during starvation.

The overlap between the V3F and DBD2 represents the number of genes present in both datasets but not the ΔV3. Therefore, as the DBD2 shows the same as the V3F and is seemingly able to rescue the phenotype observed in the ΔV3, these genes

seem to require the presence of dFoxO but not a functional DBD to be regulated appropriately.
There were 445 genes in this overlap that were therefore potentially modulated in a dFoxO-dependent DNA-binding independent manner during starvation, making up 15% and 13% of the V3F and DBD2 DEG lists respectively.

A number of genes were also found to only change in the ΔV3 (1,360) or the DBD2 (978). Gene ontology (GO) analysis was carried out on these individual gene lists in an attempt to assess their function (*Table 5.1*).

Genotype	Fold enrichment	Enrichment FDR	Functional category
V3F	13.4	2.4E-2	Heparin metabolic process
V3F	4.5	1.4E-2	Synaptic target recognition
V3F	2.5	2.5E-2	Tissue migration
V3F	1.8	3.0E-2	Positive regulation of signal transduction
V3F	1.7	2.5E-2	Neuron development
ΔV3	3.2	1.8E-6	Toll signalling pathway
ΔV3	2.7	3.8E-13	Synapse organization
ΔV3	2.3	3.5E-6	Photoreceptor cell differentiation
ΔV3	1.9	2.8E-7	Cell-cell signalling
ΔV3	1.8	1.3E-7	Neuron development
DBD2	1.4	2.7E-12	Macromolecule metabolic process
DBD2	1.5	1.9E-11	Cellular nitrogen compound metabolic process
DBD2	1.5	1.3E-10	Gene expression
DBD2	1.5	1.1E-9	Cellular biosynthetic process
DBD2	1.9	1.8E-8	Cell cycle

Table 5.1. **Gene ontology (GO) analysis of the genes differentially expressed only in one mutant.**
Gene ontology (GO) analysis of the genes found to only be differentially expressed during starvation in the individual genotypes alone. Each enriched GO term shows the enrichment score based on hypergeometric analysis (i.e., the degree to which the genes in a gene list fall into that specific category) and false discovery rate (FDR) correction (i.e., the significance of the enrichment score taking into account false positives) with a cut off of 0.05, and the functional category (i.e., biological process) for which the genes likely fall into. This list is not exhaustive and only shows the most over-represented category for a specific process.

Enriched GO terms for the V3F include those involved with neurological processes such as synapse target recognition and neuron development, as well as tissue migration and positive regulation of signal transduction.

Similar enriched GO terms are seen for the genes only found to be differentially expressed during starvation in the ΔV3, these include synapse organisation, cell-cell signalling, and neuron development.

Different GO terms are seemingly enriched in the genes only differentially expressed in the DBD mutant, including macromolecule metabolic process, gene expression, cellular biosynthetic process, and cell cycle.

Therefore, due to the stark difference in the DBD2 mutant specific genes of interest related to metabolic function in the DBD2 only gene list were identified (*Figure 5.6).*

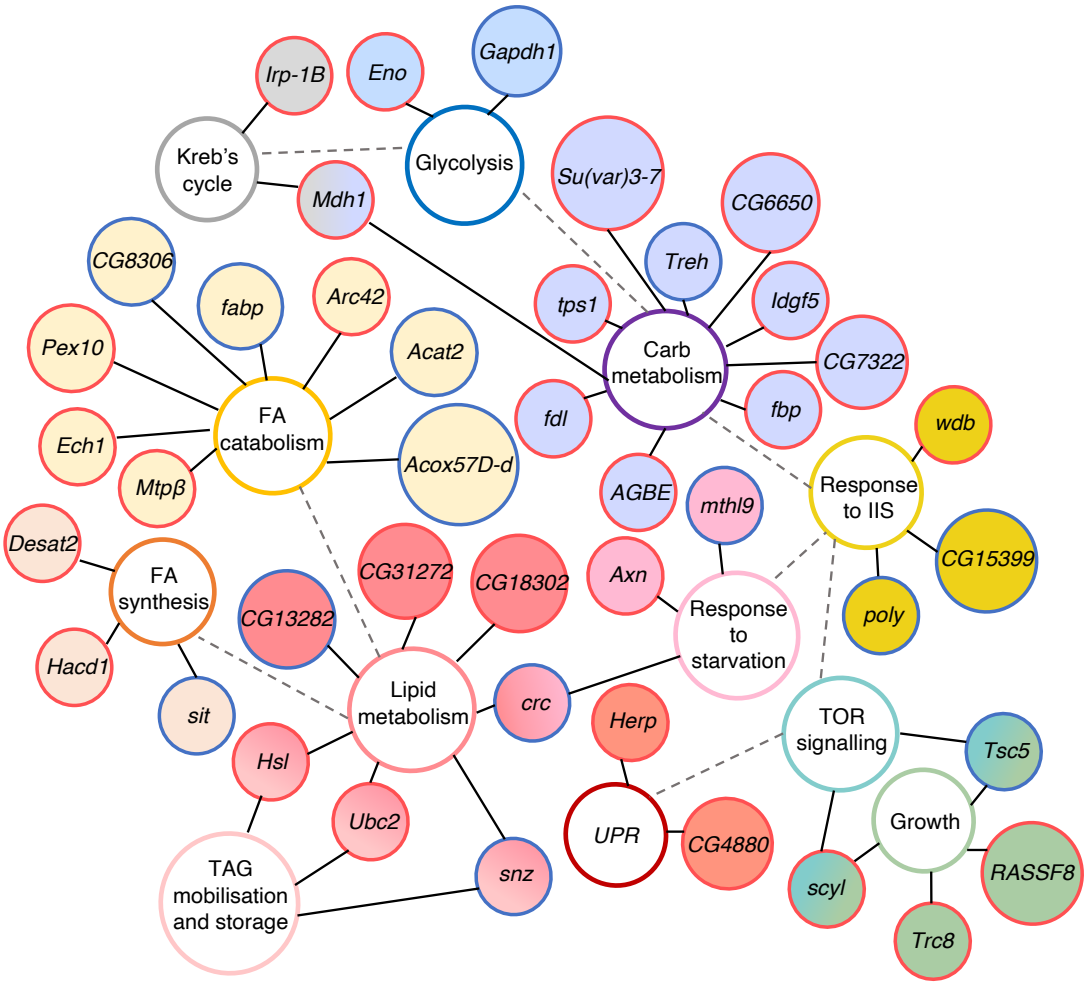

Figure 5.6. **Differentially expressed genes modulated during starvation in only dFoxO-DBD2 mutants.**
Cluster map showing the different metabolism-related genes found to be significantly differentially expressed ($p < 0.05$) in only the DBD2 mutants during starvation. Genes are grouped based on their biological process given by Flybase indicated by solid lines. Related processes are connected via dashed lines. Red outlined circles indicate upregulated genes (logFC > 0), and blue outlined circles indicate downregulated genes (logFC < 0). No logFC exceeds 2 or falls below -2. FA: fatty acid, IIS: insulin/insulin-like growth factor signalling, TAG: triglyceride, TOR: target of rapamycin, UPR: unfolded protein response.

Genes of interest in this DBD only gene list include those involved with general lipid metabolism (*CG13282, CG31272*, and *CG18302*), lipid storage and mobilisation (*Hsl, Ubc2,* and *snz*), carbohydrate metabolism (*tps1, Treh, Idgf5, fdl*, *AGBE*, and *Su(var)3-7*), the unfolded protein response (*Herp* and *CG4880*), response to starvation (*Axn, crc,* and *mthl9*), regulation of the IIS (*wdb, poly*, and *CG15399*), the Kreb's cycle and

glycolysis (*Mdh1, Irp-1B, Gapdh1*, and *Eno*), and growth (*Tcs5, scyl, Trc8,* and *RASSF8*).

After analysing genes only found in the gene lists of the ΔV3 and DBD2 mutants, genes identified as dFoxO-independent (all mutants), dFoxO-dependent DNA-binding dependent (V3F only), and dFoxO-dependent DNA-binding independent (V3F and DBD2 only) were analysed in more depth.
Several genes related to metabolic function present in the dFoxO-independent list were identified (*Figure 5.7*).

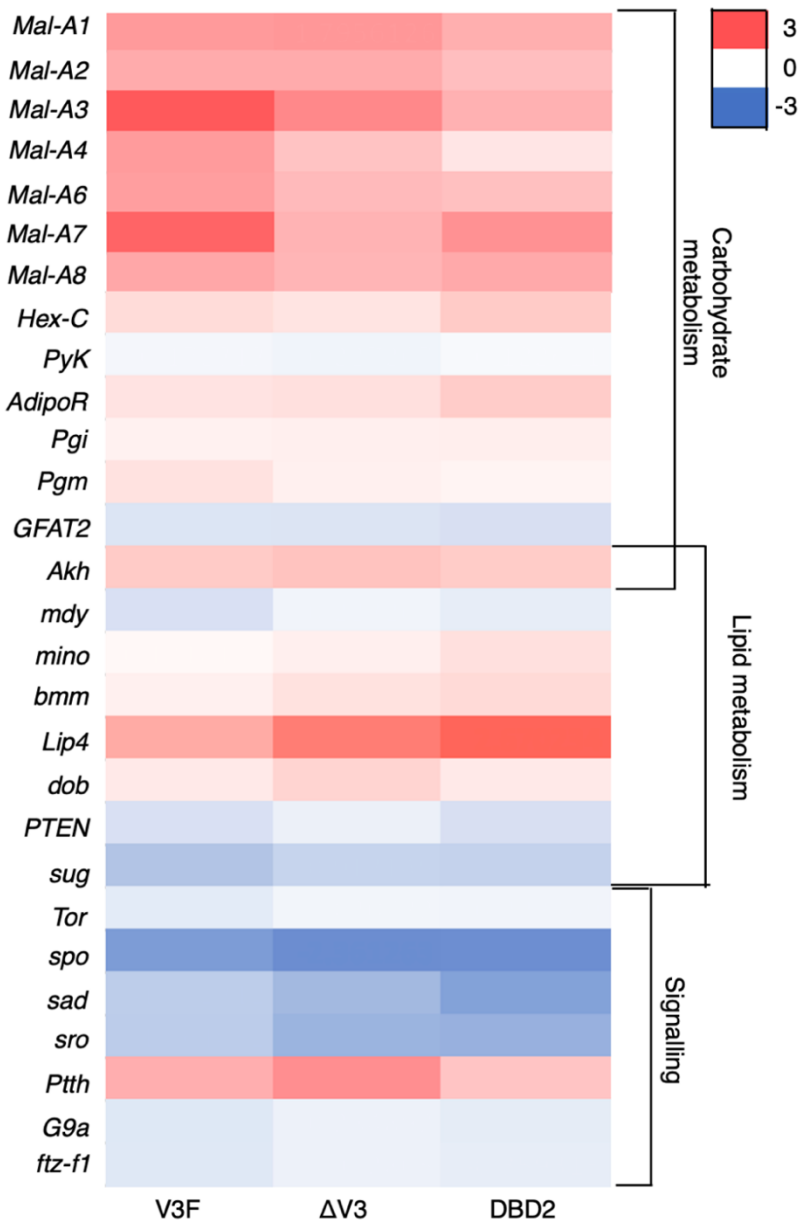

Figure 5.7. **Differential expression of genes modulated during starvation in *dFoxO* mutants.**
Heatmap showing the differential expression (log2 fold change (logFC)) of genes modulated in a dFoxO-independent manner during starvation in *dFoxO* mutants of the indicated genotypes. Expression of all indicated genes are significantly different between the fed and starved state of all mutants ($p < 0.05$). Red indicates upregulated genes (logFC > 0), and blue indicates downregulated genes (logFC < 0). No logFC exceeds 3 or falls below -3. Genes are grouped based on their biological processes given by Flybase.

A number of metabolic genes showed a significant differential expression in all *dFoxO* mutants ($p < 0.05$). These genes included those involved with carbohydrate

metabolism particularly glycogen metabolism and glycolysis (*PyK*, *HexC*, *GFAT2*, *Pgi*, *AdipoR, MalA-1, 2, 3, 4, 6, 7, 8,* and *Pgm*), lipid metabolism (*bmm*, *dob*, *mino*, *Lip4, sug, PTEN,* and *mdy*), both carbohydrate and lipid metabolism (*Akh*), and signalling pathways (*Tor*, *spo, sad, sro, Ptth, G9a,* and *ftz-f1*).

Genes found to only be modulated during starvation in V3F mutants (i.e., genes thought to be modulated in a dFoxO-dependent DNA-binding dependent manner), as well as associated with phenotypes modulated in a dFoxO-dependent DNA-binding dependent manner were also identified from the RNA-seq data (*Table 5.2*). These genes were thought to be involved with the modulation of DNA-binding dependent processes or at least require a functional DNA-binding domain, as otherwise they would also be in the list of differentially expressed genes from the DBD2 mutants as well).

Gene	LogFC	Biological process
Atg3	-0.37	Autophagy
daw	-0.46	Autophagy / regulation of adult lifespan
Fs	0.61	Regulation of BMP and activin signalling
Mys	-0.30	Regulation of adult lifespan
RagA-B	-0.28	Autophagy / regulation of TORC1
Samtor	0.27	Negative regulation of TORC1
EcR	-0.30	Oogenesis / autophagy
egh	-0.33	Regulation of oviposition and oocyte development
HLH106	-0.30	Fatty acid synthesis / autophagy
dILP3	-1.31	IIS / mating behaviour
dILP4	-0.61	IIS / feeding behaviour
bigmax	0.38	Feeding behaviour / regulation of transcription
Pdk1	-0.16	Apoptosis
dILP6	-0.33	Regulation of IIS
Jheh1	-1.06	JH catabolism / epoxide metabolism
Jheh2	-0.20	JH catabolism / epoxide metabolism
NLaz	0.43	Response to oxidative stress / regulation of adult lifespan
cue	-0.22	TAG homeostasis
Nrg	-0.23	Female courtship behaviour
GstD9	-0.31	Glutathione metabolic process
Lkr	0.65	Regulation of feeding behaviour
PEK	-0.30	Autophagy / unfolded protein response
Obp28a	0.81	Sensory perception of chemical stimulus
Obp83b	0.70	Sensory perception of chemical stimulus
lush	0.74	Olfactory behaviour / courtship behaviour

Table 5.2. **Differential expression of genes modulated during starvation only in V3F mutants.**

The differential expression of genes modulated in a dFoxO-dependent DNA-binding dependent manner during starvation (i.e., only in V3F mutants). Expression of all indicated genes are significantly different between the fed and starved state ($p < 0.05$). Log2 fold change (logFC) and associated biological process given by Flybase for each gene is shown, where upregulated genes have a logFC > 0 and downregulated a logFC < 0.

A number of genes associated with the phenotypes thought to be modulated in a dFoxO-dependent DNA-binding dependent manner showed a significant differential expression in only V3F mutants ($p < 0.05$).

These genes included those associated with the regulation of lifespan (*Fs*, *daw*, *Atg3*, *RagA-B*, *Mys, and Samtor*), fecundity (*cue, egh*, *Nrg*, *dILP6*, *EcR*, and *HLH106*), feeding behaviour (*dILP3*, *dILP4*, *bigmax*, *Pdk1*, *Obp28a* and *83b*, *lush*, and *Lkr*), and responses to stress (*Jheh-1*, *Jheh-2*, *PEK*, *Gst9D*, and *NLaz*).

Of the 445 genes seemingly modulated in a DNA-binding independent manner by dFoxO (i.e., genes only differentially expressed in the V3F and DBD2 during starvation), several related to the dFoxO-related phenotypes that seem to also be modulated in a dFoxO-dependent DNA-binding independent manner were identified (*Figure. 5.8*).

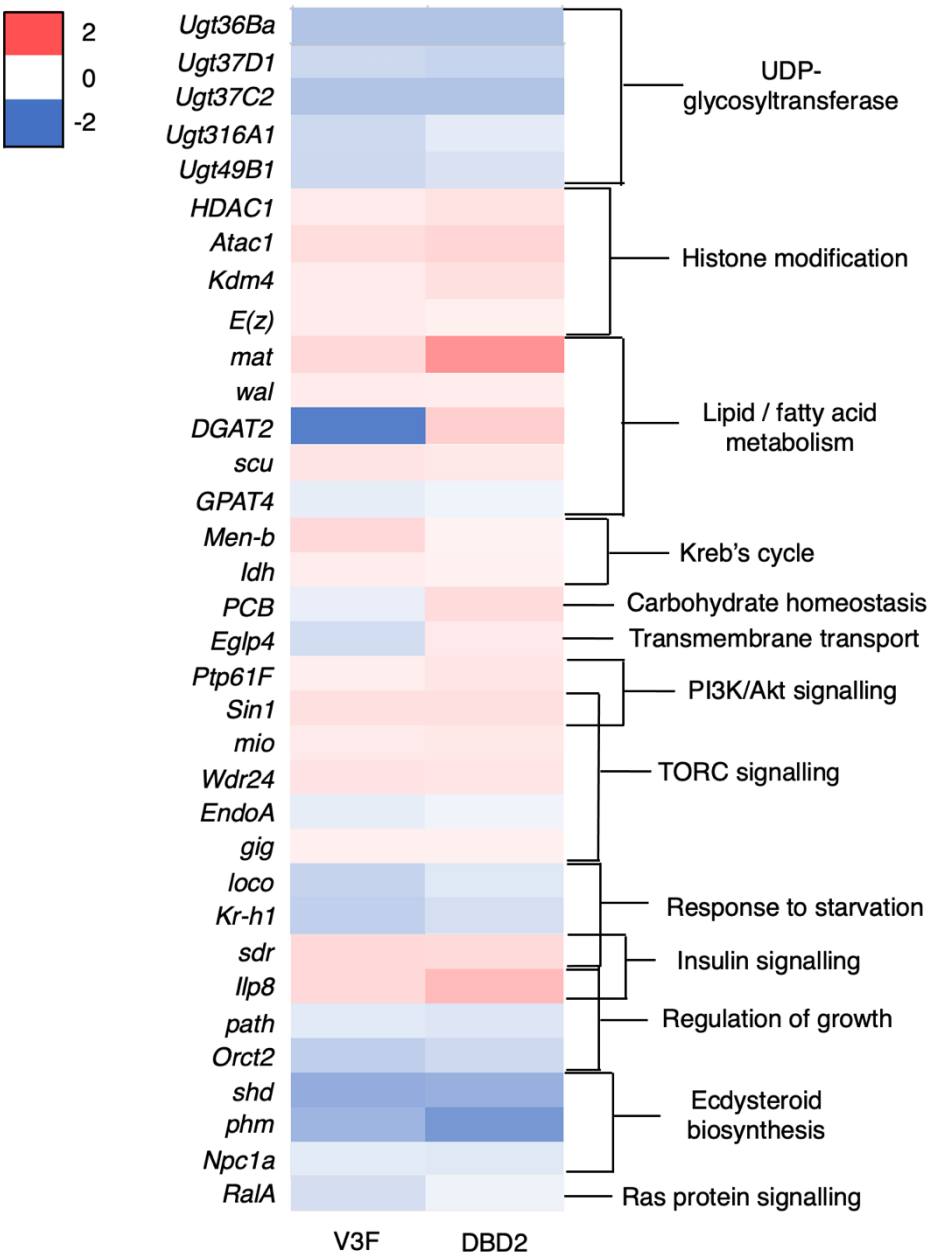

Figure 5.8. **Differential expression of genes modulated during starvation in V3F and DBD2 mutants.**

Heatmap showing the differential expression (log2 fold change (logFC)) of genes modulated in a dFoxO-dependent DNA-binding independent manner during starvation in *dFoxO* mutants of the indicated genotypes. Expression of all indicated genes are significantly different between the fed and starved state of both mutants but not the ΔV3 ($p < 0.05$). Red indicates upregulated genes (logFC > 0), and blue indicates downregulated genes (logFC < 0). No logFC exceeds 2 or falls below -2. Genes are grouped based on their biological processes given by Flybase.

Genes in this dFoxO-dependent DNA-binding independent DEG list included UDP-glycosyltransferases (*Ugt37D1*, *Ugt37C2*, *Ugt316A1*, *Ugt36Ba* and *Ugt49B1*), those

involved with histone modification (*HDAC1*, *Atac1*, *Kdm4*, and *E(z)*), lipid metabolism (*mat*, *wal*, *DGAT2*, *scu*, *Kr-h1*, and *GPAT4*), carbohydrate metabolism (*PCB*), and the Kreb's cycle (*Idh and Men-b*).

There were also many genes involved with various signalling pathways present in this list including ecdysone signalling (*shd*, *phm*, and *Npc1a*), mTOR signalling (*path*, *mio*, *Sin1*, *Wdr24*, *and gig*), Ras protein signalling (*RalA*), insulin signalling (*Ptp61F*, *sdr*, *Orct2*, and *dILP8*), and G-protein coupled receptor signalling (*loco*). Other genes of interest include those involved transmembrane transport (*Eglp4*).

Additionally, 16% (71) of genes in this list were found to have an unknown function or identity.

GO analysis was used to identify biological functions or processes attributed to the genes potentially modulated in a dFoxO-dependent DNA-binding independent manner, to possibly uncover potential mechanisms of dFoxO activity that do not require a functional DBD.

GO analysis revealed several enriched terms within this dFoxO-dependent DNA-binding independent DEG list (*Table 5.3*).

Fold enrichment	Enrichment FDR	Functional category
11.7	2.6E-2	UDP-glucose metabolic process
9.8	1.9E-3	Syncytial blastoderm mitotic cell cycle
5.2	1.6E-2	Regulation of cell division
2.2	1.6E-3	Cell cycle process
1.8	1.4E-2	Chromosome organisation
1.8	2.3E-2	Female gamete generation
1.5	1.6E-3	Nucleobase-containing compound metabolic process
1.4	2.8E-3	Heterocycle metabolic process
1.4	2.8E-3	Organic cyclic compound metabolic process
1.4	3.2E-3	Cellular aromatic compound metabolic process
1.4	7.7E-3	Nucleic acid metabolic process
1.4	1.4E-2	Regulation of metabolic process
1.4	2.3E-2	Regulation of cellular metabolic process
1.4	2.4E-2	Organelle organisation
1.2	1.4E-2	Biological regulation

Table 5.3. **Enriched gene ontology (GO) terms for the genes potentially modulated in a dFoxO-dependent DNA-binding independent manner.**
Gene ontology (GO) analysis for the genes found to be modulated by dFoxO in a DNA-binding independent manner. Each enriched GO term shows the enrichment score based on hypergeometric analysis (i.e., the degree to which the genes in a gene list fall into that specific category) and false discovery rate (FDR) correction (i.e., the significance of the enrichment score taking into account false positives) with a cut off of 0.05, and the functional category (i.e., biological process) for which the genes likely fall into. This list is not exhaustive and only shows the most over-represented category for a specific process.

These results show that many of the genes modulated in a dFoxO-dependent DNA-binding independently manner fall into categories associated with chromosome organisation and various metabolic processes such as regulation of metabolic process, cellular metabolic process, and UDP-glucose metabolic process.

5.3.1.4 Verification of dFoxO-ΔV3 mutants

To check RNA-seq analysis was carried out appropriately, the regulation of the *dFoxO* gene between the ΔV3 and V3F mutant control under fully fed conditions was checked. This gene was chosen as due to the *dFoxO* null mutation in the ΔV3 mutants, this gene would have an expected change in expression between the two

(i.e., *dFoxO* in the ΔV3 mutants should be significantly decreased compared to the V3F mutant control) (*Table 5.4)*.

Comparison	LogFC	Adjusted p-value
V3F fed to ΔV3 fed	0.19	0.001
V3F fed to DBD2 fed	-0.05	0.42

Table 5.4. **Comparisons of the differential expression of the *dFoxO* gene between *dFoxO* mutants under fully fed conditions.**
Results of RNA-seq analysis comparing the ΔV3 or DBD2 mutants to the V3F mutant control under fully fed conditions for the *dFoxO* gene. Log2 fold change (logFC) and adjusted p-value (i.e., p-value adjusted using the Benjamini-Hochberg procedure to reduce false positives) are shown. The significance threshold was $p < 0.05$, with upregulated genes showed a logFC > 0 and downregulated genes a logFC < 0.

Under fully fed conditions the ΔV3 mutants showed a significant increase ($p = 0.001$) in *dFoxO* gene expression compared to the V3F mutant controls. A response not observed in the DBD2, which showed no significant difference in *dFoxO* expression compared to the V3F mutant control.

These results were somewhat unexpected and so quantitative reverse transcription-polymerase chain reaction (qRT-PCR) was carried out.
First, an appropriate reference gene for qRT-PCR was identified by selecting a list of candidate genes from the RNA-seq data that did not show any change in expression across all conditions (genotype or nutritional state). Three genes were chosen for further expression stability analysis: *EMC10* encoding an extracellular matrix

component, *Cog6* encoding a component of oligomeric golgi complex 6, and the E3 ubiquitin protein ligase*, gzl* (*Figure 5.9*).

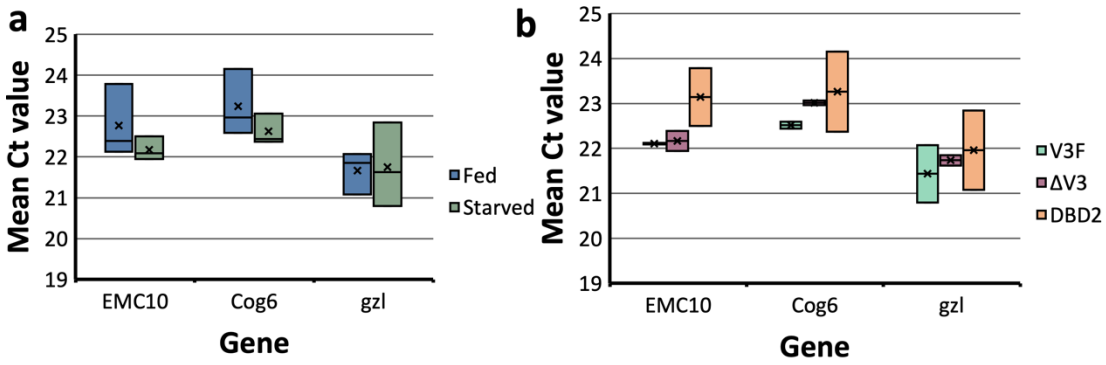

c

Gene	Group Diff	Group SD	Stability	Comparison
EMC10	0.22	0.33	0.19	Nutritional status
Cog6	0.24	0.52	0.23	Nutritional status
gzl	0.46	1.16	0.66	Nutritional status
EMC10	0.51	0.23	0.16	Genotype
Cog6	0.30	0.56	0.30	Genotype
gzl	0.33	1.42	0.76	Genotype

Figure 5.9. **Identification of an appropriate reference gene for qRT-PCR.** Identification of an appropriate reference gene using qRT-PCR for 3 genes identified from the RNA-seq data: *EMC10, gzl,* and *Cog6*. (a) mean Ct values for genotype (in pooled fed and starved states) and (b) nutritional state (pooled genotypes). (c) Normfinder results table output showing gene expression stability across genotypes and nutritional state. Group diff represents the measure of the difference in means between groups, group SD represents weighted average of the intragroup variance (common standard deviation), stability gives a stability measure with a high stability value indicating higher variability and lower expression stability. Comparison indicates sample grouping for stability analysis based on genotype and nutritional state (fed vs starved) (n = 5 replicates of each genotype of 15 pooled female flies).

Mean cycle threshold (Ct) values (i.e., the number of cycles needed for the fluorescent signal to cross the threshold and exceed background level) showed some variation in expression of all three genes across different genotypes and between fed versus starved conditions. However, both *EMC10* and *Cog6* showed less variable expression across groups than *gzl*.

Normfinder analysis was then used to determine overall stability in the expression of the three potential reference genes in response to either genotype or nutritional state. Of the three genes analysed, *EMC10* showed the lowest stability score across both genotype and nutritional state indicative of a more stable expression in response to these variables. Therefore, in subsequent qRT-PCR analysis, *EMC10* was used as a reference gene for normalisation of candidate gene expression.

After identification of a suitable reference gene, qRT-PCR was carried out on the three mutants to analyse whether this discrepancy in *dFoxO* expression was observed using a different technique for measuring gene expression (*Figure 5.10)*.

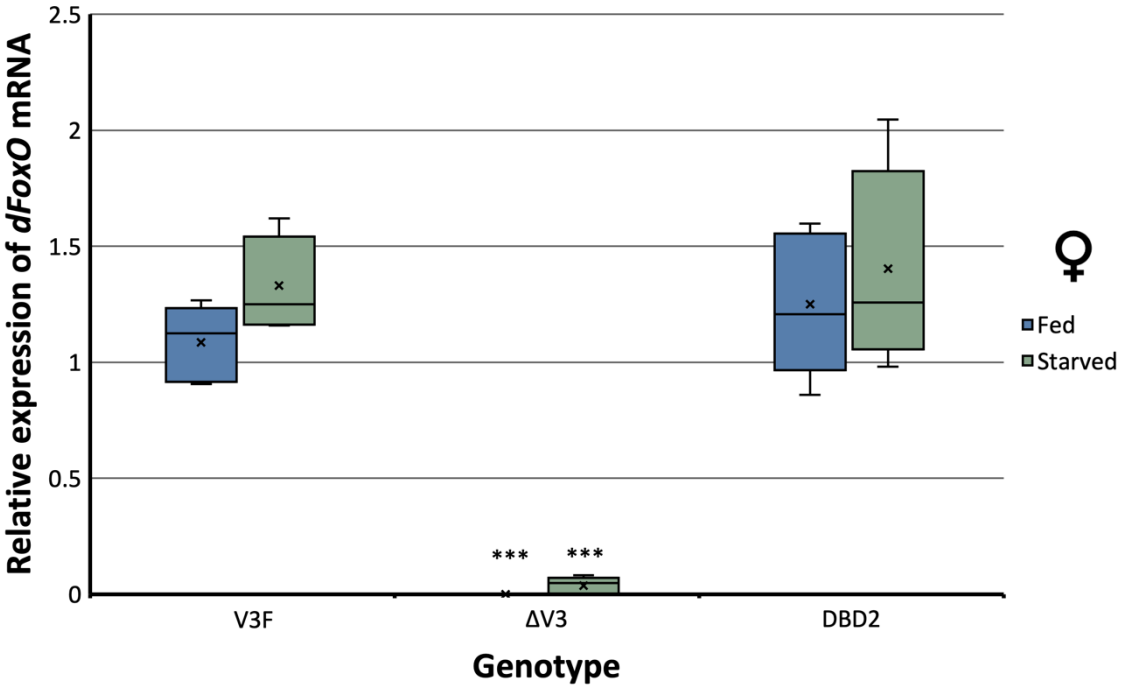

Figure 5.10. **Analysis of the expression of *dFoxO* by qRT-PCR.**
dFoxO mRNA expression was analysed by qRT-PCR and normalised relative to expression of *EMC10* mRNA in 7-day old adult female *Drosophila* of the indicated genotypes. All flies were either fully fed or subjected to 72-hours of starvation. Standard curves were created using fully fed w^{Dah} 7-day old adult female *Drosophila.* Data represent relative *dFoxO* mRNA levels for the indicated genotypes and conditions (n = 5 replicates of 15 pooled flies for each genotype, $p < 0.001$ ***, Welch's t-test compared to V3F flies).

No significant differences in *dFoxO* gene expression were observed between the V3F and the DBD2 mutants in either the fed or starved state for qRT-PCR.
Further, there were no significant differences in *dFoxO* gene expression when comparing the fed and the starved of the same mutant, for either the V3F or DBD2.
These results corroborated with the results observed during RNA-seq analysis.

Unlike in the RNA-seq data, however, there was a significant reduction in *dFoxO* expression in the ΔV3 flies compared to the V3F controls in both fed and starved states (100% decrease in expression whilst fed (p = 1.2E-4) and 97% decrease in expression whilst starved (p = 1.9E-4)).
Furthermore, there was no significant difference observed between the fed and starved states for the ΔV3 flies, where the RNA-seq data showed a significant

increase in the starved state. However, an upward trend is observable and power analysis indicates this could reach significance with a sample size of 12.

To investigate the possible basis for this discrepancy within the RNA-seq data and expected qRT-PCR analysis for *dFoxO* expression, the aligned RNA-seq reads were viewed in the Integrated Genomics Viewer (IGV) (*Figure 5.11*).

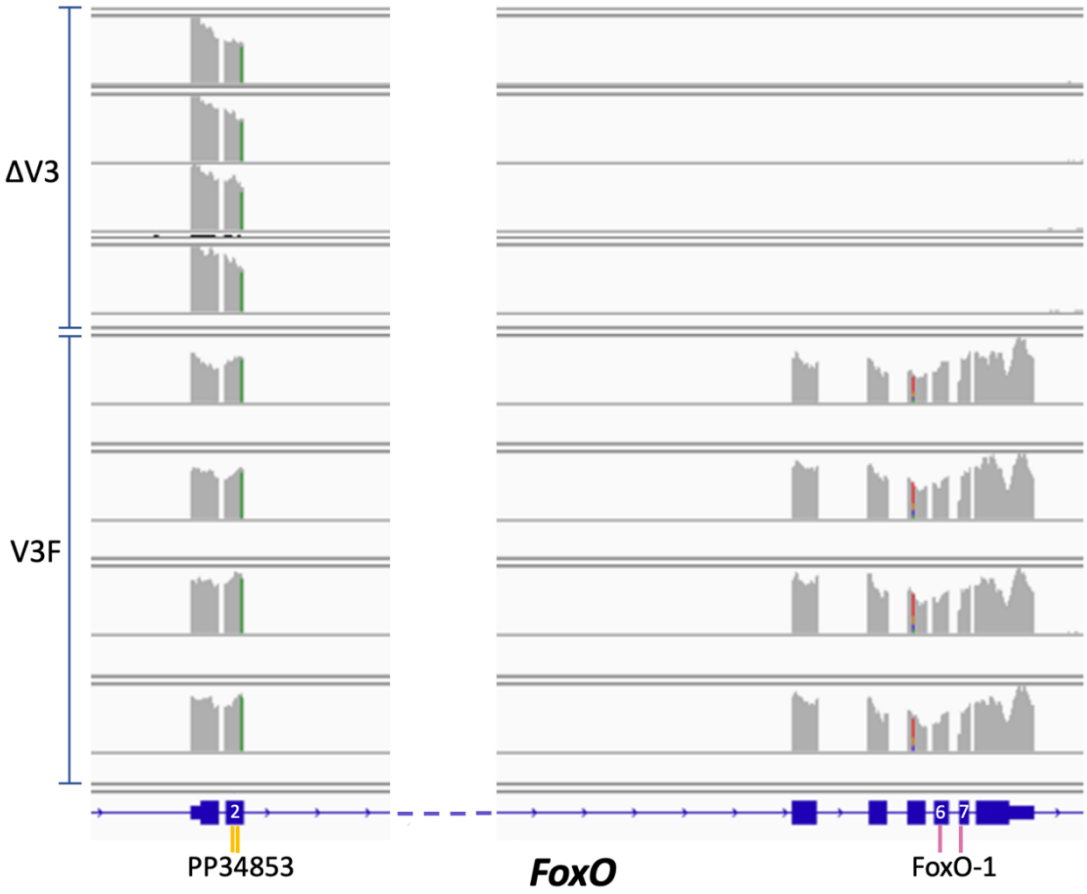

***Figure 5.11*. Analysis of *dFoxO* gene expression in the dFoxO-V3F and -ΔV3 mutants using the Integrated Genomics Viewer (IGV).**
Integrated Genomics Viewer (IGV) tracks visualising the mapped.bam RNA STAR output files produced during RNA-seq analysis with the first four tracks belonging to ΔV3 reads and the bottom four tracks reads from the V3F flies. Relevant exons and positions of primers used in qRT-PCR are indicated. PP34853 indicates primers that amplify a region with exon 2, and FoxO-1 indicates primers that amplify a region spanning exons 6 and 7.

At the *dFoxO* locus, reads mapped across all 8 exons of the gene in the V3F flies. However, in the ΔV3 mutants, reads were only mapped to exons 1 and 2. Furthermore, there were approximately 4.7-fold more reads mapped to these two exons in the ΔV3 mutants than across the gene in the V3F flies.

The original qRT-PCR primers used to assess *dFoxO* expression amplified a region spanning exons 6 and 7 (primers FoxO-1), a region which is removed in the ΔV3 mutants. Therefore, the qRT-PCR was repeated using primers that target exon 2 (primers PP34853), a region of the *dFoxO* gene that is not removed in the ΔV3 mutants and is the location of these mapped reads (*Figure 5.12*).

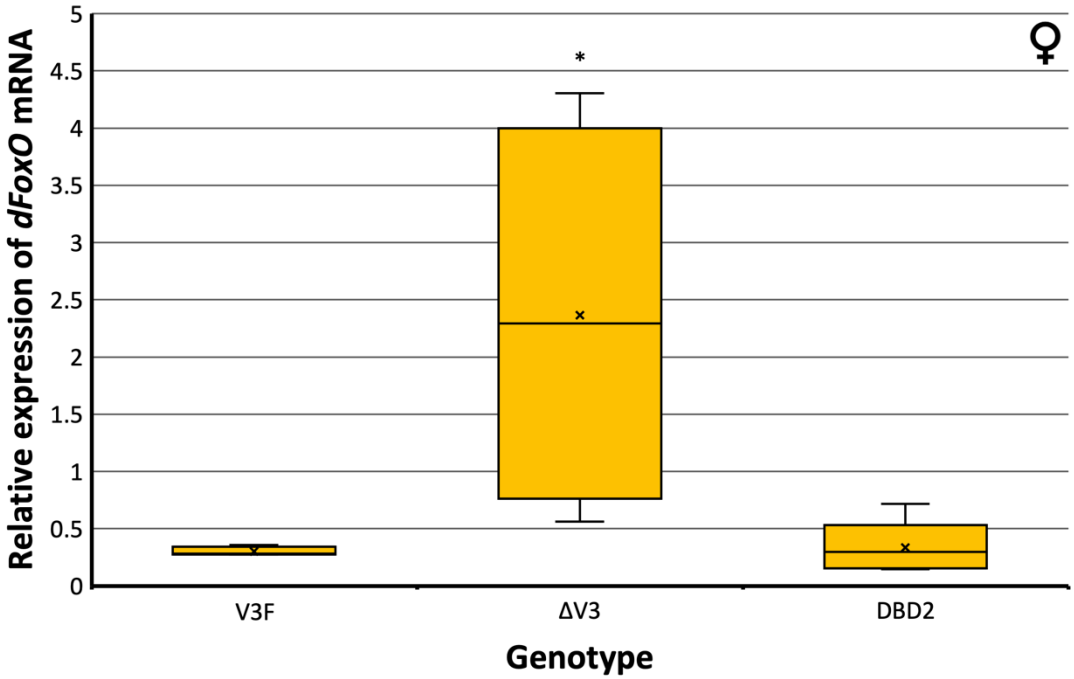

Figure 5.12. **Analysis of *dFoxO* gene expression in the dFoxO-ΔV3 mutant.** *dFoxO* mRNA expression was analysed by qRT-PCR and normalised relative to expression of *EMC10* mRNA in 7-day old adult female *Drosophila* of the indicated genotypes using primers targeting exon 2 of the *dFoxO* gene. All flies were fully fed. Standards were created using fully fed w^{Dah} 7-day old adult female *Drosophila.* Data represent relative *dFoxO* mRNA levels of 5 biological replicates for the indicated genotypes (n = 5 replicates of 15 pooled flies for each genotype, $p < 0.05$ *, Welch's t-test compared to V3F flies).

qRT-PCR analysis of *dFoxO* gene expression using primers targeting the second exon of the *dFoxO* gene showed a significant increase ($p = 0.04$) in the expression of *dFoxO* in the ΔV3 female compared to the V3F.

As before, there were no significant differences observed between the V3F and DBD2 mutants.

This data suggests that the *dFoxO* gene in the ΔV3 mutants is still being regulated and transcribed, however due to the mutation it is likely producing a truncated transcript.

Therefore, to determine whether this transcript produces any form of the dFoxO protein, western blot analysis was performed using an anti-dFoxO antibody (*Figure 5.13*).

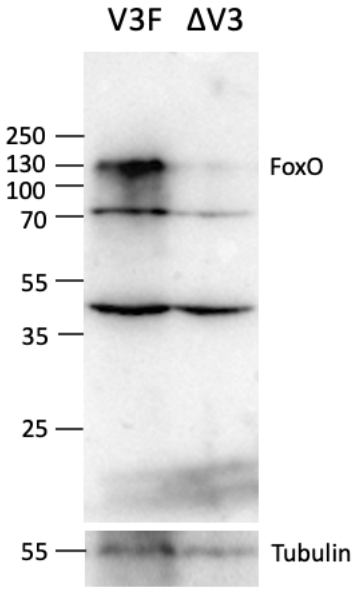

Figure 5.13. **Western blot for the dFoxO protein in the dFoxO-ΔV3 mutant.** Analysis of protein extracts from whole 7-day old adult female *Drosophila* of the indicated genotypes to enable detection of dFoxO protein expression. Blots were probed with an anti-dFoxO antibody, as well as an anti-tubulin antibody as a loading control. A large band was present at the expected size for a dFoxO protein (~130 kDa) in the V3F but not the ΔV3, whereas non-specific bands were observed in both (~60 and 40 kDa) (n = 1 replicate of 5 pooled flies for each genotype).

Western blot analysis for dFoxO protein expression identified a band present at ~130 kDa, the size expected for the dFoxO protein, in the V3F protein extracts but not in the extracts from ΔV3 mutants.

Lower molecular weight proteins (~60 and 40 kDa) were also bound by the dFoxO antibody in both V3 and ΔV3 protein extracts indicating some non-specific binding of the anti-FoxO antibody. However, no additional smaller bands were observed in the ΔV3 protein extracts suggesting that a truncated dFoxO protein is not expressed in these flies.

Taken together this data suggests that regulation of the *dFoxO* gene is still occurring in the ΔV3 mutant flies, leading to increases in the number of reads present in this mutant compared to the V3F mutant control. It also suggests that the partial transcript produced due to this, does not seem to produce any form of truncated protein,

therefore it should not cause any phenotypic effect. However, loss of one of the two antibody epitopes may affect the results for the ΔV3 mutant flies.
Furthermore, this is not observed in either the V3F or DBD mutants indicating there is normally feedback on the *dFoxO* gene that is possibly modulated in a dFoxO-dependent DNA-binding independent manner.

5.3.1.5 Verification of RNA-seq data and analysis

5.3.1.5.2 Quantitative reverse transcription PCR (qRT-PCR) verification of RNA-seq analysis

The verification of the analysis of the RNA-seq was an important stage of analysing the differential expression between mutants. Therefore, to verify the gene expression changes identified within the RNA-seq analysis, a subset of genes was independently analysed using qRT-PCR.

qRT-PCR was performed on a selected group of metabolically related genes identified as differentially expressed from the initial RNA-seq analysis. These genes were: *bmm* (*Figure 5.14*), *tps1* (*Figure 5.15*), and *bigmax* (*Figure 5.16*).

a

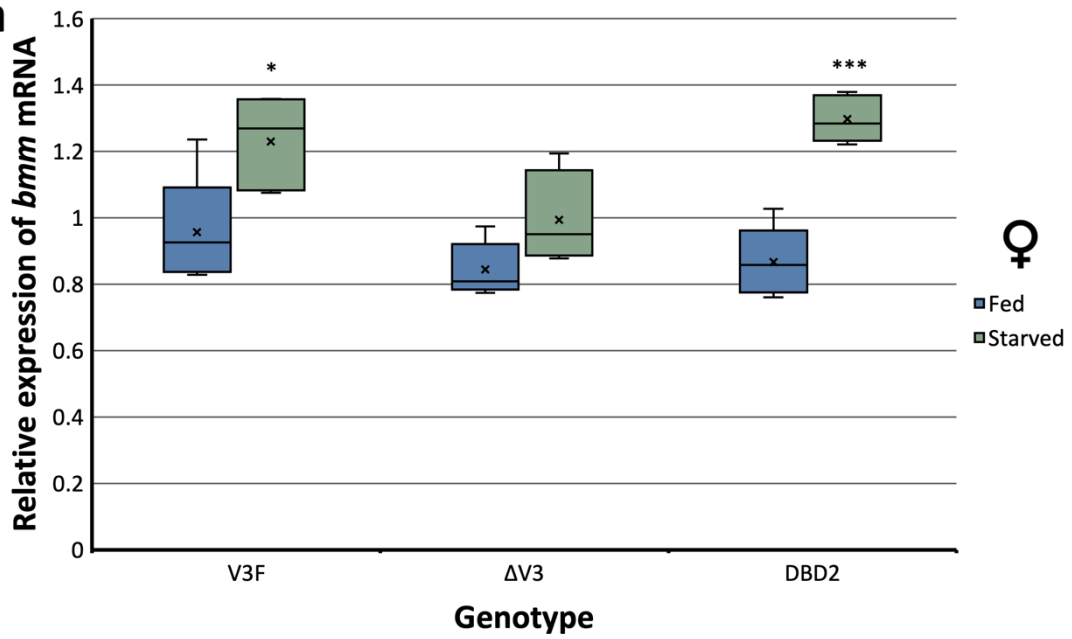

b

Comparison	LogFC	Adjusted p-value
V3F fed to V3F starved	0.27	0.0004
ΔV3 fed to ΔV3 starved	0.52	2.78E-14
DBD2 fed to DBD2 starved	0.65	2.63E-15
V3F fed to ΔV3 fed	-0.11	0.04
V3F fed to DBD2 fed	-0.19	0.01

Figure 5.14. **Analysis of the expression of *bmm* by qRT-PCR.**
bmm mRNA expression was analysed by qRT-PCR and normalised relative to expression of *EMC10* mRNA in 7-day old adult female *Drosophila* of the indicated genotypes. All flies were either fully fed or subjected to 72-hours of starvation. Standard curves were created using fully fed w^{Dah} 7-day old adult female *Drosophila.* (a) Data represent relative *bmm* mRNA levels for the indicated genotypes and conditions (n = 5 replicates of 15 pooled flies for each genotype, $p < 0.05$ *, $p < 0.001$ ***, Welch's t-test comparing fed to the starved of each genotype). (b) Results of RNA-seq analysis of the *bmm* gene showing log2 fold change (logFC) and adjusted p-value (i.e., p-value adjusted using the Benjamini-Hochberg procedure to reduce false positives) for each comparison.

RNA-seq data showed significant increases for *bmm* gene expression in the starved state when compared to the fed state of the same mutant for all genotypes.

There were also significant decreases in *bmm* gene expression in the fully fed ΔV3 and DBD2 mutants compared to the fully fed V3F mutant.

qRT-PCR showed significant increases in both the V3F and DBD2 starved mutants compared to the fed mutants of the same genotype ($p = 0.02$ for the V3F and $p = 1.2E-4$) for the DBD2 comparisons). This was in line with the RNA-seq data.

Unlike the RNA-seq data, the ΔV3 starved mutants showed no significant difference compared to the ΔV3 fed mutants. However, expression was shown to be trending upwards which power analysis indicated could reach statistical significance with a sample size of 12.
Furthermore, no significant differences were observed between the fed ΔV3 or DBD2 mutants compared to the fed V3F mutant.

a

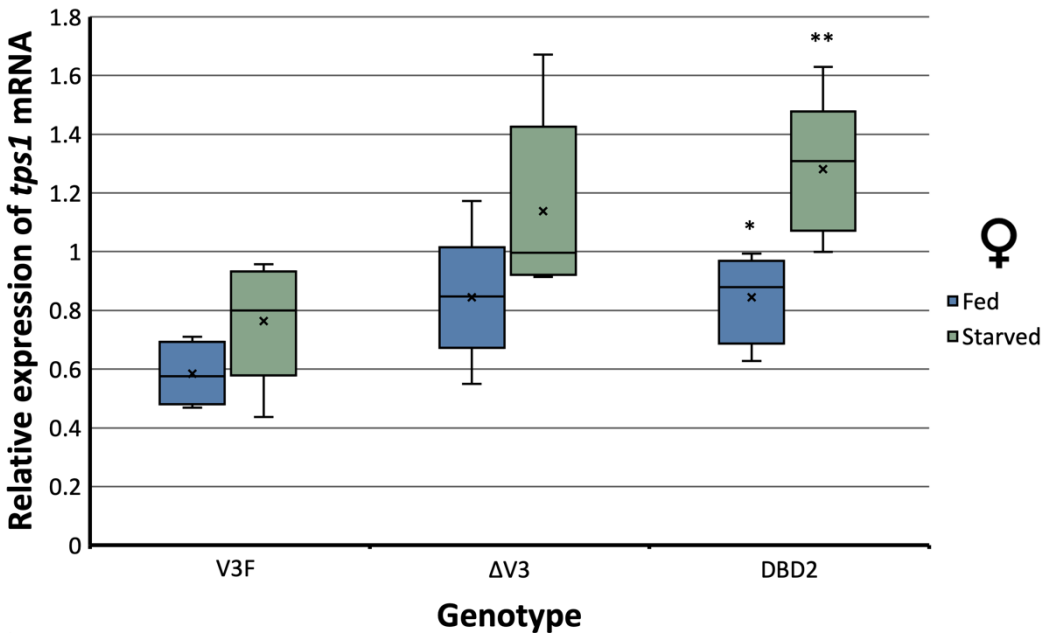

b

Comparison	LogFC	Adjusted p-value
V3F fed to ΔV3 fed	0.37	0.001
V3F fed to DBD2 fed	0.25	0.01
V3F starved to ΔV3 starved	0.69	0.001
V3F starved to DBD2 starved	0.86	3.87E-6
DBD2 fed to DBD2 starved	0.49	2.82E-6

***Figure 5.15*. Analysis of the expression of *tps1* by qRT-PCR.**
tps1 mRNA expression was analysed by qRT-PCR and normalised relative to expression of *EMC10* mRNA in 7-day old adult female *Drosophila* of the indicated genotypes. All flies were either fully fed or subjected to 72-hours of starvation. Standard curves were created using fully fed w^{Dah} 7-day old adult female *Drosophila*. (a) Data represent relative *tps1* mRNA levels for the indicated genotypes (n = 5 replicates of 15 pooled flies for each genotype, $p < 0.05$ *, $p < 0.01$ **, Welch's t-test compared to the V3F). (b) Results of RNA-seq analysis of the *tps1* gene showing log2 fold change (logFC) and adjusted p-value (i.e., p-value adjusted using the Benjamini-Hochberg procedure to reduce false positives) for each comparison.

RNA-seq data showed significant increases for *tps1* gene expression in the fully fed ΔV3 and DBD2 mutants compared to the fully fed V3F mutant. Significant increases were also observed in the starved ΔV3 and DBD2 mutants compared to the starved

V3F mutant. There was also a significant increase in *tps1* gene expression in the starved DBD2 mutant compared to the fed DBD2 mutant.

qRT-PCR showed significant increases in the DBD2 mutants in both the fed and starved states compared to the V3F mutants under the same conditions ($p = 0.04$ for the fed and $p = 0.006$ for the starved comparisons). There was also a significant increase in *tps1* expression in the DBD2 starved mutants compared to the DBD2 fed mutants ($p = 0.01$). These observations were in line with the RNA-seq data.

Unlike the RNA-seq data, the ΔV3 fed and starved mutants showed no significant difference compared to the V3F mutants under the same conditions. However, expression was shown to be trending upwards which power analysis indicated could reach statistical significance with sample sizes of 11 and 12 for fed and starved states respectively.

a

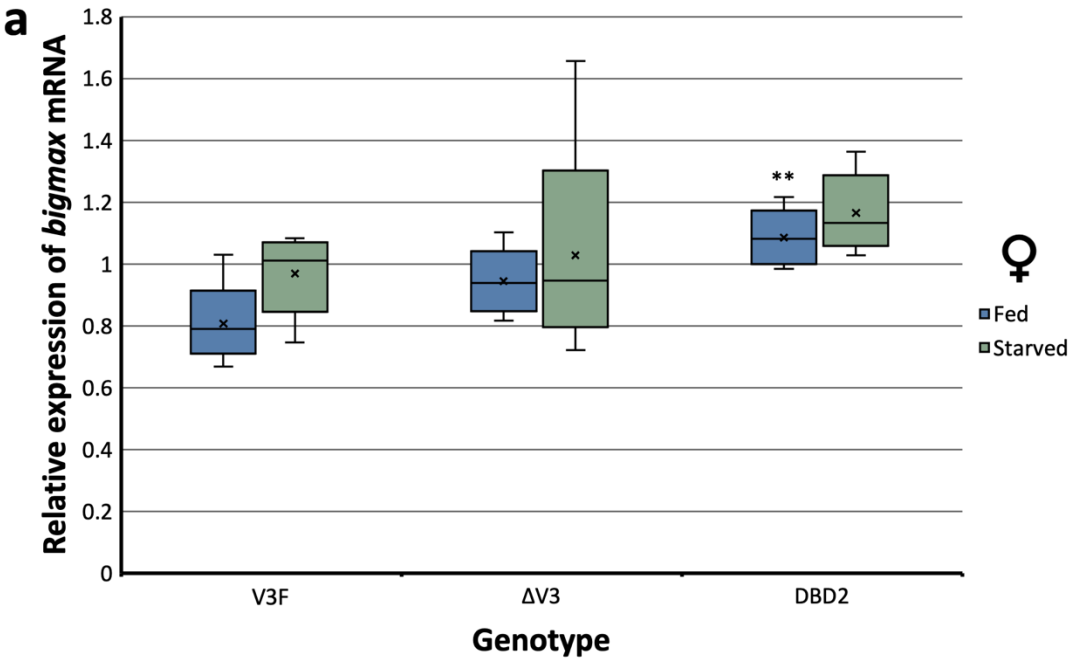

b

Comparison	LogFC	Adjusted p-value
V3F fed to ΔV3 fed	0.5	7.95E-12
V3F fed to DBD2 fed	0.6	1.84E-15
V3F starved to DBD2 starved	0.20	0.04
V3F fed to V3F starved	0.38	6.03E-5

Figure 5.16. **Analysis of the expression of *bigmax* by qRT-PCR.**
bigmax mRNA expression was analysed by qRT-PCR and normalised relative to expression of *EMC10* mRNA in 7-day old adult female *Drosophila* of the indicated genotypes. All flies were either fully fed or subjected to 72-hours of starvation. Standard curves were created using fully fed w^{Dah} 7-day old adult female *Drosophila*. (a) Data represent relative *bigmax* mRNA for the indicated genotypes (n = 5 replicates of 15 pooled flies for each genotype, $p < 0.01$ **, Welch's t-test compared to the V3F). (b) Results of RNA-seq analysis of the *bigmax* gene showing log2 fold change (logFC) and adjusted p-value (i.e., p-value adjusted using the Benjamini-Hochberg procedure to reduce false positives) for each comparison.

RNA-seq data showed significant increases for *bigmax* gene expression in the fully fed ΔV3 and DBD2 mutants compared to the fully fed V3F mutant. Significant increases were also observed in the starved DBD2 mutant compared to the starved V3F mutant, and in the starved V3F mutant compared to the fed V3F mutant.

qRT-PCR showed a significant increase in the DBD2 fed mutants compared to the V3F mutants under the same condition ($p = 0.006$). No significant differences were observed when comparing the fed ΔV3 and DBD2 mutants to starved mutants of the same genotype or when comparing the ΔV3 mutants to the V3F mutants in the starved state. These observations were in line with the RNA-seq data.

However, no significant differences were observed for the other comparisons. Although, expression did appear to be trending upwards for these comparisons. Where power analysis indicated the ΔV3 fed compared to the V3F fed, the DBD2 starved compared to the V3F starved, and the V3F starved compared to the V3F fed could all reach statistical significance with sample sizes of 13, 11, and 15 respectively.

Taken together the results of the qRT-PCR align relatively well with the results observed in the RNA-seq analysis. However, due to there being some discrepancies mostly due to expression changes not reaching statistical significance, a gene with a large fold change was chosen to further support this verification.
Therefore, as the *Drosophila insulin-like peptide 3* (*dILP3*) gene showed large log2 fold changes across conditions, qRT-PCR analysis was carried out on this gene as well (*Figure 5.17*).

a

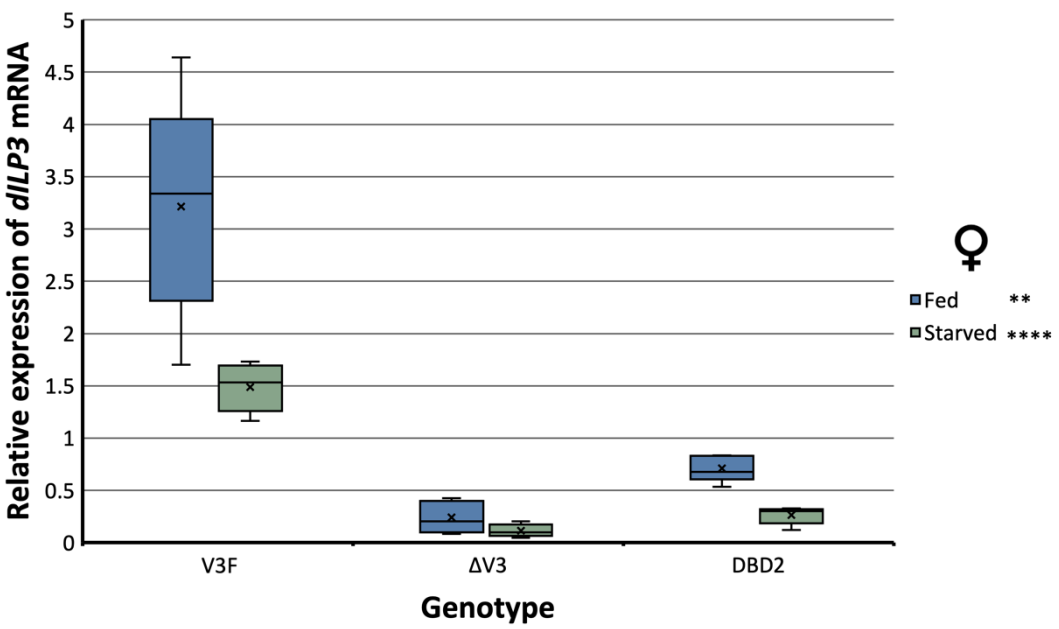

b

Comparison	LogFC	Adjusted p-value
V3F fed to ΔV3 fed	-2.16	2.60E-21
V3F fed to DBD2 fed	-1.98	7.39E-17
V3F fed to ΔV3 starved	-1.77	3.67E-6
V3F starved to DBD2 starved	-1.37	0.0001
V3F fed to V3F starved	-1.31	6.31E-8

***Figure 5.17*. Analysis of the expression of *dILP3* by qRT-PCR.**
dILP3 mRNA expression was analysed by qRT-PCR and normalised relative to expression of *EMC10* mRNA in 7-day old adult female *Drosophila* of the indicated genotypes. All flies were either fully fed or subjected to 72-hours of starvation. Standard curves were created using fully fed w^{Dah} 7-day old adult female *Drosophila*. (a) Data represent relative *dILP3* mRNA levels for the indicated genotypes (n = 5 replicates of 15 pooled flies for each genotype, $p < 0.01$ **, $p < 0.0001$ ****, Welch's t-test compared to the V3F). (b) Results of RNA-seq analysis of the *dILP3* gene showing log2 fold change (logFC) and adjusted p-value (i.e., p-value adjusted using the Benjamini-Hochberg procedure to reduce false positives) for each comparison.

RNA-seq data showed significant decreases for *dILP3* gene expression in the fully fed ΔV3 and DBD2 mutants compared to the fully fed V3F mutant. Significant decreases were also observed in the starved ΔV3 and DBD2 mutants compared to

the starved V3F mutant. There was also a significant decrease in *dILP3* gene expression in the starved V3F mutant compared to the fed V3F mutant.

qRT-PCR showed a significant decrease in both the ΔV3 and DBD2 fed mutants compared to the V3F mutants under the same condition ($p = 0.005$ for the ΔV3 and $p = 0.01$ for the DBD2). There was also a significant decrease in both the ΔV3 and DBD2 starved mutants compared to the V3F starved mutant condition ($p = 3E-7$ for both ΔV3 and DBD2). A significant decrease was also observed in the V3F starved mutant compared to the fully fed V3F mutant ($p = 0.02$). There was no significant difference observed between the ΔV3 fed and ΔV3 starved mutant. These observations were all in line with the RNA-seq data.

Interestingly, an additional significant decrease in *dILP3 gene expression* in the DBD2 starved mutant compared to the DBD2 fed mutant was also observed in the qRT-PCR data ($p = 2E-4$). This was not found in the RNA-seq data.

Taken together, this *dILP3* qRT-PCR expression data further supports the results obtained during the RNA-seq analysis, whilst also indicating discrepancies seen between the qRT-PCR and RNA-seq data of other genes could be due to low fold changes and variability. The difference in transcription of this gene during starvation in the V3F and DBD2 mutants compared to the ΔV3 mutants also potentially highlights this gene as being modulated in a dFoxO-dependent DNA-binding independent manner.

As qRT-PCR verification was found to align with the RNA-seq data for female flies, qRT-PCR was also carried out on RNA extracted from male V3F, ΔV3, and DBD2 mutants under fully fed or starved conditions. This was done to determine if male flies responded in the same manner as female flies to changes in nutritional status or genotype, or if any sexually dimorphic changes in gene expression occurred.
Therefore, qRT-PCR was performed on the *dFoxO* gene using both primer sets used for the female qRT-PCR analysis (*Figure 5.18).*

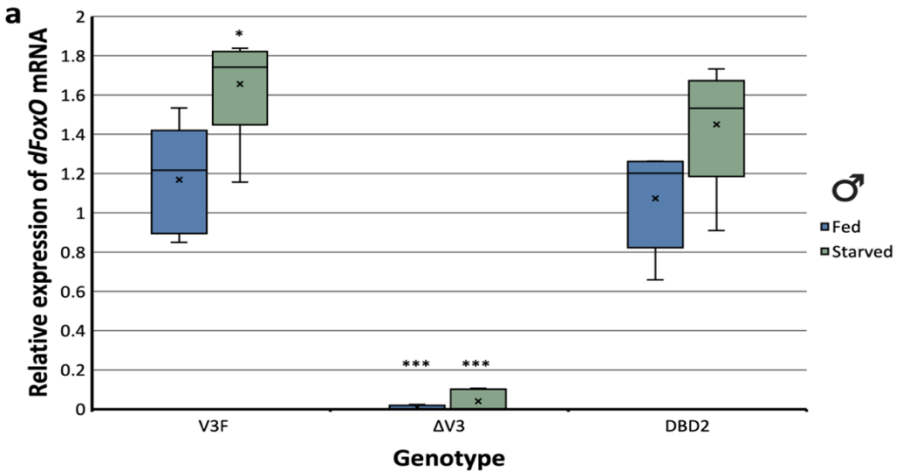

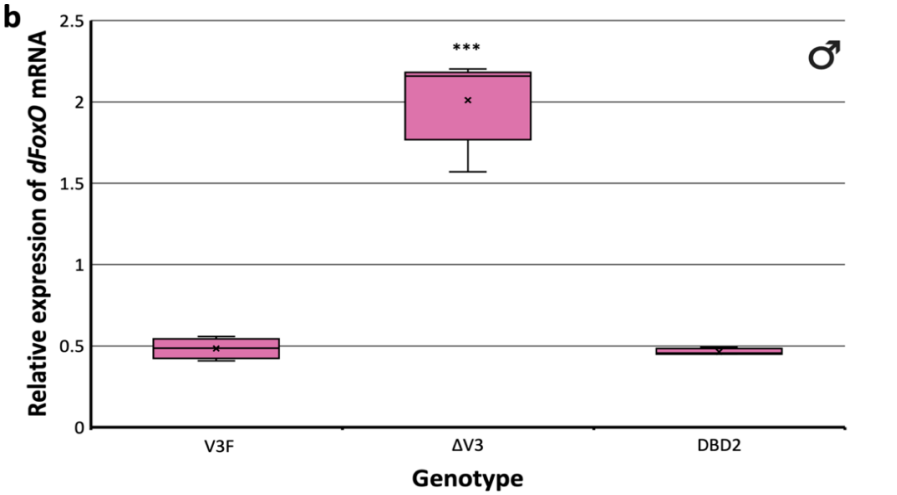

c

♀

Comparison	qRT-PCR using primers targeting: Exon 2	Exon 6 & 7
V3F fed	0.30 (+/- 0.04)	1.08 (+/- 0.16)
ΔV3 fed	2.38 (+/- 1.64)	1.09E-13 (+/- 2.16E-13)
DBD2 fed	0.33 (+/- 0.23)	1.25 (+/- 0.31)
V3F starved	-	1.33 (+/- 0.20)
ΔV3 starved	-	0.04 (+/- 0.04)
DBD2 starved	-	1.40 (+/- 0.43)

Figure 5.18. **Analysis of *dFoxO* expression in the male dFoxO-ΔV3 mutant.** *dFoxO* mRNA expression was analysed by qRT-PCR and normalised relative to expression of *EMC10* mRNA in 7-day old adult male *Drosophila* of the indicated genotypes. Standard curves were created using fully fed w^{Dah} 7-day old adult female *Drosophila.* Primers targeting (a) exons 6 and 7 of the *dFoxO* gene for flies either fully fed or after 72-hours of starvation, and (b) exon 2 of the *dFoxO* gene for fully fed flies were used. Data represent relative *dFoxO* mRNA levels for the indicated genotypes. (c) Relative mRNA expression of female qPCR data for comparison with standard deviation in brackets (n = 5 replicates of 30 pooled flies for each genotype, $p < 0.05$ *, $p < 0.001$ ***, Welch's t-test compared to V3F flies).

qRT-PCR analysis for *dFoxO* expression, using primers that target the 6th and 7th exons of the *dFoxO* gene, showed a significant decrease in ΔV3 males in both the fed and the starved state compared to V3F males under the same conditions (99% decrease for *dFoxO* in the fed state p = 7.3E-4, and 98% decrease for *dFoxO* in the starved state p = 2E-4). However, when using primers targeting exon 2 of the *dFoxO* gene, there was a significant increase in *dFoxO* mRNA in the fully fed ΔV3 males compared to fully fed V3F males (p = 2E-4).
No significant differences in *dFoxO* gene expression were observed between the V3F and DBD2 mutant males when using either primer set, or when comparing the fed and the starved of the same mutant for either the ΔV3 or DBD2.
These observations are consistent with the results observed for female flies.

Unlike the female data, however, the V3F starved mutant males showed a significant increase compared to the V3F fed mutants (p = 0.03). However, female *dFoxO* expression when comparing this condition was shown to be trending upwards.

Taken together, this data showed that with regard to *dFoxO* expression male mutants behaved similarly to females. A difference was present, although the observation in female data did show results trending in the same direction that mirrors this male data even though they did not reach significance.

5.3.1.5.3 Comparisons of transcriptional responses to loss of dFoxO

After qRT-PCR results showed alignment to those produced via RNA-seq, further verification of the dFoxO-ΔV3 mutant could be made by comparing the transcriptional response to loss of dFoxO in a previously published dataset.

Genes that showed significant differential expression between the ΔV3 mutants and the V3F mutant controls under fully fed conditions were identified alongside their fold change in expression (*Figure 5.19*).

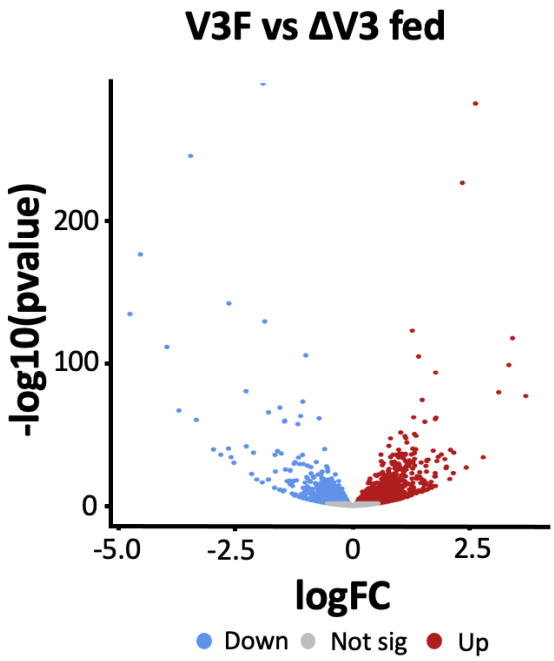

Figure 5.19. **Visualisation of differentially expressed genes comparing the fully fed V3F and ΔV3 mutants.**
Volcano plot comparing the V3F and ΔV3 mutant RNA-seq data sets under fully fed conditions. Plots show the -log10(pvalue) for each gene plotted against log2 fold change (logFC). Significantly upregulated genes (logFC > 0) are highlighted in red and downregulated genes (logFC < 0) in blue ($p < 0.05$). Genes that show no significant differences in expression are in grey.

There were a large number of genes (4190) that showed a significant ($p < 0.05$) differential expression between the ΔV3 mutants and the V3F mutant controls under fully fed conditions. Approximately 50% were upregulated (2197) and approximately 50% were downregulated (1993) in the comparisons between these two *dFoxO* mutants.

As this indicated changes in genes expression between the ΔV3 mutants and the V3F mutant control, this data was then compared to a previously published dataset that analysed transcriptional responses to loss of dFoxO activity.
This previously published dataset was an existing microarray dataset produced by Alic *et al.* (2011) comparing a previously characterised *dFoxO* null allele ($dFoxO^{\Delta 94}$) to controls (*Figure 5.20*).

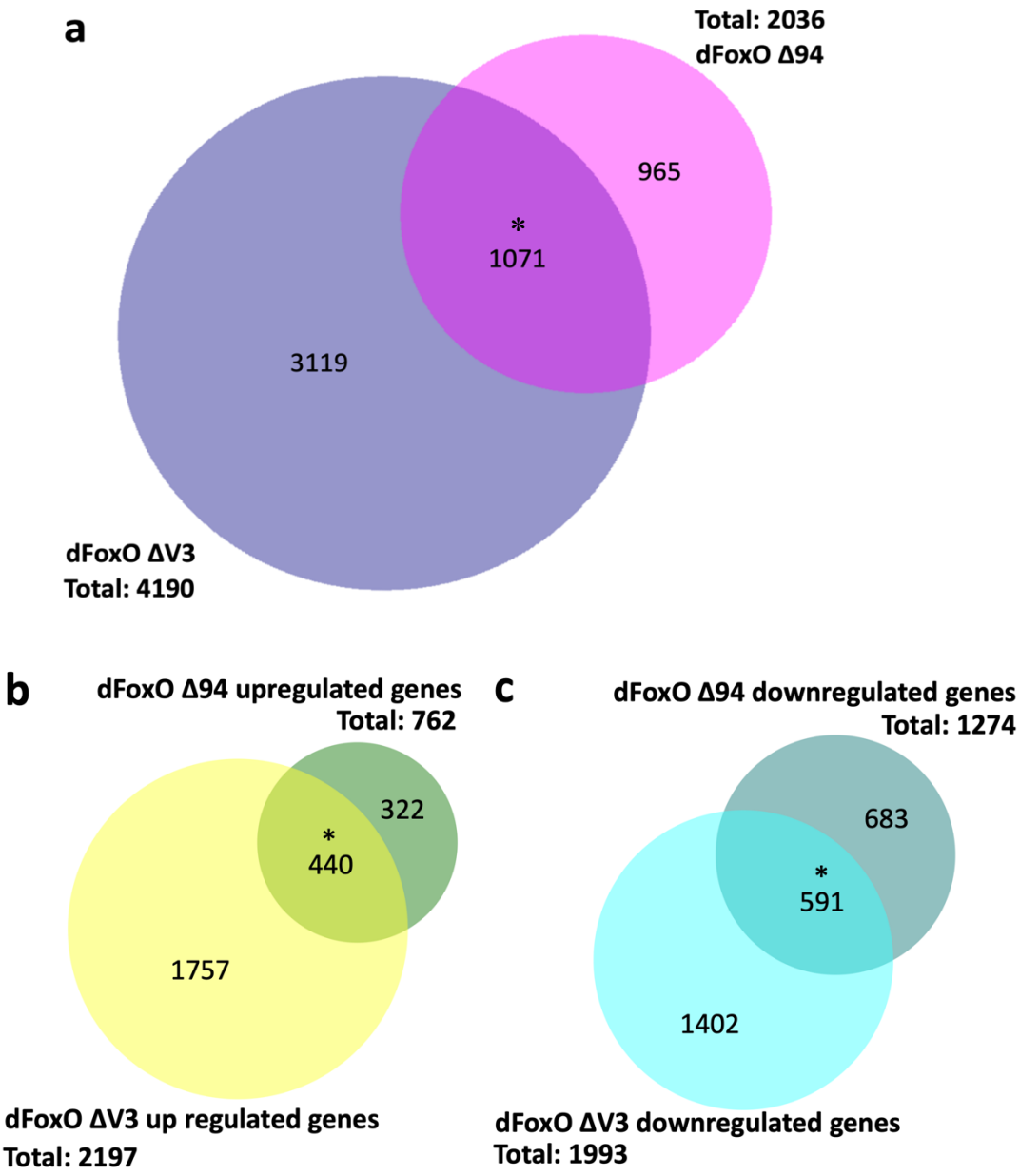

***Figure 5.20*. Comparison of differentially expressed genes identified in the dFoxO-ΔV3 mutant with differentially expressed genes characterised in an additional *dFoxO* null allele.**

(a) Proportional Venn diagram comparing the differentially expressed gene lists identified in the fully fed dFoxO-ΔV3 mutants and those identified in *dFoxO*$^{\Delta 94}$ mutants. A significant overlap was identified between the two data sets (p = 1.58E-119 *, hypergeometric analysis). Differentially expressed genes were separated into those that showed upregulated (b) and (c) downregulated expression. Again, significant overlaps were identified between the data sets (up: p = 2.99E-167 *, down: p = 1.21E-190 *, hypergeometric analysis). Numbers indicate the number of genes in each category.

The gene lists from microarray experiments described in Alic *et al.* (2011) were much smaller than those produced in the RNA-seq experiments described here for the ΔV3 mutants (approximately half the size). However, there was a significant overlap between the genes that were identified as differentially expressed in *dFoxO*$^{\Delta 94}$ null mutants and those differentially expressed in dFoxO-ΔV3 mutants (p = 1.58E-119) compared to their appropriate control. Thus, 52.6% of the total number of differentially expressed genes in *dFoxO*$^{\Delta 94}$ nulls were shared with the dFoxO-ΔV3 mutants.

Furthermore, when the gene lists were subdivided into up- or down-regulated genes, significant overlaps were again identified (p= 2.99E-167 for the upregulated genes, and p = 1.21E-190 for the downregulated genes) with 58% of the upregulated genes and 46% of the downregulated genes downregulated in in *dFoxO*$^{\Delta 94}$ nulls showing similar up- and down-regulation in the dFoxO-ΔV3 mutants.

Taken together, this demonstrated relatively consistent changes in gene expression between the two independently isolated *dFoxO* alleles, despite the presence of a GAL4 (i.e., in the *dFoxO*$^{\Delta 94}$) and different methods of gene analysis.

5.4. Discussion

In the previous chapters, it was determined that the normal starvation response is dependent on dFoxO activity but does not depend on a functional DBD. Therefore, the main aim of this chapter was to further investigate the mechanisms by which the DBD mutants modulate normal responses to starvation by comparing gene expression changes induced by starvation in the DBD2 mutants to ΔV3 mutants. The hypothesis stated that there would be an observable difference in gene expression in these *dFoxO* mutants during starvation, that could lead to the observed differences in dFoxO metabolic activity.

5.4.1 RNA-sequencing of *Drosophila FoxO* mutants

5.4.1.1 Quality control of the RNA-sequencing data, mapping, and alignment

Using the FastQC and MultiQC quality control tools, raw sequence data was initially assessed for basic overall quality to ensure fewer errors were produced during these and later analyses. These errors are caused by limitations in the sequencing techniques used, however as an Illumina sequencing platform (Illumina 1.9) was used to generate the sequence reads for this project, these errors were less of a concern. This is because Illumina uses an ensemble-based sequencing by synthesis technique, which produces a low error rate of <1% and with most of these errors produced via single nucleotide mismatches (Kukurba & Montgomery, 2015). Therefore, it is unsurprising that these analyses showed good overall quality for all reads across different replicates of all the genotypes with one not being worse than the other that can often be the case with reverse reads and high levels of duplication, which is expected of RNA-seq data (Kwon *et al.* 2013). Further quality assessment showed successful mapping of reads to the reference genome, as nearly all the reads were mapped to a unique region of the reference genome, primarily to exonic regions, confirming good quality RNA-seq data with no genomic DNA contamination or bias across the gene body. This uniformity in gene body coverage suggests that there was no 5' or 3' end bias, supporting the assumption that there was no RNA degradation occurring during sequencing (Wang *et al.* 2016a). Most genes were shown to be mapped to chromosomes 2, 3, and X, which is expected as the samples were taken from female *Drosophila* and therefore there would be no Y chromosome present for reads to be sequenced from. Of the 3 other *Drosophila* chromosomes (2, 3, and 4), 2

and 3 carry the most genes from the genome as the 4th chromosome, also known as the dot chromosome due to its diminutive size, only carries ~3.5% of the genome therefore large percentages of genes being mapped to it would be unlikely (Sun *et al.* 2000).

Together this indicated both sample and library preparation were carried out appropriately and the resulting gene expression analysis would draw accurate conclusions.

5.4.1.2 VERIFICATION OF THE RNA-SEQ RESULTS AND ANALYSIS

To ensure that the RNA-seq data was analysed appropriately various verification steps were taken, including qRT-PCR and comparisons to previously published data sets. Firstly, the genes that were identified as differentially expressed in the ΔV3 mutant flies compared to the V3F controls were compared to those identified as differentially expressed by microarray analysis in an independently derived *dFoxO* mutant allele, *dFoxO*$^{\Delta 94}$ (Alic *et al.* 2011). This experiment used 4 biological replicates of 10 females per replicate and an Affymetrix Drosophila Genome 2.0 GeneChip™ which analyses over 18,500 *Drosophila* transcripts (Alic *et al.* 2011). This comparison showed a significant overlap in the genes differentially expressed between the two *dFoxO* null mutants and their controls. Comparing these datasets also supported the use of RNA-seq as an experimental method for this project, as not only was the microarray dataset ~50% the size of that produced here by RNA-seq but the log-fold changes observed were all relatively small. Furthermore, several studies comparing the two methods have shown the advantages of using RNA-seq technology over microarray. For example, in the comparison for studying rat toxicogenomics, RNA-seq not only showed additional DEGs compared to microarray data but also identified non-coding DEGs that could improve the understanding of the specific molecular mechanisms involved (Rao *et al.* 2019). In addition, in the transcriptome profiling of activated T-cells, RNA-seq data surpassed other methods in detecting low-level transcripts and differentiating between isoforms (Zhao *et al.* 2014). Detection of lowly expressed transcripts is key when studying the dynamics of FoxO activity and gene transcription as many of FoxO's interactions are transient, and therefore changes in gene expression can often occur at lower and harder to detect levels (Glauser *et al.* 2007; Accili & Arden, 2004). As well as the overlap between differentially expressed genes in the microarray and RNA-seq data sets, it was also shown that the directions of regulation of those genes in these two datasets were also relatively consistent, with

the same genes showing either up- or down-regulation in both. There were, however, some discrepancies between the datasets where genes were missing from one dataset or regulated in the opposite direction between datasets. Examples of genes not present within the microarray data, but present in the RNA-seq data include the insulin-like peptide, *dILP6,* the insulin receptor, InR, and the fatty-acid--CoA ligase, *pdgy,* genes that would be expected to change expression in a *dFoxO* mutant as they are known direct FoxO targets (Birnbaum *et al.* 2019; Xu *et al.* 2012).

Examples of genes that show the opposite regulation include the gene *Bendless (Ben),* which encodes an E2 ubiquitin-conjugating enzyme that regulates cell death (Ma *et al.* 2014), which is downregulated in the RNA-seq data but upregulated in the microarray. Which direction of transcription is accurate is hard to determine as a link between Ben and dFoxO has yet to be made, however, dFoxO has been known to suppress the expression of the JNK-kinase, Hep, which in turn is known to suppress Ben (Wang *et al.* 2005; Ma *et al.* 2014). Therefore, a loss of dFoxO would reduce Hep suppression, increasing Hep activity and increased suppression of Ben, lowering its expression leading to the response seen in the RNA-seq data.

It should be noted that the flies used in the $dFoxO^{\Delta 94}$ microarray experiments (both *dFoxO* nulls and controls) were also carrying the daGAL4 driver (Alic *et al.* 2011). The daGAL4 driver drives ubiquitous expression of the GAL4 transcription factor but should only activate gene transcription in the presence of its upstream activation sequence (UAS). However, there are some suggestions that its presence may interfere with endogenous gene expression even in the absence of the UAS via interactions with other signalling or transcriptional components. For example, in mice even in the absence of the UAS, a GAL4 line has been linked to toxicity and phenotypic abnormalities (Halpern *et al.* 2008). Furthermore, the microarray analysis employed used the limma tool (as opposed to the DESeq2 used in the RNA-seq analysis), this could cause some differences between results produced as the limma tool uses a linear relationship and normalised data to analyse gene expression whereas a negative binomal relationship and raw data is used in DESeq2 (Liu *et al.* 2021). This could affect results as, as with all statistical analysis, various different assumptions are made in each analysis (e.g., limma assumes a normal distribution and DESeq2 does not) that will result in observable differences in gene expression. In addition, it has been found that microarray measurements can correlate well RNA counts in optimal ranges but can suffer from bias and reduced precision outside of the optimum (Richard *et al.* 2014). This, alongside RNA-seq showing a higher

dynamic range than microarray allowing for the identification of low abundance transcripts, could therefore leave comparisons between microarray and RNA-seq data lacking, with inconsistencies between them being found in comparative studies (van der Kloet *et al.* 2020). For example, one study found that comparisons between microarray and RNA-seq data ranged in correlation coefficents from 0.62-0.75 (i.e., moderate to strong correlation) but correlation between data of the same methods was on average 0.96 (i.e., very strong correlation) (Fu *et al.* 2009b). However, relatively recent preliminary findings have shown that by transforming both analysis outputs using relevant gene enrichment scores, the correlation between the results can be increased (van der Kloet *et al.* 2020). Due to these reasonings, therefore, this could explain some of the discrepancies between the RNA-seq and microarray datasets. Furthermore, future re-analysis of these datasets may show increased correlation as these computational data analysis techniques progress.

The most surprising difference found between the microarray and RNA-seq data was the expression of *dFoxO* itself. As expected in a *dFoxO* null mutant, in the microarray data *dFoxO* expression was significantly downregulated but was surprisingly upregulated in the RNA-seq data from *dFoxO* ΔV3 mutants that should also function as a genetic null.

Further examination of the location of the mapped reads in the ΔV3 mutants and analysis of *dFoxO* expression by qRT-PCR using primers that amplify different regions of the *dFoxO* transcript showed that indeed there was an increase in expression of a 5' region of the *dFoxO* transcript. This is possible as the ΔV3 null mutant is only a partial deletion of the *dFoxO* gene removing exons 3-8 compared to the $dFoxO^{\Delta 94}$ which represents a much larger deletion that also removes part of the promoter (Slack *et al.* 2011). Importantly, the truncated transcripts expressed within the ΔV3 mutants did not produce a detectable protein possibly due to instability of the gene transcripts preventing translation. However, it must be noted that the dFoxO antibody used was raised against two peptide sequences PTDELDSTKAS-NQQL (amino acids 56–70) and ETSRYEKRRGRAKKR (amino acids 192–206) (Giannakou *et al.* 2007), and the coding sequence for the latter peptide sequence is absent in the ΔV3 allele. Therefore, whilst it is possible that there is no protein produced, it is unclear whether the antibody would still bind in the absence of one of the peptide sequences and so it is possible that the antibody may not be able to detect any FoxO protein present within the ΔV3 mutant flies.

Interestingly, therefore, it appears that expression of the *dFoxO* gene itself is being negatively regulated by the dFoxO protein, where this regulation is lost in the ΔV3 mutants leading to an increase in *dFoxO* gene expression. It appeared that this modulation could be independent of dFoxO's ability to bind to DNA, as in the DBD mutants there is no change in *dFoxO* gene expression indicating this negative regulation is still intact. It is also possible that when dFoxO is absent other dFoxO-independent methods of transcriptional feedback occur on the *dFoxO* gene increasing expression due to the lack of phenotypic responses that would be expected if a functional dFoxO was present. However, again as this is not seen in the DBD mutants these phenotypic responses that act as regulatory 'sensors' seemingly occur in a DNA-binding independent manner.

Unlike the regulation of FoxO via post-translational modification, transcriptional modulation of *FoxO* gene expression is less widely reported. Evidence has been reported for the regulation of the *FoxO* gene by KRIT1 (a Krev-1/rap1a binding protein) in mammals, where KRIT1-/- mouse embryonic fibroblasts showed a significant reduction in *FoxO* mRNA expression compared to controls (Goitre *et al.* 2010). Furthermore, the *FoxO3* gene has been identified as a direct target of the tumour suppressor, p53 in mouse embryonic fibroblasts and thymocytes in response to exposure to DNA-damaging agents indicating *FoxO3* transcriptional regulation by p53 could be a major role in both age-related health declines and cancer (Renault *et al.* 2011). Similarly, *FoxO3a* mRNA (but not *FoxO1* or *FoxO4*) is upregulated in response to hypoxic stress by the hypoxia-induced factor 1 (HIF1) in both normal and cancerous cells to regulate HIF1-dependent apoptosis and maintain cell survival (Bakker *et al.* 2007).

Other Fox proteins have also been implicated in *FoxO* gene expression, where knockdown of *FoxC1* mRNA via siRNA leads to decreased *FoxO1* expression in human trabecular meshwork cells identifying a method of *FoxO* regulation in disordered eye function (e.g., Axenfeld–Rieger syndrome) (Berry *et al.* 2008). As well as FoxC proteins, the FoxO also seems to regulate its own expression. In *C. elegans,* SWSN1 (a core subunit of the chromatin modifying SWI/SNF complex) regulates expression of the FoxO homologue, *DAF16*, by co-localising to the DAF-16 promoter after direct interaction with the DAF-16 protein itself to regulate longevity and stress resistance (Bansal *et al.* 2014). Similarly, in mammals FoxO3a binds not only to its own promoter but that of *FoxO1* and *FoxO4* in the process of wound healing (Roupé *et al.* 2014).

However, despite these examples of the regulation of *FoxO* gene expression there is still little information regarding the regulation of the *FoxO* gene in non-disordered conditions. Therefore, to identify the reasons behind the increase in *dFoxO* gene expression in the ΔV3 mutants and dFoxO's possible role in modulating its own gene expression, further research in this area would be of interest.

In conjunction with the RNA-seq analysis, qRT-PCR analysis was used to independently verify some of the gene expression changes observed. The accuracy in which qRT-PCR results mapped directly onto the RNA-seq data was approximately 68% (i.e., 25 comparisons of a total of 37 were replicated exactly in the qRT-PCR data). This is quite low considering the RNA extractions used for both experiments were the same. However, despite being highly sensitive and therefore ideal as an independent verification method compared to the high-throughput status of RNA-seq, qRT-PCR is considered a medium-throughput technique (Nonis *et al.* 2014; Muniesa *et al.* 2014). This potential lowered sensitivity of qRT-PCR is reflected in the results from the power analysis, which showed that observable trends in 7 of the comparisons that did not reflect the results shown in the RNA-seq data would reach significance with a larger sample size.

Of the remaining 5 comparisons, 2 issues arose when comparing the expression of the *dFoxO* gene, where qRT-PCR was only showing significant decreases caused by the loss of exons 3-8 and the RNA-seq data was observing significant increases due to the presence of the remaining exons. This effect was due to the RNA-seq anaylsis covering the entirety of the *dFoxO* gene, including the portion of the *dFoxO* gene remaining in the null mutant, but the initial qRT-PCR analysis only focussing on exons 6 and 7 which were removed in the null mutant. Therefore, subsequent analysis was able to prove that these 2 discrepancies were due to the location of the initial *dFoxO* primers in the qRT-PCR results, as subsequent qRT-PCR with primers located in exon 2 (i.e., one of the remaining exons in the null) replicated the results seen in the RNA-seq analysis exactly.

Ultimately, there were only 3 comparisons made that were not easily explainable by technique sensitivity or primers location. These were the lack of a significant decrease in *bmm* expression in the fed state of the ΔV3 and DBD2 mutants compared to the V3F during qRT-PCR analysis, and the significant increase in the DBD2 starved compared to the DBD2 fed mutants that was observed in the qRT-PCR but not the

RNA-seq. However, it could be possible that differences in significance between qRT-PCR analysis and RNA-seq analysis could be due to reference gene instability. This is a plausible explanation as even though *EMC10* showed a non-significant change in expression between conditions in the RNA-seq data a logFC was observed. Furthermore, the cut-off for appropriate stability using the Normfinder programme used to measure stability is often 0.15 (Köhsler *et al.* 2020), whereas a result of between 0.16 and 0.19 was found here for the *EMC10* gene. Ultimately, *EMC10* was chosen as it had the lowest scores of the three genes analysed, had one of the highest non-significant p values in the RNA-seq data, and had verified primers already available. Therefore, whilst this instability may affect significance levels, trends were still observable between conditions and was able to adequately verify the RNA-seq analysis.
However, even with these few potentially unexplained discrepancies the overall accuracy when considering the reasoning given above (e.g., assay sensitivity and primer location) is approximately 92%.

This accuracy is also reflected when comparing the male and female *dFoxO* qRT-PCR analysis male *dFoxO* gene expression seemed to reflect that observed in the female data, possibly indicating why both males and females showed similar phenotypic responses in the presence of the various *dFoxO* mutations. In contrast, the male V3F showed a significant increase in *dFoxO* expression in the starved state compared to the fed, however a non-significant trend was seen in the female data indicating a similar response is occurring. These more significant responses in male analysis to female analysis could be due to sex-specific genetic regulation caused by X chromosome variations or because of sexually divergent transcriptomic changes that appear in challenging nutritional environments (Stocks *et al.* 2015; Camus *et al.* 2019).

All together this showed that the use and analysis of the RNA-seq data was appropriate and reasonably accurate. Analysis also interestingly identifies *dFoxO* gene expression as an area of research for further development in the area of dFoxO-dependent DNA-binding independent activity.

5.4.1.3 Analysis of differential gene expression

To identify differentially expressed genes the DESeq2 tool was used as compared to other forms of RNA-seq analysis, it showed a distinct performance advantage by showing a higher detection accuracy (Rapaport *et al.* 2013). Therefore, as PCA plots showed little variation between replicates of the same genotype, there was little concern over batch effects affecting the resulting differentially expressed gene lists.

Subsequent filitering showed there were a large number of significant differentially expressed genes found in all mutants during starvation (approximately 2,900-3,900). Such a large number of genes could be considered surprising given only 17.559 total genes were identified in the samples indicating 16.5-22% of the total genes are involved in this starvation response. However, previous study has found that during long-term starvation stress (i.e., flies were collected at the starvation half-life) approximately 25% of the genome was involved in the transcriptional response (Harbison *et al.* 2005). Therefore, the number of DEGs found during the RNA-seq analysis in this project aligns with previous study and can therefore be considered relatively accurate for further analysis.

5.4.1.3.1 Genes modulated in a dFoxO-independent manner

Previously observed phenotypes which seemed to be modulated in a dFoxO-independent manner included production of key metabolic macromolecules (e.g., carbohydrates glycogen and trehalose, and the lipid TAG) in the storage of energy, and the mobilisation of both carbohydrate energy stores. Interestingly, there are several genes shown in this RNA-seq data that seem to be involved in these processes.

For example, in the regulation of glycogen synthesis and breakdown *Hexokinase-C* (*Hex-C*), which is orthologous to human glucokinase and a key regulator in glycogen storage through phosphorylation of glucose using ATP (Cárdenas *et al.* 1998; Matschinsky & Wilson, 2019), is found in this gene list. Similarly, *glutamine:fructose-6-phosphate aminotransferase 2* (*GFAT2*) which allows for commitment into the hexosamine biosynthetic pathway (HBP) by using glutamine and fructose-6-phosphate to form glucosamine-6-phosphate (GlcN6P) in a highly conserved process important for regulating anabolic activity, including glycogen synthesis (Chen *et al.* 2020; Akella *et al.* 2019; Singh & Crook, 2000), is also seemingly regulated independently of dFoxO.

In the mobilisation of glycogen stores a gene of interest found to potentially be regulated independently of dFoxO is *Akh. Akh is* the adipokinetic hormone and *Drosophila* counterpart to mammalian glucagon and regulates both stored and circulating carbohydrates, particularly glycogen, through its G-protein coupled Akh receptor located in the fat body (Song *et al.* 2017; Gáliková *et al.* 2015; Bednářová *et al*. 2018). As well as glycogen catabolism, the regulation of this gene also helps to explain the modulation of both trehalose and glucose levels being independent of dFoxO activity. This is because it has also been shown via analysis of haemolymph trehalose and glucose levels that Akh-null mutants showed a distinct hypoglycaemia, possibly due to Akh regulating glucose and trehalose synthesis and levels of these circulating sugars particularly during starvation (Gáliková *et al.* 2015; Song *et al.* 2017; Mochanová *et al*. 2018). Furthermore, in the synthesis of trehalose and glucose is the gene *Pgi*, a glucose-6-phosphate isomerase which catalyses the reversible isomerisation of glucose-6-phosphate to fructose-6-phosphate or *vice versa*, a key step not just in the glycolytic pathway but also in gluconeogenesis (Grauvogel *et al.* 2007; Fermo *et al*. 2019). The regulation of this gene therefore could also explain how these sugars are able to be reduced independently of dFoxO activity. However, this phenotype could also be explained by the genes, *Pgm* (the phosphoglucomutase), *Pyk, AdipoR,* and those encoding various α-glucosidases (MalA group of enzymes). Where whole body glucose homeostasis and glycolysis are known to be regulated by *Pyk,* a critical pyruvate kinase enzyme in the modulation of gluconeogenesis, and *AdipoR,* the adiponectin receptor responsible for regulating AMPK and peroxisome proliferator-activated receptor (PPAR)-α in the control carbohydrate homeostasis (Israelsen & Vander Heiden, 2015; Long & Zierath, 2006; Peeters & Baes, 2010; Park *et al.* 2016).

Previous research has also shown that both the juvenile hormone (JH) and 20-hydroxyecdysone (20E) signalling pathways have been implicated in the expression of trehalose metabolic genes (Shukla *et al.* 2015). This is interesting as a number of genes involved with these signalling pathways were identified as being differentially expressed independently of dFoxO during starvation. For example, the Halloween genes *sro*, *spo*, and *sad,* and the gene encoding the prothoracicotropic hormone *Ptth* are all genes associated with ecdysteroid biosynthesis, particularly during development (Niwa *et al.* 2010; Chanut-Delalande *et al.* 2014; Warren *et al.* 2002; Kim *et al.* 1997) and are also regulated in a dFoxO-independent manner in this RNA-seq data. In addition, the histone modifier G9a is also involved with ecdysteroid

regulatory pathways (Stabell *et al.* 2006). These genes, alongside, the transcription factor ftz-f1, that modulates JH signalling and trehalose circulation by increasing trehalose transport and *trehalase* expression (Nishimura, 2020), suggests a dFoxO-independent method of trehalose metabolism that explains the phenotypes observed using these *dFoxO* mutants.

There are also genes in this dFoxO-independent gene list that link the modulation of lipid stores to dFoxO-independent activity that explains the lack of effect of *dFoxO* mutation in lipid storage and long-term lipid mobilisation.
With regard to lipid synthesis genes regulated in this dFoxO-independent manner include the glycerol-3-phosphate 1-O-acyltransferase (GPAT) *mino,* which converts glycerol-3-phosphate into lysophosphatidic acid playing a key role in lipid biosynthesis and lipid droplet formation, and *mdy* the diacylglycerol O-acyltransferase 1 that is critical in catalysing the conversion of DAG to TAG (Fantin *et al.* 2019).
In a similar vein the genes, *Tor*, *sug*, and *PTEN* were also found to be regulated in this dFoxO-independent manner. The target of rapamycin, *Tor* is interesting because it has a central role in the cellular nutrient sensing network and controls a variety of cell metabolism processes, such as amino acid synthesis and glucose homeostasis (Wullschleger *et al.* 2006). This gene also relates to PTEN's role in the modulation of lipogenesis via SREBP-1c, a transcription factor with key lipogenic targets (such as, *fatty acid synthase* (*FASN*) and *acetyl-CoA carboxylase* (*ACC*)); as this process is Tor-dependent (Haeusler *et al.* 2014). Furthermore, PTEN can regulate energy homeostasis and excess energy storage by regulating glycolysis and insulin signalling (Chen *et al.* 2018; Venniyoor, 2020). This role in regulating lipogenesis is also carried out by sugarbabe (sug), a transcription factor regulated by Mondo/Mlx and activin signalling that leads to the regulation of a subset of Mondo/Mlx-dependent processes such as lipogenesis, carbohydrate metabolism, and nutrient transport and digestion (Mattila *et al.* 2015).

Even though there was a delay in lipid mobilisation in the ΔV3 mutants, ultimately lipid stores were still mobilised in all mutants after long periods of starvation. This was surprising given FoxO's known role in lipid breakdown, however similar to lipid storage many genes were found in the RNA-seq analysis of these *dFoxO* mutants that could explain the seemingly dFoxO-independent nature of this phenotype.

For example, genes such as the TAG lipases *bmm, dob,* and *Lip4* are all present within this gene list. Starvation in all three *dFoxO* mutants induced the upregulation of *bmm* expression, the *Drosophila* homologue to mammalian adipose triglyceride lipase, and its paralogue *doppelganger von brummer* (*dob*). This was surprising given that *bmm* is a well-studied dFoxO target gene (Birnbaum *et al.* 2019). However, *bmm* has been shown to be modulated by several other signalling pathways (including hedgehog and mTOR) (Chatterjee & Perrimon 2021; Zhang *et al.* 2020b). Furthermore, it has also been reported that *bmm* expression is more influential in basal lipolysis and only plays a supporting role in lipolysis induced by stress (Bi *et al.* 2012; Wat *et al.* 2020). Similar findings have been reported for Lip4, which is a known dFoxO target and regulator of lipolysis (Vihervaara & Puig, 2008). However, the human orthologue LipA is known to also be regulated by the mTORC1-regulated basic helix-loop-helix transcription factor, TFEB, during nutrient restriction (Dubland & Francis, 2015). Therefore, it is possible that due to these enzymes being of such importance they are modulated by multiple signalling pathways, and therefore the lack of functional dFoxO proteins in some of the mutants does not affect the expression of these genes as they can be rescued by these other pathways.

Taken together the apparent modulation of the expression of these genes independently of dFoxO explains the phenotypes observed previously in this project, and therefore confirms that the production of the key energy stores in *Drosophila* (namely, glycogen, trehalose, and TAG), the modulation of haemolymph sugars, and the mobilisation of carbohydrate, and to a lesser extent lipid, stores during fasting or stress all seemingly can occur independently of dFoxO activity.

5.4.1.3.2 Genes modulated in a dFoxO-dependent DNA-binding dependent manner

There were also a variety of genes whose expression was dependent on FoxO activity as well as its ability to bind to DNA (or at least the use of a functional DNA-binding domain) and seemed to be essential in the modulation of key biological processes such as lifespan, fecundity, and stress resistance. Processes that have already been shown in previous research to be dependent on dFoxO activity (Slack *et al.* 2011).
This is interesting as one of the previous phenotypes found in this project to not just require the presence of dFoxO but also the presence of a functional DBD was the

modulation of normal lifespan. Genes associated with this phenotype found in the RNA-seq data include those such as *daw, Fs, Mys, Atg3, RagA-B, and Samtor.*

daw and *Fs* allow for the regulation of the highly conserved activin signalling pathway in an insulin/dFoxO-dependent manner that subsequently modulates autophagy a well-known longevity assurance mechanism (Bai *et al.* 2013). Further study has also shown that *daw*, a known direct dFoxO target, is able to regulate adult *Drosophila* lifespan by mediating 26S proteasome function in adult muscle (Langerak *et al.* 2018; Bai *et al.* 2013). This modulation of 26S proteasome activity influences protein homeostasis by allowing for the removal of misfolded or dysfunctional proteins that accumulate and affect intracellular trafficking and cell membrane permeability, ultimately leading to deterioration of tissues (Langerak *et al.* 2018). Another direct target of dFoxO in female *Drosophila* and well-researched autophagy-related gene found in this RNA-seq analysis is *Atg3*, which has been shown to play a pivotal role in autophagosome formation and recruitment of dysfunctional or damaged proteins and organelles (Birnbaum *et al.* 2019; Metlagel *et al.* 2013).

Additionally, the gene *Mys* found in this RNA-seq analysis is also linked to lifespan, as *Mys* encodes the X-linked myospheroid, one of the 2 β-integrins identified in *Drosophila* that have been identified as integral to normal healthy ageing by regulating functional senescence (Goddeeris *et al.* 2003).

Further modulation of lifespan in these flies seemingly involves the mTOR signalling pathway based on several genes found via the RNA-seq to be modulated in a dFoxO-dependent DNA-binding dependent manner. mTOR has already been widely regarded as a core regulator of ageing across species in association with insulin signalling and FoxO (Lamming *et al.* 2012; Robida-Stubbs *et al.* 2012; Powers *et al.* 2006; Kapahi *et al.* 2004; Vellai *et al.* 2003; Jia *et al.* 2004), therefore the idea of genes such as *RagA-B* and *Samtor* being found in this gene list is not surprising. Although, Samtor has not been shown to directly regulate lifespan both of these factors represent positive and negative regulators of mTORC1 signalling respectively, allowing for an indirect affect in lifespan as mTORC1 is known to affect key hallmarks of ageing such as, energy homeostasis and mitochondrial function, nutrient availability, cellular senescence, proteostasis, and stem cell stemness (Papadopoli *et al.* 2019; Bar-Peled & Sabatini, 2014; Gu *et al.* 2017; Kitada *et al.* 2019).

Another phenotype found to be modulated in a dFoxO-dependent DNA-binding dependent manner using these *dFoxO* mutants was fecundity, and similar to lifespan

there were several genes found (e.g., *egh, cue, Nrg, HLH106,* and *EcR*) within the RNA-seq analysis using these same mutants that could explain this.

For example, *egh* is vital in the male-derived sex-peptide response and subsequent egg laying in female *Drosophila* (Soller *et al.* 2006). Furthermore, transcription of this gene is considerably downregulated in a viable but sterile female *Drosophila* model (Soller *et al.* 2006). This also reflects what is seen in models of *cue*, where dysregulation of this gene leads to semi-sterile female *Drosophila* (Castrillon *et al.* 1993), as well as models of *Nrg* a member of highly conserved L1-type cell adhesion molecules that lowers the sexual receptivity of female *Drosophila* possibly affecting subsequent egg laying (Goossens *et al.* 2011; Kerr *et al.* 1996).

Another gene of interest in this list is the *HLH106*, the only *Drosophila* SREBP isoform, which is interestingly well-known in the regulation of autophagy and is a key mediator in the lifespan-extending process of caloric restriction (Kobayashi *et al.* 2018; Theopold *et al.* 1996). In reproduction, however, it has also been associated with the control of lipid synthesis in the germline of *Drosophila* females (Sieber & Spradling, 2015).

A further well studied and overall essential gene found in this gene list is the ecdysone receptor gene, *EcR*. The modulation of this gene has implications in a variety of processes, for example mutations in this receptor exhibit both lifespan extension and stress resistance providing a connection between this ecdysone signalling pathway and longevity in *Drosophila* (Simon *et al.* 2003; Tricoire *et al.* 2009). Furthermore, EcR mutant females also have defective oogenesis from aberrant egg chamber formation to loss of vitellogenesis (i.e., yolk formation and nutrient deposition) therefore indicating EcR as a key component of normal female reproduction (Carney & Bender, 2000).

As with lifespan and fecundity, xenobiotic metabolism and response to oxidative stress were also identified as dFoxO-dependent DNA-binding dependent processes with related genes found within the RNA-seq analysis of the *dFoxO* mutants. These genes include *Jheh1* and *Jheh2*, a cluster of genes involved with responses to both oxidative and xenobiotic stress, particularly in responses and possible resistance to paraquat (Guio *et al.* 2014). Where the *Jheh* gene of the silkworm *Bombyx mori* has been shown to contain a FoxO binding site within its promoter, thereby supporting this assertion this could also be a FoxO target gene in *Drosophila* (Zeng *et al.* 2017).

Other genes include *NLaz*, a *Drosophila* lipocalin family member homologous to apolipoprotein D and retinol binding protein 4 (Hull-Thompson *et al.* 2009). This gene has the ability to repress the IIS and anabolic pathways to enable resistance to stress and influence lifespan (Hull-Thompson *et al.* 2009). As well as *GstD9*, which encodes a glutathione-s-transferase that transfers glutathione, a potent antioxidant, onto xenobiotics allowing for their subsequent excretion and prevention of cellular stress (Piper *et al.* 2008; Wang *et al.* 2014; Sipes *et al.* 1986). There is also a potential further role for this enzyme in the reduction and detoxification of reactive oxygen species (Huang *et al.* 2004).

Also of interest in this RNA-seq analysis is PEK*,* the pancreatic eIF-2α kinase that resides within the endoplasmic reticulum and phosphorylates eukaryotic translation initiation factor 2α leading to the immediate switch from translation to activation of stress response genes (Iida *et al.* 2007; Pomar *et al.* 2003; Ghosh *et al.* 2011). Interestingly, PEK induction has also been related to the regulation of autophagy and the cellular unfolded protein response (UPR) (Nagy *et al.* 2013), possibly indicating a role for this gene in the modulation of lifespan as well as stress resistance.

Another gene of interest is *dILP6*, this is a gene that encodes insulin-like peptide 6 a component of the IIS pathway in *Drosophila* which shares structures and functionality with the mammalian insulin growth factor 1 (IGF-1) (Okamoto *et al.* 2009). Previous research has shown that dILP6 overexpression in the fat body is able to extend both lifespan and oxidative stress resistance (Bai *et al.* 2012). Interestingly, *dILP6* expression has already been linked to dFoxO activity, where not only is *dILP6* expression both environmentally and developmentally dFoxO-dependent but several dFoxO binding sites have been identified upstream of the *dILP6* gene (Slaidina *et al*. 2009).

Compellingly, two other insulin-like peptides *dILP3* and *dILP4* seem to be modulated by dFoxO as well as requiring a functional DBD. *dILP3* has been shown to influence *Drosophila* appetite both in consumption and regulation of food palatability, and *dILP4* mutants showed a 1.2-fold increase in consumption of yeast autolysate solution compared to controls on most experimental diets (Semaniuk *et al.* 2018). Interestingly proper regulation of *dILP3* also seems to have effects in longevity with ablated *dILP3* mutants showing a significant increase in lifespan (Broughton *et al.* 2005). The fact these genes seem to be modulated in this manner based on RNA-seq analysis could

therefore help to explain why feeding behaviour was also observed as being a dFoxO-dependent DNA-binding dependent phenotype using these *dFoxO* mutants.
Interestingly, this dFoxO modulation of the dILPs could elicit some form of feedback onto dFoxO activity itself and subsequent dILP production, as these peptides bind to the dInR causing dFoxO inactivation (Puig & Tjian, 2005). This identifies the potential need for a stringent balance on the modulation of these dILPs and dFoxO activity to ensure normal feeding behaviours and stress resistance.

Other interesting genes that are potentially modulated in this DNA-binding dependent manner and are involved in the apparent modulation of feeding behaviour in *Drosophila* include *bigmax*, *Pdk1*, *Lkr*, and various *Obp* genes (e.g., *Obp28a* and *83b*, and *lush*). These are of interest as for example, *bigmax* the *Drosophila* equivalent to the carbohydrate response element binding protein (ChREBP) binding partner, Mlx, has been shown to regulate feeding behaviour via its interactions with its partner Mondo (i.e., the *Drosophila* homologue of ChREBP) allowing for the regulation of nutrient-dependent feeding behaviour (Sassu *et al.* 2012). *Pdk1*, is a gene encoding 3-phosphoinositide-dependent protein kinase-1, that regulates feeding behaviour through the integration of insulin and leptin signalling pathways balancing the release of POMC and AgRP in mice (Iskandar *et al.* 2010; Cao *et al.* 2011). And *Lkr* encodes the leucokinin receptor, where mutations in this and other components of the leucokinin signalling pathway led to altered food intake, metabolic rate, water homeostasis, and stress regulation (Al-Anzi *et al.* 2010; Zandawala *et al.* 2018; Ohashi & Sakai, 2018).
This modulation of feeding behaviour could also be through the modulation of various odorant binding proteins (Obp) (including, *Obp28a* and *83b,* and *lush*). These Obps are a large family of ~52 *Drosophila* proteins, however they share very little amino acid similarity (on average ~20%) (Sun *et al.* 2018). These sensory proteins have been linked to the regulation of feeding behaviour, including food searching and regulating volume of food consumed (Oh *et al.* 2021). In addition, *lush* is also required for pheromone-sensing neurons, which are essential for modulating social behaviours including those vital for survival and mating (Ha & Smith, 2006; Xu *et al.* 2005). Despite this, there is little information into the precise mechanisms into how Obps are able to modulate these processes highlighting a further area of interest to be explored. However, these Obps have also been connected to lifespan where exposure to yeast odorants decreased lifespan in diet-restricted flies (Pletcher, 2009). Therefore, this

could indicate that lack of proper modulation of the transcription of these genes in the *dFoxO* could also help to explain the effects in lifespan.

All together this RNA-seq data includes genes that confirms the responses found in previous phenotypic analysis, identifying processes including lifespan, fecundity, feeding behaviour, responses to oxidative stress, and xenobiotic metabolism are seemingly modulated in a dFoxO-dependent DNA-binding dependent manner.

5.4.1.3.3 Genes modulated in a dFoxO-dependent DNA-binding independent manner

Previously in this project, both growth and the response to starvation were identified as being phenotypes that whilst requiring dFoxO, did not require the presence of a functional DBD. Therefore, it was interesting to find that there were 445 genes that seemed to be modulated in this same manner during RNA-seq analysis that could explain the phenotypic differences between the ΔV3 and DBD mutants.

All in all, these genes respresent many ways in which metabolic phenotypes can be modulated in a dFoxO-dependent DNA binding independent manner. Interestingly, this is further supported by gene ontology analysis that showed enrichment of various metabolic processes (including, UDP-glucose metabolism, regulation of metabolic process, and regulation of cellular metabolic processes).

An over-represented group of downregulated genes in this list are the UDP-glycosyltransferases (e.g., *Ugt316A1* and *Ugt36Ba*). These enzymes are of interest as not only do they catalyse the addition of sugars to a wide variety of lipophilic molecules, where the UGT3 family of enzymes commonly utilises UDP-glucose, UDP-xylose, and UDP-N-acetylglucosamine to regulate the elimination endogenous metabolic by-products, in the maintenance of normal tissue function, but are also required for lipid droplet formation and interactions with proteins involved with many metabolic processes, such as those involved with fatty acid degradation (e.g., ACOT8 and ECH1), glucagon signalling (e.g., PHKG2 and PHKA2), and glycolysis (e.g., GAPDH and GFPT1) (Meech *et al.* 2019; Hu *et al.* 2019).

Interestingly, one of the phenotypes determined to possibly underly effects in starvation survival and growth was the mobilisation of lipid stores. A phenotype that could be explained further by the seemingly dFoxO-dependent DNA-binding independent modulation of the histone modifier Kdm4, a demethylase modulated in

response to metabolic fluctuations due to its key substrate being a Kreb's cycle intermediate, α-ketoglutarate (Tran *et al.* 2017). This influence of metabolism allows Kdm4 to activate a critical growth factor E2F1 which in turn induces pyruvate dehydrogenase kinases allowing for the inactivation of pyruvate dehydrogenases and modulation of metabolic flexibility switching from glucose to fatty acid utilisation (Zhang *et al.* 2014a).

Another histone modifier present in this dFoxO-dependent DNA-binding independent gene list was the histone deacetylase 1 (HDAC1). This enzyme has been shown in a human epithelial cell line to reduce lipogenesis when overexpressed by suppressing SREBP-1c promoter activity (Shin *et al.* 2021). Furthermore, this gene has been identified as the key to surviving starvation through the increased expression of ribosomal RNA synthesis and autophagic genes, where ultimately loss of *HDAC1* causes sensitivity to starvation (Nakajima *et al.* 2016).

The upregulation of these genes during starvation in the V3F and DBD mutants would therefore allow for the increased switch from anabolic to catabolic pathways, as well as from carbohydrate to lipid utilisation, allowing for the production of energy from metabolic stores in addition to the reservation of energy produced via carbohydrates for organs that cannot derive energy from lipid stores.

This effect in lipid metabolism is also found in the dFoxO-dependent DNA-binding independent modulation of other genes including *mat, scu*, and *wal*. These upregulated genes are important during starvation as the product of *mat* removes lipids from the haemolymph preventing lipid peroxidation and oxidative stress, and both *scu* and *wal* are absolutely essential for fatty acid β oxidation through 17β-hydroxysteroid dehydrogenase 10 and mitochondrial electron transport activity respectively (Li *et al.* 2020; Moeller & Adamski, 2006; Henriques *et al*. 2021; Lammers *et al.* 2019).

Another important aspect of this lipid utilisation comes via the modulation of Kr-h1, this gene is downregulated in a dFoxO-dependent DNA-binding independent manner during starvation allowing for the repressive action of Kr-h1 on lipolysis to be lifted preventing the severely altered lipid metabolism observed in Kr-h1 mutants (Kang *et al.* 2017). This effect in lipid utilisation is also seen in the upregulation of genes involved with the Kreb's cycle that produces energy from metabolic stores, such as lipids. Two such genes are *Men-b* and *Idh*, a malate dehydrogenase that converts malate into oxaloacetate as a means of providing energy and an isocitrate dehydrogenase, that works alongside the malic enzymes in the Kreb's cycle to

catalyse the decarboxylation of isocitrate to 2-oxoglutarate to produce energy (Minárik *et al.* 2002; Williamson *et al.* 1980). Therefore, these genes too help to explain the dFoxO-dependent DNA-binding independent phenotypes observed, particularly the effects on lipid mobilisation.

Importantly in the modulation of the mobilisation of lipid stores is the modulation of the lipid droplet (LD), the main storage vesicle for lipids such as TAG. There are several genes found to be regulated independently of dFoxO's ability to bind to DNA that relate to this organelle. For example, RalA, a member of the Ras family of GTPases, encodes an important protein for maintaining lipid droplets during starvation to allow for the removal of toxic lipids produced via autophagy and to provide further energy for fatty acid β-oxidation (Hussain *et al.* 2021). This gene in the RNA-seq data showed downregulation, however RalA is also key in mTORC1 signalling during fasting conditions and GLUT4 translocation to enable glucose transport into the adipose tissue (Hussain *et al.* 2021). Therefore, a balance must be struck with this gene and so this unexpected modulation may simply be caused by the necessary fluctuations needed for appropriate metabolic homeostasis during starvation responses, where lipolysis could temporarily be halted due to saturation of fatty acid oxidation pathways thereby ensuring efficient usage of lipid stores so energy can be maintained for as long as possible.

Another gene associated with this role in lipid homeostasis is *gig*, an upregulated mTOR signalling and tumour suppressor that antagonises mTORC1 via interactions with the TSC1 protein leading to inactivation of TOR (Gao *et al.* 2002). This interaction has effects in lipid homeostasis due to its roles as a fat body nutrient sensor, regulation of lipid droplets, and in the positive regulation of autophagy and lipophagy (Gutierrez *et al.* 2007; Tang *et al.* 2018).

Other LD-associated genes included downregulated *diacylglycerol acyltransferase-2* (*DGAT2*) and *glycerol-3-phosphate acyltransferase 4* (*GPAT4*), which interact with LDs to catalyse TAG synthesis and LD expansion with mutants leading to dysfunctional metabolic regulation (McFie *et al.* 2018; Wilfling *et al.* 2013; Yao *et al.* 2018; Yan *et al.* 2015).

These effects on the metabolic pathways in the LDs also relates to other downregulated genes found in this dFoxO-dependent DNA-binding independent gene list such as *PCB* and *Eglp4* which are both involved with glyceroneogenesis and lipid

formation through pyruvate carboxylase activity or glycerol transport respectively (Reshef *et al.* 2003; Calamita *et al*. 2018).
Altogether, the fact these genes seem to be modulated in a dFoxO-dependent DNA-binding independent manner in the RNA-seq analysis correlates with the dFoxO-dependent DNA-binding independent phenotypes observed using the same *dFoxO* mutants, particularly in response to starvation and lipid mobilisation.

The modulation of normal growth phenotypes was also observed as being modulated independently of dFoxO's ability to bind to DNA. As growth is a well-known energy-dependent process, alongside starvation, it was not surprising that a number of genes connected to both metabolism and growth were found during the RNA-seq analysis. For example, genes such as *sdr*, *Orct2*, and *Ptp61F* could all regulate growth in a nutrient-dependent dFoxO-dependent DNA-binding independent manner. *Ptp61F* is an upregulated protein tyrosine phosphatase, which has the ability to negatively regulate IIS allowing for the regulation of proper growth (Buszard *et al.* 2013). *Orct2* (also known as, calderón) is required for the proliferation of tissues in *Drosophila* larvae and co-ordinates nutritional-sensing and growth (Herranz *et al.* 2006). And finally, *sdr* (or, the secreted decoy receptor) is a decoy insulin receptor secreted into the haemolymph to negatively regulate insulin signalling via the interactions with various dILPs making it indispensable for regulating the IIS under adverse nutrient conditions fine tuning stress responses and growth (Okamoto *et al.* 2013). The dILP with the highest affinity for this decoy is dILP3, the lipogenic peptide known to regulate growth, via the increase of the expression of SREBP-1c and inhibition of FoxO activity, with ablation of this dILP leading to increased starvation resistance (Toprak, 2020; Rulifson *et al.* 2002; Broughton *et al.* 2005). Therefore, increased expression of *sdr* as seen in this RNA-seq data shows that a reduction in anabolic pathways could be associated with a proper response to starvation, which seems to be modulated in a dFoxO-dependent DNA-binding independent manner.
Alongside the regulation of the IIS in relation to growth and metabolism is the regulation of the mTOR signalling pathway, as mTOR is an essential pathway in the nutrient-dependent regulation of cellular growth and metabolism (Saxton *et al.* 2017). One such gene is *path,* a positive regulator of mTOR signalling, that can enable the modulation of overall growth with research showing that mutations in this gene lead to growth reductions in *Drosophila* (Goberdhan *et al.* 2005). Therefore, ensuring the appropriate regulation of this gene would seem to be key in regulating normal growth

phenotypes, possibly explaining why this phenotype was different between the ΔV3 and DBD mutants. Another is *Sin1* (or stress-activated protein kinase-interacting protein 1), a core phosphorylating component of the mTORC2 complex this kinase activity enables the activation of Akt and regulation of cell growth and survival, as well as apoptosis in response to growth factor signalling (Yang *et al.* 2006; Lamming & Sabatini, 2013). mTORC2 has also been shown to be upregulated during nutrient withdrawal to replenish Kreb's cycle intermediates (Moloughney *et al.* 2016), which would be indispensable in energy homeostasis and the starvation response fitting in well with the RNA-seq analysis which shows this *Sin2* gene is upregulated during starvation.

Furthermore, in the regulation of mTOR, there was differential expression of two genes that encode components of the GTPase-activating protein toward Rags 2 (GATOR2) complex, *Wdr24* and *mio*. This complex is known to enhance mTORC1 signalling allowing for the promotion of cell growth in a variety of *Drosophila* tissues, where ultimately suppression of any individual GATOR2 sub-unit leads to suppression of mTORC1 (Cai *et al.* 2016; Bar-Peled *et al.* 2013). Therefore, the modulation of these genes would likely be necessary for the modulation of proper growth, helping to explain why this phenotype was observed as being modulated in a dFoxO-dependent DNA-binding independent manner.

However, Wdr24 and mio both also have mTOR-independent functions in cellular metabolism, where they regulate autophagy and lysosome dynamics, including lysosome acidification (Cai *et al.* 2016). This is essential as proper lysosome function, including acidification, is critical to the maintenance of healthy tissues preventing knock-on effects in inflammation and mitochondrial function (Yambire *et al.* 2019). Therefore, as autophagy is considered an important process when considering responses to starvation (Finn & Dice, 2006; Shang *et al.* 2011), it is possible that these two genes also help to explain the dFoxO-dependent DNA-binding independent nature of the response to starvation as well as growth.

Aside from these roles in connecting metabolism and growth, genes that have links to development and growth but are not necessarily directly tied to metabolism were also found in this this dFoxO-dependent DNA-binding independent gene list that could also help to explain the stunted growth that was observed in the ΔV3 mutants but not the DBD mutants. One such gene is *Atac1*, the product of which associates with numerous subunits (i.e., dAda2A, dGcn5, dAda3, and dHCF) to acetylate histones 3

and 4 (Guelman *et al.* 2006). Histone acetylation has been tightly associated with metabolic regulation due to its responsiveness to acetyl-coA produced from the breakdown of fatty acids (McDonnell *et al.* 2016). This acetylation has also been linked to the regulation of mammalian development, where disassembly of the similar mammalian ATAC2 complex led to stunted growth or death during early embryogenesis in mice (Guelman *et al.* 2009). Another such gene is *E(z)*, a methyltransferase that is known to methylate lysine residues 9 and 27 of histone 3, a process well-regarded as being critical in normal development, as it regulates interconnected networks of gene expression to enable normal organogenesis and cell differentiation (Czermin *et al.* 2002; Jambhekar *et al.* 2019).

Further genes that could relate to the DNA-binding independent nature of the growth phenotype, include those involved in the modulation of the ecdysone signalling pathway. Although, this has already been shown above to be modulated in part in a dFoxO-dependent DNA-binding dependent manner, there are also areas of this signalling pathway that seem to be modulated in a dFoxO-dependent DNA-binding independent manner. This is shown via the downregulation of the Halloween genes *shd* and *phm,* and the Niemann pick type c1a, *Npc1a*. These three genes are all critical in the biosynthesis of the active form of the ecdysone steroid 20E (Petryk *et al.* 2003; Warren *et al.* 2004; Huang *et al.* 2007). 20E is the hormone responsible for most insect growth, metamorphosis, and final adult size (Koyama *et al.* 2020). However, it has been suggested that the role of these genes in the production of this hormone is nutrient-dependent with a strong association with the IIS (Koyama *et al.* 2020). For example, overexpression of the dILPs in the insulin producing cells leads to a distinct upregulation of several so-called Halloween genes including *phm* (Walkiewicz & Stern, 2009). Interestingly one of the dILPs, *dILP8* is also upregulated in this dFoxO-dependent DNA-binding independent manner. This dILP has been shown to be required for organ growth and organism maturation by suppression of ecdysone biosynthesis in larvae (Garelli *et al.* 2012), possibly connecting the modulation to this gene to those above. However, it also has a connection to lipid metabolism, where in the mosquito *Aedes aegypti* ILP8 (as well as ILP7) was a target for the regulation of lipid mobilisation by microRNAs (Ling *et al.* 2017). Therefore, this upregulation of *dILP8* could also help to explain why lipid mobilisation is observed to be a dFoxO-dependent DNA-binding independent phenotype.

Further to the genes above, there are a few genes found in this DBD-independent list that are directly associated with responses to starvation correlating well with the phenotypes observed. For example, both *EndoA* and *loco* are connected to responses to starvation due to their roles in autophagy and mediation of G-protein signalling via GTPase-activating activity respectively (Soukup *et al.* 2016; Lin *et al.* 2011). Where downregulation of *loco* (as is found in this RNA-seq data) is found to convey lifespan extensions and stronger resistance to stress, including heat and starvation (Lin *et al.* 2011).

It is also important to consider that ~16% of the genes in this DEG list have an unknown function. This is important to note as these genes could potentially have roles related to metabolism, as for example there are many uncharacterised lipases in the *Drosophila* genome (Wat *et al.* 2020). Therefore, there may be unknown genes effecting these dFoxO-dependent DNA-binding independent phenotypes that cannot be identified at this time.

Furthermore, some of the identifiable genes show a different expression change during starvation than what would generally be expected based on the knowledge of these genes. However, metabolism is a complex process where even during periods of fasting homeostasis needs to be maintained to allow for efficient usage of metabolic stores. It has even been found in Zebrafish that starvation can induce lipogenesis with aberrant metabolic states leading to hepatic steatosis (Xu *et al.* 2021). Therefore, it is possible at the moment the flies were collected for RNA-seq analysis, different stages of metabolism are being modulated or the genes are having potentially unknown or less well-characterised effects such as those seen with *Wdr24* and *mio* and their mTOR-independent effects. Another explanation that is important to note, it that the RNA used for RNA-seq analysis was extracted from whole flies immediately snap frozen on liquid nitrogen, and as different tissues may respond to stimuli differently in order to produce a coordinated response there may be fluctuations in gene expression between flies at the precise moment they were frozen resulting in the unexpected modulation observed.

As well as these genes found to be overlapping with the V3F, there were also several genes found to be modulated only in the ΔV3 or DBD2 mutant and not the others. Interestingly, the gene ontology analysis for the genes present in only the V3F or the ΔV3 lists showed very similar processes being enriched (e.g., synaptic signalling and

neuron development). This is likely to indicate that the ΔV3 mutants are modulating different genes to modulate the same processes, presumably independent of dFoxO, to rescue essential phenotypes (e.g., proper brain function) disturbed by the lack of dFoxO.

However, the genes only found to be differentially expressed in the DBD2 during starvation represent an entirely different set of biological processes, namely macromolecule metabolism and biosynthetic processes. Interestingly, many of the genes (such as *Hsl*, *Ubc2*, and *snz*) are key in TAG homeostasis and mobilisation or are critical in maintaining protective responses to stress (such as *Treh*, *Herp*, *crc*, and *Axn*) (Bi *et al.* 2012; Beller *et al.* 2008; Ugrankar *et al.* 2019; Hibshman *et al.* 2017; Kang & Ryoo, 2009; Zhang *et al.* 2014b; Seo *et al.* 2009). This indicates these mutants do not just represent a wild-type without a functional DBD but produce a protein that has a behaviour distinct from the wild-type, something that is also seen in the DBD mutant produced in human cells providing another indication that the observations made in *Drosophila* in this project are evolutionarily conserved (Ramaswamy *et al.* 2002). This distinct phenotype may be caused by loss of DNA-binding allowing for dFoxO to produce interactions it wouldn't normally as it would be occupied at the DNA, or due to sequestering other proteins away from the DNA to inhibit other proteins effects. Ultimately, this distinct response seems to identify another set of dFoxO-dependent DNA-binding independent genes and sheds further light on why these DBD mutants are not phenotypically divergent from the V3F wild-type.

Overall, it is clear from the data presented that by using RNA-seq analysis there are a variety of genes modulated in a dFoxO-dependent DNA-binding independent manner that can help to explain the phenotypes observed previously. For example, aspects of processes such as lipid metabolism, autophagy, and nutrient switching are potentially modulated by dFoxO but independently of its ability to bind to DNA. Therefore, further analysis of the modulation of these differentially expressed genes may elucidate the underlying mechanisms of dFoxO's DNA-binding independent activity.

Chapter 6

Analysis of potential dFoxO binding partners

6. Analysis of potential FoxO binding partners

6.1 Introduction

As a transcription factor, FoxO's main mechanism of action is mediated by its ability to bind to DNA and regulate the expression of a specific set of target genes ensuring accurate regulation of a variety of biological processes and organismal homeostasis. However, FoxO also has another method of modulating gene expression where it can interact directly with other proteins including other transcription factors, which leads to indirect gene regulation by FoxO. This is possible due to the presence of a variety of domains within the FoxO protein structure that allow for protein-protein interactions. For example, the hormone receptor box also known as the "LXXLL" motif found within the transactivation domain (TAD) of mammalian FoxO proteins, has been shown to interact with Sirt1 allowing Sirt1 to exert enhancing effects on FoxO transcriptional activity particularly on genes involved with carbohydrate metabolism (such as, *glucose-6-phosphatase c* (*G6pc*)), although this still requires FoxO's ability to bind to DNA (Nakae *et al*. 2006; Frescas *et al.* 2005). Another such region is the polyglutamine (polyQ) region, which forms coiled-coil-coiled-coil interactions with polyQ regions of other proteins due to electrostatic interactions and hydrogen bonds (Grigoryan & Keating, 2008). In *Drosophila* FoxO (dFoxO) this Q-rich region is relatively large and contains two coiled-coil regions (amino acids 429-449 and 543-578) (Kwon *et al.* 2018). These coiled-coil regions can interact with coiled-coil regions of other proteins, such as pathogenic spinocerebellar ataxia type 3 (SCA3) proteins leading to neurodegeneration (Kwon *et al.* 2018).

Furthermore, FoxO protein activity has also shown to be regulated by the Krüppel-like homologue 1 (Kr-h1), where Kr-h1 binding to FoxO's TAD represses FoxO's ability to activate transcription of the triglyceride (TAG) lipase *brummer* (*bmm*) during development; a crucial intersection in the regulation of metabolism and growth (Kang *et al.* 2017). However, similar to other examples this regulation of dFoxO target genes caused by dFoxO-Kr-h1 binding still requires dFoxO's ability to bind to DNA (Kang *et al.* 2017).

These examples set a precedence that FoxO proteins are able to influence and be influenced by the activity of other proteins through direct interactions, however there is still little in-depth knowledge about FoxO modulating another proteins activity (rather than *vice versa*) without having to bind to DNA in any capacity, particularly in the context of metabolic homeostasis. Therefore, as the importance of FoxO interactions with other proteins is becoming more apparent – identifying these protein

partners and how these interactions influence FoxO activity is essential to fully understand the regulatory role that FoxO plays in processes such as metabolic regulation.

6.2 Aims and objectives

Previously, phenotypic differences (e.g., response to starvation, growth, and TAG mobilisation) were observed between the null (ΔV3) and DNA binding domain (DBD) *dFoxO* mutants. Further, a set of genes were also identified as being differentially modulated between the ΔV3 and DBD mutants during starvation.

In this chapter, the main aim was to identify and assess the potential binding partners of dFoxO that could alter the expression of these identified genes to modulate metabolic homeostasis. The hypothesis was that the differentially expressed genes found to modulated in a dFoxO-dependent DNA-binding independent manner would identify enriched transcription factors, which could be modulating the expression of these genes alongside dFoxO.

To achieve this, enrichment of transcription factor binding sites within the starvation responsive genes that were differentially expressed in the DBD mutants compared to the ΔV3 mutants was analysed. RNA-sequencing (RNA-seq) and chromatin immunoprecipitation (ChIP)-sequencing (ChIP-seq) data for transcription factors, and therefore potential FoxO binding partners, identified from this analysis were found in the literature, reanalysed, and subsequently compared to the set of genes potentially modulated in a dFoxO-dependent DNA-binding independent manner during starvation.

This set of experiments helps to fulfil the overall aim of the project by identifying dFoxO co-factors, which could determine potential mechanisms for dFoxO in modulating metabolic phenotypes independently of its ability to bind to DNA.

6.3 Results

6.3.1 Transcription factor binding motif enrichment analysis

Transcription factors bind to specific sequences in the DNA known as 'motifs', which affects the transcription of nearby genes (Rubin *et al.* 2021). Due to extensive and robust research identifying the sequences that various proteins bind to using ChIP assays, linking a specific transcription factor to observed changes in gene expression is possible (Rubin *et al.* 2021). This process is known as transcription factor binding motif enrichment analysis.

Transcription factors enriched in the list of genes shown to be modulated in a dFoxO-dependent DNA-binding independent manner were identified (*Table 6.1*).

Transcription factor	Normalised enrichment score
Hp1b	3.33
Sin3a	3.16
Hp1c	3.12
Eip74ef	3.03

Table 6.1. **Enriched transcription factors for the genes potentially modulated in a dFoxO-dependent DNA-binding independent manner.**
Transcription factor binding motif enrichment analysis carried out on the 445 dFoxO-dependent DNA-binding independent starvation-associated genes, showing the enriched transcription factor name and the normalised enrichment score for that transcription factor (i.e., the degree in which the transcription factor is enriched normalised to a random sample). A normalised enrichment score of over 2.5 for RNA-seq data is considered enriched by i-cisTarget (Herrmann *et al.* 2012).

The regulatory regions of the genes potentially modulated in a dFoxO-dependent DNA-binding independent manner during starvation were analysed for enrichment of transcription factor binding motifs. This identified four transcriptional regulators whose binding motifs were over-represented in this gene list, showing normalised enrichment scores of 3.33 for Hp1b, 3.16 for Sin3a, 3.12 for Hp1c, and 3.03 for Eip74ef.
Therefore, the top 2 ranked enriched factors (Hp1b and Sin3a) were chosen for further analysis.

6.3.2 ChIP-sequencing analysis of transcription factors of interest

Similar to RNA-seq analysis, ChIP-seq is a deep-sequencing analysis used to identify enrichment within the genome in relation to a specific DNA-binding event (Nakato & Sakata, 2021). Therefore, by using antibodies targeting the protein of interest any cross-linked DNA is separated from the remaining genomic DNA and either identified via DNA-sequencing (i.e., ChIP-seq) or microarray hybridisation (i.e., ChIP-chip) (Landt *et al.* 2012).

Therefore Gene Expression Omnibus, a publicly accessible database, was searched for next generation sequencing data that analysed genomic binding sites for both Hp1b and Sin3a by ChIP-seq. Genomic binding sites for Hp1b 3rd instar larvae were found to be described in Schoelz *et al.* (2021) and for Sin3a embryos in Das *et al.* (2012). ChIP-seq data for Hp1b ChIP-seq data was produced for two replicates for both the control (i.e., all DNA produced from 3rd instar larvae) and the Hp1b replicates (i.e., DNA associated with Hp1b binding after immunoprecipitation with a rabbit polyclonal Hp1b antibody produced by Smothers & Henikoff (2001)) (Schoelz *et al.* 2021). ChIP-seq data for Sin3a was produced for two replicates for the Sin3a replicates (i.e., DNA associated with Sin3a binding after immunoprecipitation with a rabbit polyclonal Sin3a antibody) and one replicate for the input control (i.e., all DNA produced from embryos) (Das *et al.* 2012).

Quality control on the ChIP-seq datasets was carried out for both Sin3a and Hp1b datasets, assessing correlation and signal strength to determine whether replicates of the same sample carry similar ChIP signals and whether those signals are strong enough to produce accurate analyses (*Figure 6.1*).

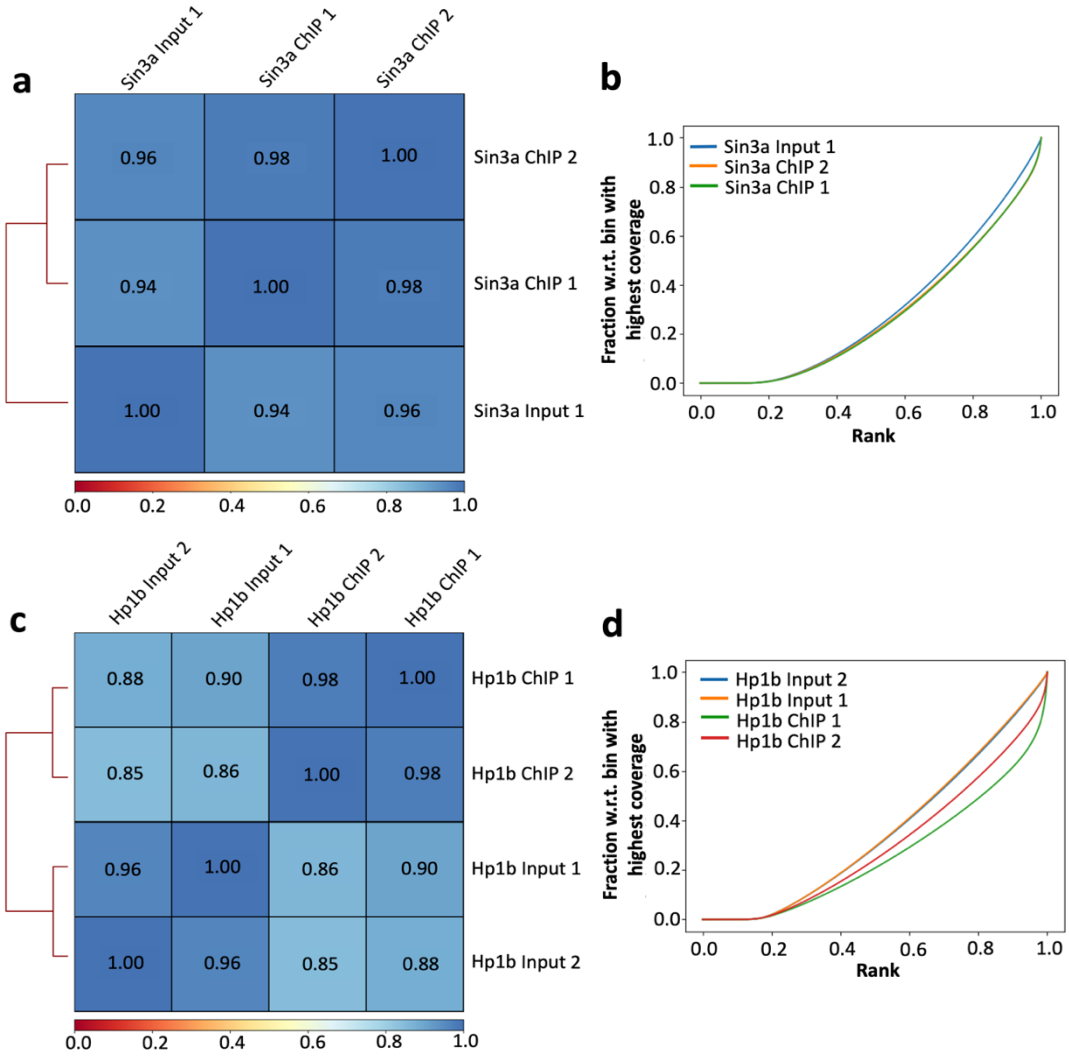

Figure 6.1. **Correlation heatmaps and signal strength fingerprints for Sin3a and Hp1b *Drosophila* ChIP-seq analysis.**
Correlation heatmaps for (a) Sin3a and (c) Hp1b, alongside signal extraction scaling (SES) fingerprint plots for (b) Sin3a and (d) Hp1b *Drosophila* ChIP-seq data. The genome is divivded into equal sized bins and the number of reads in each bin is calculated. This information can be used to create correlation heatmaps, which identify similarity in the signals produced between the replicates of the same condition and the different conditions (i.e., input (total amount of DNA present) or IP (amount of DNA associated with the binding of a particular protein), and SES fingerprints, which identify and evaluate the ChIP signal. Fraction and rank are the percentage of the reads and the genome respectively.

Both maps showed a relatively high similarity between input and IP replicates for both sets of data.

Signal extraction scaling (SES) fingerprints showed 3% of the genome contained 25% and 30% of all reads for Sin3a and Hp1b respectively. Both curves showed a rise starting at approximately 0.18, indicating 18% of the genome contained zero reads, and a less clear differentiation between input and IP signals.
These fingerprints therefore showed a large number of genes fall into a small portion of the genome, indicating very localised and strong enrichments. Therefore, these datasets are of a good enough quality to produce accurate downstream analysis.

Genes that were found in this ChIP-seq analysis, and therefore those that are directly bound by either Hp1b or Sin3a, were then compared to the genes that were found to be potentially modulated in a dFoxO-dependent DNA-binding independent manner (*Figure 6.2*).

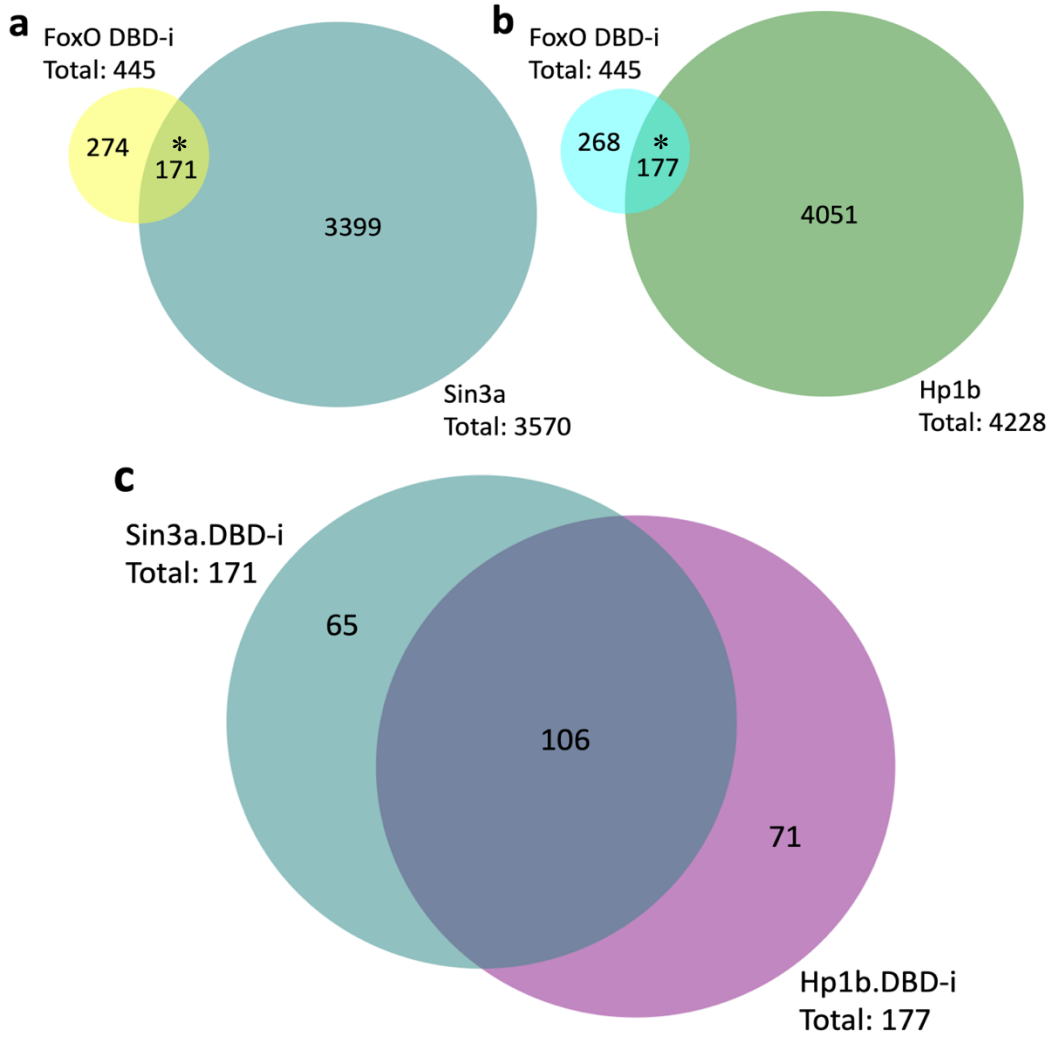

Figure 6.2. **Comparisons of genes identified as direct targets of Hp1b and Sin3a by chromatin immunoprecipitation (ChIP)-sequencing with the dFoxO-dependent DNA-binding independent differentially expressed genes.**
Proportional Venn diagram comparing genes identified as direct targets of either (a) Sin3a or (b) Hp1b by ChIP-seq from publicly available data sets (Sin3a: Das *et al.* 2012; Hp1b: Schoelz *et al.* 2021) with the genes that were differentially expressed upon starvation in a dFoxO-dependent DNA-binding independent manner. (c) Comparison between the overlaps of dFoxO-dependent DNA-binding independent Sin3a targets and dFoxO-dependent DNA-binding independent Hp1b targets. Numbers indicate the number of genes in each section of the Venn (Sin3a: p = 2.22E-8 *, Hp1b: p = 3.84E-6 *, hypergeometric analysis). DBD-i: dFoxO-dependent DNA-binding independent.

A significant overlap was observed between both sets of genes identified as direct targets of Hp1b and Sin3a by ChIP-seq and the dFoxO-dependent DNA-binding independent differentially expressed genes (p = 2.22E-8 for the overlap with Sin3a

target genes and p = 3.84E-6 for the overlap with Hp1b target genes) with 38.4% (171/445) and 39.8% (177/445) of the dFoxO-dependent DNA-binding independent differentially expressed genes identified as being directly bound by either Sin3a and Hp1b respectively.

The genes present within the two overlaps were then compared and 106 genes were present in both. Therefore, 54.4% (242 out of 445) of the genes identified as potentially modulated in a dFoxO-dependent DNA-binding independent manner were also potential direct targets of either Hp1b (71 genes), Sin3a (65 genes), or both (106 genes).

Several genes that seem to be bound by either Sin3a or Hp1b as well, as modulated in a dFoxO-dependent DNA-binding independent manner were identified (*Table 6.2*).

Gene	Bound by	Biological process
HDAC1	Hp1b	Histone modification
E(z)	Both	Histone modification
Kdm4	Both	Histone modification
shd	Hp1b	Ecdysone signalling
Npc1a	Both	Ecdysone signalling
wal	Hp1b	Lipid metabolism
Kr-h1	Hp1b	Lipid metabolism
mat	Sin3a	Lipid metabolism
GPAT4	Sin3a	Lipid metabolism
scu	Both	Lipid metabolism
path	Hp1b	mTOR signalling
gig	Sin3a	mTOR signalling
mio	Sin3a	mTOR signalling
Wdr24	Both	mTOR signalling
dILP8	Hp1b	Insulin signalling
sdr	Hp1b	Insulin signalling
PCB	Hp1b	Carbohydrate metabolism
Men-b	Both	Carbohydrate metabolism/Kreb's cycle
Ugt316A1	Both	Carbohydrate metabolism
Eglp4	Hp1b	Transmembrane transport
loco	Hp1b	Response to starvation
Idh	Both	Isocitrate metabolism/Kreb's cycle
EndoA	Both	Autophagy and apoptosis
RalA	Both	Ras protein signalling

Table 6.2. **Genes bound by Hp1b or Sin3a as well as modulated in a dFoxO-dependent DNA-binding independent manner.**
Genes found to be bound by Hp1b, Sin3a or both based on previously published ChIP-seq analysis that were also seemingly modulated in a dFoxO-dependent DNA-binding independent manner during starvation. Genes are grouped based on their biological processes given by Flybase.

Genes bound by Hp1b included those involved with histone modification (*HDAC1*), ecdysone signalling (*shd*), lipid metabolism (*wal,* and *Kr-h1*), mTOR signalling (*path*), insulin signalling (*dILP8* and *sdr*), carbohydrate metabolism (*PCB*), transmembrane transport (*Eglp4*), and response to starvation (*loco*).

Genes bound by Sin3a included those involved with lipid metabolism (*mat* and *GPAT4*), and mTOR signalling (*gig* and *mio*).
Genes bound by both Hp1b and Sin3a included those involved with histone modification (*E(z)* and *Kdm4*), ecdysone signalling (*Npc1a*), Ras protein signalling (*RalA*), lipid metabolism (*scu*), mTOR signalling (*Wdr24*), carbohydrate metabolism (*Men-b* and *Ugt316A1*), isocitrate metabolism (*Idh*), and autophagy and apoptosis (*EndoA*).

Gene ontology (GO) analysis on the differentially expressed genes that could be modulated in a dFoxO-dependent DNA-binding independent manner via interactions with either Hp1b or Sin3a revealed several enriched terms (*Table. 6.3*).

Fold enrichment	Enrichment FDR	Functional category
3.11	7.81E-4	Cell division
2.71	1.90E-5	Cell cycle
2.33	9.45E-4	Chromosome organisation
1.78	1.55E-3	Regulation of gene expression
1.76	1.44E-4	Nucleic acid metabolic process
1.72	1.81E-4	Regulation of metabolic process
1.69	1.36E-3	Organelle organisation
1.69	1.18E-3	Regulation of primary metabolic process
1.63	1.90E-5	Cellular macromolecule metabolic process
1.59	1.38E-3	Organic substance biosynthetic process
1.51	5.97E-5	Regulation of biological process
1.45	1.23E-4	Macromolecule metabolic process

Table 6.3. **Enriched gene ontology (GO) terms for the genes potentially modulated in a dFoxO-dependent DNA-binding independent manner by Hp1b and/or Sin3a.**
Gene ontology (GO) analysis for the genes found to be bound by either Hp1b or Sin3a and also modulated by FoxO in a DNA-binding independent manner. Each enriched GO term shows the enrichment score based on hypergeometric analysis (i.e., the degree to which the genes in a gene list fall into that specific category) and false discovery rate (FDR) correction (i.e., the significance of the enrichment score taking into account false positives) with a cut off of 0.05, and the functional category (i.e., biological process) for which the genes likely fall into. This list is not exhaustive and only shows the most over-represented category for a specific process.

Enriched GO terms include the regulation of various metabolic processes including macromolecule metabolic process, organic substance biosynthetic process, and nucleic acid metabolic process. Other over-represented GO terms include those involved with the cell cycle, chromosome organisation, and organelle organisation.

Altogether, these data identified a significant degree of overlap between the genes identified as being differentially expressed in response to starvation in a dFoxO-dependent DNA-binding-independent manner and genes identified as directly bound by both Sin3a and Hp1b. As such, Sin3a and Hp1b could potentially be key transcriptional regulators of those dFoxO-dependent DNA-binding-independent starvation responsive genes.

6.3.3 RNA-SEQUENCING ANALYSIS FOR TRANSCRIPTIONAL REGULATION BY SIN3A AND HP1B

The two transcriptional regulators (i.e., Sin3a and Hp1b) that could be mediating the dFoxO-dependent DNA-binding independent starvation response showed via ChIP-seq data to bind to the same subset of genes as those in the dFoxO-dependent DNA-binding independent gene list. Therefore, the next aim was to see if these two factors also modulate gene expression (i.e., alter the expression after binding) of those same genes.

For this, previously published RNA-seq data was reanalysed and compared to *dFoxO* mutant DNA-binding independent data. For Hp1b, RNA-seq had been performed on two *Hp1b* null mutants that were generated by p-element imprecise excision, $Hp1b^{86}$ and $Hp1b^{16}$. Gene expression changes in both alleles were analysed in homozygous 3rd instar larvae knockouts compared to *yw* controls (Mills *et al.* 2018). Sin3a RNA-seq experiments were conducted on *Drosophila* S2 cells in which *Sin3a* expression was significantly reduced using RNAi (Gajan *et al.* 2016).

After appropriate quality control assessments, reads were mapped to the *Drosophila* reference genome produced by the Berkeley *Drosophila* Genome Project in 2014, dm6 (dos Santos *et al.* 2015). Analysis of differential gene expression was carried out using the DESeq2 tool.

Principal component analysis (PCA) of transformed RNA-seq count data for each mutant compared to an appropriate control was performed (*Figure 6.3*).

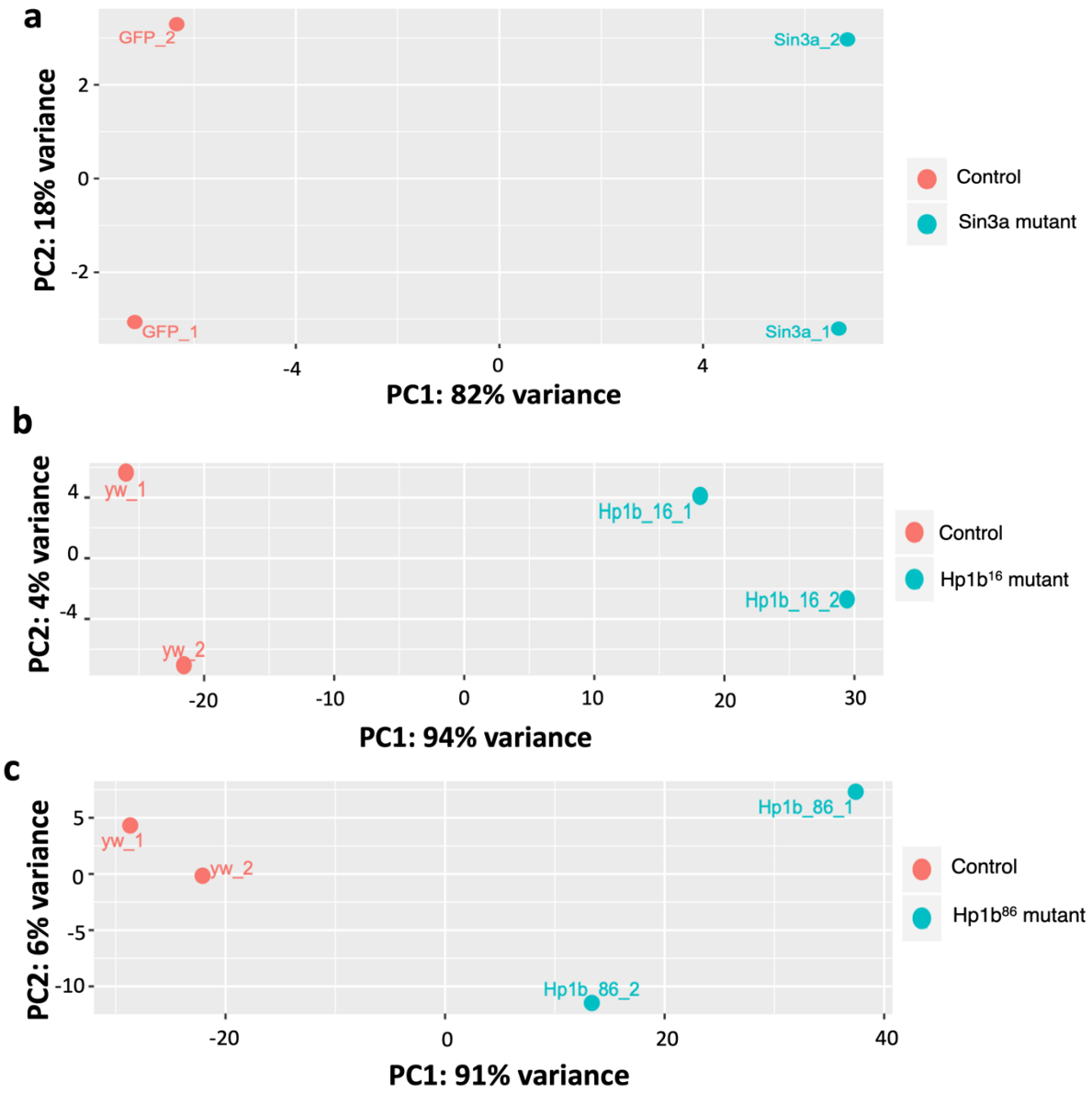

Figure 6.3. **Principal component analysis (PCA) for differential gene expression in response to loss of Sin3a and Hp1b expression.**
Scatter plot of principal component analysis (PCA) of transformed count data from DESeq2 analysis of (a) *Sin3a* knockdown, and *Hp1b* knockout mutants (b) *Hp1b*^{16} and (c) *Hp1b*^{86}. Samples are clustered as either mutants or controls (n = 2 independent biological replicates). Principal component 1 (PC1) is the variance between knockdowns or mutants and controls and principal component 2 (PC2) is the variance between replicates of the same type.

PCA revealed that between 97-100% of the total variance amongst the mutant and control was represented by two principal components. Samples were separated along the first principal component, with 82%, 94%, and 91% of the variation between samples caused by the presence of the knockdown or mutation for the *Sin3a*, *Hp1b*^{16}, and *Hp1b*^{86} flies respectively. Samples were also separated along the second principal component, with 18%, 4%, and 1% of the variation between samples being caused by variability between replicates of the same genotype for the *Sin3a*, *Hp1b*^{16}, and *Hp1b*^{86} flies respectively.

Genes that showed significant differential expression between the *Sin3a* knockdown and *Hp1b* mutants and their respective controls were identified alongside their fold change in expression (*Figure 6.4*).

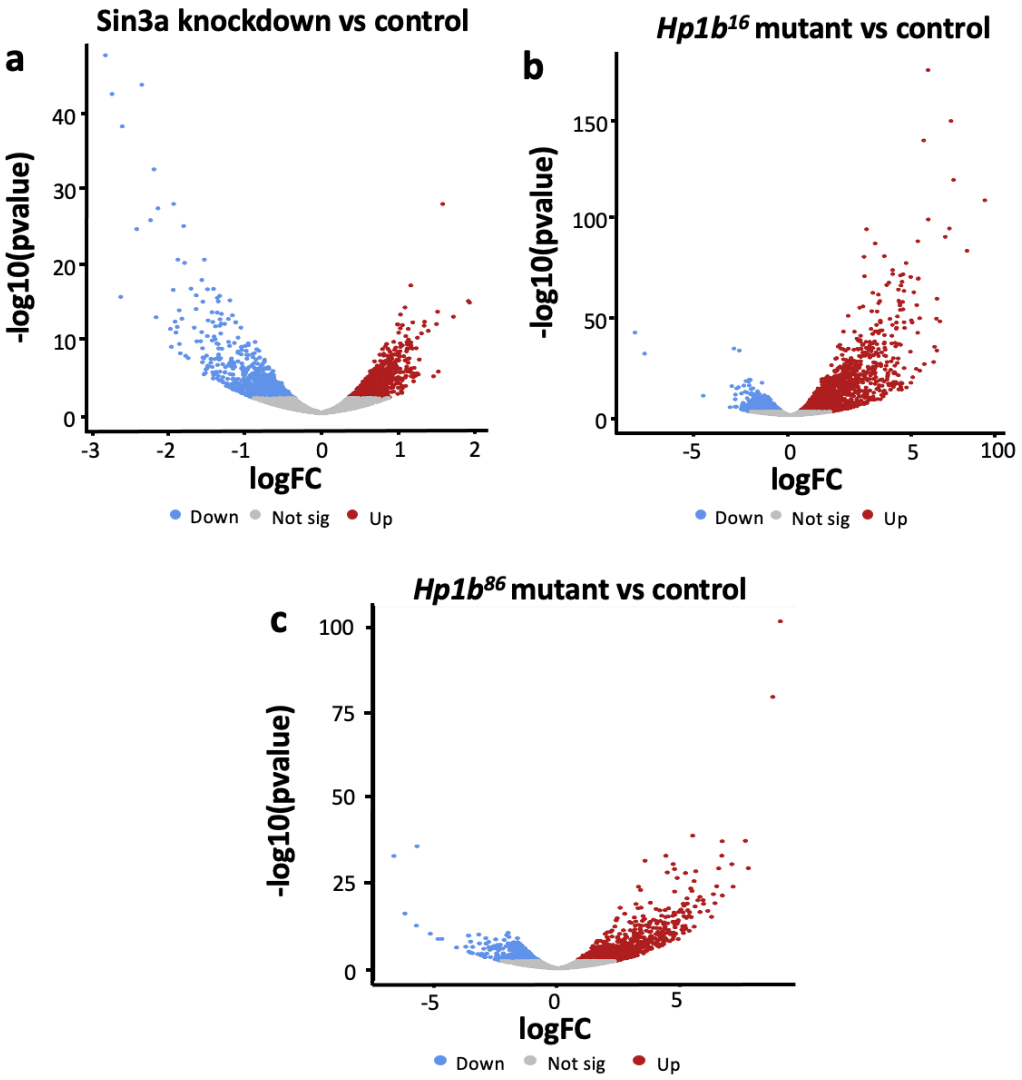

Figure 6.4. **Visualisation of differentially expressed genes in response to loss of *Sin3a* and *Hp1b* expression.**
Volcano plots showing the differentially expressed genes in (a) *Sin3a* knockdown and both (b) *Hp1b*^{16} and (c) *Hp1b*^{86} mutants compared to non-mutant controls. Plots show the -log10(pvalue) for each gene plotted against log2 fold change (logFC). Significantly upregulated genes (logFC > 0) are highlighted in red and downregulated genes (logFC < 0) in blue ($p < 0.05$). Genes that show no significant differences in expression are in grey.

In the presence of a *Sin3a* knockdown, there were a number of genes (1411) that showed a significant ($p < 0.05$) differential expression compared to the control. Approximately 52% were upregulated (739) and approximately 48% were downregulated (672).

For *Hp1b*^{16} mutants, there were a large number of genes (3740) that showed a significant ($p < 0.05$) differential expression compared to the control. Approximately 64% were upregulated (2400) and approximately 36% were downregulated (1340).

For *Hp1b*^{86} mutants, there were a number of genes (1597) that showed a significant ($p < 0.05$) differential expression compared to the control. Approximately 65% were upregulated (1044) and approximately 35% were downregulated (553).

GO analysis on these differentially expressed genes revealed several enriched terms for genes modulated by either Hp1b or Sin3a (*Table 6.4*).

a

Fold enrichment	Enrichment FDR	Functional category
2.5	1.4E-17	Organic acid catabolic process
2.3	1.1E-17	Electron transport chain
2.3	1.2E-17	ATP metabolic process
2.2	5.0E-27	Generation of precursor metabolites and energy
2.2	3.4E-12	Fatty acid metabolic process
2	1.7E-49	Oxidation-reduction process

b

Fold enrichment	Enrichment FDR	Functional category
4.2	4.5E-5	Tight junction assembly
3.2	2.3E-8	Mitochondrial gene expression
2.8	4.5E-5	Heart development
2	7.7E-8	Organophosphate metabolic process
2	6.6E-7	Cellular lipid metabolic process
2	1.4E-5	Mitotic cell cycle process

Table 6.4. **Enriched gene ontology (GO) terms for the genes potentially modulated by either Hp1b or Sin3a.**
Gene ontology (GO) analysis for the genes found to be modulated by either Hp1b or Sin3a and also modulated by FoxO in a DNA-binding independent manner. Each enriched GO term shows the enrichment score based on hypergeometric analysis (i.e., the degree to which the genes in a gene list fall into that specific category) and false discovery rate (FDR) correction (i.e., the significance of the enrichment score taking into account false positives) with a cut off of 0.05, and the functional category (i.e., biological process) for which the genes likely fall into for (a) accumulated *Hp1b* mutants and (b) *Sin3a* knockdowns. This list is not exhaustive and only shows the most over-represented category for a specific process.

Enriched GO terms for the combined *Hp1b* mutant differentially expressed gene (DEG) lists included various metabolic processes (such as, organic acid catabolism, fatty acid metabolism, and ATP metabolism), as well as oxidation-reduction process.

For the *Sin3a* knockdown DEG list, terms such as tight junction assembly, mitochondrial gene expression, mitotic cell cycle processes, and metabolic processes (including cellular lipid metabolic process) were enriched.

To determine if Hp1b or Sin3a are likely candidates in modulating the phenotypes alongside dFoxO that appear to utilise dFoxO's DNA-binding independent activity, the DEG lists produced for these three mutants were then compared to the dFoxO-dependent DNA-binding independent DEG list produced via RNA-seq of the *dFoxO* mutants (*Figure 6.5*).

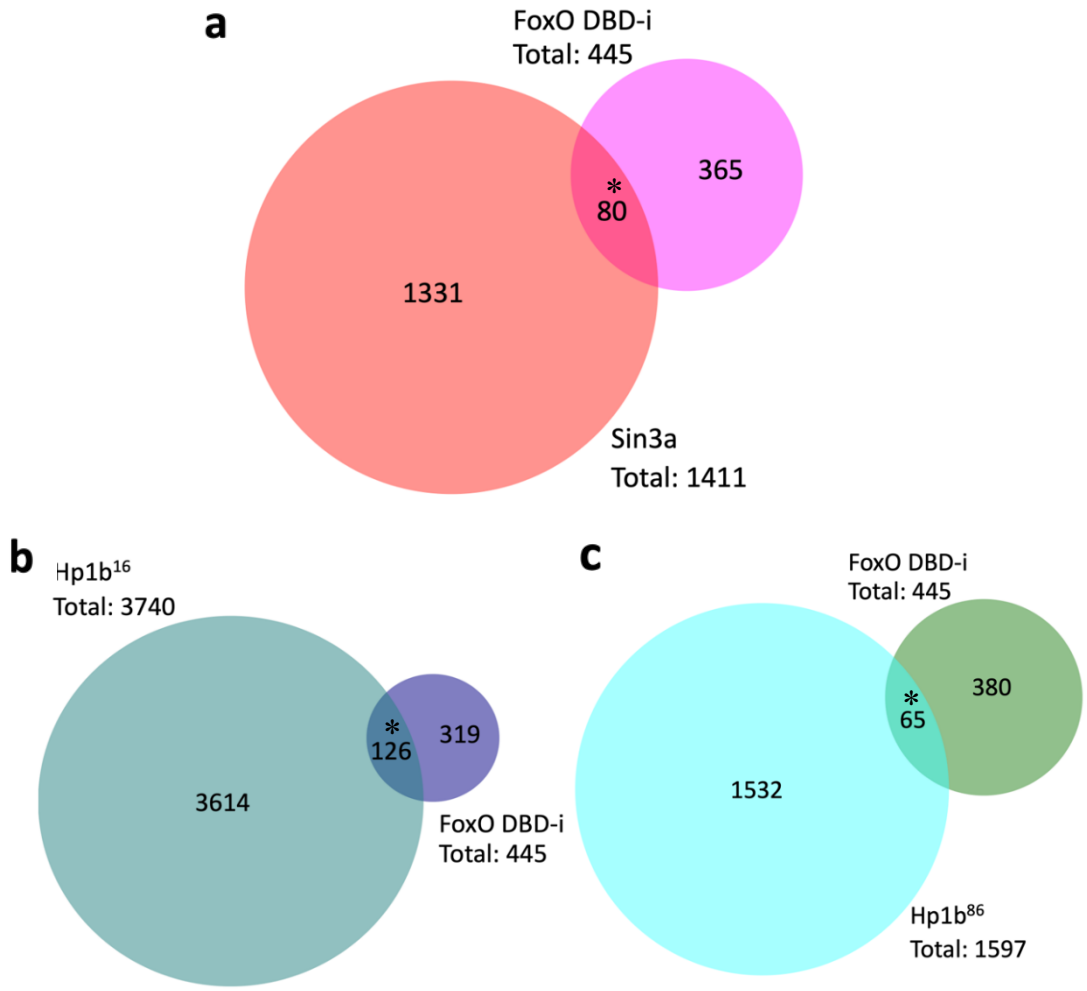

Figure 6.5. **Comparisons of genes identified as targets of Hp1b and Sin3a by RNA-sequencing with the starvation induced dFoxO-dependent DNA-binding independent differentially expressed genes.**
Proportional Venn diagrams comparing genes identified as targets of either (a) *Sin3a* RNAi knockdown S2 cells, and either (b) *Hp1b*^{16} or (c) *Hp1b*^{86} homozygous mutant 3rd instar larvae by RNA-seq from publicly available data sets (Sin3a: Gajan *et al.* 2016; Hp1b: Mills *et al.* 2018) with the genes that were differentially expressed upon starvation in a dFoxO-dependent DNA-binding independent manner. Numbers indicate the number of genes in each section of the Venn (*Sin3a*: p = 1.64E-7 *, *Hp1b*^{16}: p = 0.03 *, *Hp1b*^{86}: p = 0.01 *, hypergeometric analysis). DBD-i: dFoxO-dependent DNA-binding independent.

A significant overlap was observed between all three sets of genes identified as targets of Hp1b and Sin3a by RNA-seq and the dFoxO-dependent DNA-binding independent differentially expressed genes (p = 1.64E-7 for the overlap with Sin3a target genes, p = 0.03 for the overlap with Hp1b^{16} target genes, and p = 0.01 for the

overlap with Hp1b^{86} target genes) with 18% (80/445), 28% (126/445), and 15% (65/445) of the dFoxO-dependent DNA-binding independent differentially expressed genes identified as changing expression in the *Sin3a* knockdown, and *Hp1b^{16}* and *Hp1b^{86}* mutants respectively.

Several genes that seem to be modulated by either Sin3a or Hp1b as well as in a dFoxO-dependent DNA-binding independent manner were identified (*Figure. 6.6*).

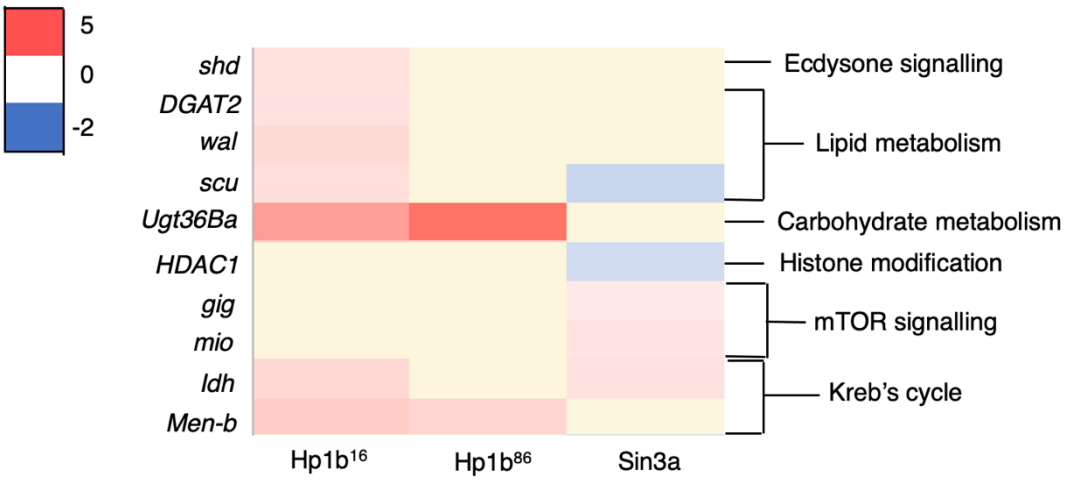

Figure 6.6. **Differential expression of genes modulated by Hp1b or Sin3a as well as in a dFoxO-dependent DNA-binding independent manner.**
Heatmap showing the differential expression (log2 fold change (logFC)) of genes identified as being modulated in a dFoxO-dependent DNA-binding independent manner in mutants of the indicated genotypes using previously published RNA-seq datasets. Expression of all indicated genes are significantly different between the knockdown (*Sin3a*) or knockout (*Hp1b*) mutants and control ($p < 0.05$). Red indicates upregulated genes ($logFC > 0$), and blue indicates downregulated genes ($logFC < 0$). Yellow indicates not present in that gene list. No logFC exceeds 5 or falls below -2. Genes are grouped based on their biological processes given by Flybase.

Genes modulated by Hp1b included those involved with ecdysone signalling (*shd*), lipid metabolism (*DGAT2* and *wal*), and carbohydrate metabolism (*Ugt36Ba* and *Men-b*).

Genes modulated by Sin3a included those involved with histone modification (*HDAC1*) and mTOR signalling (*gig* and *mio*).

Genes modulated by both Hp1b and Sin3a included those involved lipid metabolism ‘’(*scu*) and isocitrate metabolism (*Idh*).

Altogether, these results showed a large overlap of genes modulated by the chromatin modifiers Hp1b and Sin3a and genes modulated in a dFoxO-dependent DNA-binding independent manner. ChIP-seq and RNA-seq data for these two factors showed further support to indicate that these factors do play some role in modulating these genes alongside dFoxO.

6.4 Discussion

The main aim of this chapter was to identify candidate transcription factors that could be mediating the transcriptional changes observed in the dFoxO-dependent DNA-binding independent RNA-seq experiment. The subsequent aim was then to investigate identified transcription factors using previously published RNA-seq and ChIP-seq data, to ultimately assess the potential of these identified proteins as candidates for potential dFoxO binding partners in the modulation of metabolic homeostasis. The hypothesis stated that the differentially expressed genes found to modulated in a dFoxO-dependent DNA-binding independent manner during starvation would identify enriched transcription factors, which could be modulating the expression of these metabolism-related genes alongside dFoxO.

6.4.1 Transcription factor binding motif enrichment analysis

Transcription factor binding motif enrichment analysis is an accurate predictive bioinformatics method, which when paired with expression data (such as that produced via RNA-seq analysis) allows for the identification of transcription factors that are responsible for changes in gene expression caused by conditional changes (Rubin *et al.* 2021). Previous studies suggest that the use of transcription factor enrichment analysis tools on RNA-seq assays (such as, single-cell RNA-seq) are reliable and effective (Holland *et al.* 2020). This reliability stems from the high power and robustness of this sequencing technique, allowing for the visualisation of dynamic gene expression changes across different tissues or conditions in a relatively simple manner (Wang *et al.* 2009b).

Binding sites for transcriptional regulators Sin3a, Hp1b, Hp1c, and Eip74EF showed high enrichment in the list of dFoxO-dependent DNA-binding independently modulated differentially expressed genes, therefore these factors could be interacting with dFoxO in a DNA-binding independent manner to effect gene expression during starvation in a bid to maintain appropriate metabolic responses (e.g., lipid mobilisation).

Of these four factors, Sin3a and the two Hp1 proteins are known to affect chromatin structure via histone modifications (Barnes *et al.* 2018; Zeng *et al.* 2010). DNA is packaged into a dynamic chromatin structure within the nucleus where two super-helical turns of DNA are wound around each core histone protein, eight of which are altogether called a nucleosome (Banerjee & Chakravarti, 2011). Each nucleosome is linked to another via 20-60 bp of so-called ‘linker’ DNA, allowing for flexible

management of the regulation of gene expression through post-translational modification of each histone (Kouzarides, 2007; Banerjee & Chakravarti, 2011). The existence of these modifications has been well known since the late-20th century, with subsequent research identifying the numerous histone post-translational modifications that occur and how they affect chromatin structure (Bannister & Kouzarides, 2011).

A key factor of histone modifications is the various combinations and 'code' that can be imparted to allow for specific and diverse responses (Kouzarides, 2007). These modifications, which occur on over 60 histone locations, include acetylation and deacetylation, phosphorylation, methylation and demethylation, and even in some cases ubiquitylation and ADP ribosylation (Bannister & Kouzarides, 2011; Kouzarides, 2007).

Histone methylation is an integral modification caused by the transfer of a methyl group onto basic lysine (K), histidine (H), and arginine (R) residues present within histones 3 (H3) and 4 (H4), such as K4, K9, K20, R2, and R8, in either mono-, di-, or tri-methylated forms (Cheung & Lau, 2005; Greer & Shi, 2012). These various forms of methylation allow for increased diversity in the responses that can be governed by this modification process, such so that methylation is associated with both active transcription and condensed silent chromatin (Cheung & Lau, 2005; Greer & Shi, 2012). However, this process is considered to be one of the slowest post-translational histone modifications and up until the last 10 years and the discovery of the lysine specific demethylase, Kdm1a, was considered to be irreversible (Greer & Shi, 2012). Interestingly, this modification is also associated with ageing, where altering methyltransferases and demethylases had the ability to alter *Drosophila* and *C. elegans* lifespan, where the latter was affected by increased activity of the demethylase, ubiquitously transcribed TPR on X 1 (UTX-1), on insulin/insulin-like growth factor signalling (IIS) components increasing cellular age (Siebold *et al.* 2010; Jin *et al.* 2011).

Further, effects of histone methylation are also carried out by a group of key chromatin modifiers known as the heterochromatin protein 1 (Hp1) family. This is a family of highly conserved chromosomal proteins, that function in both the condensed heterochromatin and open euchromatin to affect biological processes such as fecundity, metabolism, and activity (Mills *et al.* 2018).

As with mammals, there are 3 *Drosophila* isoforms of these Hp1 proteins known as Hp1a, Hp1b, and Hp1c (α, β, γ respectively in mammals). Of these isoforms, Hp1a is

often most associated with gene silencing (i.e., heterochromatic structures), Hp1c with euchromatin and active gene transcription, and Hp1b has the potential to associate with both (Lee *et al.* 2019). With regards to methylation, the binding of Hp1 proteins to trimethylated H3K9 and the subsequent effects on gene transcription and chromatin packaging have been well-researched (Fischle *et al*. 2005; Eskeland *et al*. 2007; Zeng *et al.* 2010). In *Drosophila*, histone peptide pulldown experiments have shown decreasing levels in affinity from Hp1a, Hp1b, and Hp1c for these modifications (Lee *et al.* 2019). Unsurprisingly therefore, these different isoforms have different roles in relation to these modifications. For example, Hp1a forms a complex to repress transcriptional activity, Hp1b can seemingly counteract this activity of Hp1a in heterochromatic environments, and Hp1c creates a complex with transcription factors (such as: the stem cell differentiation associated transcription factor, without children) to enhance gene transcription in the central nervous system (Lee *et al*. 2019; Font-Burgada *et al.* 2008).

Interestingly Hp1 proteins are also associated with histone sumoylation, a process where ubiquitin-like proteins called small ubiquitin-related modifiers covalently attach to histones (or various other proteins) similar to ubiquitination (Shiio & Eisenman, 2003). Previous research has suggested that sumoylation on H4 residues recruits both Hp1 and HDAC1 proteins to mediate transcriptional repression in HeLa cells (Shiio & Eisenman, 2003).

Another example of a key histone modification is histone acetylation. Where acetyl groups are transferred to specific histone lysine residues via histone acetyltransferases (HAT), a process which is reversed via histone deacetylases (HDAC) (Gräff & Tsai, 2013; Eberharter & Becker, 2002).

This modification is known to enhance transcription across both housekeeping and more specific genes, as the modification of H3 and H4 prevents the tendency for compact chromatin to form allowing for increased transcription factor access (Eberharter & Becker, 2002). An interesting role for this modification is in both memory formation and learning, where a loss of histone acetylation is known to be associated with neurodegeneration in both disease and ageing (Gräff & Tsai, 2013).

Histone acetylation is influenced by metabolism allowing for adaptation to the environment (i.e., in a nutrient sensing manner), where the key intermediary metabolite for acetylation is acetyl-coenzyme A which is also a key component of the Kreb's cycle in the building of macromolecules (e.g., lipids) (Etchegaray &

Mostoslavsky, 2016; Fan *et al.* 2016). Furthermore, a model has been proposed for the involvement of deacetylation during fasting and starvation; where nutrient depravation produces free fatty acids which in turn increase the deacetylase efficiency of the sirtuin Sirt6 towards acetylated H3K9, resulting in decreased transcription of lipogenic and glycolytic genes (Kim *et al.* 2010).

Unsurprisingly then, it is known that FoxO can recruit chromatin modifiers such as HDACs / HATs to alter gene transcription (van der Vos & Coffer, 2008).

For example, mammalian FoxO3a is known to complex with HDAC2 allowing for increased H4K16 acetylation, thereby repressing the expression of the anti-apoptotic gene p21 (independently of the tumour suppressor p53) (Peng *et al.* 2015). ChIP shows that when FoxO3a is knocked down in the mouse brain, the enrichment of HDAC2 in the promoter region of the p21 gene is decreased (Peng *et al.* 2015). This was flagged as of interest due to the potential therapeutic uses of preventing oxidative stress induced neuronal cell death, a key component of some neurodegenerative diseases such as Huntington's, Alzheimer's, and Parkinson's (Peng *et al.* 2015, Singh *et al.* 2019).

Similarly to this, Sin3a is also known to form a complex with an HDAC, to enable its recruitment to chromatin to elicit its effects such as appropriate responses to DNA damage (Barnes *et al*. 2018). Interestingly, Sin3a is also associated with histone methylation where proteomic studies have shown that Sin3a co-immunoprecipitated with the *Drosophila* demethylase, little imaginal discs (LID; also known as Kdm5) affects the specific methylation of H3K4 in locations corresponding to the promoter regions of genes related to methionine metabolism (Liu & Pile, 2017; Spain *et al*. 2010).

Furthermore, nuclear factor kappa-light-chain-enhancer of activated B cells (NFκB)/Relish is known to affect chromatin structure by influencing deacetylation within gene loci (such as, the *bmm* gene) and FoxO modulation of these genes in a fasting-dependent manner (Molaei *et al*. 2019). ChIP-quantitative polymerase chain reaction (ChIP-qPCR) showed that during starvation in NFκB/Relish mutant *Drosophila*, there was a significant enrichment of the activation-associated histone modification H4K9ac in the *bmm* gene locus indicating that the presence of NFκB/Relish is needed for regulating these histone modifications, subsequent chromatin changes, and gene repression (Molaei *et al.* 2019).

It is also interesting to note that in aged flies, many FoxO target genes are associated with chromatin, particularly in its organisation (Birnbaum *et al.* 2019). Despite this and

the examples given above, information regarding whether FoxO is influencing chromatin modifications and assembly is somewhat lacking, identifying a novel avenue of research that could further inform future investigations into the treatment of disorders involving FoxO activity, including ageing.

In addition to these roles in chromatin modification, Sin3a and Hp1b have also been shown to influence metabolism. For example, Sin3a has been shown to affect the expression of *glucokinase* (*GCK*), which catalyses glucose into glucose-6-phosphate a metabolic hub that initiates *de novo* lipogenesis, the hexosamine biosynthetic pathway, and glycogen synthesis (Langlet *et al.* 2017; Peter *et al.* 2011). In reduced insulin environments and therefore increased FoxO activity, Sin3a directly interacts with FoxO1 which represses the expression of *GCK* when both proteins associate to the *GCK* promoter (Langlet *et al.* 2017). Furthermore, Sin3a has been shown to repress the activity of key gluconeogenic genes (e.g., *Pepck* and *G6pc*) when recruited to the fasting response factor, cAMP response element binding protein (CREB), by small heterodimer partner (Zhang *et al.* 2019b). Therefore, the fact that this transcriptional regulator has already been shown to have a direct protein-protein interaction with FoxO and is also a metabolic gene regulator is of great interest and helps to support the suggestion that Sin3a may be able to aid FoxO in the modulation of metabolic genes during starvation.
Similar to Sin3a, Hp1b has also been shown to influence metabolism in *Drosophila* where knockout *Hp1b* mutants showed decreased food intake and elevated body fat levels, as well as increased resistance to both starvation and oxidative stress (Mills *et al.* 2018). However, unlike Sin3a, there is no evidence as yet that FoxO and Hp1b have any direct interactions.

Unlike the other three factors, ecdysone-induced protein 74EF (Eip74EF) (also known as, E74) does not seem to influence chromatin regulation, however it is known to regulate gene transcription in response to differing concentrations of the steroid, 20-hydroxyecdysone (20E) particularly during *Drosophila* development (Thummel *et al.* 1990; Urness & Thummel, 1995). For example, research showed this factor is key in the maximal activation of the *head involution defective* gene, which in turn activates apoptosis during metamorphosis to eliminate redundant tissues (Jiang *et al.* 2000). In spite of this information regarding the role of Eip74EF in development, there is little information surrounding its activity in *Drosophila* adults. Due to the lack of information

surrounding Hp1c and Eip74EF compared to the other two factors, only Hp1b and Sin3a were considered for further analysis. However, their potential ability to modulate metabolism through interactions with dFoxO should not be ignored in future work.

6.4.2 ChIP-sequencing analysis of transcription factors of interest

Subsequent ChIP-seq analysis was carried out on previously published data in an attempt to support the identification of Sin3a and Hp1b as potential dFoxO binding partners (Sin3a: Das *et al.* 2012; Hp1b: Schoelz *et al.* 2021). ChIP-seq is a method of identifying sequences of DNA that a particular protein of interest is bound to, to shed light on DNA-protein interactions on a sizeable scale (Park, 2009). The use of ChIP-seq is effective in the way it is employed here as it has a higher sensitivity, specificity, and coverage than counterpart assays such as ChIP-chip, which combines chromatin immunoprecipitation with microarray hybridisation (Kharchenko *et al.* 2008; Park, 2009). There are some disadvantages to using ChIP-seq including the production of sequencing errors as well as cost, however constant improvements in computational analysis (including, alignment tools) and availability lessen the effect of these disadvantages every year (Park, 2009).

ChIP-seq analysis here showed that between input (i.e., all possible DNA sequences) and IP samples (i.e., DNA sequences associated with a specific protein) there was little variation, as well as less clear differentiation between the signals. This could mean that instead of returning tight precise peaks, the analysis could produce broad domains that do not accurately reflect the enriched motifs and specific DNA sequences (Starmer & Magnuson, 2016). However, this does not mean that the ChIP experiment failed and therefore should not be used for further analysis, for example this analysis showed that a relatively large proportion of the genome contained zero reads, and that 3% of the genome contained 25% and 30% of all the reads for the Sin3a and Hp1b data, respectively. Therefore, this identifies that there is at least a somewhat specific nature to the sequences produced by the IP sample data. Furthermore, the issue with low variation could come from the use of Spearman's Rank correlation, which does not use the raw data but rather the ranks that are produced from it, consequently Pearson's correlation could be used instead as this does use the raw data however, it is not as robust to outliers and relies only on linear relationships therefore could be less accurate (Pernet *et al.* 2013). An improvement to increase the reliability of this data and reduce the effect of possible outliers could be to increase the sample size, as the maximum number of replicates used was two

for the Hp1b analysis and the Sin3a input only had 1. For example, to achieve a p value < 0.05, with a relatively narrow confidence interval (to ensure precision), and 90% power (i.e., at least a 90% chance of obtaining a p value < 0.05) the ideal sample size would be at least 12 or 16 for Pearson's or Spearman's tests, respectively (Bonett & Wright, 2000).

A further issue with the data provided here is the fact that both Sin3a and Hp1b ChIP-seq data was produced during developmental stages of the *Drosophila* life cycle, namely from embryos for Sin3a and 3rd instar larvae for Hp1b. As these are then being compared to gene lists created using RNA-seq analysis on adult *Drosophila*, it may be that the ChIP-seq datasets do not produce a representative and therefore directly comparable state. For example, the homeobox (also known as, Hox) genes (50% of which appear in the Hp1b ChIP-seq data) are essential for the regulation of development in *Drosophila* by driving positional identity of the fly body segments, but do not play much of a role in the adult (with the exception of stem and cancer cell populations) (Lappin *et al.* 2006). Furthermore, there have also been several genes found only expressed in adult tissues, where the cytochrome p450 protein *sxe1,* the TAG lipase *sxe2,* and the female-specific gene of unknown function *fit* were only found to be expressed in adult tissues (e.g., fat body and adult male head fat cells) and not during any developmental stages (Xu *et al.* 2011; Fujii & Amrein, 2002).

However, for the purpose of using this data as supporting evidence to suggest a link between Sin3a or Hp1b and dFoxO in modulating metabolism through protein-protein interactions, it seems as if the quality and representativity of this data is adequate. For example, despite these issues there was still a significant overlap in the genes found in the Sin3a or Hp1b ChIP-seq analysis with those genes potentially modulated in a dFoxO-dependent DNA-binding independent manner, as well as a similar enrichment in GO terms. As the ChIP-seq gene lists were so large, this significance level could be overstated. However, the use of hypergeometric analysis for these comparisons, which takes into account the sample size of each gene list and the likelihood such overlaps occur by chance (Evangelou *et al*. 2012), supports the reliability of the statistical output of these analyses.

The genes that were identified in the overlap of these gene lists include histone modifiers (*E(z), Kdm4,* and *HDAC1*), lipid metabolism regulators (*RalA, Kr-h1, mat , wal, glycerol-3-phosphate acyltransferase 4* (*GPAT4*), and *scu*), ecdysone, mTOR, and insulin signalling pathway associated genes (*path, mio, Npc1a, dILP8, sdr,*

Wdr24, *shd,* and *gig*), an autophagic gene (*EndoA*), regulators of carbohydrate metabolism (*Ugt316A1, PCB, and Men-b*), genes associated with transport (*Eglp4*) and a starvation responsive gene (*loco*).

These genes are of interest when considering the dFoxO-dependent DNA-binding independent phenotypes of starvation and growth that were observed using the *dFoxO* mutants. *Kdm4* is especially of interest as it has been associated with the carbohydrate to lipid switch (Zhang *et al.* 2014a), which could in part help to explain the delayed TAG mobilisation in *dFoxO* mutants where this dFoxO-dependent DNA-binding independent modulation is not possible. This effect in lipid metabolism can also be related to deacetylation carried out via HDAC1, as this is also linked to metabolism in mammalian cells through the suppression of lipogenesis via repression of the sterol regulatory binding protein-1c (SREBP-1c) (Shin *et al.* 2021).

This link between lipid and carbohydrate metabolism and the genes seemingly modulated in a dFoxO-dependent DNA-binding independent manner is also observed in many other ways from the maintenance of lipid droplets and regulation of mTOR by RalA (Hussain *et al.* 2021), the removal of circulating lipids and subsequent ROS control by mat (Li *et al*. 2020), or the regulation of fatty acid β-oxidation via scu and wal (Moeller & Adamski, 2006; Henriques *et al*. 2021; Lammers *et al.* 2019).

Further roles for these genes include the modulation of TAG synthesis by GPAT4 and PCB, and the regulation of TAG breakdown by Kr-h1 (Yao *et al.* 2018; Reshef *et al.* 2003; Kang *et al.* 2017; Zhang *et al.* 2020a). Carbohydrate metabolism can also be affected by the UDP-glycosyltransferase Ugt316A1, where human orthologues of these genes have shown to have roles in lipid droplet formation, fatty acid degradation, glucagon signalling, and glycolysis (Hu *et al.* 2019).

With regard to the dFoxO-dependent DNA-binding independent genes associated with mTOR signalling, it seems as if *path, mio, Wdr24,* and *gig* are all genes modulated by either Hp1b and/or Sin3a. Both path and gig have opposing functions in the regulation of the mTOR pathway, leading to activation and repression of mTOR signalling, respectively (Gao *et al.* 2002; Goberdhan *et al.* 2005). The activation by path ensures proper growth during development due to mTORC1's anabolic nature, whereas gig seems to be more influential in regulating lipid metabolism and autophagy (Goberdhan *et al.* 2005; Gutierrez *et al.* 2007; Tang *et al.* 2018).

Interestingly, both *Wdr24* and *mio* are connected in their biological function, as they both translate into components of the GTPase-activating protein toward Rags 2 (GATOR2) complex which enhances mTORC1 signalling and anabolic processes

(Cai *et al.* 2016; Bar-Peled *et al.* 2013) and both also have mTOR-independent functions in autophagy (Cai *et al.* 2016). Other stress-responsive genes were also potentially bound by Hp1b or Sin3a based on this ChIP-seq data. One such gene is *loco*, a mediator of G-protein signalling with GTPase-activating activity, which has been shown to extend lifespan and produce stronger resistance to stress such as starvation when downregulated (Lin *et al.* 2011).

This influence on metabolism is also observed in the genes involved with the regulation of both the ecdysone and insulin signalling pathways. For example, the *Drosophila* insulin-like peptide (dILP) 8 and secreted decoy receptor (sdr) both influence insulin signalling possibly leading to lipid mobilisation and appropriate growth and stress responses (Ling *et al.* 2017; Okamoto *et al.* 2013).

Similar to Kdm4 and HDAC1 above, the modulation of all these genes are associated with lipid mobilisation, the switch from anabolic to catabolic pathways, and the production of energy, which taken together are important in explaining the dFoxO-dependent DNA-binding independent phenotypes of starvation and growth observed previously in this project.

In ecdysone signalling *shd,* one of the Halloween genes, and *Npc1a* were both identified in the overlap of dFoxO-dependent DNA-binding independently modulated differentially expressed genes and genes directly bound by Sin3a and/or Hp1b. These genes are crucial in the production of 20E and subsequent *Drosophila* development, but are also known to be highly connected to nutritional status as well as insulin signalling (Petryk *et al.* 2003; Warren *et al.* 2004; Huang *et al.* 2007). Curiously, despite ecdysone signalling being a critical pathway in development (Schwedes & Carney, 2012), the presence of these genes in the dFoxO-dependent DNA-binding independent gene list produced from adult *Drosophila* identifies a possible role for these genes in the adult tissues. This could therefore give another aspect to the modulation of growth, where it may not just be effects of metabolism affecting the growth of the *dFoxO* mutants but also effects in the developmental signalling pathway itself leading to this being a dFoxO-dependent DNA-binding independent phenotype. Interestingly, under half of these genes are seemingly bound by both Hp1b and Sin3a (e.g., *E(z), Kdm4*, *Npc1a*, *RalA*, *scu*, *Wdr24*, *Men-b, Ugt316A1*, and *Idh*). Therefore, future work in this area may require the use of double *Sin3a*-knockdown/*Hp1b*-knockout mutants to ensure one factor cannot rescue the absence of the other.

All together, these results identify Sin3a and Hp1b as reasonable candidates as FoxO-binding partners in the context of modulating metabolic and starvation-related genes, particularly those involved with lipid metabolism and mobilisation, and responses to starvation and growth.

6.4.3 RNA-SEQUENCING ANALYSIS OF TRANSCRIPTION FACTORS OF INTEREST

Subsequent RNA-seq analysis was carried out on previously published data in an attempt to further support Sin3a and Hp1b as potential FoxO binding partners (Sin3a: Gajan *et al.* 2016; Hp1b: Mills *et al.* 2018). To ensure that comparisons made between this previously published data and the differentially expressed gene lists produced from RNA-seq analysis on *dFoxO* mutants were accurate, the Hp1b and Sin3a raw RNA-seq data files were re-analysed in the same manner. This re-analysis is important as it has been shown that Cuffdiff (the tool used in the data analysis performed by Mills *et al.* (2018)) has a relatively low power and could not identify differentially expressed Y-chromosome specific genes when comparing male and female human data (Seyednasrollah *et al.* 2015). This disadvantage is not something that was observed with DESeq2 (the tool used in the analysis of the *dFoxO* mutants), ultimately leading to the conclusion that DESeq2 is one of the best tools to use for RNA-seq analysis (Seyednasrollah *et al.* 2015).

Significant overlaps between the genes modulated by Hp1b or Sin3a and those modulated in a dFoxO-dependent DNA-binding independent manner were still observed. However, as these datasets were so large this significance level could be overstated but using hypergeometric analysis for these comparisons, which takes into account the sample size of each gene list and the likelihood such overlaps occur by chance (Evangelou *et al.* 2012), supports the reliability of the statistical output of these analyses.

The genes identified as possibly being modulated in a Hp1b- or Sin3a-dependent dFoxO-dependent DNA-binding independent manner include *HDAC1, Idh, mio, shd, gig, scu, wal,* and *Men-b.*

Many of these genes have been discussed above, such as those involved with histone modification (e.g., *HDAC1*), mTOR and ecdysone signalling (e.g., *mio, gig*, and *shd*), and carbohydrate and lipid metabolism (e.g., *scu*, *Idh*, and *wal*).

There are a number of other genes with interesting functions that are present in this overlap such as the malate dehydrogenase *Men-b*, a component of the Kreb's cycle

alongside Idh, where the product of *Men-b* is important in the regulation of the glycolytic end-product pyruvate making it central in regulating metabolic flux with *Men-b* mutants showing increased glucose levels (Ugrankar *et al.* 2015; Zhang *et al.* 2016). Interestingly, a lot of the genes found here (such as, *Idh, mio, gig, scu, wal, and HDAC1*) are also found within the ChIP-seq data overlap, further supporting the assertion that these two factors are associated with the dFoxO-dependent DNA-binding independent modulation of these genes.

Therefore, as mentioned above, the modulation of these genes correlates well with the areas of metabolism (particularly lipid metabolism and mobilisation, and energy production) that could lead to affects in phenotypes such as starvation survival and growth, explaining why these phenotypes were observed as being modulated in a dFoxO-dependent DNA-binding independent manner.

As with the ChIP-seq data, there are possible caveats that come from using this RNA-seq data as the RNA-seq analyses were performed on 3rd instar larvae and S2 cells for Hp1b and Sin3a respectively. This may mean results are not directly comparable because, as mentioned above, comparing results during a developmental stage to those produced in the adult may differ due to the existence of stage-specific genes. Furthermore, S2 cells may not be representative of what is occurring *in vivo* as dFoxO binds to different promoter regions *in vitro*, where for example dFoxO was found to bind to the P1 promoter of the *dInR* in S2 cells and the P3 promoter in the adult fat body and gut, an area that was found to have no dFoxO binding in S2 cells (Alic *et al.* 2014). However, despite these differences in promoter binding location the same genes were regulated (i.e., both showed regulation of the *InR* gene) (Alic *et al.* 2014), therefore the use of S2 cells for the purpose of RNA-seq should be adequate.

Another possible caveat when comparing this data is that there is research suggesting genetic background can have a variety of effects on gene regulation (Mackay *et al.* 2012; Leips & Mackay, 2000; Chandler *et al.* 2013; Zimmerman *et al.* 2012; Eleftherianos *et al.* 2014). Therefore, as the *Hp1b* mutant RNA-seq analysis was carried out in an *yw* background rather than the w^{Dah} background used for the *dFoxO* mutant RNA-seq analysis, there may be issues with comparing changes in gene expression. This has been shown in previous study where contradictory results have been obtained when investigating longevity-related genes due to the use of different wild-type genetic backgrounds (Evangelou *et al.* 2019). However, there are examples of comparison made between backgrounds that have shown similarities, where for

example with regard to ecdysone signalling and Halloween gene regulation similar responses were observed in *yw* and w^{Dah} flies during desiccation (Zheng *et al.* 2018). Despite this potential hurdle, the datasets showed highly significant overlaps indicating that it is possible in this phenotype the differences in genetic background may not have much of an effect. However, whilst this analysis is adequate for the purpose used here (i.e., preliminary study of whether Hp1b is a likely dFoxO co-factor), due to these potential issues with comparing between backgrounds it highlights the necessity for further experimental analysis (including, co-immunoprecipitation and epistasis study).

It may also be stated that the Sin3a RNA-seq data does not produce a full list of the genes that could be affected by a *Sin3a* mutation, as the effect on *Sin3a* in the S2 cells is produced via RNAi, producing a knockdown of the *Sin3a* gene rather than a knockout meaning the effect could be incomplete (Mocellin & Provenzano, 2004). This diluted response could be related to the efficacy of this process which can be affected by multiple factors, such as cellular localisation of the target mRNA, rate of mRNA turnover, and off-target competition (Hong *et al.* 2014). However, the use of RNAi is extensive and is considered a powerful tool for studying mutations of specific genes, particularly *in vitro* such as here (Mocellin & Provenzano, 2004). And as Sin3a is an essential regulator during development leading to embryonic lethality when fully knocked out, producing *in vivo* knockout models of this gene is complex (Pennetta & Pauli, 1998). Therefore, the use of this form of knockdown should not have much of an effect on the comparisons made in this project.

Ultimately, significant overlaps were still observed between the RNA-seq data and the data produced using the *dFoxO* mutants therefore it seems that there is little reason to believe these issues had any major impact on the conclusions reached here.

All together this data identifies and supports Sin3a and Hp1b as reasonable candidates for FoxO-binding partners in the context of modulating metabolic genes, therefore future work should focus on genetic epistasis interactions between these *Sin3a* knockdown or *Hp1b* knockout flies in combination with *dFoxO* mutations.

Chapter 7

Discussion and conclusions

7. Discussion and conclusions

7.1 Discussion

As a transcription factor, most of the research previously conducted to understand FoxO's functions has focussed on identifying its direct target genes (i.e., how it influences gene expression via direct binding to the DNA). Recently, it has become more apparent that FoxO also mediates gene expression via protein-protein interactions as a way of regulating numerous biological processes including metabolic homeostasis (Thanh *et al.* 2020; Hardie *et al.* 2012; van der Vos & Coffer, 2008). However, many of these studies highlight that whilst FoxO is able to modulate gene expression by binding to other proteins, it still requires binding to the DNA in some capacity (van der Vos & Coffer, 2008).

However, previous research has also found by using a mammalian FoxO DNA-binding domain (DBD) mutant, that FoxO regulates a distinct set of target genes compared to when it binds to DNA (Ramaswamy *et al*. 2002). With further utilisation of this mutant in mice showing that FoxO seemingly regulates glucose metabolism in a DNA-binding dependent manner, but lipid metabolism has both DNA-binding dependent and DNA-binding independent aspects (Cook *et al.* 2015). However, despite reaching this conclusion there were few in-depth experimental results presented (such as, RNA-sequencing) and exactly which processes or genes associated with lipid metabolism affected by FoxO in a DNA-binding independent manner are still relatively unknown.

Therefore, despite an ever-growing collection of FoxO binding partners and the creation of a FoxO DNA-binding domain mutant, there are still many unanswered questions. This provides an exciting and crucial area of research to be explored as understanding FoxO's entire set of capabilities is imperative in order to design safe and effective treatments for disorders caused by aberrant FoxO activity, such as metabolic disorder. This is important as drugs that directly target FoxO have been shown to lead to a wide variety of severe side effects (such as, tumourigenesis and steatosis) (Greer & Brunet, 2005; Langlet *et al*. 2017). These side effects are possibly due to the normal processes, that when disrupted cause these disordered phenotypes, seeming to be heavily reliant on FoxO's ability to bind to DNA. As for example apoptotic genes such as *Bim-1* and *FasL* are known FoxO targets with deregulation being known to be related to tumorigenesis (Greer & Brunet, 2005; Harada & Grant, 2012). Furthermore, liver-knockout FoxO mice show hepatic steatosis on both normal and high fat diets potentially due to the loss of expression of

the FoxO target *nicotinamide phosphoribosyl transferase*, which when active is the rate-limiting enzyme in NAD^+ biosynthesis allowing for the fine tuning of cellular metabolism through the regulation of NAD^+-dependent metabolic proteins such as sirtuins, which are known to effect lipogenesis (Tao *et al.* 2011; Audrito *et al.* 2020; Kemper *et al.* 2013). Therefore, drugs targeting other factors or specifically disrupting FoxO's DNA-binding independent interactions could avoid the severe side effects often seen during FoxO-targeted treatments.

7.1.1 *Drosophila FoxO* mutant verification and phenotyping

By using *Drosophila melanogaster* as a model system, the overall aim of this project was to investigate the molecular mechanisms that *Drosophila* FoxO (dFoxO) uses to influence various metabolic phenotypes, particularly investigating those that occur independently of DNA-binding. This could then lead to the identification of dFoxO binding partners and the repercussions of these binding interactions on gene expression and metabolism. Ultimately, this would allow for the identification of potential therapeutic targets for treating metabolic disturbances linked to aberrant FoxO activity, such as diabetes.

Genomic engineering processes developed by Huang *et al.* (2009) were used as part of a previously unpublished work to create the novel *dFoxO* mutants used here. The removal of the arbitrarily named V3 region, a 3kb region spanning exons 3-8 and a portion of the DBD, created a dFoxO null (dFoxO-ΔV3) mutant using ends out homologous recombination. Reinsertion using the ϕC31 integrase system created the "wild-type" dFoxO-V3 (V3) and dFoxO-V3-3xFLAG (V3F), and two DNA-binding domain mutants dFoxO-DBD1-3xFLAG (DBD1) and dFoxO-DBD2-3xFLAG (DBD2) with H150A and H150A/N146A amino acid alterations within their DBDs respectively. The initial aim was to verify the novel *dFoxO* mutants used in this study, to ensure any subsequent findings (such as, differences in phenotypes or gene expression) were caused by the specific change in dFoxO activity. Polymerase chain reaction (PCR) and western blotting were able to confirm the identity, protein stability, and the ability of the encoded protein to undergo appropriate post-translational modification. To ensure loss of DNA-binding of the DBD mutants, chromatin immunoprecipitation-quantitative PCR (ChIP-qPCR) was used to visualise the abundance of DNA associated with specific genes known to be bound by dFoxO (Alic *et al.* 2011). The ChIP-qPCR showed a reduction in the abundance of DNA associated with two dFoxO direct target genes, *GATAd* and *phl*, in both DBD mutants. However, the DBD1

mutants did not show as great a reduction as the DBD2 mutants, indicating the DBD1 mutants may still have residual DNA binding in some genes. This could lead to phenotypic differences between these mutants, especially as these genes have functions related to the regulation of *Drosophila* lifespan. Ultimately, it was determined with a high level of confidence that the *dFoxO* mutants used in this study created targeted effects on dFoxO activity, and that the introduction of the FLAG tag epitope, amino acid alterations, and presence of the reinsertion artefact sequences do not affect the expression, stability, or post translational modification of the resulting dFoxO protein.

7.1.2 dFoxO-dependent DNA-binding dependent phenotypes

After this successful verification, the aim was to use the *dFoxO* mutants to characterise known dFoxO-regulated phenotypes as DNA-binding dependent or independently regulated processes. Then subsequently, RNA-sequencing (RNA-seq) analysis was used to determine what changes in gene expression were occurring to potentially cause these phenotypic effects. The hypothesis stated that there were DNA-binding independent roles in dFoxO's activity caused by changes in gene expression due to protein-protein interactions, which impact on metabolic function.

RNA-seq analysis was used over other methods (e.g., microarray) as it is a deep-sequencing method, therefore it is commonly used in biological research to quantify and discover transcriptional changes under a vast array of different conditions at a high level of sensitivity and accuracy (Han *et al.* 2015). This sensitivity is essential as it allows for the identification of differentially expressed genes that are regulated by processes or transcription factors, like FoxO, which occur transiently or at low levels (Perkins *et al.* 2010). Other advantages include the high reproducibility of data produced via this method, as there is unique mapping of sequences within the genome, and a lack of background relative to other techniques (such as, microarrays) (Wang *et al.* 2009b). The RNA-seq analysis in this project showed the overall production of good quality sequences spanning a large area of the genome with no bias or mapping irregularities. There was also little variability between replicates of the same condition, ensuring this data should be easily reproducible. Differentially expressed genes were then determined using the DESeq2 tool, one of the best tools for identifying differentially expressed genes due to its high power, a consequence of its high precision and sensitivity (Seyednasrollah *et al.* 2015; Love *et al.* 2014). To

support the results observed using RNA-seq analysis, quantitative reverse transcription-polymerase chain reaction (qRT-PCR) was used to verify the differential expression observed in the RNA-seq analysis with an overall accuracy of 68% rising to 92% when considering sample size, qRT-PCR sensitivity, variability, and primer location.

It was determined that the proper modulation of a number of phenotypes required dFoxO's ability to bind to DNA, including fecundity, lifespan, feeding behaviour, and oxidative and xenobiotic stress survival.

Based on previous research, dFoxO requiring the ability to bind to DNA to properly modulate lifespan is not surprising as many dFoxO targets genes are associated with this phenotype, including the proteosomal regulator, *daw* (Morris *et al.* 2015; Slack *et al.* 2011; Bai *et al.* 2013; Langerak *et al.* 2018).

The RNA-seq analysis carried out on these *dFoxO* mutants supports this as *daw* was found to be modulated in a dFoxO-dependent DNA-binding dependent manner. Further genes found within this RNA-seq data that require dFoxO's ability to bind to DNA and could explain this phenotype include *Atg3* and genes related to mTOR signalling (e.g., *RagA-B*). This is interesting as Atg3, an already known dFoxO target, plays a critical role in autophagosome function and regulation of dysfunctional proteins and organelles to appropriately modulate adult *Drosophila* lifespan (Birnbaum *et al.* 2019; Metlagel *et al.* 2013). Furthermore, mTOR signalling is of interest as it is a well-known ageing-related signalling pathway and its regulation effects key aspects of ageing including energy homeostasis, cellular senescence, and proteostasis (Papadopoli *et al.* 2019).

One thing of note with the lifespan data was that there were some deviations from the expected outcome, where there were significant differences between genotypes that would be expected to behave similarly (e.g., between the w^{Dah}, V3, and V3F or between the ΔV3, DBD1, and DBD2). These differences are possibly due to the natural variations in the genetic background affecting the genotype. Between each generation new genetic variations can occur (Mackay, 2010), therefore carrying out backcrossing should eliminate these genetic differecnces in nuclear and mitochrondiral DNA excepting the mutation of interest (Hospital, 2005). However, these lifespan experiments were carried out approximately at least 15 generations post-backcrossing possibly allowing for these intergenerational mutations to occur leading to altered phenotypes, particularly those that are highly-sensitive (e.g.,

lifespan) (Burnett *et al.* 2011; Mackay, 2010). Genetic variance can be protected against by using balancer chromosomes (Mackay, 2010). However, only the DBD2 and ΔV3 mutant stocks had retained the balancer at this stage due to poor fitness and all experimental mutant flies were used as homozygotes (i.e., without the balancer) therefore it is possible that genetic variation could occur in all genotypes. It is also likely that this effect is only seen in lifespan, as it is a quantitative genetic trait (i.e., variation of lifespan in natural populations can be attributed to a number of different loci) affected by a minimum of 19 different trait loci (Mackay, 2002), which could make it more sensitive to intergenerational variation than the other phenotypes assessed in this project. Therefore, it is unlikely that genetic background is playing any decisive role in these phenotypes especially as these differences showed very small levels of significance compared to those between genotypes where differences were expected, and in every other assay performed these divergences were not observed.

It was noted that perhaps the DBD1 still had some residual DNA-binding activity, which could be causing such a large significant difference over the ΔV3 and DBD2 mutants. However, previously unpublished data shows via luciferase reporter assays that unlike the wild-type flies these DBD mutants were not able to induce luciferase expression under two different promoters (i.e., 4xFOXO responsive elements and insulin receptor (InR)), indicating a sufficient loss of DNA-binding even with just one amino acid alteration. However, ChIP-qPCR showed residual DNA-binding activity for the DBD1 mutant indicating potential residual DNA-binding, at least for genes such as *GATAd* and *phl.* These could be of interest regarding effects in lifespan as *phl,* also known as *Raf* (the *Drosophila* counterpart to mammalian MAPKKK), is a key component in Raf/MEK/ERK signalling which has been shown to have a critical role in ageing in *Drosophila* (Kučerová *et al.* 2016; Slack *et al.* 2015). Furthermore, GATAd has been shown to be overrepresented at the promoters of genes that are upregulated in long-lived insulin/insulin-like growth factor signalling (IIS) mutants (Afschar *et al.* 2016). Therefore, it is possible that genes that affect lifespan could still be regulated by the DBD1 mutant, but not in the DBD2 explaining why these mutants show a different phenotype. Importantly, this phenotype was the only one in which these two mutants differed so it is possible that as with genetic background effects, lifespan could just be more sensitive to this residual activity than other phenotypes.

In the modulation of fecundity, other *dFoxO* null mutants have been shown to lay significantly fewer eggs compared to controls (Slack *et al.* 2011), complementing the phenotype observed in this project. However, the mechanisms FoxO uses to modulate *Drosophila* fecundity are not well-established, therefore despite previous research identifying this as a dFoxO-dependent process the genes that are responsible for this phenotype are not well known. Interestingly, the RNA-seq analysis carried out here identified several genes that could explain this. For example, genes such as *egh, HLH106,* and *EcR* were found to be modulated in a dFoxO-dependent DNA-binding dependent manner. These are of interest as *egh* is a core component of the female *Drosophila* sex-peptide response vital to egg laying and preventing sterility, *HLH106* (the only *Drosophila* sterol regulatory element binding protein (SREBP) isoform) is known to regulate germline lipid synthesis in *Drosophila* females, and *EcR* (the ecdysone receptor) whilst being well known in lifespan extension and stress resistance is also known to effect oogenesis through egg formation and nutrient deposition (Soller *et al.* 2006; Sieber & Spradling, 2015; Simon *et al.* 2003; Carney & Bender, 2000). Excepting *HLH106*, no previous evidence was found to suggest these genes are direct FoxO targets however, the links between the ecdysone signalling pathway and FoxO are already clear (Hossain *et al.* 2013; Colombani *et al.* 2005). Therefore, due to this lack of knowledge surrounding FoxO and *Drosophila* fecundity investigating this potential direct FoxO action on these specific genes could be of interest, especially in the field of *Drosophila* reproduction.

In contrast however, the role of FoxO in modulating genes related to feeding behaviour is more well-known. For example, FoxO has been shown to directly upregulate the expression of orexigenic peptides (Hong *et al.* 2012; Ma *et al.* 2015), however, in this study there was a lack of effect of *dFoxO* mutation on orexigenic peptide expression in the RNA-seq data. Despite this discrepancy, this lack of effect on orexigenic peptide expression could explain why no effect of *dFoxO* mutation was observed on meal frequency or size. Interestingly however, there seemed to be an effect on volume of food consumed after several days indicating a possible cumulative effect. This seems to be replicated in previous research, which suggested that a loss of FoxO inhibition on leptin signalling can lead to cumulative effects on food consumption in rats (Yang *et al.* 2009a). Although this seemingly has not been previously identified in *Drosophila*, the 3-phosphoinositide-dependent protein kinase, PDK-1, found to be modulated in a dFoxO-dependent DNA-binding dependent

manner during the RNA-seq analysis could help to explain this. As this enzyme can integrate the insulin and leptin signalling pathways to balance the release of orexigenic and anorexigenic peptides from their respective neurons (Iskandar *et al.* 2010; Cao *et al.* 2011). Therefore, loss of this integration could lead to aberrant leptin signalling and a disrupted and cumulative effect on food consumption.

Other genes also modulated in a dFoxO-dependent DNA-binding dependent manner that could cause differences in the feeding behaviour in the different *dFoxO* mutants included the *Drosophila* counterpart to the binding partner of the carbohydrate response element binding protein (ChREBP), bigmax, which is known to modulate feeding behaviour particularly in association with environmental cues (Sassu *et al.* 2012). Further genes found in this RNA-seq analysis included the *Drosophila* insulin like peptides (dILP) 3 and 4, both of which have been shown to affect *Drosophila* appetite and food palatability (Semaniuk *et al.* 2018). Curiously, dILP3 also seems to have effects in longevity with *dILP3* knockout mutants showing a significant increase in lifespan (Broughton *et al.* 2005), which could also help to explain the dFoxO-dependent DNA-binding dependent nature of the modulation of normal lifespan. However, one interesting point of note was during the qRT-PCR verification of the RNA-seq data, qRT-PCR data could suggest that *dILP3* mRNA is modulated in a DNA-binding independent manner rather than the DNA-binding dependent manner suggested by the RNA-seq data. Therefore, there is a small possiblity that dILP3 is not contributing to the feeding behaviour or lifespan phenotypes observed in this project.

Similar to feeding behaviour, there are also many examples of FoxO's role in modulating oxidative stress responses and xenobiotic metabolism (Slack *et al.* 2011; Huang & Tindall, 2007; Kops *et al.* 2002; Piper *et al.* 2008; Wang *et al.* 2014; Sipes *et al.* 1986). This again is supported by the results produced during the RNA-seq analysis, where genes related to oxidative stress and xenobiotic responses were found to be modulated by dFoxO and required its ability to bind to DNA. One such example is that of *dILP6*, a known FoxO target that shares vast similarity to the mammalian insulin growth factor 1 (IGF-1) and confers stress resistance when overexpressed in the fat body (Slaidina *et al.* 2009; Okamoto *et al.* 2009; Bai *et al.* 2012). Other examples include the juvenile hormone epoxide hydrolases *Jheh1* and *Jheh-2*, which make up a gene cluster associated with oxidative stress and xenobiotic responses particularly in the presence of paraquat (Guio *et al.* 2014), and the Neural

Lazarillo lipocalin family member, *NLaz* which represses anabolic pathways (such as, IIS) to confer stress resistance and lifespan extension (Hull-Thompson *et al.* 2009). Of interest is also the gene *PEK,* the pancreatic eIF-2α kinase in the endoplasmic reticulum, which phosphorylates eukaryotic translation initiation factor 2α switching to activation of stress response genes (Iida *et al.* 2007; Pomar *et al.* 2003; Ghosh *et al.* 2011). Like *dILP6* these genes have also previously been associated with FoxO activity, where the *Jheh* gene of the silkworm *Bombyx mori* contains a FoxO binding site within its promoter and where both *NLaz* and *PEK* are significantly downregulated in a dFoxO null mutant (Zeng *et al.* 2017; Alic *et al.* 2011).

Altogether, the phenotypes observed in this project as being modulated in a dFoxO-dependent DNA-binding dependent manner support the findings of previous research and can be adequately explained by the differences in gene expression between *dFoxO* mutants that are observed during RNA-seq analysis.

7.1.3 dFoxO-dependent DNA-binding independent phenotypes

Importantly however there were two phenotypes, namely starvation survival and growth, that seemingly required the presence of dFoxO but did not require FoxO's DNA-binding ability to be regulated appropriately. This was interesting as both phenotypes are highly energy dependent, as metabolic stores need to be produced during periods of feeding, then mobilised and utilised efficiently during fasting or the non-feeding developmental stages, so that essential biological processes can be maintained whilst energy sources are limited (Álvarez-Rendón *et al.* 2018; Shingleton *et al.* 2005). It is unclear whether the same links between starvation survival and metabolism are those that connect growth and metabolism however, larvae without sufficient nutrition (e.g., through starvation) yield smaller, but still fertile, adults (Gilette *et al.* 2021) as is seen in this project, indicating that growth can be affected by metabolic state, particularly starvation. And furthermore, as this phenotype is observed in dFoxO-null but not dFoxO-DBD mutants similar to starvation survival, there could be similar mechanisms that relates metabolism to these phenotypes.

7.1.3.1 dFoxO-independent activity in metabolic processes

Subsequent experimentation into these metabolic processes (e.g., storage and utilisation) identified that there were no issues in any of the *dFoxO* mutant or wild-type

flies in producing the three major metabolic stores (i.e., the carbohydrates, glycogen and trehalose, and lipid, triglyceride (TAG)). This was also true for the mobilisation of both carbohydrate stores when under starvation conditions, therefore neither of these phenotypes seemed to require dFoxO activity at all let alone its ability to bind to DNA. The FoxO independent nature of the anabolic processes was partly expected, as this often occurs during the fed state when FoxO activity is at its lowest. For example, the production of glycogen stores not relying on FoxO activity was not unsurprising, as glycogen synthesis relies on the dFoxO-independent expression of factors such as protein phosphorylase-1 (PP1) and Mef2 to regulate key genes such as *hexokinase C* (Berg *et al.* 2002; Clark *et al.* 2013). This was supported in the RNA-seq analysis carried out during this project, as the modulation of *hexokinase C* was found to be independent of dFoxO activity.

The fact that TAG storage was unaffected by *dFoxO* mutations was slightly unexpected. As FoxO is known to repress lipogenic pathways by disrupting transcription carried out by the lipogenic SREBP-1c and the modulation of genes such as *fatty acid synthase (FASN)* (Deng *et al.* 2012; Sekiya *et al.* 2007). Consequently, the loss of FoxO activity would lead to an expected increase in the storage of lipids, something that is not replicated in the results of this study. However, TAG storage can be regulated both dependently and independently of FoxO, as the IIS is not the only signalling pathway implicated in modulating lipogenesis. For example, the Mondo-Mlx signalling pathway can also induce lipogenesis and TAG storage in *Drosophila* through the activation of the transcription factor sugarbabe (sug), which in turn activates *FASN* and *acetyl-coA carboxylase* (*ACC*) both key drivers of lipogenesis (Mattila *et al.* 2015). Furthermore, the glycogenic transcription factor Mef2, mentioned above with regards to glycogenesis, also has lipogenic capabilities as it has been shown to influence the expression of both *FASN* and *ACC*, as well as the diacylglycerol (DAG) transferase, *midway* (*mdy*) (Clark *et al.* 2013). This is also supported by the RNA-seq analysis carried out here, where *sug, mdy,* and *ACC* are found to be dFoxO-independently regulated genes. Therefore, it is likely that the normal modulation of lipid stores is able to continue even in the absence of normal FoxO activity due to these other pathways. Interestingly dFoxO-independent responses in lipid storage have also been observed in mice with liver-specific knock outs of FoxO1 and a FoxO1-DBD mutant not showing any change in *ACC* transcription levels compared to controls (Cook *et al.* 2015). Therefore, not only

supporting the phenotypes observed in this project, but also indicating this is a potentially evolutionarily conserved response.

Another unexpected response was the fact that carbohydrate catabolism was unaffected. For example, in glycogen breakdown the key enzyme involved in the catalysis of the terminal step in glycogen breakdown into glucose, glucose-6-phosphatase (G6pc), is a well-known dFoxO target (Salih & Brunet, 2008). However, as with TAG storage, FoxO-independent glycogenolysis can also be regulated by glucagon and the FoxO-independent inhibition of PP1 through activation of the cAMP/PKA signalling pathway and G6pc (Janah *et al.* 2019; Wu *et al.* 2018). As before, there were also dFoxO-independently regulated genes identified during RNA-seq analysis in this project that are associated with glycogenolysis (such as the phosphoglucomutase, *Pgm*, and various α-glucosidases), therefore this could explain this seemingly dFoxO-independent modulation of glycogen breakdown.

In addition, trehalose synthesis and breakdown also showed unexpected outcomes as FoxO is a known regulator of both of these processes as it modulates the trehalose synthesis genes, *tps-1* and *trehalose phosphatase* (*CG5177*), as well as the gene encoding the enzyme responsible for trehalose breakdown, *trehalase* (Hibshman *et al.* 2017). However as before, there has been research to suggest that in the absence of dFoxO all these processes could be rescued by other signalling pathways. For example, trehalose production and breakdown could be regulated by either the juvenile hormone (JH) and 20-hydroxyecdysone (20E) independently of dFoxO, as both have been implicated in the control of trehalose metabolic genes (Shukla *et al.* 2015). For example, JH has been associated with trehalase expression to maintain proper starvation survival in the red flour beetle, *Tribolium castaneum*, whereby concurrent reductions of trehalase and JH in the fat body, decrease carbohydrate metabolism and increase starvation resistance (Xu *et al.* 2013). This is also supported by the differentially expressed genes found in the RNA-seq analysis, where genes associated with these signalling pathways were found to be regulated independently of dFoxO. These included *ftz-f1*, which encodes a transcription factor that alongside ecdysteroid signalling (which can be influenced by genes such as *spo, sad, sro, ptth,* and *G9a,* all of which are also found in this RNA-seq data) can regulate the modulation of circulating trehalose by increasing trehalose transport and *trehalase* expression (Nishimura, 2020).

Interestingly, it was important to note that trehalose stores did not seem to initially be affected by starvation or *Drosophila* genotype when using whole fly extracts.

Therefore, the use of haemolymph metabolic assays was employed in the assessment of this phenotype, which showed an observable difference during starvation. This was most likely caused by smaller alterations being 'masked' when using whole fly extracts, as most trehalose is found in the haemolymph. This is a conclusion supported by observations using *Akh* mutants, where whole body extracts from *Akh* mutant *Drosophila* showed little changes in trehalose concentration to controls, but haemolymph extracts showed observable differences (Gáliková *et al.* 2015).

An additional advantage of using the haemolymph assays was the ability to quantify the circulating glucose levels, which ultimately showed a similar phenotype to trehalose metabolism. Again, it is not surprising that the metabolism of glucose also seems to be independent of FoxO activity, as there are also many FoxO-independent ways in which glucose can be utilised (Berg *et al.* 2002; Watford, 2015). Again, this is supported by the RNA-seq data produced using these *dFoxO* mutants, as genes potentially involved with these processes were found to be regulated independently of dFoxO activity. These genes included *PyK*, *AdipoR*, and *Akh*. *Pyk* encodes pyruvate kinase, a key enzyme in the regulation glucose homeostasis through the modulation of gluconeogenesis (Israelsen & Vander Heiden, 2015). *AdipoR*, the adiponectin receptor responsible for regulating AMPK and peroxisome proliferator-activated receptor (PPAR)-α enabling the regulation of whole-body glucose homeostasis and glycolysis (Long & Zierath, 2006; Peeters & Baes, 2010). And lastly, *Akh* (the counterpart to mammalian glucagon) has been shown in previous research to increase in expression during starvation leading to increased control of circulating sugars in the haemolymph (Mochanová *et al.* 2018).

Overall, the phenotypes observed in this project that are associated with metabolic storage and carbohydrate mobilisation are seemingly regulated independently of dFoxO entirely. This is supported not only by previous research, but also by the genes identified during RNA-seq analysis. All in all, the lack of dysfunction in these phenotypes excludes these processes as having an effect in the dFoxO-dependent DNA-binding independent phenotypes.

7.1.3.2 dFoxO-dependent DNA-binding independent lipid mobilisation

The most important phenotype assessed was lipid mobilisation, as the initial stages of this process seemed to be slower during starvation in dFoxO-null mutant flies

compared to all other mutants and controls, indicating that this is a process potentially modulated in a dFoxO-dependent DNA-binding independent manner. The effects of this slower mobilisation seemed to correct itself after a longer period of starvation (i.e., lipids were eventually mobilised), although by this time point the majority of the dFoxO-null flies were dead. However, the fact that lipids were mobilised at all in these nulls was unexpected as lipolysis is a process well-known to be modulated by FoxO activity as *bmm,* the gene encoding a core TAG lipase (homologous to mammalian adipose TAG lipase (ATGL)), is known to be a dFoxO target (Birnbaum *et al.* 2019). Although, as with many of the processes outlined above, the modulation of this gene alongside other lipases such as *Lip4* and *dob* and core lipid droplet associated proteins such as *Lsd-1*, were shown in this RNA-seq analysis to be regulated independently of dFoxO activity. Something which fits with other research as *bmm* is such a key lipolytic enzyme, it can be regulated by other signalling pathways including hedgehog and mTOR signalling (Chatterjee & Perrimon 2021; Zhang *et al.* 2020b).

Interestingly, there was a more obvious delay in lipid mobilisation in response to starvation in the males compared to the females. This sexual dimorphism in TAG mobilisation was attributed to females having a more complicated lipid biology as differing reproductive needs have to be considered. For example, the nutritional status of *Drosophila* females (such as, the onset of starvation) can affect the egg chamber with nutrient deprivation leading to apoptosis and the reabsorption of macromolecules (e.g., lipids) from the lipid droplets within these egg chambers into other tissues for use as energy (Terashima & Bownes, 2006; Welte, 2015). In conjunction, lipid metabolism is also affected by the sex peptide (an essential component of *Drosophila* seminal fluid), which alters female lipid metabolism via modulating gene expression to ensure the metabolic demands of reproduction are met (White *et al.* 2021). Therefore, improvements in phenotyping the females could be to use virgin females or females reared in a controlled-mated environment preventing reproduction from having such a strong effect. Furthermore, lipid analysis using mass spectrometry or quantitative magnetic resonance would also be a vast improvement as they would allow for identification of exact species and quantities of lipids present or allow for estimations of fat and lean body mass respectively. A further additional technique that could be used in conjunction with these metabolic assays is analysing the respiratory quotient, which by using the ratio of CO_2 produced to O_2 consumption can identify which fuel (e.g., carbohydrates, fat, or protein) is primarily being used to fuel metabolic

processes in that moment (Wat *et al.* 2020). This may help to pinpoint a more specific area to focus on in future work, as genes found in the RNA-seq analysis in this project represented those from a wide range of metabolic processes (including, the Kreb's cycle, fatty acid oxidation, and the carbohydrate to lipid switch).

However, despite the sexually dimorphic response, the methods used were appropriate for the scope of this study based on cost-effectiveness and sensitivity.

As with other phenotypes, this effect on lipid mobilisation is also supported by the changes in gene expression found via the RNA-seq analysis, where 445 genes were found to be differentially expressed during starvation, indicating that there is a relatively large number of genes that are potentially modulated in a dFoxO-dependent DNA-binding independent manner during starvation.

These genes are involved with processes such as chromosome organisation, organelle organisation, and various metabolic processes such as regulation of metabolic process, cellular metabolic process, and UDP-glucose metabolic process. Therefore, due to this high enrichment of metabolism-related processes, there were several genes that could be of interest in explaining this dFoxO-dependent DNA-binding independent phenotype.

For example the histone modifiers HDAC1 and Kdm4 are associated with metabolic homeostasis and lipid metabolism, as HDAC1 suppresses the activity of the lipogenic master regulator SREBP-1c, and Kdm4 is both influenced by the nutritional environment as its key substrate is the Kreb's cycle intermediate, α-ketoglutarate, as well as influences metabolic homeostasis via the activation of E2F1, the subsequent inhibition of pyruvate dehydrogenase, and the initiation of the carbohydrate to lipid energy switch (Tran *et al.* 2017; Shin *et al.* 2021; Zhang *et al.* 2014a). Another step of the Kreb's cycle that is potentially affected in this DNA-binding independent manner is the conversion of malate into oxaloacetate by malate dehydrogenase (encoded by the gene *Men-b*) allowing for the production of energy (Minárik *et al.* 2002).

The switch to fatty acid oxidation as a form of energy production carried out via Kdm4, is also related to the upregulation of the electron transfer flavoprotein, wal, and short-chain dehydrogenase/reductase, scu, that also enable fatty acid breakdown (Shafqat *et al.* 2003; Henriques *et al.* 2021; Lammers *et al.* 2019).

Transport-related genes were also found in to be modulated in a DNA-binding independent manner. One such gene is *mat*, an upregulated lipid binding protein that removes lipids from the circulation as a key process in the inhibition of oxidative stress, cellular damage, and impaired ATP synthesis and insulin secretion by

reducing the likelihood of lipid peroxidation and the formation of toxic by-products (Li *et al.* 2020; Bielka & Przezak, 2021). Another such gene important in transport is *Eglp4,* which encodes the aquaglyceroporin (AQP) entomoglyceroporin 4, which transports glycerol, the backbone of complex lipids such as TAG, across cellular membranes for lipid synthesis (Calamita *et al*. 2018). This in concert with the modulation of *PCB*, which encodes pyruvate carboxylase a lipogenic gene that produces glycerol allowing for the build-up of lipid stores and removal free fatty acids from the circulation (Reshef *et al.* 2003), could also help to effect lipid mobilisation by switching from anabolic to catabolic processes. This switch is also represented by the dFoxO-dependent DNA-binding independent downregulation of Kr-h1*,* which has been shown to be linked to inhibiting TAG lipolysis and the crosstalk of developmental signalling in *Drosophila* with metabolism where Kr-h1 mutants display severely altered lipid metabolism (Kang *et al.* 2017).

This DNA-binding independent modulation of lipid mobilisation could also be affected by genes encoding proteins associated with the lipid droplet (LD), namely *DGAT2* and *GPAT4. DGAT2* encodes the diacylglycerol O-acyltransferase 2 that interacts with and saturates the surface of LDs to enable the catalysis of the final TAG synthesis step, the conversion of diacylglycerol (DAG) to TAG (McFie *et al.* 2018; Wilfling *et al.* 2013). The role of *GPAT4* which encodes the glycerol-3-phosphate acyltransferase 4, is very similar sharing DGAT2's role in LD growth and TAG synthesis with mutants often being developmental lethal or incurring developmental defects and dysfunctional metabolic regulation (Yan *et al.* 2015; Yao *et al.* 2018). By appropriately modulating these genes there would also be a proper modulation of anabolic processes (e.g., lipogenesis), allowing for the appropriate switching to catabolic processes.

Interestingly, as mentioned above, based on the qRT-PCR data dILP3 could also potentially be modulated in a dFoxO-dependent DNA-binding independent manner. This could be important when determining the cause of these lipid mobilisation defects, as ablation of dILP3 which leads to increased starvation resistance and lifespan possibly through its effects on SREBP-1c activation (Toprak, 2020).

This effect on the dILPs is also potentially affected by the upregulation of the *secreted decoy receptor* (*sdr*) gene. The product of this gene has a high sequence similarity to the extracellular portion of the *Drosophila* insulin receptor and can therefore bind dILPs (specifically the lipogenic dILP3, but also dILP1, 2, 5, 6, and 7) with a high affinity in the circulation antagonising the IIS to fine tune responses to stress and

growth signals (Okamoto *et al.* 2013; Toprak, 2020; Rulifson *et al.* 2002; Broughton *et al.* 2005).
Another dILP that is seemingly affected by dFoxO independent of its ability to bind to DNA is dILP8, the upregulation of this gene is interesting as dILP8 has already been linked to larval growth and ecdysone suppression in *Drosophila* but has recently also been found to modulate lipid mobilisation in the mosquito *Aedes aegypti* (Garelli *et al.* 2012; Ling *et al.* 2017).

Therefore, taken together, these results show dFoxO-dependendent DNA-binding independent effects in lipid metabolism and mobilisation, and responses to starvation that support the observed dFoxO-dependendent DNA-binding independent nature of the modulation of growth and starvation survival.

An interesting observation made during the RNA-seq analysis identified that there were sets of genes found to only be modulated in a single mutant. However, the genes present in only the V3F or the dFoxO-null lists, showed enrichment of very similar biological processes (e.g., synaptic signalling and neuron development). Therefore, this indicates that to rescue essential phenotypes (e.g., proper brain function) disrupted by loss of dFoxO, the dFoxO-null mutants modulate different genes to modulate the same processes independently of dFoxO activity.
However, the genes only found to be differentially expressed in the DBD2 during starvation are associated with a completely distinct set of biological processes (e.g., macromolecule metabolism and biosynthetic processes). There are even several genes that are essential in modulating TAG homeostasis and mobilisation (such as, *Hsl*, *Ubc2*, and *snz*) or are critical in maintaining protective responses to stress (such as, *Treh*, *Herp*, *crc*, and *Axn*) (Bi *et al.* 2012; Beller *et al.* 2008; Ugrankar *et al.* 2019; Hibshman *et al.* 2017; Kang & Ryoo, 2009; Zhang *et al.* 2014b; Seo *et al.* 2009). Therefore, it is likely that these DBD mutants do not function as a wild-type with a dysfunctional DBD, but produce a distinct phenotype of their own. Interestingly, this mimics the observations found in human cells (Ramaswamy *et al.* 2002), providing another indication that these observations made in *Drosophila* in this project are evolutionarily conserved. This distinct phenotype could be due to the loss of DNA-binding allowing for dFoxO to produce interactions it would not normally due to it being occupied at the DNA, or due to sequestering other proteins away from the DNA to inhibit their effects. Ultimately, this response seems to highlight another set of dFoxO-

dependent DNA-binding independent genes, which complements the already identified dFoxO-dependent DNA-binding independent genes in the processes they modulate (e.g., lipid metabolism and mobilisation, mTOR signalling and growth, and reponses to IIS and starvation) shedding further light on why these DBD mutants are not phenotypically divergent from the V3F wild-type in some areas.

Another interesting find that would be interesting to pursue, not related to FoxO's role in metabolism, is the regulation of the *FoxO* gene itself. This is because transcriptional modulation of *FoxO* is still relatively unknown, as most of the focus is on the regulation of the FoxO protein via post translational modifications. The qRT-PCR used to verify the RNA-seq analysis showed that in the fed state, *dFoxO* expression was significantly upregulated in null flies compared to the V3F control. This response was determined to not produce a viable protein indicating this truncated transcript could be unstable. However, the antibody used was raised against two peptides (Giannakou *et al.* 2007), one of which is missing in this dFoxO-null therefore it is also possible that the antibody is not able to bind appropriately, and the truncated protein cannot be visualised. It was also determined that *dFoxO* gene regulation does not require FoxO's ability to bind to DNA, as in the DBD mutants there is no change in *dFoxO* gene expression compared to the V3F mutants indicating this negative regulation is still intact. As well as the possibility that dFoxO is modulating its own expression through protein-protein interactions, it is also plausible that due to the absence of dFoxO's DNA-binding independent activity, the lack of phenotypic effect that would occur if a functional dFoxO protein was present leads to an increase in *dFoxO* expression independent of dFoxO.

As outlined above, transcriptional regulation of the *FoxO* gene is not well studied and therefore whether this type of feedback is plausible is hard to determine from the literature. There are some examples of *FoxO* gene regulation for example, in mammalian myocytes, where *FoxO3* was shown to be a target gene of the tumour suppressor p53 in the presence of DNA-damaging agents (Renault *et al.* 2011). In addition, the *FoxO* gene was also shown to be regulated by the hypoxia-induced factor (HIF) 1 to regulate apoptotic and cell survival pathways during hypoxic stress (Bakker *et al.* 2007). Despite this, many of these examples only refer to the modulation of the *FoxO* gene during disorder and little is reported on its modulation under normal conditions. Interestingly, however, it has been suggested that FoxO is able to modulate transcription of the *FoxO* gene directly. For example, in *Caenorhabditis*

elegans a core subunit of a complex associated with chromatin modification, SWSN1, modulates the gene for the *C. elegans* FoxO homologue *DAF-16* after direct interaction with the DAF-16 protein and subsequent binding to the promoter (Bansal *et al.* 2014). However, as this latter example seemingly still required FoxO's ability to bind to DNA, this dFoxO-dependent DNA-binding independent modulation of the *FoxO* gene observed here could potentially be a novel find that has not been previously reported.

7.1.3.3 dFoxO-dependent DNA-binding independent growth effects

Even though growth is a highly-energy dependent process with genes that regulate metabolism in *Drosophila* also playing large roles in growth regulation (Nayak & Mishra, 2021), there are many genes highlighted in this dFoxO-dependent DNA-binding independent gene lists that identify a possible connection between critical growth pathways and metabolism-related dFoxO-dependent DNA-binding independent modulation, on top of the effects in lipid mobilisation.

For example, *scu* has already been shown to be a metabolic gene that connects lipid metabolism to early development in *Drosophila* (Thanh *et al.* 2020). Furthermore, research has also shown that the regulation of genes involved with 20E production can also be influenced by nutritional status and the IIS, where overexpression of several dILPs concurrently increased Halloween gene expression (Koyama *et al.* 2020; Walkiewicz & Stern, 2009). There are several genes related to ecdysone signalling in this gene list, where *Npc1a*, and the Halloween genes, *shd* and *phm,* are all potentially downregulated by dFoxO in a DNA-binding independent manner. These genes are all essential in generating the active form of ecdysone, 20E, a steroid essential in insect growth and modulation of final adult size (Petryk *et al.* 2003; Warren *et al.* 2004; Huang *et al.* 2007). Therefore, they have the potential to co-ordinate ecdysone signalling with metabolism, which could be vital during development, creating another link between metabolism and disordered growth.

The IIS and ecdysone pathways are not the only signalling pathways or growth-related processes that are influenced by genes modulated in a DNA-binding independent manner. As there are several genes related to mTOR signalling that are also found to be modulated in this way. For example, both *mio* and *Wdr24,* components of the GTPase-activating protein toward Rags 2 (GATOR2) complex that enhances mTORC1 activity promoting cell growth (Cai *et al.* 2016; Bar-Peled *et al.* 2013), are upregulated in a DNA-binding independent manner. In addition, these both

also have mTOR-independent functions in metabolic regulation, where they can modulate both autophagy and lysosome function in the maintenance of health tissues (Cai *et al.* 2016; Yambire *et al.* 2019). Other mTOR-related genes found to potentially be modulated in a dFoxO-dependent DNA-binding independent manner, include the downregulated *path* and the upregulated *gig*. *Path* like the above genes (e.g., *mio* and *Wdr24*), is a positive regulator of mTOR signalling to ensure the maintenance of proper growth (Goberdhan *et al.* 2005), and *gig* opposes the functions of the above genes by antagonising mTORC1 signalling via interactions with the TSC1 protein that binds to and inhibits TOR, effecting lipid metabolism via regulation of LDs and autophagy, and sensing of nutrients in the fat body (Gao *et al.* 2002; Gutierrez *et al.* 2007; Tang *et al.* 2018).

Taken together, the dFoxO-dependent DNA-binding independent modulation of these genes could identify another link to the defects in the modulation of normal growth observed and dFoxO's DNA-binding independent activity, in addition to the potential link with lipid mobilisation identified above.

7.1.4 Identification of dFoxO binding partners

Using these differentially expressed genes that are seemingly modulated in a dFoxO-dependent DNA-binding independent manner, the final aim was to attempt to identify potential binding partners with which dFoxO binds to during starvation to indirectly modulate the expression of these metabolically related genes. The hypothesis was that the differential expression in the identified genes would lead to transcription factor enrichment, identifying co-factors with which dFoxO could be interacting with to directly impact on metabolism independent of dFoxO's ability to bind to DNA.

Transcription factor binding motif enrichment analysis was employed and four enriched factors were recognised, including Sin3a, Hp1b, Hp1c, and Eip74EF. Little is known of Eip74EF, although previous research has connected it to regulating gene expression in response to 20E during development (Thummel *et al.* 1990; Urness & Thummel, 1995). However, Sin3a and heterochromatin 1 (Hp1) family members Hp1b and Hp1c are known to be associated with chromatin modifications such as histone deacetylation and lysine methylation respectively (Barnes *et al.* 2018; Nielsen *et al.* 2002). Interestingly, Sin3a has already been associated with FoxO binding in mammals where direct interactions with FoxO cause the repression of the Sin3a target gene *glucokinase* (*GCK*) in the regulation of glycolysis and lipogenesis (Langlet

et al. 2017). Furthermore, this protein-protein interaction has also already been successfully disrupted via the use of small molecule inhibitors, however whilst these compounds were able to remove FoxO activity at some promoters (e.g., *G6pc*) it failed to do so at others (e.g., *GCK*) (Calissi *et al.* 2020; Langlet *et al.* 2017). In addition to this, although not as yet associated with FoxO function, Hp1b has been associated with lipid metabolism in *Drosophila,* where *Hp1b* mutants showed reduced food consumption and elevated body fat compared to controls (Mills *et al.* 2018). As with Eip74EF less information is available for Hp1c, particularly in comparison to Hp1b and Sin3a. Therefore, as the two most enriched factors subsequent analyses concentrated on these two proteins.

To ensure that these factors were reasonable candidates for dFoxO binding partners, the next aim was to compare gene expression analyses associated with these two factors and compare their target genes to the RNA-seq analysis produced using the *dFoxO* mutants.

Previously published RNA-seq data (Sin3a: Gainan *et al.* 2016; Hp1b: Mills *et al.* 2018) using *Drosophila* larvae or S2 cells with *Hp1b* mutations or reduced *Sin3a* expression respectively was reanalysed and compared to the dFoxO-dependent DNA-binding independent genes. The reanalysation of the publicly accessible data was important as the published research used a different analysis toolkit to the one used here, which can produce variable results that do not lend themselves to precise comparisons. This is evident by the outcomes of various studies, where for example DESeq2 (the tool used to analyse the *dFoxO* mutant data) and CuffDiff (the tool used to analyse the Hp1b and Sin3a data originally) were shown to differ, where CuffDiff had an overall lower statistical power compared to other tools (including, DESeq2) and struggled to differentiate the expression of even Y chromosome specific genes between male and female samples (Seyednasrollah *et al.* 2015). ChIP-sequencing (ChIP-seq) data was also used to support this RNA-seq reanalysis. This was done as ChIP-seq is another deep-sequencing method, similar to RNA-seq, that allows for the identification of enriched DNA sequences associated with the binding of a particular transcription factor or regulator (Nakato & Sakata, 2021). The advantage of sequencing is that it gives a greater representation of the sequences present due to its higher sensitivity, especially compared to methods such as ChIP-chip, the combination of ChIP with microarray hybridisation (Kharchenko *et al.* 2008; Park, 2009). When published ChIP-seq data (Sin3a: Das *et al.* 2012; Hp1b: Schoelz *et al.*

2021) was reanalysed, it was found that there was not much variation between the input signal (i.e., all the DNA present) compared to the IP signal (i.e., only the DNA associated with binding by the factor of interest). This could be a disadvantage as it may be harder to differentiate between the signals of the different conditions; therefore, instead of returning tight peaks, broad domains may be produced which do not accurately reflect the enriched motifs (Starmer & Magnuson, 2016). However, it was determined that a large proportion of the reads were found in a small part of the genome with an ample area of the genome containing zero reads for both sets of data. Thereby identifying that there was at least a somewhat specific nature to the sequences produced by the ChIP sample data, and therefore the results produced would be reliable enough for the proposed application.

Downstream analysis of both the ChIP-seq and RNA-seq datasets identified a large overlap in the enriched gene ontology terms produced for the Hp1b-, Sin3a- and dFoxO-related differentially expressed gene lists. For example, terms associated with various metabolic processes (such as, macromolecule metabolic process, organic substance biosynthetic process, and nucleic acid metabolic process), as well as regulation of the cell cycle and chromosome organisation were found to be enriched in all datasets. There were also a number of genes associated with Hp1b and Sin3a binding, including lipid metabolism regulators (*Kr-h1, mat, Eglp4, PCB, scu, GPAT4,* and *wal*), histone modifiers (*Kdm4* and *HDAC1*), and signalling pathway components (*dILP8, sdr, shd, Npc1a, path, Wdr24, mio,* and *gig*), that also seem to be modulated in a dFoxO-dependent DNA-binding independent manner, which seemingly could be affecting the mobilisation of lipids as outlined above. This supports these genes as being modulated by dFoxO alongside either Sin3a or Hp1b, and that there is a possible connection between these factors and to the dFoxO-dependent DNA-binding independent modulation of their expression.

Despite these successes, there are possibly limitations with using previously published results as comparisons. Firstly, both the RNA-seq and ChIP-seq analyses were not carried out on adult flies as used for the *dFoxO* mutant RNA-seq analysis. They were either in the developmental stages (embryos for Sin3a ChIP-seq or 3rd instar larvae both Hp1b datasets) or in S2 cells (Sin3a RNA-seq data). This is challenging because during development different genes are regulated compared to the adult, where for example several genes (such as, *sxe2* and *fit*) are expressed in

the adult but not during earlier developmental stages (Xu *et al.* 2011; Fujii & Amrein, 2002). In addition, many genes involved in the developmental pathways, such as the JH and ecdysone pathways, have been identified as existing in adults but information on their roles is often lacking making it harder to create connections with observed phenotypes. Furthermore, S2 cells may not be wholly representative or comparable to *in vivo* analyses, as some transcription factors, including dFoxO, bind to different promoter regions when *in vitro* (Alic *et al.* 2014). However, despite the difference in promoter binding, the genes that were assessed in these experiments were regulated both *in vitro* and *in vivo* (i.e., in both circumstances the *InR* gene was expressed) (Alic *et al.* 2014).

Furthermore, the Hp1b RNA-seq data uses *Drosophila* of an *yw* background compared to the w^{Dah} used in the *dFoxO* mutant experiments and research has suggested that genetic background can play a part in changes in gene expression and phenotype (Zheng *et al.* 2018; Leips & Mackay, 2000; Chandler *et al.* 2013; Zimmerman *et al.* 2012; Eleftherianos *et al.* 2014). Even though this is not ideal, in previous experiments when directly comparing both *yw* and w^{Dah} flies, they show similar responses for certain phenotypes (Zheng *et al.* 2018).

An additional disadvantage of using this RNA-seq data also occurs in the method of production, where a reduction in *Sin3a* expression in S2 cells was produced using interference RNA (RNAi). The resulting change in expression of *Sin3a* is not as ideal, as RNAi only produces knockdowns rather than knockouts (Mocellin & Provenzano, 2004). However, these methods have been used extensively in the past and are considered powerful tools for studying molecular mechanisms or creating genetic mutants (Mocellin & Provenzano, 2004), and due to the essential nature of the protein, *Sin3a* mutants are unusable.

Altogether, whilst these limitations should be acknowledged, there is much supporting evidence to suggest these disadvantages are not as detrimental as they may seem, and the presence of significant overlaps between the different datasets used in this study make it reasonable to assume this data is able to make reliable comparisons in this context. Therefore, it is likely that Hp1b and Sin3a could be co-regulating these dFoxO-dependent DNA-binding independent genes alongside dFoxO in some manner.

Altogether this showed that maintaining efficient lipid utilisation during the initial stages of starvation or periods of non-feeding may be most critical in ensuring normal starvation survival and growth respectively. Firstly, it appears that due to unaffected nutrient storage developing flies and fully fed adults can function appropriately, and in the case of the former reach critical weight (i.e., the minimum weight in which sufficient nutrient stores have been acquired to survive to adulthood (Zeng *et al.* 2020)). Then as carbohydrates can be mobilised appropriately, the production of energy to survive and regulate key processes in the initial stages of development and starvation is possible. However, when fasting is extensive the main source of energy in the dFoxO-nulls cannot be effectively switched to the lipid stores, due to issues in modulating genes involved with lipid metabolism. This then prevents either the reservation of carbohydrate energy for obligate glucose utilisers causing premature death during starvation, or the production of enough energy to produce a fly of normal adult size as this is determined after the critical weight checkpoint is reached (Shingleton *et al.* 2005). As this is not observed in the other *dFoxO* mutants (e.g., DBD mutants) and the controls, therefore this process seems to be modulated in a dFoxO-dependent DNA-binding independent manner via interactions with factors such as Hp1b or Sin3a (*Figure 7.1*).

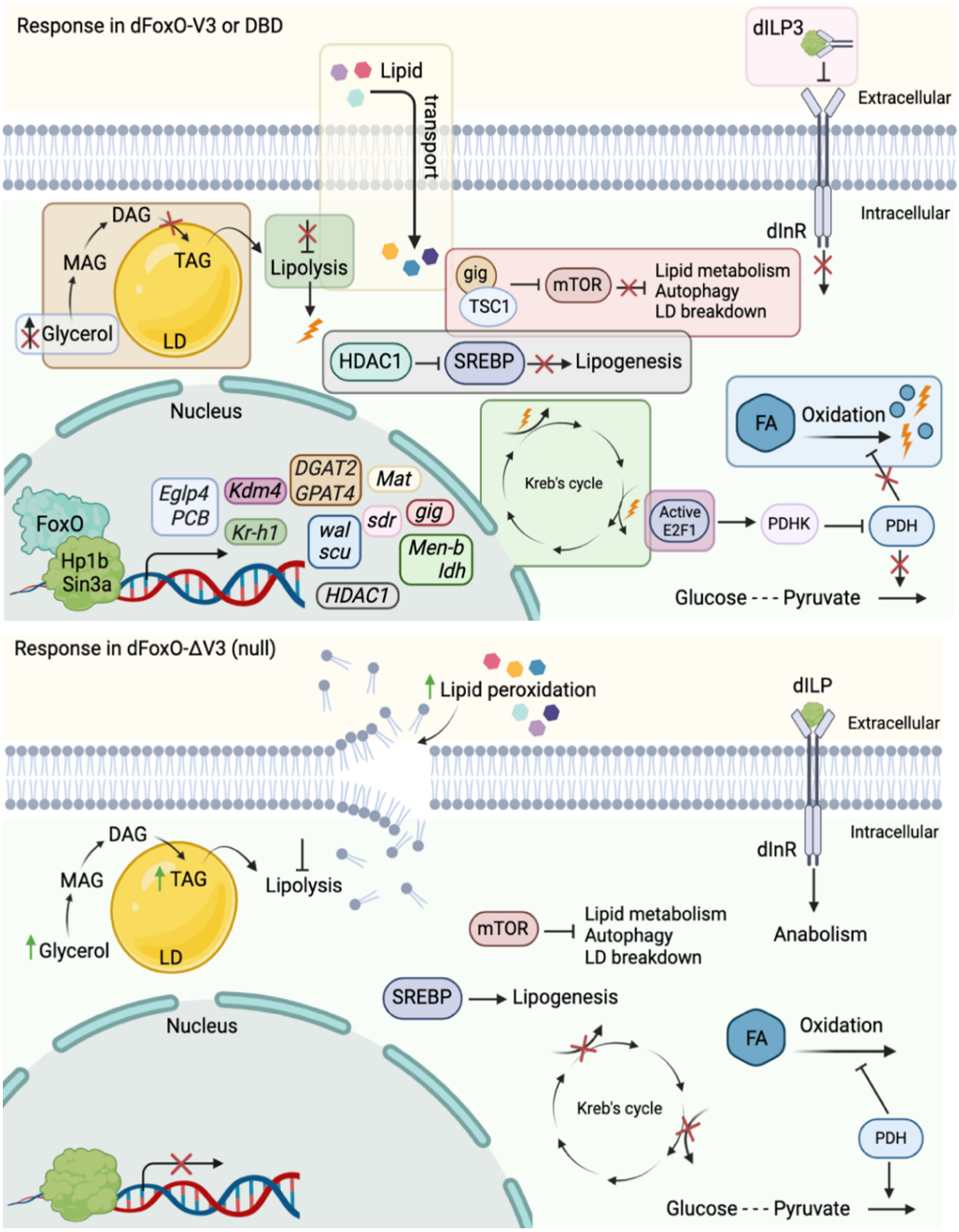

Figure 7.1. **Graphical representation of dFoxO's hypothesised DNA-binding independent modulation of metabolism.**
FoxO, alongside Hp1b or Sin3a, can modulate genes involved processes such as transport (*Eglp4/Mat*), fatty acid breakdown (*wal/scu)*, nutrient switch (*Kdm4)*, TAG synthesis and lipolysis (*DGAT2/GPAT4/PCB/HDAC1/Kr-h1)*, insulin and mTOR signalling (*sdr/gig),* and the Kreb's cycle (*Men-b/ldh)*. Lightning bolts represent energy. LD: lipid droplet; dInR: *Drosophila* insulin receptor; PDH/PDHK: pyruvate dehydrogenase kinase; PDH: pyruvate dehydrogenase; dILP: *Drosophila* insulin-like peptide; MAG: monoacylglycerol; DAG: diacylglycerol; TAG: triglyceride; FA: fatty acid; TSC1: tuberous sclerosis 1; HDAC1: histone deacetylase 1; mTOR: mammalian target of rapamycin; SREBP: sterol regulatory element binding protein. The genes represented here are not an exhaustive list of those involved (Created in Biorender).

One point of note is that it does not seem as if it is just one specific gene or process that is involved with the modulation of proper metabolic function in a dFoxO-dependent DNA-binding independent manner. Where it seems as if a collection of processes are modulated in this way, which when disrupted cause knock on effects in specific metabolic-related phenotypes (such as, growth and starvation survival).
It is also important to highlight that many of the genes identified as being dFoxO-dependent DNA-binding independent and Hp1b- or Sin3a-dependent have unknown or less well characterised functions. For example, *loco* which is downregulated under these circumstances in a DNA-binding independent manner is known to have GTPase-activating activity that extends lifespan, produces a stronger resistance to starvation stress, and lowers lipid content when downregulated (Lin *et al.* 2011). However, how these processes are modulated is not clearly established. Therefore, further work should also consider attempting to characterise these unknown or less well-known genes, to be able to give a clearer picture in the collection of processes that is affecting metabolism in a dFoxO-dependent DNA-binding independent and Hp1b- or Sin3a-dependent manner.

The hypothesis produced from this project for further consideration states that either or both Hp1b and Sin3a are FoxO co-factors, allowing FoxO to modulate metabolic processes (such as, starvation survival and TAG mobilisation) independently of its DNA-binding activity. Therefore, making Hp1b and/or Sin3a potential targets for future therapeutics in the treatment of metabolic disorder.
To answer this hypothesis, future work should focus on objectively assessing whether Sin3a and/or Hp1b are binding partners of dFoxO, as currently the only method of verification of the association between proteins was the use of previously published ChIP-seq and RNA-seq data. To do this, co-immunoprecipitation and FRET-FLIM of tagged Hp1b and Sin3a alongside dFoxO would be utilised to definitively visualise the potential interactions between these proteins. If successful, this would then be expanded upon to identify the exact regions through which these interactions occur using co-immunoprecipitation using full-length and partial protein constructs as seen in Kang *et al.* (2017). Furthermore, it would be imperitive to phenotypically test whether removing Hp1b or Sin3a alongside the dFoxO-DBD mutations would affect the metabolic DNA-binding independent phenotypes observed in this project. To do this however, starvation survival and TAG mobilisation would be assessed as whilst Hp1b is not developmentally essential Sin3a is, as *Sin3a* mutants are embryonic

lethal (Mills *et al.* 2018; Pennetta & Pauli, 1998). Due to this, growth would not be able to be assayed as it is a phenotype determined during development (Shingleton *et al.* 2005). This would aim to elucidate whether Hp1b and/or Sin3a are co-factors which aid FoxO in the modulation of metabolic phenotypes, identifying new potential mechanisms that could be targeted for future therapeutic treatments for metabolic disorder.

Secondary points of interest that could also be explored further are the distinct DBD mutant phenotypes and the modulation of the *dFoxO* gene itself. This would help to inform other future work that involves dFoxO in general or that specifically utilises these *dFoxO* mutants, allowing for more accurate analyses.

7.3 Conclusion

Overall, this project aimed to identify potential protein-protein interactions produced by dFoxO that influenced changes in gene expression, which subsequently leads to changes in the modulation of metabolic processes. Research showed that novel previously unpublished *dFoxO* mutants created via genomic engineering were appropriate for this investigation producing 'wild-type' and null dFoxO proteins as well as dFoxO-DBD mutants. These latter mutants were still able to undergo suitable post translational modification but lacked DNA-binding. This then allowed for the classification of phenotypes based on dFoxO transcriptional activity, where DNA-binding independent roles impacted by metabolic function were identified (namely, growth and starvation survival). The key metabolic process that could seemingly be influencing these phenotypes was identified as the initial stages of lipid mobilisation. Subsequently, RNA-seq and transcription factor binding analysis showed that there was a significant difference in the expression of a relatively large subset of genes. Many of which modulated processes involved in lipid metabolism and growth and could be potentially leading to the observed differences caused by dFoxO interactions with regulators such as Hp1b and Sin3a.

Future work should focus on producing concrete supporting evidence to suggest that dFoxO and Hp1b and/or Sin3a produce protein-protein interactions, and how those interactions are structurally mediated. Altogether this enables a greater in-depth understanding of FoxO activity in a previously acknowledged but not well-studied area, allowing for the identification of potential therapeutic targets for treating metabolic disorders linked to disordered FoxO activity, such as diabetes, without

disrupting the essential DNA-binding dependent processes FoxO must fulfil thereby preventing the onset of severe side effects, such as cancer.

References

References

Accili, D. & Arden, K. C. (2004) FoxOs at the crossroads of cellular metabolism, differentiation, and transformation. *Cell*. 117 (4), pp. 421-426.

Achari, A. E. & Jain, S. K. (2017) Adiponectin, a therapeutic target for obesity, diabetes, and endothelial dysfunction. *International Journal of Molecular Sciences.* 18 (6), pp. 1321.

Afgan, E., Baker, D., Batut, B., van den Beek, M., Bouvier, D., Čech, M., Chilton, J., Clements, D., Coraor, N., Grüning, B., Guerler, A., Hillman-Jackson, J., Jalili, V., Rasche, H., Soranzo, N., Goecks, J., Taylor, J., Nekrutenko, A. & Blankenberg, D. (2018) The Galaxy platform for accessible, reproducible and collaborative biomedical analyses: 2018 update. *Nucleic Acids Research.* 46 (W1), pp. W537–W544. doi:10.1093/nar/gky379

Afschar, S., Toivonen, J. M., Hoffmann, J. M., Tain, L. S., Wieser, D., Finlayson, A. J., Driege, Y., Alic, N., Emran, S., Stinn, J., Froehlich, J., Piper, M. D. & Partridge, L. (2016) Nuclear hormone receptor DHR96 mediates the resistance to xenobiotics but not the increased lifespan of insulin-mutant *Drosophila*. *Proceedings of the National Academy of Sciences of the United States of America*. 113 (5), pp. 1321-1326.

Agha, M. & Agha, R. (2017) The rising prevalence of obesity: part A: impact on public health. *International Journal of Surgery*: *Oncology*. 2 (7), pp. e17.

Akella, N. M., Ciraku, L. & Reginato, M. J. (2019) Fueling the fire: emerging role of the hexosamine biosynthetic pathway in cancer. *BMC Biology.* 17 (52). doi: 10.1186/s12915-019-0671-3.

Al-Anzi, B. & Zinn, K. (2010) Colorimetric measurement of triglycerides cannot provide an accurate measure of stored fat content in *Drosophila. PLoS One.* 5 (8), pp. e12354.

Al-Anzi, B., Armand, E., Nagamei, P., Olszewski, M., Sapin, V., Waters, C., Zinn, K., Wyman, R. J. & Benzer, S. (2010) The leucokinin pathway and its neurons regulate meal size in *Drosophila. Current Biology.* 20, pp. 969-978.

Alic, N., Andrews, T. D., Giannakou, M. E., Papatheodorou, I., Slack, C., Hoddinott, M. P., Cochemé, H. M., Schuster, E. F., Thornton, J. M. & Partridge, L. (2011) Genome-wide dFOXO targets and topology of the transcriptomic response to stress and insulin signalling. *Molecular Systems Biology.* 7, pp. 502. doi: 10.1038/msb.2011.36

Alic, N., Giannakou, M. E., Papatheodorou, I., Hoddinott, M. P., Andrews, T. D., Bolukbasi, E. & Partridge, L. (2014) Interplay of dFoxO and two ETS-family transcription factors determines lifespan in *Drosophila melanogaster. PLoS Genetics.* 10 (9), pp. e1004619.

Altomonte, J., Cong, L., Harbaran, S., Richter, A., Xu, J., Meseck, M. & Dong, H. H. (2004) Foxo1 mediates insulin action on apoC-III and triglyceride metabolism. *The Journal of Clinical Investigation*. 114 (10), pp. 1493-1503.

Álvarez-Rendón, J. P. Salceda, R. & Riesgo-Escovar, J. R. (2018) *Drosophila melanogaster* as a model for Diabetes Type 2 progression. *BioMed Research International.* doi: 10.1155/2018/1417528

Andersen, C. L., Jensen, J. L. & Ørntoft, T. F. (2004) Normalisation of real time quantitative reverse transcription PCR data: a model-based variance estimation approach to identify genes suited for normalisation, applied to bladder and colon cancer data sets. *Cancer Research.* 64 (15). doi: 10.1158/0008-5472.CAN-04-0496

Andrews, S. (2010) FastQC a quality control tool for high throughput sequence data [Online]. Available at: http://www.bioinformatics.babraham.ac.uk/projects/fastqc/ (Accessed: 15th October 2020).

Arriola, D. J., Mayo, S. L., Skarra, D. V., Benson, C. A. & Thackray, V. G. (2012) FoxO1 transcription factor inhibits luteinizing hormone β gene expression in pituitary gonadotrope cells. *Journal of Biological Chemistry.* 287 (40), pp. 33424-33435.

Atanesyan, L., Günther, V., Dichtl, B., Georgiev, O. & Schaffner, W. (2012) Polyglutamine tracts as modulators of transcriptional activation from yeast to mammals. *Biological Chemistry.* 393 (1-2). doi: 10.1515/BC-2011-252.

Audrito, V., Messana, V. G. & Deaglio, S. (2020) NAMPT and NAPRT: two metabolic enzymes with key roles in inflammation. *Frontiers in Oncology*. 10, pp. 358.

Baar, M. P., Brandt, R. M. C., Putavet, D. A., Klein, J. D. D., Derks, K. W. J., Bourgeois, B. R. M., Stryeck, S., Rijksen, Y., van Willigenburg, H., Feijtel, D. A., van der Pluijm, I., Essers, J., van Cappellen, W. A., van Ijcken, W. F. J., Houtsmuller, A. B., Pothof, J., de Bruin, R. W. F., Madl, T., Hoeijmakers, J. H. J., Campisi, J. & de Keizer, P. L. J. (2017) Targeted apoptosis of senescent cells restores tissue homeostasis in reponse to chemotoxicity and aging. *Cell.* 169 (1), pp. 132-147.

Bai, H., Kang, P. & Tatar, M. (2012) *Drosophila* insulin-like peptide-6 (dilp6) expression from fat body extends lifespan and represses secretion of *Drosophila* insulin-like peptide-2 from the brain. *Aging Cell.* 11 (6), pp. 978-985.

Bai, H., Kang, P., Hernandez, A. M. & Tatar, M. (2013) Activin signalling targeted by insulin/dFOXO regulates aging and muscle proteostasis in *Drosophila. PLoS Genetics.* 9 (11), pp. e1003941.

Bailey, C. J., Path, M. R. C. & Turner, R. (1996) Metformin. *The New England Journal of Medicine.* 334, pp. 574-579.

Baker, K. D. & Thummel, C. S. (2007) Diabetic larvae and obese flies—emerging studies of metabolism in *Drosophila. Cell Metabolism.* 6 (1), pp. 257-266.

Bakker, W. J., Harris, I. S., & Mak, T. W. (2007) FOXO3a is activated in response to hypoxic stress and inhibits HIF1-induced apoptosis via regulation of CITED2. *Molecular Cell*. 28 (6), pp. 941-953.

Banerjee, T. & Chakravarti, D. (2011) A peek into the complex realm of histone phosphorylation. *Molecular and Cellular Biology*. 31 (24), pp. 4858-4873.

Bannister, A. J. & Kouzarides, T. (2011) Regulation of chromatin by histone modifications. *Cell Research.* 21, pp. 381-395.

Bansal, A., Kwon, E. S., Conte, D., Liu, H., Gilchrist, M. J., MacNeil, L. T., & Tissenbaum, H. A. (2014) Transcriptional regulation of *Caenorhabditis elegans* FOXO/DAF-16 modulates lifespan. *Longevity & Healthspan*. 3 (1), pp. 1-15.

Bar-Peled, L. & Sabatini, D. M. (2014) Regulation of mTORC1 by amino acids. *Trends in Cell Biology*. 24 (7), pp. 400-406.

Bar-Peled, L., Chantranupong, L., Cherniack, A. D., Chen, W. W., Ottina, K. A., Grabiner, B. C., Spear, E. D., Carter, S. L., Meyerson, M. & Sabatini, D. M. (2013) A tumor suppressor complex with GAP activity for the Rag GTPases that signal amino acid sufficiency to mTORC1. *Science*. 340 (6136), pp. 1100-1106.

Barbieri, M., Bonafé, M., Franceschi, C. & Paolisso, G. (2003) Insulin/IGF-1-signalling pathways: an evolutionary conserved mechanism of longevity from yeast to humans. *American Journal of Physiology, Endocrinology, and Metabolism.* 285 (5), pp. e1064-e1071.

Barnes, V. L., Laity, K. A., Pilecki, M. & Pile, L. A. (2018) Systematic analysis of SIN3 histone modifying complex components during development. *Scientific Reports.* 8. doi: 10.1038/s41598-018-35093-0

Barthel, A., Schmoll, D. & Unterman, T. G. (2005) FoxO proteins in insulin action and metabolism. *Trends in Endocrinology and Metabolism.* 16 (4), pp. 183-189.

Bass, T. M., Grandison, R. C., Wong, R., Martinez, P., Partridge, L. & Piper, M. D. W. (2007) Optimization of dietary restriction protocols in *Drosophila*. *The Journals of Gerontology Series A: Biological Sciences and Medical Sciences.* 62 (10), pp. 1071-1081.

Baumbach, J., Xu, Y., Hehlert, P. & Kühnlein, R. P. (2014) Gαq, Gγ1 and Plc21C control *Drosophila* body fat storage. *Journal of Genetics and Genomics.* 41 (5), pp. 283-292.

Bednářová, A., Tomčala, A., Mochanová, M., Kodrík, D. & Krishnan, N. (2018) Disruption of adipokinetic hormone mediated energy homeostasis has subtle effects on physiology, behavior and lipid status during aging in *Drosophila. Frontiers in Physiology.* 9, pp. 949. doi: 10.3389/fphys.2018.00949.

Beller, M., Sztalryd, C., Southall, N., Bell, M., Jäckle, H., Auld, D.S. & Oliver, B. (2008) COPI Complex is a regulator of lipid homeostasis. *PLoS Biology*. 6 (11), pp. e292.

Benayoun, B. A., Caburet, S. & Veitia, R. A. (2011) Forkhead transcription factors: key players in health and disease. *Trends in Genetics.* 27 (6), pp. 224-232.

Berg, J. M., Tymoczko, J. L. & Stryer, L. (2002) *Biochemistry*. 5th edition. W. H. Freeman, New York.

Berry, F. B., Skarie, J. M., Mirzayans, F., Fortin, Y., Hudson, T. J., Raymond, V., Link, B. A. & Walter, M. A. (2008) FOXC1 is required for cell viability and resistance to oxidative stress in the eye through the transcriptional regulation of FOXO1A. *Human Molecular Genetics* 17 (4), pp. 490-505.

Bi, J., Xiang, Y., Chen, H., Liu, Z., Grönke, S., Kühnlein, R. P. & Huang, X. (2012) Opposite and redundant roles of the two *Drosophila* perilipins in lipid mobilisation. *Journal of Cell Science.* 125 (15), pp. 3568-3577.

Bielka, W. & Przezak, A. (2021) The role of FOXO transcription factors in the development of type 2 diabetes and related potential therapeutic possibilities. *Clinical Diabetology.* 10. doi: 10.5603/DK.a2021.0021

Birnbaum, A., Wu, X., Tatar, M., Liu, N. & Bai, H. (2019) Age-Dependent changes in transcription factor FOXO targeting in female *Drosophila. Frontiers in Genetics*. 10, pp. 312-324. doi: 10.3389/fgene.2019.00312.

Blice-Baum, A. C., Guida, M. C., Hartley, P. S., Adams, P. D., Bodmer, R. & Cammarato, A. (2019) As time flies by: investigating cardiac aging in the short-lived *Drosophila* model. *Biochimica et Biophysica Acta (BBA)-Molecular Basis of Disease*. 1865 (7), pp. 1831-1844.

Bonett, D.G. & Wright, T.A. (2000) Sample size requirements for estimating Pearson, Kendall and Spearman correlations. *Psychometrika*. 65, pp. 23–28.

Booth, L. N. & Brunet, A. (2016) The ageing epigenome. *Molecular Cell.* 62 (5), pp. 728-744.

Bouabe, H. & Okkenhaug, K. (2013) Gene targeting in mice: a review. *Methods in Molecular Biology*. 1064, pp. 315-336.

Brenkman, A. B., de Keizer, P. L. J., van den Broek, N. J. F., Jochemsen, A. G. & Burgering, B. M. (2008) Mdm2 induces mono-ubiquitination of FoxO4. *PLoS ONE.* 3 (7), e2819. doi: 10.1371/journal.pone.0002819

Brent, M. M., Anand, R. & Marmorstein, R. (2008a) Structural basis for DNA recognition by FoxO1 and its regulation by posttranslational modification. *Structure*. 16 (9), pp. 1407-1416.

Brent, M.M., Anand, R. & Marmorstein, R. (2008b) Crystal Structure of FoxO1 DBD Bound to DBE2 DNA. doi: 10.2210/pdb3CO7/pdb

Bridge, D., Theofiles, A. G., Holler, R. L., Marcinkevicius, E., Steele, R. E. & Martinez, D. E. (2010) FoxO and stress responses in the Cnidarian *Hydra vulgaris*. *PLoS One.* 5 (7), pp. e11686. doi: 10.1371/journal.pone.0011686

Broad Institute (n.d.) Picard. Broad Institute, GitHub repository. *GitHub*. http://broadinstitute.github.io/picard/.

Broughton, S. J., Piper, M. D. W., Ikeya, T., Bass, T. M., Jacobson, J., Driege, Y., Martinez, P., Hafen, E., Withers, D. J., Leevers, S. J. & Partridge, L. (2005) Longer lifespan, altered metabolism, and stress resistance in *Drosophila* from ablation of cells making insulin-like ligands. *Proceedings of the National Academy of Sciences of the United States of America.* 102 (8), pp. 3105-3110.

Brown, E. B., Slocumb, M. E., Szuperak, M., Kerbs, A., Gibbs, A. G., Kayser, M. S. & Keene, A. C. (2019) Starvation resistance is associated with developmentally specified changes in sleep, feeding and metabolic rate. *Journal of Experimental Biology.* 222 (3). doi: 10.1242/jeb.191049.

Burnett, C., Valentini, S., Cabreiro, F., Goss, M., Somogyvári, M., Piper, M. D., Hoddinott, M., Sutphon, G. L., Leko, V., McElwee, J. J., Vazquez-Manrique, R. P., Orfila, A., Ackerman, D., Au, C., Vinti, G., Riesen, M., Howard, K., Neri, C., Bedalov, A., Kaeberlein, M., Söti, C., Partridge, L. & Gems, D. (2011) Absence of effects of Sir2 overexpression on lifespan in *C. elegans* and *Drosophila. Nature.* 477, pp. 482-485.

Buse, M. G. (2006) Hexosamines, insulin resistance, and the complications of diabetes: current status. *American Journal of Physiology-Endocrinology and Metabolism.* 290 (1), pp. E1-E8.

Buszard, B. J., Johnson, T. K., Meng, T., Burke, R., Warr, C. G. & Tiganis, T. (2013) The nucleus- and endoplasmic reticulum-targeted forms of protein tyrosine phosphatase 61F regulate *Drosophila* growth, life span, and fecundity. *Molecular and Cellular Biology.* 33 (7), pp. 1345-1356.

Buteau, J., & Accili, D. (2007) Regulation of pancreatic β-cell function by the forkhead protein FoxO1. *Diabetes, Obesity and Metabolism*. 9, pp. 140-146.

Cai, W., Wei, Y., Jarnik, M., Reich, J. & Lilly, M. A. (2016) The GATOR2 component Wdr24 regulates TORC1 activity and lysosome function. *PLoS Genetics*. 12 (5), e1006036.

Calamita, G., Perret, J. & Delporte, C. (2018) Aquaglyceroporins: drug targets for metabolic diseases? *Frontiers in Physiology*. 9, 851.

Calissi, G., Lam, E. W. F. & Link, W. (2020) Therapeutic strategies targeting FoxO transcription factors. *Nature Reviews: Drug Discovery.* 20, pp. 21-38.

Calnan, D. R. & Brunet, A. (2008) The FoxO code. *Oncogene*. 27 (16), pp. 2276-2288.

Calnan, D. R., Webb, A. E., White, J. L., Stowe, T. R., Goswami, T., Shi, X., Espejo, A., Bedford, M. T., Gozani, O., Gygi, S. P. & Brunet, A. (2012) Methylation by Set9 modulates FoxO3 stability and transcriptional activity. *Aging (Albany, NY).* 4 (7), pp. 462-479.

Camus, M. F., Piper, M. D. & Reuter, M. (2019) Sex-specific transcriptomic responses to changes in the nutritional environment. *elife*. 8, e47262.

Cao, Y., Nakata, M., Okamoto, S., Takano, E., Yada, T., Minokoshi, Y., Hirata, Y., Nakajima, K., Iskandar, K., Hayashi, Y., Ogawa, W., Barsh, G. S., Hosoda, H., Kangawa, K., Itoh, H., Noda, T., Kasuga, M. & Nakae, J. (2011) PDK1-Foxo1 in agouti-related peptide neurons regulates energy homeostasis by modulating food intake and energy expenditure. *PLoS One.* 6 (4), pp. e18324.

Cárdenas, M. L., Cornish-Bowden, A. & Ureta, T. (1998) Evolution and regulatory role of the hexokinases. *Biochimica et Biophysica Acta.* 1401, pp. 242-264.

Carney, G. E. & Bender, M. (2000) The *Drosophila* ecdysone receptor (EcR) gene is required maternally for normal oogenesis. *Genetics.* 154 (3), pp. 1203-1211.

Castrillon, D. H., Gönczy, P., Rawson, A. R., Eberhart, C. G., Viswanathan, S., DiNardo, S. & Wasserman, S. A. (1993) Toward a molecular genetic analysis of spermatogenesis in *Drosophila melanogaster*: characterization of male-sterile mutants generated by single P element mutagenesis. *Genetics.* 135 (2), pp. 489-505.

Celotto, A. M., Liu, Z., VanDemark, A. P. & Palladino, M. J. (2012) A novel *Drosophila* SOD2 mutant demonstrates a role for mitochondrial ROS in neurodevelopment and disease. *Brain and Behavior*. 2 (4), pp. 424-434.

Chae, Y. C., Kim, J. Y., Park, J. W., Kim, K. B., Oh, H., Lee, K. H. & Seo, S. B. (2019) FoxO1 degradation via G9a-mediated methylation promotes cell proliferation in colon cancer. *Nucleic Acids Research.* 47 (4), pp. 1692-1705.

Chakrabarti, P. & Kandror, K. V. (2009) FoxO1 controls insulin-dependent adipose triglyceride lipase (ATGL) expression and lipolysis in adipocytes. *Journal of Biological Chemistry*. 282 (20), pp. 13289-13300.

Chandler, C. H., Chari, S. & Dworkin, I. (2013) Does your gene need a background check? How genetic background impacts the analysis of mutations, genes, and evolution. *Trends in Genetics*. 29 (6), pp. 358-366.

Chanut-Delalande, H., Hashimoto, Y., Pelissier-Monier, A., Spokony, R., Dib, A., Kondo, T., Bohère, J., Niimi, K., Latapie, Y., Inagaki, S., Dubois, L., Valenti, P., Polesello, C., Kobayashi, S., Moussian, B., White, K. P., Plaza, S., Kageyama, Y. & Payre, F. (2014) Pri peptides are mediators of ecdysone for the temporal control of development. *Nature Cell Biology.* 16 (11), pp. 1035-1044.

Chatterjee, S. & Perrimon, N. (2021) What fuels the fly: energy metabolism in *Drosophila* and its application to the study of obesity and diabetes. *Science Advances.* 7 (24), pp. eabg4336.

Chatterjee, S., Khunti, K. & Davies, M. J. (2017) Type 2 diabetes. *The Lancet.* 389 (10085), pp. 2239-2251.

Chen, C. Y., Chen, J., He, L. & Stiles, B. L. (2018) PTEN: tumor suppressor and metabolic regulator. *Frontiers in Endocrinology.* 9 (338). doi: 10.3389/fendo.2018.00338.

Chen, P., Visokay, S. & Abrams, J. M. (2020) *Drosophila* GFAT1 and GFAT2 enzymes encode obligate developmental functions. *Fly (Austin).* 14 (1-4), pp. 3-9.

Cheng, Z. & White, M. F. (2011) Targeting Forkhead BOX O1 from the concept to metabolic diseases: lessons from mouse models. *Antioxidants & Redox Signalling*. 14 (4), pp. 649-661.

Cheung, P. & Lau, P. (2005) Epigenetic regulation by histone methylation and histone variants. *Molecular Endocrinology.* 19 (3), pp. 563-573.

Cho, N., Shaw, J. E., Karuranga, S., Huang, Y. D., da Rocha Fernandes, J. D., Ohlrogge, A. W. & Malanda, B. (2018) IDF Diabetes Atlas: Global estimates of diabetes prevalence for 2017 and projections for 2045. *Diabetes Research and Clinical Practice*. 138, pp. 271-281.

Choi, H. E., Kim, Y., Lee, H. J. & Cheon, H. G. (2021) Novel FoxO1 inhibitor, JY-2, amerliorates palmitic acid-induced lipotoxicity and gluconeogenesis in a murine model. *European Journal of Pharmacology.* 899, pp. 174011.

Clark, R. I., Tan, S. W. S., Péan, C. B., Roostalu, U., Vivancos, V., Bronda, K., Pilátová, M., Fu, J., Walker, D. W., Berdeaux, R., Geissmann, F. & Dionne, M. S. (2013) MEF2 is an in vivo immune-metabolic switch. *Cell.* 155 (2), pp. 435-447.

Colombani, J., Bianchini, L., Layalle, S., Pondeville, E., Dauphin-Villemant, C., Antoniewski, C., Carré, C., Noselli, S. & Léopold, P. (2005) Antagonistic actions of ecdysone and insulins determine final size in *Drosophila*. *Science.* 310 (5748), pp. 667-670.

Cook, J. R., Matsumoto, M., Banks, A. S., Kitamura, T., Tsuchiya, K. & Accili, D. (2015) A mutant allele encoding DNA binding–deficient FoxO1 differentially regulates hepatic glucose and lipid metabolism. *Diabetes*. 64 (6), pp. 1951-1965.

Copeland, R. J., Bullen, J. W. & Hart, G. W. (2008) Cross-talk between GlcNAcylation and phosphorylation: roles in insulin resistance and glucose toxicity. *American Journal of Physiology-Endocrinology and Metabolism*. 295 (1), pp. E17-E28.

Czermin, B., Melfi, R., McCabe, D., Seitz, V., Imhof, A. & Pirrotta, V. (2002) *Drosophila* enhancer of Zeste/ESC complexes have a histone H3 methyltransferase activity that marks chromosomal Polycomb sites. *Cell.* 111 (2), pp. 185-196.

Das, T. K., Sangodkar, J., Negre, N., Narla, G. & Cagan, R. L. (2012) Sin3a acts through a multi-gene module to regulate invasion in *Drosophila* and human tumors. *Oncogene*. 32, pp. 3184-3197.

Davies, B. R., Greenwood, H., Dudley, P., Crafter, C., Yu, D. H., Zhang, J., Li, J., Gao, B., Ji, Q., Maynard, J., Ricketts, S., Cross, D., Cosulich, S., Chresta, C. C., Page, K., Yates, J., Lane, C., Watson, R., Luke, R., Ogilvie, D. & Pass, M. (2012) Preclinical pharmacology of AZD5363, an inhibitor of AKT: pharmacodynamics, antitumor activity, and correlation of monotherapy activity with genetic background. *Molecular Cancer and Therapeutics.* 11 (4). doi: 10.1158/1535-7163.MCT-11-0824-T.

de Mendoza, A., Jones, J. W. & Friedrich, M. (2016) Methuselah/Methuselah-like G protein-coupled receptors constitute an ancient metazoan gene family. *Scientific Reports.* 6, 21801. doi: 10.1038/srep21801.

Deng, X., Zhang, W., O'Sullivan, I., Williams, J. B., Dong, Q., Park, E. A., Raghow, R., Unterman, T. G. & Elam, M. B. (2012) FoxO1 Inhibits Sterol Regulatory Element-binding Protein-1c (SREBP-1c) gene expression via transcription factors Sp1 and SREBP-1c. *Journal of Biological Chemistry.* 287 (24), pp. 20132-20143.

DiMeglio, L. A., Evans-Molina, C. & Oram, R. A. (2018) Type 1 diabetes. *The Lancet.* 391 (10138), pp. 2449-2462.

Dobi, K. C., Halfon, M. S. & Baylies, M. K. (2014) Whole-genome analysis of muscle founder cells implicates the chromatin regulator Sin3A in muscle identity. *Cell Reports*. 8 (3), pp. 858-870.

Dobin, A., Davis, C. A., Schlesinger, F., Drenkow, J., Zaleski, C., Jha, S., Batut, P., Chaisson, M. & Gingeras, T. R. (2012) STAR: ultrafast universal RNA-seq aligner. *Bioinformatics*. 29 (1), pp. 15–21. doi: 10.1093/bioinformatics/bts635.

Dolatabadi, J. E. N. & Omidi, Y. (2016) Solid lipid-based nanocarriers as efficient targeted drug and gene delivery systems. *Trends in Analytical Chemistry*. 77, pp. 100-108. doi: 10.1016/j.trac.2015.12.016.

dos Santos, G., Schroeder, A. J., Goodman, J. L., Strelets, V. B., Crosby, M. A., Thurmond, J., Emmert, D. B., Gelbart, W. M. & the Flybase Consortium (2015) FlyBase: introduction of the *Drosophila melanogaster* Release 6 reference genome assembly and large-scale migration of genome annotations. *Nucleic Acids Research.* 43, D690-D697.

Dowell, P., Otto, T. C., Adi, S. & Lane, M. D. (2003) Convergence of peroxisome proliferator-activated receptor gamma and Foxo1 signaling pathways. *Journal of Biological Chemistry.* 278 (46), pp. 45485-45491.

Dubland, J. A. & Francis, G. A. (2015) Lysosomal acid lipase: at the crossroads of normal and atherogenic cholesterol metabolism. *Frontiers in Cell and Developmental Biology*. 3, pp. 3.

Eberharter, A. & Becker, P. B. (2002) Histone acetylation: a swtich between repressive and permissive chromatin. *EMBO Reports.* 3 (3), pp. 224-229.

Eijkelenboom, A. & Burgering, B. M. (2013) FOXOs: signalling integrators for homeostasis maintenance. *Nature Reviews Molecular Cell Biology*. 14 (2), pp. 83-97.

Eleftherianos, I., More, K., Spivack, S., Paulin, E., Khojandi, A. & Shukla, S. (2014) Nitric oxide levels regulate the immune response of *Drosophila melanogaster* reference laboratory strains to bacterial infections. *Infection and Immunity*. 82 (10), pp. 4169-4181.

Eriksen, K. K., Hauser, F., Schiøtt, M., Pedersen, K. M., Søndergaard, L. & Grimmelikhuijzen, C. J. P. (2000) Molecular cloning, genomic organisation, developmental regulation, and a knock-out mutant of a novel Leu-rich repeats-containing G protein-coupled receptor (DLGR-2) from *Drosophila melanogaster. Genome Research.* 10 (7), pp. 924-938.

Eskeland, R., Eberharter, A. & Imhof, A. (2007) HP1 binding to chromatin methylated at H3K9 is enhanced by auxiliary factors. *Molecular and Cellular Biology.* 27 (2), pp. 453-465.

Essafi, A., Fernández de Mattos, S., Hassen, Y. A. M., Soeiro, I., Mufti, G. J., Thomas, N. S. B., Medema, R. H. & Lam, E. W. F. (2005) Direct transcriptional regulation of Bim by FoxO3a mediates STI571-induced apoptosis in Bcr-Abl-expressing cells. *Oncogene.* 24, pp. 2317-2329.

Essers, M. A. G., Weijzen, S., de Vries-Smits. A. M. M., Saarloos, I., de Ruiter, N. D., Bos, J. L. & Burgering, B. M. T. (2004) FoxO transcription factor activation by oxidative stress mediated by the small GTPase Ral and JNK. *EMBO Journal.* 23 (24), pp. 4802-4812.

Etchegaray, J. P. & Mostoslavsky, R. (2016) Interplay between metabolism and epigenetics: a nuclear adaptation to environmental changes. *Molecular Cell*. 62 (5), pp. 695-711.

Evangelou, A., Ignatiou, A., Antoniou, C., Kalanidou, S., Chatzimatthaiou, S., Shianiou, G., Ellina, S., Athanasiou, R., Panagi, M., Apidianakis, Y. and Pitsouli, C. (2019) Unpredictable effects of the genetic background of transgenic lines in physiological quantitative traits. *G3: Genes, Genomes, Genetics.* 9 (11), pp. 3877-3890.

Evangelou, M., Rendon, A., Ouwehand, W. H., Wernisch, L. & Dudbridge, F. (2012) Comparison of methods for competitive tests of pathway analysis. *PLoS One*. 7 (7), e41018.

Ewels, P., Magnusson, M., Lundin, S. & Käller, M. (2016) MultiQC: summarize analysis results for multiple tools and samples in a single report. *Bioinformatics*. 32 (19), pp. 3047-3048.

Fan, J., Krautkramer, K. A., Feldman, J. L. & Denu, J. M. (2016) Metabolic regulation of histone post-translational modifications. *ACS Chemical Biology.* 10 (1), pp. 95-108.

Fan, W., Imamura, T., Sonoda, N., Sears, D. D., Patsouris, D., Kim, J. J. & Olefsky, J. M. (2009) FoxO1 transrepresses peroxisome proliferator-activator receptor γ transactivation, coordinating an insulin-induced feed-forward response in adipocytes. *Journal of Biological Chemistry.* 284 (18), pp. 12188-12197.

Fantin, M., Garelli, F., Napoli, B., Forgiarini, A., Gumeni, S., De Martin, S., Montopoli, M., Vantaggiato, C. & Orso, G. (2019) Flavonoids regulate lipid droplets biogenesis in *Drosophila melanogaster. Natural Product Communications.* 14 (5). doi: 10.1177/1934578X19852430.

Feehan, R. P. & Shantz, L. M. (2016) Negative regulation of the FOXO3a transcription factor by mTORC2 induces a pro-survival response following exposure to ultraviolet-B irradiation. *Cellular Signalling.* 28 (8), pp. 798-809.

Feng, J., Liu, T., Qin, B., Zhang, Y. & Liu, X. S. (2012) Identifying ChIP-seq enrichment using MACS. *Nature Protocols*. 7 (9), pp. 1728–1740. doi: 10.1038/nprot.2012.101

Fermo, E., Vercellati, C., Marcello, A. P., Zaninoni, A., Aytac, S., Cetin, M., Capolsini, I., Casale, M., Paci, S., Zanella, A., Barcellini, W. & Bianchi, P. (2019) Clinical and molecular spectrum of glucose-6-phosphate isomerase deficiency. Report of 12 new cases. *Frontiers in Physiology.* 10, pp. 476. doi: 10.3389/fphys.2019.00467.

Finn, P. & Dice, J. F. (2006) Proteolytic and lipolytic responses to starvation. *Nutrition*. 22 (7-8), pp. 830-844.

Fischle, W., Tseng, B. S., Dormann, H. L., Ueberheide, B. M., Garcia, B. A., Shabanowitz, J., Hunt, D. F., Funabiki, H. & Allis, C. D. (2005) Regulation of HP1-chromatin binding by histone H3 methylation and phosphorylation. *Nature.* 438, pp. 1116-1122.

Fonseca, S. G., Gromada, J. & Urano, F. (2011) Endoplasmic reticulum stress and pancreatic β-cell death. *Trends in Endocrinology & Metabolism*. 22 (7), pp. 266-274.

Font-Burgada, J., Rossell, D., Auer, H. & Azorín, F. (2008) *Drosophila* HP1c isoform interacts with the zinc-finger proteins WOC and Relative-of-WOC to regulate gene expression. *Genes & Development*. 22 (21), pp. 3007-3023.

Fontana, L., Partridge, L. & Longo, V. D. (2010) Extending healthy life span–from yeast to humans. *Science.* 328, pp. 321–326. doi:10.1126/science.1172539.

Freathy, R. M., Timpson, N. J., Lawlor, D. A., Pouta, A., Ben-Shlomo, Y., Ruokonen, A., Ebrahim, S., Shields, B., Zeggini, E., Weedon, M. N., Lindgren, C. M., Lango, H., Melzer, D., Ferrucci, L., Paolisso, G., Neville, M. J., Karpe, F., Palmer, C. N. A., Morris, A. D., Elliott, P., Jarvelin, M. R., Smith, G. D., McCarthy, M. I., Hattersley, A. T. & Frayling, T. M. (2008) Common variation in the *FTO* gene alters diabetes-related metabolic traits to the extent expected given its effect on BMI. *Diabetes.* 57 (5), pp. 1419-1426.

Frescas, D., Valenti, L. & Accili, D. (2005) Nuclear trapping of the forkhead transcription factor FoxO1 via Sirt-dependent deacetylation promotes expression of glucogenetic genes. *Journal of Biological Chemistry*. 280, pp. 20589–20595.

Friedman, J. R. & Kaestner, K. H. (2006) The Foxa family of transcription factors in development and metabolism. *Cellular and Molecular Life Sciences.* 63 (19-20), pp. 2317-2328.

Fu, W., Ma, Q., Chen, L., Li, P., Zhang, M., Ramamoorthy, S., Nawaz, Z., Shimojima, T., Wang, H., Yang, Y., Shen, Z., Zhang, Y., Zhang, X., Nicosia, S. V., Zhang, Y., Pledger, J. W., Chen, J. & Bai, W. (2009a) MDM2 acts downstram of p53 as an E3 ligase to promote FOXO ubiquitination and degradation. *Journal of Biological Chemistry.* 284 (21), pp. 13987-14000.

Fu, X., Fu, N., Guo, S., Yan, Z., Xu, Y., Hu, H., Menzel, C., Chen, W., Li, Y., Zeng, R. & Khaitovich, P. (2009b) Estimating accuracy of RNA-Seq and microarrays with proteomics. *BMC Genomics.* 10 (1), pp.1-9.

Fujii, S. & Amrein, H. (2002) Genes expressed in the *Drosophila* head reveal a role for fat cells in sex-specific physiology. *The EMBO Journal*. 21 (20), pp. 5353-5363.

Fukuoka, M., Daitoku, H., Hatta, M., Matsuzaki, H., Umemura, S. & Fukamizu, A. (2003) Negative regulation of forkhead transcription factor AFX (Foxo4) by CBP-induced acetylation. *International Journal of Molecular Medicine.* 12 (4), pp. 503-508.

Gajan, A., Barnes, V. L., Liu, M., Saha, N. & Pile, L. A. (2016) The histone demethylase dKDM5/LID interacts with the SIN3 histone deacetylase complex and shares functional similarities with SIN3. *Epigenetics & Chromatin*. 9 (4). doi: 10.1186/s13072-016-0053-9.

Gáliková, M., Diesner, M., Klepsatel, P., Hehlert, P., Xu, Y., Bickmeyer, I., Predel, R. & Kühnlein, R. P. (2015) Energy homeostasis control in *Drosophila* adipokinetic hormone mutants. *Genetics.* 201 (2), pp. 665-683.

Gao, T., McKenna, B., Li, C., Reichert, M., Nguyen, J., Singh, T., Yang, C., Pannikar, A., Doliba, N., Zhang, T., Stoffers, D.A., Edlund, H., Matschinsky, F., Stein, R. & Stanger, B. Z. (2014) Pdx1 maintains β cell identity and function by repressing an α cell program. *Cell Metabolism*. 19 (2), pp. 259-271.

Gao, X., Zhang, Y., Arrazola, P., Hino, O., Kobayashi, T., Yeung, R.S., Ru, B. & Pan, D. (2002) Tsc tumour suppressor proteins antagonize amino-acid–TOR signalling. *Nature Cell Biology*. 4 (9), pp. 699-704.

Garelli, A., Gontijo, A. M., Miguela, V., Caparros, E. & Dominguez, M. (2012) Imaginal discs secrete insulin-like peptide 8 to mediate plasticity of growth and maturation. *Science*. 336 (6081), pp. 579-582.

Garofalo, R. S. (2002) Genetic analysis of insulin signaling in *Drosophila. Trends in Endocrinology and Metabolism.* 13 (4), pp. 156-162.

Ge, S. X., Jung, D. & Yao, R. (2020) ShinyGO: a graphical gene-set enrichment tool for animals and plants. *Bioinformatics.* 36 (8), pp. 2628-2629.

Gemayel, R., Vinces, M. D., Legendre, M. & Verstrepen, K.J. (2010) Variable tandem repeats accelerate evolution of coding and regulatory sequences. *Annual Review of Genetics*. 44, pp. 445–477. doi:10.1146/annurev-genet-072610-155046.

Ghosh, H. S., Reizis, B. & Robbins, P. D. (2011) SIRT1 associates with eIF2-alpha and regulates the cellular stress response. *Scientific Reports.* 1, pp. 150. doi: 10.1038/srep00150.

Giannakou, M. E., Goss, M., Jacobson, J., Vinti, G., Leevers, S. J. & Partridge, L. (2007) Dynamics of the action of dFOXO on adult mortality in *Drosophila*. *Aging Cell.* 6, 429–438. doi:10.1111/j.1474-9726.2007.00290.x.

Gilette, C. M., Tennessen, J. M. & Reis, T. (2021) Balancing energy expenditure and storage with growth and biosynthesis during *Drosophila* development. *Developmental Biology*. 475, pp. 234-244.

Glauser, D. A., & Schlegel, W. (2007) The emerging role of FOXO transcription factors in pancreatic β cells. *Journal of Endocrinology*. 193 (2), pp. 195-207.

Goberdhan, D. C., Meredith, D., Boyd, C. A. & Wilson, C. (2005) PAT-related amino acid transporters regulate growth via a novel mechanism that does not require bulk transport of amino acids. *Development*. 132 (10), pp. 2365-2375.

Goddeeris, M. M., Cook-Wiens, E., Horton, W. J., Wolf, H., Stoltzfus, J. R., Borrusch, M. & Grotewiel, M. S. (2003) Delayed behavioural ageing and altered mortality in *Drosophila* β integrin mutants. *Aging Cell.* 2, pp. 257-264.

Goitre, L., Balzac, F., Degani, S., Degan, P., Marchi, S., Pinton, P., & Retta, S. F. (2010). KRIT1 regulates the homeostasis of intracellular reactive oxygen species. *PloS One*. 5 (7), e11786.

Goossens, T., Kang, Y. Y., Wuytens, G., Zimmermann, P., Callaerts-Végh, Z., Pollarolo, G., Islam, R., Hortsch, M. & Callaerts, P. (2011) The *Drosophila* L1CAM homolog Neuroglian signals through distinct pathways to control different aspects of mushroom body axon development. *Development.* 138 (8), pp. 1595-1605.

Gräff, J. & Tsai, L. H. (2013) Histone acetylation: molecular mnemonics on the chromatin. *Nature Reviews: Neuroscience.* 14, pp. 97-111.

Graham, P. & Pick, L. (2017) *Drosophila* as a model for diabetes and diseases of insulin resistance. *Current Topics in Developmental Biology.* 121 (1), pp. 397-419.

Grauvogel, C., Brinkmann, H. & Petersen, J. (2007) Evolution of the glucose-6-phosphate isomerase: the plasticity of primary metabolism in photosynthetic eurkaryotes. *Molecular Biology and Evolution.* 24 (8), pp. 1611-1621.

Greer, E. L. & Brunet, A. (2005) FOXO transcription factors at the interface between longevity and tumor suppression. *Oncogene*. 24 (50), pp. 7410-7425.

Greer, E. L. & Shi, Y. (2012) Histone methylation: a dynamic mark in health, disease and inheritance. *Nature Reviews Genetics.* 13 (5), pp. 343-357.

Greer, E. L., Dowlatshahi, D., Banko, M. R., Villen, J., Hoang, K., Blanchard, D., Gygi, S. P. & Brunet, A. (2007) An AMPK-FoxO pathway mediates longevity induced by a novel method of dietary restriction in *C. elegans. Current Biology.* 17 (19), pp. 1646-1656.

Grigoryan, G. & Keating, A. E. (2008) Structural specificity in coiled-coil interactions. *Current Opinion in Structural Biology*. 18 (4), pp. 477-483.

Grönke, S., Mildner, A., Fellert, S., Tennagels, N., Petry, S., Müller, G., Jäckle, H. & Kühnlein, R. P. (2005) Brummer lipase is an evolutionary conserved fat storage regulator in *Drosophila. Cell Metabolism.* 1 (5), pp. 323-330.

Grönke, S., Müller, G., Hirsch, J., Fellert, S., Andreou, A., Haase, T., Jäckle, H. & Kühnlein, R. P. (2007) Dual lipolytic control of body fat storage and mobilization in *Drosophila*. *PLoS Biology*. 5 (6), pp. e137.

Gross, D. N., Van den Heuvel, A. P. J. & Birnbaum, M. J. (2008) The role of FoxO in the regulation of metabolism. *Oncogene*. 27 (16), pp. 2320-2336.

Gu, X., Orozco, J. M., Saxton, R. A., Condon, K. J., Liu, G. Y., Krawczyk, P. A., Scaria, S. M., Harper, J. W., Gygi, S. P. & Sabatini, D. M. (2017) SAMTOR is an S-adenosylmethionine sensor for the mTORC1 pathway. *Science.* 358 (6364), pp. 813-818.

Guelman, S., Kozuka, K., Mao, Y., Pham, V., Solloway, M. J., Wang, J., Wu, J., Lill, J. R. & Zha, J. (2009) The double-histone-acetyltransferase complex ATAC is essential for mammalian development. *Molecular and Cellular Biology.* 29 (5), pp. 1176-1188.

Guelman, S., Suganuma, T., Florens, L., Swanson, S. K., Kiesecker, C. L., Kusch, T., Anderson, S., Yates, J. R., Washburn, M. P., Abmayr, S. M. & Workman, J. L. (2006) Host cell factor and an uncharacterized SANT domain protein are stable components of ATAC, a novel dAda2A/dGcn5-containing histone acetyltransferase complex in *Drosophila*. *Molecular and Cellular Biology.* 26 (3), pp. 871-882.

Guio, L., Barrón, M. G. & González, J. (2014) The transposable element *Bari-Jheh* mediates oxidative stress response in *Drosophila. Molecular Ecology.* 23 (8), pp. 2020-2030.

Gutierrez, E., Wiggins, D., Fielding, B. & Gould, A. P. (2007) Specialized hepatocyte-like cells regulate *Drosophila* lipid metabolism. *Nature*. 445 (7125), pp. 275-280.

Ha, T. S. & Smith, D. P. (2006) A pheromone receptor mediates 11-cis-vaccenyl acetate-induced responses in *Drosophila. Journal of Neuroscience.* 26 (34), pp. 8727-8733.

Haeusler, R. A., Hartil, K., Vaitheesvaran, B., Arrieta-Cruz, I., Knight, C. M., Cook, J. R., Kammoun, H. L., Febbraio, M. A., Gutierrez-Juarez, R., Kurland, I. J. & Accili, D. (2014) Integrated control of hepatic lipogenesis versus glucose production requires FoxO transcription factors. *Nature Communications.* 5 (5190). doi: 10.1038/ncomms6190.

Haeusler, R. A., Pratt-Hyatt, M., Welch, C. L., Klaassen, C. D. & Accili, D. (2012) Impaired generation of 12-hydroxylated bile acids links hepatic insulin signalling with dyslipidaemia. *Cell Metabolism.* 15 (1), pp. 65-74.

Hall, J. A., Tabata, M., Rodgers, J. T. & Puigserver, P. (2014) USP7 attenuates hepatic gluconeogenesis through modulation of FoxO1 gene promoter occupancy. *Molecular Endocrinology*. 28, pp. 912–924.

Halpern, M. E., Rhee, J., Goll, M. G., Akitake, C. M., Parsons, M., & Leach, S. D. (2008) Gal4/UAS transgenic tools and their application to zebrafish. *Zebrafish*. 5 (2), 97-110.

Han, Y., Gao, S., Muegge, K., Zhang, W. & Zhou, B. (2015) Advanced applications of RNA sequencing and challenges. *Bioinformatics and Biology Insights.* 9, BBI-S28991.

Hannenhalli, S. & Kaestner, K. H. (2009) The evolution of Fox genes and their role in development and disease. *Nature Reviews Genetics.* 10 (4), pp. 233-240.

Harada, H. & Grant, S. (2012) Targeting the regulatory machinery of BIM for cancer therapy. *Critical Reviews™ in Eukaryotic Gene Expression*. 22 (2).

Harbison, S. T., Chang, S., Kamdar, K. P., & Mackay, T. F. (2005) Quantitative genomics of starvation stress resistance in *Drosophila. Genome Biology*. 6 (4), pp. 1-15.

Hardie, D. G. (2012) Organismal carbohydrate and lipid homeostasis. *Cold Spring Harbor Perspectives in Biology.* 4 (5), pp. a006031. doi: 10.1101/cshperspect.a006031.

Hardy, C. M., Burke, M. K., Everett, L. J., Han, M. V., Lantz, K. M. & Gibbs, A. G. (2018) Genome-wide analysis of starvation-selected *Drosophila melanogaster* – a genetic model of obesity. *Molecular Biology and Evolution*. 35 (1), pp. 50-65.

Harshman, L. G. & Schmid, J. L. (1997) Evolution of starvation resistance in *Drosophila melanogaster*: aspects of metabolism and counter-impact selection. *Evolution*. 52 (6), pp. 1679-1685.

Hawley, S. A., Gadalla, A. E., Olsen, G. S. & Hardie, D. G. (2002) The antidiabetic drug metformin activates the AMP-activated protein kinase cascade via an adenine nucleotide-independent mechanism. *Diabetes.* 51 (8), pp. 2420-2425.

Henriques, B. J., Olsen, R. K., J., Gomes, C. M. & Bross, P. (2021) Electron transfer flavoprotein and its role in mitochondrial energy metabolism in health and disease. *Gene.* 776, 145407.

Herranz, H., Morata, G. & Milán, M. (2006) *calderón* encodes an organic cation transporter of the major facilitator superfamily required for cell growth and proliferation of *Drosophila* tissues. *Development.* 133, pp. 2617-2625.

Herrmann, C., Van de Sande, B., Potier, D. & Aerts, S. (2012) i-cisTarget: an integrative genomics method for the prediction of regulatory features and cis-regulatory modules. *Nucleic Acids Research*. doi: 10.1093/nar/gks543.

Hesp, K., Smant, G. & Kammenga, J. E. (2015) *Caenorhabditis elegans* DAF-16/FOXO transcription factor and its mammalian homologs associate with age-related disease. *Experimental Gerontology*. 72, pp. 1-7.

Hibshman, J. D., Doan, A. E., Moore, B. T., Kaplan, R. E. W., Hung, A., Webster, A. K., Bhatt, D. P., Chitrakar, R., Hirschey, M. D. & Baugh, L. R. (2017) daf-16/FoxO promotes gluconeogenesis and trehalose synthesis during starvation to support survival. *eLife*. 6, pp. e30057. doi: 10.7554/eLife.30057.

Hildebrandt, A., Bickmeyer, I., Kühnlein, R. P. (2011) Reliable *Drosophila* body fat quantification by a coupled colorimetric assay. *PLoS One*. 6 (9), pp. e32796.

Hill, R., Kalathur, R. K. R., Callejas, S., Calaço, L., Brandão, R., Serelde, B., Cebriá, A., Blanco-Aparicio, C., Pastor, J., Futschik, M., Dopazo, A. & Link, W. (2014) A novel phosphatidylinositol 3-kinase (PI3K) inhibitor directs a potent FOXO-dependent, p53-independent cell cycle arrest phenotype characterized by the differential induction of a subset of FOXO-regulated genes. *Breast Cancer Research.* 16 (482). doi: 10.1186/s13058-014-0482-y.

Hirota, K., Daitoku, H., Matsuzaki, H., Araya, N., Yamagata, K., Asada, S., Sugaya, T. & Fukamizu, A. (2003) Hepatocyte nuclear factor-4 is a novel downstream target of insulin via FKHR as a signal-regulated transcriptional inhibitor. *Journal of Biological Chemistry.* 278 (15), pp. 13056–13060.

Hirota, K., Sakamaki, J., Ishida, J., Shimamoto, Y., Nishihara, S., Kodama, N., Ohta, K., Yamamoto, M., Tanimoto, K. & Fukamizu, A. (2008) A combination of HNF-4 and

Foxo1 is required for reciprocal transcriptional regulation of glucokinase and glucose-6-phosphatase genes in response to fasting and feeding. *Journal of Biological Chemistry.* 283 (47), pp. 32432-32441.

Holland, C. H., Tanevski, J., Perales-Patón, J., Gleixner, J., Kumar, M. P., Mereu, E., Joughin, B. A., Stegle, O., Lauffenburger, D. A., Heyn, H., Szalai, B. & Saez-Rodriguez, J. (2020) Robustness and applicability of transcription factor and pathway analysis tools on single-cell RNA-seq data. *Genome Biology*. 21 (1), pp. 1-19.

Hong, S. H., Lee, K. S., Kwak, S. J., Kim, A. K., Bai, H., Jung, M. S., Kwon, O. Y., Song, W. J., Tatar, M. & Yu, K. (2012) Minibrain/Dyrk1a regulates food intake through the Sir2-FoxO-sNPF/NPY pathway in *Drosophila* and mammals. *PLoS Genetics*. 8 (9). doi: 10.1371/journal.pgen/1002857.

Hong, S. W., Jiang, Y., Kim, S., Li, C. J. & Lee, D. K. (2014) Target gene abundance contributes to the efficiency of siRNA-mediated gene silencing. *Nucleic Acid Therapeutics*. 24 (3), pp. 192-198.

Hoogeboom, D., Essers, M. A. G., Polderman, P. E., Voets, E., Smits, L. M. M. & Burgering, B. M. T. (2008) Interaction of FOXO with beta-catenin inhibits beta-catenin/T cell factor activity. *Journal of Biological Chemistry.* 283 (14), pp. 9224-9230.

Hospital, F. (2005) Selection in backcross programmes. *Philosophical Transactions of the Royal Society B: Biological Sciences.* 360 (1459), pp. 1503-1511.

Hossain, M. S., Liu, Y., Zhou, S., Li, K., Tian, L. & Li, S. (2013) 20-hydroxyecdysone-induced transcriptional activity of FoxO upregulates *brummer* and *acid lipase-1* and promotes lipolysis in *Bombyx* fat body. *Insect Biochemistry and Molecular Biology.* 43 (9), pp. 829-838.

Housley, M.P., Rodgers, J.T., Udeshi, N.D., Kelly, T.J., Shabanowitz, J., Hunt, D.F., Puigserver, P. & Hart, G.W. (2008) O-GlcNAc regulates FoxO activation in response to glucose. *Journal of Biological Chemistry*. 283 (24), pp. 16283-16292.

Hu, D. G., Hulin, J. A., Nair, P. C., Haines, A. Z., McKinnon, R. A., Mackenzie, P. I. & Meech, R. (2019) The UGTome: the expanding diversity of UDP glycosyltransferases and its impact on small molecule metabolism. *Pharmacology & Therapeutics.* 204, 107414.

Hu, Y., Sopko, R., Foos, M., Kelley, C., Flockhart, I., Ammeux, N., Wang, X., Perkins, L., Perrimon, N. & Mohr, S. E. (2013) FlyPrimerBank: an online database for *Drosophila melanogaster* gene expression analysis and knockdown evaluation of RNAi reagents. *G3 (Bethesda).* 3 (9), pp. 1607-1616.

Huang, H. & Tindall, D. J. (2007) Dynamic FoxO transcription factors. *Journal of Cell Science*. 120 (1), pp. 2479-2487.

Huang, H. & Tindall, D. J. (2011) Regulation of FOXO protein stability via ubiquitination and proteasome degradation. *Biochimica et Biophysica Acta (BBA) – Molecular Cell Research.* 1813 (11), pp. 1961-1964.

Huang, J., Tan, P. H., Tan, B. K. H. & Bay, B. H. (2004) GST-pi expression correlates with oxidative stress and apoptosis in breast cancer. *Oncology Reports.* 12 (4), pp. 921-925.

Huang, J., Zhou, W., Dong. W., Watson, A. M. & Hong, Y. (2009) Directed, efficient, and versatile modifications of the *Drosophila* genome by genomic engineering. *Proceedings of the National Academy of Sciences of the United States of America.* 106 (20), pp. 8284-8289.

Huang, X., Warren, J. T., Buchanan, J. A., Gilbert, L. I. & Scott, M. P. (2007) *Drosophila* Niemann-Pick Type C-2 genes control sterol homeostasis and steroid biosynthesis: a model of human neurodegenerative disease. *Development.* 134 (20), pp. 3733-3742.

Hull-Thompson, J., Muffat, J., Sanchez, D., Walker, D. W., Benzer, S., Ganfornina, M. D. & Jasper, H. (2009) Control of metabolic homeostasis by stress signaling is mediated by the lipocalin NLaz. *PLoS Genetics.* doi: 10.1371/journal.pgen.1000460.

Hulsen, T., de Vlieg, J. & Alkema, W. (2008) BioVenn - a web application for the comparison and visualization of biological lists using area-proportional Venn diagrams. *BMC Genomics.* 9 (1), pp. 488.

Hussain, S. S., Tran, T. M., Ware, T. B., Luse, M. A., Prevost, C. T., Ferguson, A. N., Kashatus, J. A., Hsu, K. L. & Kashatus, D. F. (2021) RalA and PLD1 promote lipid droplet growth in response to nutrient withdrawal. *Cell Reports*. 36 (4), pp.109451.

Hwangbo, D. S., Gersham, B., Tu, M. P., Palmer, M. & Tatar, M. (2004) *Drosophila* dFOXO controls lifespan and regulates insulin signalling in brain and fat body. *Nature*. 429 (6991), pp. 562-566.

Iida, K., Li, Y., McGrath, B. C., Frank, A. & Cavener, D. R. (2007) PERK eIF2 alpha kinase is required to regulate the viability of the exocrine pancreas in mice. *BMC Cell Biology.* 8 (38). doi: 10.1186/1471-2121-8-38.

Imrichová, H., Hulselmans, G., Kalender-Atak, Z., Potier, D. & Aerts, S. (2015) i-cisTarget 2015 update: generalized cis-regulatory enrichment analysis in human, mouse and fly. *Nucleic Acids Research*. doi: 10.1093/nar/gkv395.

Intergalactic Utilities Commission (n.d. a) Volcano Plot. Intergalactic Utilities Commission, GitHub Repository. *GitHub.* https://github.com/galaxyproject/tools-iuc/tree/master/tools/volcanoplot.

Intergalactic Utilities Commission (n.d. b) heatmap2. Intergalactic Utilities Commission, GitHub Repository. *GitHub.* https://github.com/galaxyproject/tools-iuc/tree/master/tools/heatmap2.

Iskandar, K., Cao, Y., Hayashi, Y., Nakata, M., Takano, E., Yada, T., Zhang, C., Ogawa, W., Oki, M., Chua, S., Itoh, H., Noda, T., Kasuga, M. & Nakae, J. (2010) PDK-1/FoxO1 pathway in POMC neurons regulates pomc expression and food intake. *American Journal of Physiology, Endocrinology and Metabolism.* 298 (4), pp. e787-e798.

Israelsen, W. J. & Vander Heiden, M. G. (2015) Pyruvate kinase: function, regulation and role in cancer. *Seminars in Cell & Developmental Biology*. 43, pp. 43-51.

Itskov, P. M., Moreira, J. M., Vinnik, E., Lopes, G., Safarik, S., Dickinson, M. H. & Ribeiro, C. (2014) Automated monitoring and quantitative analysis of feeding behaviour in *Drosophila*. *Nature Communications.* 5 (1), pp. 1-10.

Jambhekar, A., Dhall, A. & Shi, Y. (2019) Roles and regulation of histone methylation in animal development. *Nature Reviews Molecular Cell Biology.* 20 (10), pp. 625-641.

Janah, L., Kjeldsen, S., Galsgaard, K. D., Winther-Sørensen, M., Stojanovska, E., Pedersen, J., Knop, F. K., Holst, J. J. & Albrechtsen, N. J. W. (2019) Glucagon receptor signalling and glucagon resistance. *International Journal of Molecular Sciences*. 20 (13), pp. 3314. doi:10.3390/ijms20133314.

Jeon, S. M. (2016) Regulation and function of AMPK in physiology and diseases. *Experimental & Molecular Medicine.* 48, e245.

Jia, K., Chen, D. & Riddle, D. L. (2004) The TOR pathway interacts with the insulin signaling pathway to regulate *C. elegans* larval development, metabolism and life span. *Development.* 131 (16), pp. 3897-3906.

Jiang, C., Lamblin, A. F. J., Steller, H. & Thummel, C. S. (2000) A steroid-triggered transcriptional hierarchy controls salivary gland cell death during *Drosophila* metamorphosis. *Molecular Cell*. 5 (3), pp. 445-455.

Jin, C., Li, J., Green, C. D., Yu, X., Tang, X., Han, D., Xian, B., Wang, D., Huang, X., Cao, X., Yan, Z., Hou, L., Liu, J., Shukeir, N., Khaitovich, P., Chen, C. D., Zhang, H., Jenuwein, T. & Han, J. D. J. (2011) Histone demethylase UTX-1 regulates *C. elegans* life span by targeting the insulin/IGF-1 signaling pathway. *Cell Metabolism.* 14 (2), pp. 161-172.

Jünger, M. A., Rintelen, F., Stocker, H., Wasserman, J. D., Végh, M., Radimerski, T., Greenberg, M. E. & Hafen, E. (2003) The *Drosophila* forkhead transcription factor

FOXO mediates the reduction in cell number associated with reduced insulin signaling. *Journal of Biology*. 2 (3), pp. 1-17.

Kamei, Y., Mizukami, J., Miura, S., Suzuki, M., Takahashi, N., Kawada, T., Taniguchi, T. & Ezaki, O. (2003) A forkhead transcription factor FKHR upregulates lipoprotein lipase expression in skeletal muscle. *FEBS Letters*. 536 (1-3), pp. 232–236.

Kang, M.J. & Ryoo, H.D. (2009) Suppression of retinal degeneration in *Drosophila* by stimulation of ER-associated degradation. *Proceedings of the National Academy of Sciences of the United States of America*. 106 (40), pp. 17043--17048.

Kang, P., Chang, K., Liu, Y., Bouska, M., Birnbaum, A., Karashchuk, G., Thakore, R., Zheng, W., Post, S., Brent, C. S., Li, S., Tatar, M. & Bai, H. (2017) *Drosoophila* Kruppel homologue 1 represses lipolysis through interaction with dFOXO. *Scientific Reports*. 7 (1), pp. 1-15. doi:10.1038/s41598-017-16638-1.

Kanoski, S. E., Ong, Z. Y., Fortin, S. M., Schlessinger, E. S. & Grill, H. J. (2014) Liraglutide, leptin and their combined effects on feeding: additive intake reduction through common intracellular signalling mechanisms. *Diabetes, Obesity, and Metabolism*. 17 (3), pp. 285-293.

Kapahi, P., Zid, B. M., Harper, T., Koslover, D., Sapin, V. & Benzer, S. (2004) Regulation of lifespan in *Drosophila* by modulation of genes in the TOR signalling pathway. *Current Biology.* 14 (10), pp. 885-890.

Kawahito, S., Kitahata, H. & Oshita, S. (2009) Problems associated with glucose toxicity: role of hyperglycemia-induced oxidative stress. *World Journal of Gastroenterology*. 15 (33), pp. 4137.

Kemper, J. K., Choi, S. E. & Kim, D. H. (2013) Sirtuin 1 deacetylase: a key regulator of hepatic lipid metabolism. *Vitamins & Hormones*. 91, pp. 385-404.

Kerr, C., Ringo, J., Dowse, H. & Johnson, E. (1996) Icebox, a recessive X-linked mutation in *Drosophila* causing low sexual receptivity. *Journal of Neurogenetics.* 11 (3-4), pp. 213-229.

Kharchenko, P. V., Tolstorukov, M. Y. & Park, P. J. (2008) Design and analysis of ChIP-seq experiments for DNA-binding proteins. *Nature Biotechnology*. 26 (12), pp. 1351-1359.

Kim, A. J., Cha, G. H., Kim, K., Gilbert, L. I. & Lee, C. C. (1997) Purification and characterization of the prothoracicotropic hormone of *Drosophila melanogaster*. *Proceedings of the National Academy of Sciences of the United States of America*. 94 (4), pp. 1130-1135.

Kim, H. S., Mittenthal, J. E. & Caetano-Anollés, G. (2006) MANET: tracing evolution of protein architecture in metabolic networks. *BMC Bioinformatics.* 7 (351). doi: 10.1186/1471-2105-7-351.

Kim, H.S., Xiao, C., Wang, R.H., Lahusen, T., Xu, X., Vassilopoulos, A., Vazquez-Ortiz, G., Jeong, W.I., Park, O., Ki, S.H., Gao, B. & Deng, C. X. (2010) Hepatic-specific disruption of SIRT6 in mice results in fatty liver formation due to enhanced glycolysis and triglyceride synthesis. *Cell Metabolism*. 12 (3), pp. 224-236.

Kim, J. H., Hwang, J., Jung, J. H., Lee, H. J., Lee, D. Y. & Kim, S. H. (2019) Molecular networks of FOXP family: dual biologic functions, interplay with other molecules and clinical implications in cancer progression. *Molecular Cancer*. 18 (1), pp. 1-19.

Kim, J. J., Buzzio, O. L., Li, S. & Lu, Z. (2005) Role of FoxO1a in the regulation of insulin-like growth factor-binding protein-1 in human endometrial cells: interaction with progesterone receptor. *Biology of Reproduction.* 73 (4), pp. 833-839.

Kim, Y. H., Nakayama, T. & Nayak, J. (2018) Glycolysis and the hexosamine biosynthetic pathway as novel targets for upper and lower airway inflammation. *Allergy, Asthma & Immunology Research*. 10 (1), pp. 6-11.

Kitada, M., Ogura, Y., Monno, I. & Koya, D. (2019) The impact of dietary protein intake on longevity and metabolic health. *EBioMedicine.* 43, pp. 632-640.

Kitamura, T. & Kitamura, Y. I. (2007) Role of FoxO proteins in pancreatic β cells. *Endocrine Journal*. 54 (4), pp. 507. doi: 10.1507/endocrj.KR-109.

Kitamura, T., Kitamura, Y.I., Funahashi, Y., Shawber, C.J., Castrillon, D.H., Kollipara, R., DePinho, R.A., Kitajewski, J. & Accili, D. (2007) A Foxo/Notch pathway controls myogenic differentiation and fiber type specification. *The Journal of Clinical Investigation.* 117 (9), pp. 2477-2485.

Kitamura, T., Nakae, J., Kitamura, Y., Kido, Y., Biggs, W. H., Wright, C. V. E., White, M. F., Arden, K. C. & Accili, D. (2002) The forkhead transcription factor FoxO1 links insulin signalling PDX1 regulation of pancreatic β cell growth. *The Journal of Clinical Investigation*. 110 (12), pp. 1839-1847.

Klepsatel, P., Gáliková, M., Xu, Y. & Kühnlein, R. P. (2016) Thermal stress depletes energy reserves in *Drosophila. Scientific Reports.* 6, 33667.

Klotz, L. O. & Steinbrenner, H. (2017) Cellular adaptation to xenobiotics: interplay between xenosensors, reactive oxygen species, and FOXO transcription factors. *Redox Biology*. 13, pp. 646-654.

Klotz, L. O., Sánchez-Ramos, C., Prieto-Arroyo, I., Urbánek, P., Steinbrenner, H. & Monsalve, M. (2015) Redox regulation of FoxO transcription factors. *Redox Biology*. 6, pp. 51-72.

Kobayashi, M., Fukii, N., Narita, T. & Higami, Y. (2018) SREBP-1c-dependent metabolic remodelling of white adipose tissue by caloric restriction. *International Journal of Molecular Sciences.* 19 (11), pp. 3335.

Kobayashi, Y., Furukawa-Hibi, Y., Chen, C., Horio, Y., Isobe, K., Ikeda, K. & Motoyama, N. (2005) SIRT1 is critical regulator of FOXO-mediated transcription in response to oxidative stress. *International Journal of Molecular Medicine.* 16, pp. 237-243.

Kodani, N. & Nakae, J. (2020) Tissue-specific metabolic regulation of FOXO-binding protein: FOXO does not act alone. *Cells.* 9. doi: :10.3390/cells9030702.

Köhsler, M., Leitsch, D., Müller, N. & Walochnik, J. (2020) Validation of reference genes for the normalization of RT-qPCR gene expression in *Acanthamoeba spp*. *Scientific Reports*. 10 (1), pp. 1-12.

Kops, G. J., Dansen, T. B., Polderman, P. E., Saarloos, I., Wirtz, K. W., Coffer, P. J., Huang, T. T., Bos, J. L., Medema, R. H. & Burgering, B. M. (2002) Forkhead transcription factor FoxO3a protects quiescent cells from oxidative stress. *Nature.* 419 (6904), pp. 316-321.

Kousteni, S. (2012) FoxO1, the transcriptional chief of staff of energy metabolism. *Bone*. 50 (2), pp. 437-443.

Kouzarides, T. (2007) Chromatin modifications and their function. *Cell.* 128 (4), pp. 693-705.

Koyama, T., Texada, M. J., Halberg, K. A. & Rewitz, K. (2020) Metabolism and growth adaptation to environmental conditions in *Drosophila. Cellular and Molecular Life Sciences.* 77, pp. 4523-4551.

Kramer, J. M., Davidge, J. T., Lockyer, J. M. & Staveley, B. E. (2003) Expression of *Drosophila* FoxO regulates growth and can phenocopy starvation. *BMC Developmental Biology*. 3 (5), pp. 1-14. doi: 10.1186/1471-213X-3-5.

Kramer, J. M., Slade, J. D. & Staveley, B. E. (2008) FoxO is required for resistance to amino acid starvation. *Genome.* 51, pp. 668-672. doi:10.1139/G08-047.

Kréneisz, O., Chen, X., Fridell, Y. W. C. & Mulkey, D. K. (2010) Glucose increases activity and Ca^{2+} in adult *Drosophila* insulin producing cells. *Neuroreport*. 21 (17), pp. 1116.

Kučerová, L., Kubrak, O. I., Bengtsson, J. M., Strnad, H., Nylin, S., Theopold, U. & Nässel, D. R. (2016) Slowed aging during reproductive dormancy is reflected in genome-wide transcriptome changes in *Drosophila melanogaster. BMC Genomics*. 17 (1), pp. 1-25.

Kühnlein, R. P. (2012) Lipid droplet-based storage fat metabolism in *Drosophila. Journal of Lipid Research*. 53 (8), pp. 1430-1436.

Kukurba, K. R. & Montgomery, S. B. (2015) RNA sequencing and analysis. *Cold Spring Harbour Protocols.* 11, pp. 951-969.

Kwon, M. J., Han, M. H., Bagley, J. A., Hyeon, D. Y., Ko, B. S., Lee, Y. M., Cha, I. J., Kim, S. Y., Kim, D. Y., Kim, H. M., Hwang, D., Lee, S. B. & Jan, Y. N. (2018) Coiled-coil structure-dependent interactions between polyQ proteins and FoxO lead to dendrite pathology and behavioural defects. *Proceedings of the National Academy of Sciences of the United States of America.* 115 (45), pp. e10748-e10757.

Kwon, S., Park, S., Lee, B. & Yoon, S. (2013) In-depth analysis of interrelation between quality scores and real errors in Illumina reads. *Annual International Conference of the IEEE Engineering in Medicine and Biology Society.* pp. 635-638. doi: 10.1109/EMBC.2013.6609580.

Lammers, M., Kraaijeveld, K., Mariën, J. & Ellers, J. (2019) Gene expression changes associated with the evolutionary loss of a metabolic trait: lack of lipogenesis in parasitoids. *BMC Genomics.* 20, pp. 309.

Lamming, D. W & Sabatini, D. M. (2013) A central role for mTOR in lipid homoestasis. *Cell Metabolism.* 18 (4), pp. 465-469.

Lamming, D. W., Ye, L., Katajisto, P., Goncalves, M. D., Saitoh, M., Stevens, D. M., Davis, J. G., Salmon, A. B., Richardson, A., Ahima, R. S., Guertin, D. A., Sabatini, D. M. & Baur, J. A. (2012) Rapamycin-induced insulin resistance is mediated by mTORC2 loss and uncoupled from longevity. *Science.* 335 (6076), pp. 1638-1643.

Landt, S. G., Marinov, G. K., Kundaje, A., Kheradpour, P., Pauli, F., Batzoglou, S., Bernstein, B. E., Bickel, P., Brown, J. B., Cayting, P., Chen, Y., DeSalvo, G., Epstein, C., Fisher-Aylor, K. I., Euskirchen, G., Gerstein, M., Gertz, J., Hartemink, A. J., Hoffman, M. M., Iyer, V. R., Jung, Y. L., Karmakar, S., Kellis, M., Kharchenko, P. V., Li, Q., Liu, T., Liu, X. S., Ma, L., Milosavljevic, A., Myers, R. M., Park, P. J., Pazin, M. J., Perry, M. D., Raha, D., Reddy, T. E., Rozowsky, J., Shoresh, N., Sidow, A., Slattery, M., Stamatoyannopoulos, J. A., Tolstorukov, M. Y., White, K. P., Xi, S., Farnham, P. J., Lieb, J. D., Wold, B. J. & Snyder, M. (2012) ChIP-seq guidelines and practices of the ENCODE and modENCODE consortia. *Genome Research*. 22 (9), pp. 1813-183.

Langerak, S., Kim, M. J., Lamberg, H., Godinez, M., Main, M., Winslow, L., O'Connor, M. B. & Zhu, C. C. (2018) The *Drosophila* TGF-beta/activin-like ligands Dawdle and Myoglianin appear to modulate adult lifespan through regulation of 26S proteasome function in adult muscle. *Biology Open.* 7 (4), pp. bio029454.

Langlet, F., Haeusler, R. A., Lindén, D., Ericson, E., Norris, T., Johansson, A., Cook, J. R., Aizawa, K., Wang, L., Buettner, C. & Accili, D. (2017) Selective inhibition of FoxO1 activator/repressor balance modulates hepatic glucose handling. *Cell.* 171 (4), pp. 824-835.

Lappin, T. R. J., Grier, D. G., Thompson, A. & Halliday, H. L. (2006) *HOX* genes: seductive science, mysterious mechanisms. *Ulster Medical Journal.* 75 (1), pp. 23-31.

Larkin, A., Marygold, S. J., Antonazzo, G., Attrill, H., dos Santos, G., Garapati, P. V., Goodman, J. L., Gramates, L. S., Millburn, G., Strelets, V. B., Tabone, C. J., Thurmond, J. & the FlyBase Consortium (2021) FlyBase: updates to the *Drosophila melanogaster* knowledge base. *Nucleic Acids Research*. 49 (D1), D899–D907.

Lee, D. H., Ryu, H. W., Kim, G. W. & Kwon, S. H. (2019) Comparison of three heterochromatin protein 1 homologs in *Drosophila. Journal of Cell Science.* 132 (3). doi:10.1242/jcs.222729.

Lee, S. & Dong, H. H. (2017) FoxO integration of insulin signalling with glucose and lipid metabolism. *Journal of Endocrinology*. 233 (2), pp. R67-R79.

Leips, J. & Mackay, T. F. (2000) Quantitative trait loci for life span in *Drosophila melanogaster*: interactions with genetic background and larval density. *Genetics*. 155 (4), pp. 1773-1788.

Li, C., Zhang, Y., Yun, X., Wang, Y., Sang, M., Liu, X., Hu, X. and Li, B. (2014) Methuselah-like genes affect development, stress resistance, lifespan and reproduction in *Tribolium castaneum*. *Insect Molecular Biology*. 23 (5), pp. 587-597.

Li, H. H., Willis, M. S., Lockyer, P., Miller, N., McDonough, H., Glass, D. J. & Patterson, C. (2007) Atrogin-1 inhibits Akt-dependent cardiac hypertrophy in mice via ubiquitin-dependent coactivation of Forkhead proteins. *The Journal of Clinical Investigation.* 117 (11), pp. 3211-3223.

Li, H. & Durbin, R. (2010) Fast and accurate long-read alignment with Burrows–Wheeler transform. *Bioinformatics*. 26 (5), pp. 589–595. doi: 10.1093/bioinformatics/btp698.

Li, H., Handsaker, B., Wysoker, A., Fennell, T., Ruan, J., Homer, N., Marth, G., Abecasis, G. & Durbin, R. (2009) The Sequence Alignment/Map format and

SAMtools. *Bioinformatics*. 25 (16), pp. 2078–2079. doi: 10.1093/bioinformatics/btp352.

Li, J., Dai, S., Chen, X., Liang, X., Qu, L., Jiang, L., Guo, M., Zhou, Z., Wei, H., Zhang, H., Chen, Z., Chen, L. & Chen, Y. (2021) Mechanism of forkhead transcription factors binding to a novel palindromic DNA site. *Nucleic Acids Research.* doi: 10.1093/nar/gkab086.

Li, L., Edgar, B. A. & Grewal, S. S. (2010) Nutritional control of gene expression in *Drosophila* larvae via TOR, Myc and a novel cis-regulatory element. *BMC Cell Biology*. 11 (1), pp. 1-13.

Li, X., Rommelaere, S., Kondo, S. & Lemaitre, B. (2020) Renal purge of hemolymphatic lipids prevents the accumulation of ROS-induced inflammatory oxidized lipids and protects *Drosophila* from tissue damage. *Immunity.* 52 (2), pp. 374-387.

Li, Y., Ma, Z., Jiang, S., Hu, W., Li, T., Di, S., Wang, D. & Yang, Y. (2017) A global perspective on FOXO1 in lipid metabolism and lipid-related diseases. *Progress in Lipid Research*. 66, pp. 42-49.

Liao, Y., Smyth, G. K. & Shi, W. (2014) featureCounts: an efficient general purpose program for assigning sequence reads to genomic features. *Bioinformatics.* 30 (7), pp. 923-30. doi: 10.1093/bioinformatics/btt656.

Lin, Y. R., Kim, K., Yang, Y., Ivessa, A., Sadoshima, J. & Park, Y. (2011) Regulation of longevity by regulator of G-protein signaling protein, *Loco. Aging Cell*. 10 (3), pp. 438-447.

Ling, L., Kokoza, V. A., Zhang, C., Aksoy, E. & Raikhel, A. S. (2017) MicroRNA-277 targets *insulin-like peptides 7* and *8* to control lipid metabolism and reproduction in *Aedes aegypti* mosquitoes. *Proceedings of the National Academy of Sciences of the United States of America.* 114 (38), pp. e8017-8024.

Link, W. (2019) *FoxO transcription factors.* Humana Press, New Jersey.

Liu, L., Zheng, L. D., Zou, P., Brooke, J., Smith, C., Long, Y. C., Almeida, F. A., Liu, D. & Cheng, Z. (2016) FoxO1 antagonist suppresses autophagy and lipid droplet growth in adipocytes. *Cell Cycle.* 15 (15), pp. 2033-2041.

Liu, M. & Pile, L. A. (2017) The transcriptional corepressor Sin3 directly regulates genes involved with methionine catabolism and affects histone methylation, linking epigenetics and metabolism. *Journal of Biological Chemistry.* 292 (5), pp. 1970-1976.

Liu, S., Wang, Z., Zhu, R., Wang, F., Cheng, Y. & Liu, Y. (2021) Three Differential Expression Analysis Methods for RNA Sequencing: limma, EdgeR, DESeq2. *Journal of Visualized Experiments: JoVE*. (175).

Liu, Q. & Jin, L. H. (2017) Organ-to-organ communication: a *Drosophila* gastrointestinal tract perspective. *Frontiers in Cell and Developmental Biology*. 5, pp. 29.

Liu, X., Greer, C. & Secombe, J. (2014) KDM5 interacts with Foxo to modulate cellular levels of oxidative stress. *PLoS Genetics*. 10 (10), pp. e1004676.

Long, Y. C. & Zierath, J. R. (2006) AMP-activated protein kinase signaling in metabolic regulation. *The Journal of Clinical Investigation*. 116 (7), pp. 1776-1783.

Love, M. I., Huber, W. & Anders, S. (2014) Moderated estimation of fold change and dispersion for RNA-seq data with DESeq2. *Genome Biology.* 15 (550). doi: 10.1186/s13059-014-0550-8.

Lu, H. & Huang, H. (2011) FOXO1: a potential target for human diseases. *Current Drug Targets*. 12 (9), pp. 1235-1244.

Ma, W., Fuentes, G., Shi, X., Verma, C., Radda, G. K. & Han, W. (2015) FoxO1 negatively regulates leptin-induced POMC transcription through its direct interaction with STAT3. *Biochemical Journal.* 466 (1), pp. 291-298.

Ma, X., Li, W., Yu, H., Yang, Y., Li, M., Xue, L. & Xu, T. (2014) Bendless modulates JNK-mediated cell death and migration in *Drosophila*. *Cell Death & Differentiation*. 21 (3), pp. 407-415.

Machanick, P. & Bailey, T. L. (2011) MEME-ChIP: motif analysis of large DNA datasets. *Bioinformatics*. 27 (12), pp. 1696–1697. doi: 10.1093/bioinformatics/btr189.

Mackay, T. F. (2002) The nature of quantitative genetic variation for *Drosophila* longevity. *Mechanisms of Ageing and Development*. 123 (2-3), pp. 95-104.

Mackay, T. F. (2010) Mutations and quantitative genetic variation: lessons from *Drosophila. Philosophical Transactions of the Royal Society B: Biological Sciences*. 365(1544), pp. 1229-1239.

Mackay, T. F., Richards, S., Stone, E. A., Barbadilla, A., Ayroles, J. F., Zhu, D., Casillas, S., Han, Y., Magwire, M. M., Cridland, J. M., Richardson, M. F., Anholt, R. R. H., Barrón, M., Bess, C., Blankenburg, K. P., Carbone, M. A., Castellano, D., Chaboub, L., Duncan, L., Harris, Z., Javaid, M., Jayaseelan, J. C., Jhangiani, S. N., Jordan, K. W., Lara, F., Lawrence, F., Lee, S. L., Librado, P., Linheiro, R. S., Lyman, R. F., Mackey, A. J., Munidasa, M., Muzny, D. M., Nazareth, L., Newsham, I., Perales, L., Pu, L., Qu, C., Ràmia, M., Reid, J. G., Rollmann, S. M., Rozas, J., Saada, N.,

Turlapati, L., Worley, K. C., Wu, Y., Yamamoto, A., Zhu, Y., Bergman, C. M., Thornton, K. R., Mittelman, D. & Gibbs, R. A. (2012) The *Drosophila melanogaster* genetic reference panel. *Nature*. 482 (7384), pp. 173-178.

Maiese, K. (2015) New insights for oxidative stress and diabetes mellitus*. Oxidative Medicine and Cellular Longevity.* doi: 10.1155/2015/875961.

Mardilovich, K., Pankratz, S. L. & Shaw, L. M. (2009) Expression and function of the insulin receptor substrate proteins in cancer. *Cell Communication and Signaling.* 7 (14). doi: 10.1186/1478-811X-7-14.

Marseglia, L., Manti, S., D'Angelo, G., Nicotera, A., Parisi, E., Di Rosa, G., Gitto, E. & Arrigo, T. (2015) Oxidative stress in obesity: a critical component in human disease. *International Journal of Molecular Sciences*. 16 (1), pp. 378-400.

Marshall, S., Bacote, V. & Traxinger, R. R. (1991) Discovery of a metabolic pathway mediating glucose-induced desensitization of the glucose transport. system. Role of hexosamine biosynthesis in the induction of insulin resistance. *Journal of Biological Chemistry*. 266 (88), pp. 4706–4712.

Martin, M. (2011) Cutadapt removes adapter sequences from high-throughput sequencing reads. *EMBnet.Journal*. 17 (1), pp. 10. doi: 10.14806/ej.17.1.200.

Martins, R., Lithgow, G. J. & Link, W. (2016) Long live FOXO: unravelling the role of FOXO proteins in aging and longevity. *Aging Cell.* 15 (2), pp. 196-207.

Matschinsky, F. M. & Wilson, D. F. (2019) The central role of glucokinase in glucose homeostasis: a perspective 50 years after demonstrating the presence of the enzyme in islets of Langerhans. *Frontiers in Physiology.* 10, pp. 148. doi: 10.3389/fphys.2019.00148.

Matsushita, R. & Nishimura, T. (2020) Trehalose metabolism confers developmental robustness and stability in *Drosophila* by regulating glucose homeostasis. *Communications Biology*. 3 (170). doi: 10.1038/s42003-020-0889-1.

Matsuzaki, H., Daitoku, H., Hatta, M., Aoyama, H., Yoshimochi, K. & Fukamizu, A. (2005) Acetylation of Foxo1 alters its DNA-binding ability and sensitivity to phosphorylation. *Proceedings of the National Academy of Sciences of the United States of America.* 102, pp. 11278–11283.

Mattila, J. & Hietakangas, V. (2017) Regulation of carbohydrate energy metabolism in *Drosophila melanogaster. Genetics*. 207 (4), pp. 1231-1253.

Mattila, J., Bremer, A., Ahonen, L., Kostiainen, R. & Puig, O. (2009) *Drosophila* FoxO regulates organism size and stress resistance through an adenylate cyclase. *Molecular and Cellular Biology*. 29 (19), pp. 5357-5365.

Mattila, J., Havula, E., Suominen, E., Teesalu, M., Surakka, I., Hynynen, R., Kilpinen, H., Väänänen, J., Hovatta, I., Käkelä, R., Ripatti, S., Sandmann, T. & Hietakangas, V. (2015) Mondo-Mlx mediates organismal sugar sensing through the Gli-similar transcription factor Sugarbabe. *Cell Reports.* 13 (2), pp. 350-364.

McClain, D. A., Lubas, W. A., Cooksey, R. C., Hazel, M., Parker, G. J., Love, D. C. & Hanover, J. A. (2002) Altered glycan-dependent signaling induces insulin resistance and hyperleptinemia. *Proceedings of the National Academy of Sciences of the United States of America.* 99 (16), pp. 10695-10699.

McDonel, P., Demmers, J., Tan, D. W. M., Watt, F. & Hendrich, B. D. (2012) Sin3a is essential for the genome integrity and viability of pluripotent cells. *Developmental Biology.* 363-318 (1-12), pp. 62-73.

McDonnell, E., Crown, S. B., Fox, D. B., Kitir, B., Ilkayeva, O. R., Olsen, C. A., Grimsrud, P. A. & Hirschey, M. D. (2016) Lipids reprogram metabolism to become a major carbon source for histone acetylation. *Cell Reports*. 17 (6), pp. 1463-1472.

McFie, P. J., Banman, S. L. & Stone, S. J. (2018) Diacylglycerol acyltransferase-2 contains a c-terminal sequence that interacts with lipid droplets. *Biochimica et Biophysica Acta (BBA) – Molecular and Cell Biology of Lipids.* 1863 (9), pp. 1068-1081.

Meech, R., Hu, D. G., McKinnon, R. A., Mubarokah, S. N., Haines, A. Z., Mair, P. C., Rowland, A. & Mackenzie, P. I. (2019) The UDP-glycosyltransferase (UGT) superfamily: new members, new functions, and novel paradigms. *Physiological Reviews.* 99 (2), pp. 1153-1222.

Meek, T. H. & Morton, G. J. (2012) Leptin, diabetes, and the brain. *Indian Journal of Endocrinology and Metabolism*. 16 (Suppl 3), S534.

Mergenthaler, P., Lindauer, U., Dienel, G. A. & Meisel, A. (2013) Sugar for the brain: the role of glucose in physiological and pathological brain function. *Trends in Neuroscience*. 36 (10), pp. 587-597.

Metlagel, Z., Otomo, C., Takaesu, G. & Otomo, T. (2013) Structural basis of ATG3 recognition by the autophagic ubiquitin-like protein ATG12. *Proceedings of the National Academy of Sciences of the United States of America.* 110 (47), pp. 18844-18849.

Mills, B. B., Thomas, A. D. & Riddle, N. C. (2018) HP1B is a euchromatic *Drosophila* HP1 homolog with links to metabolism. *PLoS One.* doi: 10.1371/journal.pone.0205867.

Minárik, P., Tomásková, N., Kollárová, M. & Antalík, M. (2002) Malate dehydrogenases – structure and function. *General Physiology and Biophysics.* 21 (3), pp. 257-265.

Mocellin, S. & Provenzano, M. (2004) RNA interference: learning gene knock-down from cell physiology. *Journal of Translational Medicine*. 2 (1), pp. 1-6.

Mochanová, M., Tomčala, A., Svobodová, Z. & Kodrík, D. (2018) Role of adipokinetic hormone during starvation in *Drosophila*. *Comparative Biochemistry and Physiology Part B: Biochemistry and Molecular Biology*. 226, pp. 26-35.

Moeller, G. & Adamski, J. (2006) Multifunctionality of human 17β-hydroxysteroid dehydrogenases. *Molecular and Cellular Endocrinology.* 248 (1-2), pp. 47-55.

Molaei, M., Vandehoef, C. & Karpac, J. (2019) NF-κB shapes metabolic adaptation by attenuating FoxO-mediated lipolysis in *Drosophila. Developmental Cell.* 49 (5), pp. 802-810.

Moloughney, J. G., Kim, P. K., Vega-Cotto, N. M., Wu, C., Zhang, S., Adlam, M., Lynch, T., Chou, P., Rabinowitz, J. D., Werlen, G. & Jacinto, E. (2016) mTORC2 responds to glutamine catabolite levels to modulate the hexosamine biosynthesis enzyme GFAT1. *Molecular Cell*. 63 (5), pp. 811-826.

Morigny, P., Houssier, M., Mouisel, E. & Langin, D. (2016) Adipocyte lipolysis and insulin resistance. *Biochimie*. 125, pp. 259-266.

Morris, B. J., Willcox, D. C., Donlon, T. A. & Willcox, B. J. (2015) FOXO3 – a major gene for human longevity. *Gerontology*. 61 (6), pp. 515-525.

Morris, S. N. S., Coogan, C., Chamseddin, K., Fernandez-Kim, S. O., Kolli, S., Keller, J. N. & Bauer, J. H. (2012) Development of diet-induced insulin resistance in adult *Drosophila melanogaster*. *Biochimica et Biophysica Acta (BBA)-Molecular Basis of Disease*. 1822 (8), pp. 1230-1237.

Muniesa, A., Ferreira, C., Fuertes, H., Halaihel, N., & de Blas, I. (2014) Estimation of the relative sensitivity of qPCR analysis using pooled samples. *PloS One.* 9 (4), e93491.

Murillo-Maldonado, J. M. & Riesgo-Escovar J. R. (2017) Development and diabetes on the fly. *Mechanisms of Development*. 144, pp. 150–155. doi: 10.1016/j.mod.2016.09.004.

Nagy, P., Varga, A., Pircs, K., Hegedüs, K. & Juhász, G. (2013) Myc-driven overgrowth requires unfolded protein response-mediated induction of autophagy and antioxidant responses in *Drosophila melanogaster. PLoS Genetics.* 9 (8), pp. e1003664.

Nahar, A., Baker, A. L., Nichols, D. S., Bowman, J. P. & Britz, M. L. (2020) Application of thin-layer chromatography-flame ionization detection (TLC-FID) to total lipid quantitation in mycolic-acid synthesizing *Rhodococcus* and *Williamsia* species. *International Journal of Molecular Sciences*. 21 (5), pp. 1670.

Nakae, J., Cao, Y., Daitoku, H., Fukamizu, A., Ogawa, W., Yano, Y. & Hayashi, Y. (2006) The LXXLL motif of murine forkhead transcription factor FoxO1 mediates Sirt1-dependent transcriptional activity. *The Journal of Clinical Investigation.* 116 (9), pp. 2473-2483.

Nakae, J., Oki, M. & Cao, Y. (2008) The FoxO transcription factors and metabolic regulation. *FEBS Letters*. 582 (1), pp. 54-67.

Nakajima, E., Shimaji, K., Umegawachi, T., Tomida, S., Yoshida, H., Yoshimoto, N., Izawa, S., Kimura, H. & Yamaguchi, M. (2016) The histone deacetylase gene *Rpd3* is required for starvation stress resistance. *PLoS One.* 11 (12), e0167554.

Nakato, R. & Sakata, T. (2021) Methods for ChIP-seq analysis: a practical workflow and advanced applications. *Methods.* 187, pp. 44-53.

Nässel, D. R., Kubrak, O. L., Liu, Y., Luo, J. & Lushchak, O. V. (2013) Factors that regulate insulin producing cells and their output in *Drosophila. Frontiers in Physiology.* 4 (1), pp. 252. doi:10.3389/fphys.2013.00252.

Nayak, N. & Mishra, M. (2021) High fat diet induced abnormalities in metabolism, growth, behavior, and circadian clock in *Drosophila melanogaster. Life Sciences.* 281, 119758.

Ni, Y. G., Wang, N., Cao, D. J., Sachan, N., Morris, D. J., Gerard, R. D., Kuro-o, M., Rothermel, B. A. & Hill, J. A. (2007) FoxO transcription factors activate Akt and attenuate insulin signaling in heart by inhibiting protein phosphatases. *Proceedings of the National Academy of Sciences of the United States of America.* 104 (51), pp. 20517-20522.

Nielsen, P. R., Nietlispach, D., Mott, H. R., Callaghan, J., Bannister, A., Kouzarides, T., Murzin, A. G., Murzina, N. V. & Laue, E. D. (2002) Structure of the HP1 chromodomain bound to histone H3 methylated at lysine 9. *Nature*. 416 (6876), pp.103-107.

Nishimura, T (2020) Feedforward regulation of glucose metabolism by steroid hormones drives a developmental transition in *Drosophila*. *Current Biology*. 30 (18), pp. 3624-3632.

Niwa, R., Namiki, T., Ito, K., Shimada-Niwa, Y., Kiuchi, M., Kawaoka, S., Kayukawa, T., Banno, Y., Fujimoto, Y., Shigenobu, S., Kobayashi, S., Shimada, T., Katsuma, S.

& Shinoda, T. (2010) Non-molting glossy/shroud encodes a short-chain dehydrogenase/reductase that functions in the 'Black Box' of the ecdysteroid biosynthesis pathway. *Development*. 137 (12), pp. 1991-1999.

Nonis, A., De Nardi, B. & Nonis, A. (2014) Choosing between RT-qPCR and RNA-seq: a back-of-the-envelope estimate towards the definition of the break-even-point. *Analytical and Bioanalytical Chemistry.* 406, pp. 3533-3536.

Nwadozi, E., Roudier, E., Rullman, E., Tharmalingam, S., Liu, H. Y., Gustafsson, T. & Haas, T. L. (2016) Endothelial FoxO proteins impair insulin sensitivity and restrain muscle angiogenesis in response to a high-fat diet. *The FASEB Journal*. 30 (9), pp. 3039-3052.

Obsil, T. & Obsilova, V. (2011) Structural basis for DNA recognition by FOXO proteins. *Biochimica et Biophysica Acta (BBA)-Molecular Cell Research*. 1813 (11), pp. 1946-1953.

Oh, S. M., Jeong, K., Seo, J. T. & Moon, S. J. (2021) Multisensory interactions regulate feeding behavior in *Drosophila. Proceedings of the National Academy of Sciences of the United States of America.* 118 (7), pp. e2004523118.

Ohashi, H. & Sakai, T. (2018) Leucokinin signaling regulates hunger–driven reduction of behavioral responses to noxious heat in *Drosophila. Biochemical and Biophysical Research Communications.* 499 (2), pp. 221-226.

Okamoto, N., Nakamori, R., Murai, T., Yamauchi, Y., Masuda, A. & Nishimura, T. (2013) A secreted decoy of InR antagonizes insulin/IGF signaling to restrict body growth in *Drosophila*. *Genes & Development*. 27 (1), pp. 87-97.

Okamoto, N., Yamanaka, N., Yagi, Y., Nishida, Y., Kataoka, H., O'Connor, M. B., & Mizoguchi, A. (2009) A fat body-derived IGF-like peptide regulates postfeeding growth in *Drosophila*. *Developmental Cell*. 17 (6), pp. 885-891.

Olmos, Y., Valle, I., Borniquel, S., Tierrez, A., Soria, E., Lamas, S. & Monsalve, M. (2009) Mutual dependence of FoxO3a and PGC-1α in the induction of oxidative stress genes. *Journal of Biological Chemistry.* 284 (21), pp. 14476-14484.

Owusu-Ansah, E. & Perrimon, N. (2014) Modeling metabolic homeostasis and nutrient sensing in *Drosophila*: implications for aging and metabolic diseases. *Disease Models & Mechanisms*. 7 (3), pp. 343-350.

Pal-Nath, D., Didi-Cohen, S., Shtaida, N., Nath, P. R., Samani, T., Boussiba, S. & Khozin-Goldberg, I. (2017) Improved productivity and oxidative stress tolerance under nitrogen starvation is associated with the ablated Δ5 desaturation in the green microalga *Lobosphaera incisa*. *Algal Research*. 26, pp. 25-38.

Pan, C.W., Jin, X., Zhao, Y., Pan, Y., Yang, J., Karnes, R.J., Zhang, J., Wang, L. & Huang, H. (2017) AKT-phosphorylated FOXO 1 suppresses ERK activation and chemoresistance by disrupting IQGAP 1-MAPK interaction. *The EMBO Journal*. 36 (8), pp.995-1010.

Pandey, U. B. & Nichols, C. D. (2011) Human disease models in *Drosophila melanogaster* and the role of the fly in therapeutic drug discovery. *Pharmacological Reviews*. 63 (2), pp. 411-436.

Papadopoli, D., Boulay, K., Kazak, L., Pollak, M., Mallette, F. A., Topisirovic, I. & Hulea, L. (2019) mTOR as a central regulator of lifespan and aging. *F1000 Research.* 8, F1000 Faculty Rev-998.

Park, H. S., Lim, J. H., Kim, M. Y., Kim, Y., Hong, Y. A., Choi, S. R., Chung, S., Kim, H. W., Choi, B. S., Kim, Y. S., Chang, Y. S. & Park, C. W. (2016) Resveratrol increases AdipoR1 and AdipoR2 expression in type 2 diabetic nephropathy. *Journal of Translational Medicine*. 14 (1), pp. 1-13.

Park, P. J. (2009) ChIP–seq: advantages and challenges of a maturing technology. *Nature Reviews Genetics*. 10 (10), pp. 669-680.

Peeters, A. & Baes, M. (2010) Role of PPAR α in hepatic carbohydrate metabolism. *PPAR Research*. doi: 10.1155/2010/572405.

Pendse, J., Ramachandran, P.V., Na, J., Narisu, N., Fink, J.L., Cagan, R.L., Collins, F. S. & Baranski, T. J. (2013) A *Drosophila* functional evaluation of candidates from human genome-wide association studies of type 2 diabetes and related metabolic traits identifies tissue-specific roles for dHHEX. *BMC Genomics*. 14 (1), pp. 1-11.

Peng, S., Li, W., Hou, N. & Huang, N. (2020) A review of FoxO1-regulated metabolic diseases and related drug discoveries. *Cells*. 9 (1), pp. 184.

Peng, S., Xiao, W., Ju, D., Sun, B., Hou, N., Liu, Q., Wang, Y., Zhao, H., Gao, C., Zhang, S., Cao, R., Li, P., Huang, H., Ma, Y., Wang, Y., Lai, W., Ma, Z., Zhang, W., Huang, S., Wang, H., Zhang, Z., Zhao, L., Cai, T., Zhao, Y. L., Wang, F., Nie, Y., Zhi, G., Yang, Y. G., Zhang, E. E. & Huang, N. (2019) Identification of entacapone as a chemical inhibitor of FTO mediating metabolic regulation through FOXO1. *Science Translational Medicine.* 11 (488). doi: 10.1126/scitranslmed.aau7116.

Peng, S., Zhao, S., Yan, F., Cheng, J., Huang, L., Chen, H., Liu, Q., Ji, X. & Yuan, Z. (2015) HDAC2 selectively regulates FoxO3a-mediated gene transcription during oxidative stress-induced neuronal cell death. *The Journal of Neuroscience.* 35 (3), pp. 1250-1259.

Pennetta, G. & Pauli, D. (1998) The *Drosophila* Sin3 gene encodes a widely distributed transcription factor essential for embryonic viability. *Development Genes and Evolution*. 208 (9), pp. 531-536. doi: 10.1007/s004270050212.

Pennington, K. L., Chan, T. Y., Torres, M. P. & Andersen, J. L. (2018) The dynamic and stress-adaptive signaling hub of 14-3-3: emerging mechanisms of regulation and context dependent protein-protein interactions. *Oncogene.* 37, pp. 5587-5604.

Peregrín-Alvarez, J. M., Sanford, C. & Parkinson, J. (2009) The conservation and evolutionary modularity of metabolism. *Genome Biology.* 10 (R63). doi: 10.1186/gb-2009-10-6-r63.

Perkins, J. R., Diboun, I., Dessailly, B. H., Lees, J. G. & Orengo, C. (2010) Transient protein-protein interactions: structural, functional, and network properties. *Structure.* 18 (10), pp. 1233-1243.

Pernet, C. R., Wilcox, R. R. & Rousselet, G. A. (2013) Robust correlation analyses: false positive and power validation using a new open source Matlab toolbox. *Frontiers in Psychology*. 3, 606.

Pertseva, M. N. & Shpakov, A. O. (2002) Conservatism of the insulin signaling system in evolution of invertebrate and vertebrate animals. *Journal of Evolutionary Biochemistry and Physiology.* 38, pp. 547-561.

Peter, A., Stefan, N., Cegan, A., Walenta, M., Wagner, S., Königsrainer, A., Königsrainer, I., Machicao, F., Schick, F., Häring, H. U. & Schleicher, E. (2011) Hepatic glucokinase expression is associated with lipogenesis and fatty liver in humans. *Journal of Clinical Endocrinology & Metabolism*. 96 (7), pp. E1126-30. doi: 10.1210/jc.2010-2017.

Petryk, A., Warren, J. T., Marqués, G., Jarcho, M. P., Gilbert, L. I., Kahler, J., Parvy, J., Li, Y., Dauphin-Villemant, C. & O'Connor, M. B. (2003) Shade is the *Drosophila* P450 enzyme that mediates the hydroxylation of ecdysone to the steroid insect molting hormone 20-hydroxyecdysone. *Proceedings of the National Academy of Sciences of the United States of America.* 100 (24), pp. 13773-13778.

Piper, M. D. W., Selman, C., McElwee, J. J. & Partridge, L. (2008) Separating cause from effect: how does insulin/IGF signalling control lifespan in worms, flies and mice? *Journal of Internal Medicine*. 263 (2). doi: 10.1111/j.1365-2796.2007.01906.x.

Pletcher, S. D. (2009) The modulation of lifespan by perceptual systems. *Annals of the New York Academy of Sciences.* 1170 (1), pp. 693-697.

Pomar, N., Berlanga, J. J., Campuzano, S., Hernández, G., Elías, M. & de Haro, C. (2003) Functional characterization of *Drosophila melanogaster* PERK eukaryotic

initiation factor 2α (eIF2α) kinase. *European Journal of Biochemistry.* 270 (2), pp. 293-306.

Pouwels, M. J., Jacobs, J. R., Span, P. N., Lutterman, J. A., Smits, P. & Tack, C. J. (2001) Short-term glucosamine infusion does not affect insulin sensitivity in humans. *Journal of Clinical Endocrinology and Metabolism*. 86, pp. 2099–2103.

Powers, R. W., Kaeberlein, M., Caldwell, S. D., Kennedy, B. K. & Fields, S. (2006) Extension of chronological life span in yeast by decreased TOR pathway signaling. *Genes & Development.* 20 (2), pp. 174-184.

Puig, O. & Tjian, R. (2005) Transcriptional feedback control of insulin receptor by dFOXO/FOXO1. *Genes & Development*. 19 (20), pp. 2435-2446.

Puigserver, P., Rhee, J., Donovan, J., Walkey, C. J., Yoon, J. C., Oriente, F., Kitamura, Y., Altomonte, J., Dong, H., Accili, D. & Spiegelman, B. M. (2003) Insulin-regulated hepatic gluconeogenesis through FOXO1-PGC-1alpha interaction. *Nature.* 423 (6939), pp. 550-555.

Qiao, L. & Shao, J. (2006) SIRT1 regulates adiponectin gene expression through Foxo1-C/enhancer-binding protein alpha transcriptional complex. *Journal of Biological Chemistry.* 281 (52), pp. 39915-39924.

Qu, S., Su, D., Altomonte, J., Kamagate, A., He, J., Perdomo, G., Tse, T., Jiang, Y. & Dong, H. H. (2007) PPAR{alpha} mediates the hypolipidemic action of fibrates by antagonizing FoxO1. *American Journal of Physiology, Endocrinology, and Metabolism.* 292 (2), pp. e421-434.

Ragab, S., Abdallah, N., Hasan, N. S., Kandil, M. E., El Wasseif, M., Elhosary, Y., Ibrahim, A. A. & Mourad, A. (2014) *FOXO 1a* and *FOXO 3a* gene polymorphisms in association with metabolic syndrome. *Journal of Genetic Engineering and Biotechnology*. 12 (2), pp. 127-133.

Rajendran, R., Garva, R., Krstic-Demonacos, M. & Demonacos, C. (2011) Sirtuins: molecular traffic lights in the crossroad of oxidative stress, chromatin remodelling, and transcription. *BioMed Research International.* doi: 10.1155/2011/368276.

Ramaswamy, S., Nakamura, N., Sansai, I., Bergeron, L. & Sellers, W. R. (2002) A novel mechanism of gene regulation and tumor suppression by the transcription factor FKHR. *Cancer Cell.* 2 (1), pp. 81-91.

Ramírez, F., Ryan, D. P., Grüning, B., Bhardwaj, V., Kilpert, F., Richter, A. S., Heyne, S., Dündar, F. & Manke, T. (2016) deepTools2: a next generation web server for deep-sequencing data analysis. *Nucleic Acids Research*. 44 (W1), pp. W160–W165. doi: 10.1093/nar/gkw257

Rao, M. S., van Vleet, T. R., Ciurlionis, R., Buck, W. R., Mittelstadt, S. W., Blomme, E. A., & Liguori, M. J. (2019) Comparison of RNA-Seq and microarray gene expression platforms for the toxicogenomic evaluation of liver from short-term rat toxicity studies. *Frontiers in Genetics*. 9, 636.

Rapaport, F., Khanin, R., Liang, Y., Krek, A., Zumbo, P., Mason, C. E., Socci, N. D. & Betel, D. (2013) Comprehensive evaluation of differential expression analysis methods for RNA-seq data. *Genome Biology*. 14. doi: 10.1186/gb-2013-14-9-r95.

Rehman, K. & Akash, M. S. H. (2016) Mechanisms of inflammatory responses and development of insulin resistance: how are they interlinked? *Journal of Biomedical Science*. 23 (1), pp. 1-18.

Reiff, T., Jacobson, J., Cognigni, P., Antonello, Z., Ballesta, E., Tan, K. J., Yew, J. Y., Dominguez, M. & Miguel-Aliaga, I. (2015) Endocrine remodelling of the adult intestine sustains reproduction in *Drosophila. Developmental Biology.* 4, e06930.

Renault, V. M., Thekkat, P. U., Hoang, K. L., White, J. L., Brady, C. A., Broz, D. K., Venturelli, O. S., Johnson, T. M., Oskoui, P. R., Xuan, Z., Santo, E. E., Zhang, M. Q., Vogel, H., Attardi, L. D. & Brunet, A. (2011) The pro-longevity gene *FoxO3* is a direct target of the p53 tumor suppressor. *Oncogene*. 30 (29), pp. 3207-3221.

Reshef, L., Olswang, Y., Cassuto, H., Blum, B., Croniger, C. M., Kalhan, S. C., Tilghman, S. M., Hanson, R. W. (2003) Glyceroneogenesis and the triglyceride/fatty acid cycle. *Journal of Biological Chemistry*. 278, pp. 30413–30416.

Rhee, E. J. & Plutzky, J. (2012) Retinoid metabolism and diabetes mellitus. *Diabetes and Metabolism Journal.* 36 (3), pp. 167-180.

Rhee, J., Inoue, Y., Yoon, J. C., Puigserver, P., Fan, M., Gonzalez, F. J. & Spiegelman, B. M. (2003) Regulation of hepatic fasting response by PPARγ coactivator-1α (PGC-1): requirement for hepatocyte nuclear factor 4α in gluconeogenesis. *Proceedings of the National Academy of Sciences of the United States of America.* 100, pp. 4012–4017.

Richard, A.C., Lyons, P.A., Peters, J.E., Biasci, D., Flint, S.M., Lee, J.C., McKinney, E.F., Siegel, R.M. & Smith, K.G. (2014) Comparison of gene expression microarray data with count-based RNA measurements informs microarray interpretation. *BMC Genomics.* 15 (1), pp.1-10.

Risca, V. I. & Greenleaf, W. J. (2015) Beyond the linear genome: paired-end sequencing as a biophysical tool. *Trends in Cell Biology.* 25 (12), pp. 716-719.

Robida-Stubbs, S., Glover-Cutter, K., Lamming, D. W., Mizunuma, M., Narasimhan, S. D., Neumann-Haefelin, E., Sabatini, D. M. & Blackwell, T. K. (2012) TOR signalling

and rapamycin influence longevity by regulating SKN-1/Nrf and DAF-16/FoxO. *Cell Metabolism.* 15 (5), pp. 713-724.

Robinson, J. T., Thorvaldsdóttir, H., Winckler, W., Guttman, M., Lander, E. S., Getz, G. & Mesirov, J. P. (2011) Integrative Genomics Viewer. *Nature Biotechnology.* 29, pp. 24–26.

Roupé, K. M., Veerla, S., Olson, J., Stone, E. L., Sørensen, O. E., Hedrick, S. M., & Nizet, V. (2014) Transcription factor binding site analysis identifies FOXO transcription factors as regulators of the cutaneous wound healing process. *PloS One*. 9 (2), e89274.

Rubin, J. D., Stanley, J. T., Sigauke, R. F., Levandowski, C. B., Maas, Z. L., Westfall, J., Taatjes, D. J. & Dowell, R. D. (2021) Transcription factor enrichment analysis (TFEA) quantifies the activity of multiple transcription factors from a single experiment. *Communications Biology*. 4 (1), pp. 1-15.

Rudd, M. D., Gonzalez-Robayna, I., Hernandez-Gonzalez, I., Weigel, N. L., Bingman, W. E. & Richards, J. S. (2007) Constitutively active FoxO1a and a DNA-binding domain mutant exhibit distinct co-regulatory functions to enhance progesterone receptor A activity. *Journal of Molecular Endocrinology*. 38, pp. 673-690.

Rulifson, E. J., Kim, S. K. & Nusse, R. (2002) Ablation of insulin-producing neurons in flies: growth and diabetic phenotypes. *Science.* 296 (5570), pp. 1118-1120.

Rupp, M., Hagenbuchner, J., Rass, B., Fiegl, H., Kiechl-Kohlendorfer, U., Obexer, P. & Ausserlechner, M. J. (2017) FOXO3-mediated chemo-protection in high-stage neuroblastoma depends on wild-type TP53 and SESN3. *Oncogene.* 36 (44), pp. 6190-6203.

Salcher, S., Spoden, G., Hagenbuchner, J., Führer, S., Kaserer, T., Tollinger, M., Huber-Cantonati, P., Gruber, T., Schuster, D., Gust, R., Zwierzina, H., Müller, T., Kiechl-Kohlendorfer, U., Ausserlechner, M. J. & Obexer, P. (2019) A drug library screen identifies Carbenoxolone as novel FOXO inhibitor that overcomes FOXO3-mediated chemoprotection in high-stage neuroblastoma. *Oncogene.* 39, pp. 1080-1097.

Salih, D. A. M. & Brunet, A. (2008) FoxO transcription factors in the maintenance of cellular homeostasis during ageing. *Current Opinion in Cell Biology.* 20 (2), pp. 126-136.

Sanchez, A. M., Candau, R. B. & Bernardi, H. (2014) FoxO transcription factors: their roles in the maintenance of skeletal muscle homeostasis. *Cellular and Molecular Life Sciences*. 71 (9), pp. 1657-1671.

Saponaro, C., Gaggini, M., Carli, F. & Gastaldelli, A. (2015) The subtle balance between lipolysis and lipogenesis: a critical point in metabolic homeostasis. *Nutrients.* 7 (11), pp. 9453-9474.

Sassu, E. D., McDermott, J. E., Keys, B. J., Esmaeili, M., Keene, A. C., Birnbaum, M. J. & DiAngelo, J. R. (2012) Mio/dChREBP coordinately increases fat mass by regulating lipid synthesis and feeding behavior in *Drosophila. Biochemical and Biophysical Research Communications.* 426 (1), pp. 43-48.

Savkur, R. S. & Burris, T. P. (2008) The coactivator LXXLL nuclear receptor recognition motif. *The Journal of Peptide Research.* 63 (3), pp. 207-212.

Saxton, R. A. & Sabatini, D. M. (2017) mTOR signaling in growth, metabolism, and disease. *Cell.* 168 (6), pp. 960-976.

Schaefer, M. H., Wanker, E. E. & Andrade-Navarro, M. A. (2012) Evolution and function of CAG/polyglutamine repeats in protein-protein interaction networks. *Nucleic acids research*. 40 (10), pp. 4273–87.

Schill, D., Nord, J. & Cirillo, L. A. (2019) FoxO1 and FoxA1/2 form a complex on DNA and cooperate to open chromatin at insulin-regulated genes. *Biochemistry and Cell Biology.* 97 (2). doi: 10.1139/bcb-2018-0104.

Schmitt-Ney, M. (2020) The FOXO's advantages of being a family: considerations on function and evolution. *Cells.* 9 (3), pp. 787.

Schneider, C. A., Rasband, W. S. & Eliceiri, K. W. (2012) NIH Image to ImageJ: 25 years of image analysis. *Nature Methods*. 9 (7), pp. 671–675. doi: 10.1038/nmeth.2089.

Schoelz, J. M., Feng, J. X. & Riddle, N. C. (2021) The *Drosophila* HP1 family is associated with active gene expression across chromatin contexts. *Genetics.* 219 (1), iyab108.

Schwedes, C. C. & Carney, G. E. (2012) Ecdysone signaling in adult *Drosophila melanogaster*. *Journal of Insect Physiology.* 58 (3), pp. 293-302. doi: 10.1016/j.jinsphys.2012.01.013.

Sekiya, M., Yahagi, N., Matsuzaka, T., Takeuchi, Y., Nakagawa, Y., Takahashi, H., Okazaki, H., Iizuka, Y., Ohashi, K., Gotoda, T., Ishibashi, S., Nagai, R., Yamazaki, T., Kadowaki, T., Yamada, N., Osuga, J. & Shimano, H. (2007) SREBP-1-independent regulation of lipogenic gene expression in adipocytes. *Journal of Lipid Research.* 48, pp.1581-1591.

Sellami, A., Agricola, H. J. & Veenstra, J. A. (2011) Neuroendocrine cells in *Drosophila melanogaster* producing GPA2/GPB5, a hormone with homology to LH, FSH, and TSH. *General and Comparative Endocrinology.* 170 (3), pp. 582-588.

Semaniuk, U. V., Gospodaryov, D. V., Feden'ko, K. M., Yurkevych, I. S., Vaiserman, A. M., Storey, K. B., Simpson, S. J. & Lushchak, O. (2018) Insulin-like peptides regulate feeding preference and metabolism in *Drosophila. Frontiers in Physiology.* 9, pp.1083.

Seo, J., Fortuno, E.S., Suh, J.M., Stenesen, D., Tang, W., Parks, E.J., Adams, C.M., Townes, T. & Graff, J.M. (2009) Atf4 regulates obesity, glucose homeostasis, and energy expenditure. *Diabetes*. 58 (11), pp. 2565--2573.

Seong, K. M., Coates, B. S., Sun, W., Clark, J. M. & Pittendrigh, B. R. (2017) Changes in neuronal signaling and cell stress response pathways are associated with a multigenic response of *Drosophila melanogaster* to DDT selection. *Genome Biology and Evolution.* 9 (12), pp. 3356-3372.

Seyednasrollah, F., Laiho, A. & Elo, L. L. (2015) Comparison of software packages for detecting differential expression in RNA-seq studies. *Briefings in Bioinformatics*. 16 (1), pp. 59-70.

Shafqat, N., Marschall, H. U., Filling, C., Nordling, E., Wu, X. Q., Bjork, L., Thyberg, J., Martensson, E., Salim, S., Jornvall, H. & Oppermann, U. (2003) Expanded substrate screenings of human and *Drosophila* type 10 17-hydroxysteroid dehydrogenases (HSDs) reveal multiple specificities in bile acid and steroid hormone metabolism: characterization of multifunctional 3/7/7/17/20/21-HSD. *Biochemical Journal*. 376 (1), pp. 49-60.

Shang, L., Chen, S., Du, F., Li, S., Zhao, L. & Wang, X. (2011) Nutrient starvation elicits an acute autophagic response mediated by Ulk1 dephosphorylation and its subsequent dissociation from AMPK. *Proceedings of the National Academy of Sciences of the United States of America*. 108 (12), pp. 4788-4793.

Shiio, Y. & Eisenman, R. N. (2003) Histone sumoylation is associated with transcriptional repression. *Proceedings of the National Academy of Sciences of the United States of America.* 100 (23), pp. 13225-13230.

Shimeld, S. M., Degnan, B., Luke, G. N. (2010) Evolutionary genomics of the Fox genes: origin of gene families and the ancestry of gene clusters. *Genomics.* 95 (5), pp. 256-260.

Shin, D. J., Joshi, P., Hong, S. H., Mosure, K., Shin, D. G. & Osborne, T. F. (2012) Genome-wide analysis of FoxO1 binding in hepatic chromatin: potential involvement of FoxO1 in linking retinoid signaling to hepatic gluconeogenesis. *Nucleic Acids Research.* 40 (22), pp. 11499–11509.

Shin, H. S., Lee, Y., Shin, M. H., Cho, S. I., Zouboulis, C. C., Kim, M. K., Lee, D. H. & Chung, J. H. (2021) Histone deacetylase 1 reduces lipogenesis by suppressing SREBP1 transcription in human sebocyte cell line SZ95. *International Journal of Molecular Sciences*. 22 (9), pp. 4477.

Shingleton, A. W., Das, J., Vinicius, L. & Stern, D. L. (2005) The temporal requirements for insulin signaling during development in *Drosophila. PLoS Biology.* 3 (9), pp. e289. doi: 10.1371/journal.pbio.0030289.

Shukla, E., Thorat, L. J., Nath, B. B. & Gaikwad, S. M. (2015) Insect trehalase: physiological significance and potential applications. *Glycobiology*. 25 (4), pp. 357-367.

Sieber, M. H. & Spradling, A. C. (2015) Steroid signaling establishes a female metabolic state and regulates SREBP to control oocyte lipid accumulation. *Current Biology.* 25, pp. 993-1004.

Siebold, A. P., Banerjee, R., Tie, F., Kiss, D. L., Moskowitz, J. & Harte, P. J. (2010) Polycomb repressive complex 2 and trithorax modulate *Drosophila* longevity and stress resistance. *Proceedings of the National Academy of Sciences of the United States of America.* 107 (1), pp. 169-174.

Simon, A. F., Shih, C., Mack, A. & Benzer, S. (2003) Steroid control of longevity in *Drosophila melanogaster. Science.* 299 (5611), pp. 1407-1410.

Singh, A., Kukreti, R., Saso, L. & Kukreti, S. (2019) Oxidative stress: a key modulator in neurodegenerative diseases. *Molecules.* 24 (8), pp. 1583-1603.

Singh, A., Ye, M., Bucur, O., Zhu, S., Tanya Santos, M., Rabinovitz, I., Wei, W., Gao, D., Hahn, W. C. & Khosravi-Far, R. (2010) Protein phosphatase 2A reactivates FOXO3a through a dynamic interplay with 14-3-3 and AKT. *Molecular Biology of the Cell*. 21 (6), pp. 1140-1152.

Singh, L. P. & Crook, E. D. (2000) The effects of glucose and the hexosamine biosynthesis pathway on glycogen synthase kinase-3 and other protein kinases that regulate glycogen synthase activity. *Journal of Investigative Medicine*. 48 (4), pp. 251-258.

Sipes, I. G., Wiersma, D. A. & Armstrong, D. J. (1986) The role of glutathione in the toxicity of xenobiotic compounds: metabolic activation of 1,2-dibromoethane by glutathione. *Advances in Experimental Medicine and Biology*.197, pp. 457-467.

Slack, C., Alic, N., Foley, A., Cabecinha, M., Hoddinott, M. P. & Partridge, L. (2015) The Ras-Erk-ETS-signaling pathway is a drug target for longevity. *Cell*. 162 (1), pp. 72-83.

Slack, C., Giannakou, M. E., Foley, A., Goss, M. & Partridge, L. (2011) dFoxO-independent effects of reduced insulin-like signalling in *Drosophila. Aging Cell*. 10, pp. 735-548.

Slack, C., Werz, C., Wieser, D., Alic, N., Foley, A., Stocker, H., Withers, D.J., Thornton, J. M., Hafen, E. & Partridge, L. (2010) Regulation of lifespan, metabolism, and stress responses by the *Drosophila* SH2B protein, Lnk. *PLoS Genetics*. 6 (3), pp. e1000881.

Slaidina, M., Delanoue, R., Grönke, S., Partridge, L. & Léopold, P. (2009) A *Drosophila* insulin-like peptide promotes growth during nonfeeding states. *Developmental Cell.* 17 (6), pp. 874-884.

Slawson, C., Copeland, R. J. & Hart, G. W. (2010) O-GlcNAc signaling: a metabolic link between diabetes and cancer? *Trends in Biochemical Sciences*. 35 (10), pp. 547-555.

Smothers, J. F. & Henikoff, S. (2001) The hinge and chromo shadow domain impart distinct targeting of HP1-like proteins. *Molecular and Cellular Biology*. 21 (7), pp. 2555-2569.

Soeters, M. R., Soeters, P. B., Schooneman, M. G., Houten, S. M. & Romijn, J. A. (2012) Adaptive reciprocity of lipid and glucose metabolism in human short-term starvation. *American Journal of Physiology, Endocrinology and Metabolism.* 303 (12), pp. e1397-e1407.

Soller, M., Haussmann, I. U., Hollmann, M., Choffat, Y., White, K., Kubli, E. & Schäfer, M. A. (2006) Sex-peptide-regulated female sexual behavior requires a subset of ascending ventral nerve cord neurons. *Current Biology.* 16 (18), pp. 1771-1782.

Song, W., Cheng, D., Hong, S., Sappe, B., Hu, Y., Wei, N., Zhu, C., O'Connor, M. B., Pissios, P. & Perrimon, N. (2017) Midgut-derived activin regulates glucagon-like action in the fat body and glycemic control. *Cell Metabolism.* 25 (2), pp. 386-399.

Soukup, S. F., Kuenen, S., Vanhauwaert, R., Manetsberger, J., Hernández-Díaz, S., Swerts, J., Schoovaerts, N., Vilain, S., Gounko, N. V., Vints, K., Geens, A., De Strooper, B. & Verstreken, P. (2016) A LRRK2-dependent EndophilinA phosphoswitch is critical for macroautophagy at presynaptic terminals. *Neuron.* 92 (4), pp. 829-844.

Spain, M. M., Caruso, J. A., Swaminathan, A. & Pile, L. A. (2010) *Drosophila* Sin3 isoforms interact with distinct proteins and have unique biological functions. *Journal of Biological Chemistry.* 285 (35), pp. 27457-27467.

Sparks, D. J. & Dong, H. H. (2009) FoxO1 and hepatic lipid metabolism. *Current Opinion in Lipidology*. 20, pp. 217–226.

Stabell, M., Eskeland, R., Bjørkmo, M., Larsson, J., Aalen, R. B., Imhof, A. & Lambertsson, A. (2006) The *Drosophila* G9a gene encodes a multi-catalytic histone methyltransferase required for normal development. *Nucleic Acids Research*. 34 (16), pp. 4609-4621.

Starmer, J. & Magnuson, T. (2016) Detecting broad domains and narrow peaks in ChIP-seq data with hiddenDomains. *BMC Bioinformatics*. 17, 144. doi: 10.1186/s12859-016-0991-z.

Stedman, M., Lunt, M., Livingston, M., Fryer, A.A., Moreno, G., Bailey, S., Gadsby, R. & Heald, A. (2019) The costs of drug prescriptions for diabetes in the NHS. *The Lancet*. 393 (10168), pp. 226-227.

Stelzer, G., Rosen, R., Plaschkes, I., Zimmerman, S., Twik, M., Fishilevich, S., Iny Stein, T., Nudel, R., Lieder, I., Mazor, Y., Kaplan, S., Dahary, D., Warshawsky, D., Guan–Golan, Y., Kohn, A., Rappaport, N., Safran, M., & Lancet, D. (2016) The GeneCards Suite: From Gene Data Mining to Disease Genome Sequence Analysis, *Current Protocols in Bioinformatics.* 54, 1.30.1 - 1.30.33. doi: 10.1002/cpbi.5.

Stocks, M., Dean, R., Rogell, B., & Friberg, U. (2015). Sex-specific trans-regulatory variation on the *Drosophila melanogaster* X chromosome. *PLoS Genetics*. 11 (2), e1005015.

Subedi, R. P., Vartak, R. R. & Kale, P. G. (2017) Management of stress exerted by hydrogen peroxide in *Drosophila melanogaster* using *Abhrak bhasma*. *Journal of Applied Pharmaceutical Science*. 7 (12), pp 65-71. doi:10.7324/JAPS.2017.71208.

Subramanian, M., Metya, S. K., Sadaf, S., Kumar, S., Schwudke, D. & Hasan, G. (2013) Altered lipid homeostasis in *Drosophila* InsP3 receptor mutants leads to obesity and hyperphagia. *Disease Models and Mechanisms.* 6 (3), pp. 734-744.

Sudhakar, S. R., Pathak, H., Rehman, N., Fernandes, J., Vishnu, S. & Varghese, J. (2020) Insulin signalling elicits hunger-induced feeding in *Drosophila. Developmental Biology.* 459 (2), pp. 87-99.

Sun, F. L., Cuaycong, M. H., Craig, C. A., Wallrath, L. L., Locke, J. & Elgin, S. C. R. (2000) The fourth chromosome of *Drosophila melanogaster:* interspersed euchromatic and heterochromatic domains. *Proceedings of the National Academy of Sciences of the United States of America.* 97 (10), pp. 5340-5345.

Sun, J., Xiao, S. & Carlson, J. R. (2018) The diverse small proteins called odorant-binding proteins. *Open Biology.* 8 (12), pp. 180208.

Sunayama, J., Tsuruta, F., Masuyama, N. & Gotch, Y. (2005) JNK antagonises Akt-mediated survival signals by phosphorylating 14-3-3. *Journal of Cell Biology.* 170 (2), pp. 295-304.

Takahashi, Y., Daitoku, H., Hirota, K., Tamiya, H., Yokoyama, A., Kako, K., Nagashima, Y., Nakamura, A., Shimada, T., Watanabe, S., Yamagata, K., Yasuda, K., Ishii, N. & Fukamizu, A. (2011) Asymmetric arginine demethylation determines lifespan in *C. elegans* by regulating forkhead transcription factor DAF-16. *Cellular Metabolism.* 13 (5), pp. 505-516.

Tamemoto, H., Kadowaki, T., Tobe, K., Yagi, T., Sakura, H., Hayakawa, T., Terauchi, Y., Ueki, K., Kaburagi, Y., Satoh, S., Sekihara, H., Yoshioka, S., Horikoshi, H., Furuta, Y., Ikawa, Y., Kasuga, M., Yazaki, Y. & Aizawa, S. (1994) Insulin resistance and growth retardation in mice lacking insulin receptor substrate-1. *Nature.* 372 (6502), pp. 182-186.

Tanaka, H., Nagashima, T., Shimaya, A., Urano, Y., Shimokawa, T. & Shibasaki, M. (2010) Effects of the novel Foxo1 inhibitor AS1708727 on plasma glucose and triglyceride levels in diabetic db/db mice. *European Journal of Pharmacology.* 645 (1-3), pp. 185-191.

Tang, E., D., Nuñez, G., Barr, F. G. & Guan, K. L. (1999) Negative regulation of forkhead transcription factor FKHR by AKT. *The Journal of Biochemistry*. 274, pp. 16741-16746.

Tang, H. W., Hu, Y., Chen, C. L., Xia, B., Zirin, J., Yuan, M., Asara, J. M., Rabinow, L. & Perrimon, N. (2018) The TORC1-regulated CPA complex rewires an RNA processing network to drive autophagy and metabolic reprogramming. *Cell Metabolism*. 27 (5), pp. 1040-1054.

Tao, R., Wei, D., Gao, H., Liu, Y., Depinho, R.A. & Dong, X.C. (2011) Hepatic FoxOs regulate lipid metabolism via modulation of expression of the nicotinamide phosphoribosyltransferase gene. *Journal of Biological Chemistry*. 286, pp. 14681–14690.

Tennessen, J. M., Barry, W., Cox, J. & Thummel, C. S. (2014) Methods for studying metabolism in *Drosophila. Methods*. 68 (1), pp. 105-115.

Terashima, J. & Bownes, M. (2006) E75A and E75B have opposite effects on the apoptosis/development choice of the *Drosophila* egg chamber. *Cell Death & Differentiation.* 13 (3), pp. 454-464.

Tettweiler, G., Miron, M., Jenkins, M., Sonenberg, N. & lasko, P. F. (2005) Starvation and oxidative stress resistance in *Drosophila* are mediated through the eIF4E-binding protein, d4E-BP. *Genes and Development*. 19 (16), pp. 1840-1843.

Thanh, M. T., Pham, T. L. A., Tran, B. D., Nguyen, Y. D. H. & Kaeko, K. (2020) *Drosophila* model for studying the link between lipid metabolism and development. *Frontiers in Bioscience.* 25, pp. 147-158.

Theopold, U., Ekengren, S. & Hultmark, D. (1996) HLH106, a *Drosophila* transcription factor with similarity to the vertebrate sterol responsive element binding protein. *Proceedings of the National Academy of Sciences*. 93 (3), pp. 1195-1199.

Thermo Scientific (2010) Thermo Scientific Pierce Protein Assay Technical handbook. Accessed: May 2022. URL: http://tools.thermofisher.com/content/sfs/brochures/1602063-Protein-Assay-Handbook.pdf

Thummel, C. S., Burtis, K. C. & Hogness, D. S. (1990) Spatial and temporal patterns of E74 transcription during *Drosophila* development. *Cell.* 61 (1), pp. 101-111.

Tikhanovich, I., Cox, J. & Weinman, S. A. (2013) Forkhead box class O transcription factors in liver function and disease. *Journal of Gastroenterology and Hepatology*. 28, pp. 125-131.

Toprak, U. (2020) The role of peptide hormones in insect lipid metabolism. *Frontiers in Physiology.* 11, 434.

Totzeck, F., Andrade-Navarro, M. A. & Mier, P. (2017) The protein structure context of polyQ regions. *PLoS One.* 12 (1), e0170801. doi: 10.1371/journal.pone.0170801

Tran, T. Q., Lowman, X. H. & Kong, M. (2017) Molecular Pathways: metabolic control of histone methylation and gene expression in cancer. *Clinical Cancer Research.* 23 (15), pp. 4004-4009.

Tricoire, H., Battisti, V., Trannoy, S., Lasbleiz, C., Pret, A. & Monnier, V. (2009) The steroid hormone receptor EcR finely modulates *Drosophila* lifespan during adulthood in a sex-specific manner. *Mechanisms of Ageing and Development.* 130 (8), pp. 547-552.

Ugrankar, R., Berglund, E., Akdemir, F., Tran, C., Kim, M. S., Noh, J., Schneider, R., Ebert, B. & Graff, J. M. (2015) *Drosophila* glucome screening identifies Ck1alpha as a regulator of mammalian glucose metabolism. *Nature Communications*. 6 (1), pp. 1-10.

Ugrankar, R., Bowerman, J., Hariri, H., Chandra, M., Chen, K., Bossanyi, M.F., Datta, S., Rogers, S., Eckert, K.M., Vale, G., Victoria, A., Fresquez, J., McDonald, J.G., Jean, S., Collins, B.M. & Henne, W.M. (2019) *Drosophila* snazarus regulates a lipid droplet population at plasma membrane-droplet contacts in adipocytes. *Developmental Cell.* 50 (5), pp. 557--572.

Urness, L. D. & Thummel, C. S. (1995) Molecular analysis of a steroid-induced regulatory hierarchy: the *Drosophila* E74A protein directly regulates L71–6 transcription. *The EMBO Journal*. 14 (24), pp. 6239-6246.

van der Heide, L. P. & Smidt, M. P. (2005) Regulation of FoxO activity by CBP/p300-mediated acetylation. *Trends in Biochemical Science.* 30 (2), pp. 81-86.

van der Horst, A. & Burgering, B. (2007) Stressing the role of FoxO proteins in lifespan and disease. *Nature Reviews Molecular Cell Biology.* 8 (6), pp. 440-450.

van der Horst, A., Tertoolen, L. G. J., de Vries-Smits, L. M. M., Frye, R. A., Medema, R. H. & Burgering, B. M. T. (2004) FOXO4 is acetylated upon peroxide stress and deacteylated by the longevity protein hSir2^{SIRT1}. *Journal of Biological Chemistry.* 279 (28), pp. 28873-28879.

van der Kloet, F. M., Buurmans, J., Jonker, M. J., Smilde, A. K., & Westerhuis, J. A. (2020) Increased comparability between RNA-Seq and microarray data by utilization of gene sets. *PLoS Computational Biology*. 16 (9), e1008295.

van der Vos, K. E. & Coffer, P. J. (2008) FoxO-binding partners: it takes two to tango. *Oncogene*. 27, pp. 2289-2299.

Vellai, T., Takacs-Vellai, K., Zhang, Y., Kovacs, A. L., Orosz, L. & Müller, F. (2003) Genetics: influence of TOR kinase on lifespan in *C. elegans. Nature.* 426 (6967), pp. 620.

Vendelbo, M. H., Clasen, B. F. F., Treebak, J. T., Møller, L., Krusenstjerna-Hafstrøm, T., Madsen, M., Nielsen, T. S., Stødkilde-Jørgensen, Pedersen, S. B., Jørgensen, O. L., Goodyear, L. J., Wojtaszewski, J. F. P., Møller, N. & Jessen, N. (2012) Insulin resistance after a 72-h fast is associated with impaired AS160 phosphorylation and accumulation of lipid and glycogen in human skeletal muscle. *American Journal of Physiology, Endocrinology and Metabolism.* 302 (2), pp. e190-e200.

Venniyoor, A. (2020) PTEN: a thrifty gene that causes disease in times of plenty? *Frontiers in Nutrition.* 7 (81). doi: 10.3389/fnut.2020.00081.

Vihervaara, T. & Puig, O. (2008) dFOXO regulates transcription of a *Drosophila* acid lipase. *Journal of Molecular Biology*. 376 (5), pp. 1215-1223.

Waddell, D. S., Baehr, L. M., van den Brandt, J., Reichardt, H. M., Furlow, D. & Bodine, S. C. (2008) The glucocorticoid receptor and FOXO1 synergistically activate the skeletal muscle atrophy-associated MuRF1 gene. *American Journal of Physiology, Endocrinology and Metabolism.* 295 (4), pp. e785-e797.

Walkiewicz, M. A. & Stern, M. (2009) Increased insulin/insulin growth factor signaling advances the onset of metamorphosis in *Drosophila*. *PLoS One.* 4 (4), e5072.

Walther, T. C. & Farese, R. V. (2012) Lipid droplets and cellular lipid metabolism. *Annual Review of Biochemistry*. 81, pp. 687-714.

Wang, B, Moya, N., Niessen, S., Hoover, H., Mihaylova, M. M., Shaw, R. J., Yates, J. R., Fischer, W. H., Thomas, J. B. & Montminy, M. (2011) A hormone-dependent module regulating energy balance. *Cell.* 145 (1), pp. 596-606.

Wang, F., Chan, C. H., Chen, K., Guan, X., Lin, H. K. & Tong, Q. (2012a) Deacetylation of FOXO3 by SIRT1 or SIRT2 leads to Skp-2 mediated FOXO3 ubiquitination and degradation. *Oncogene.* 31 (12), pp. 1546-1557.

Wang, F., Marshall, C. B., Li, G. Y., Yamamoto, K., Mak, T. W. & Ikura, M. (2009a) Synergistic interplay between promoter recognition and CBP/p300 coactivator recruitment by FoxO3a. *ACS Chemical Biology.* 4 (12), pp. 1017-1027.

Wang, L., Nie, J., Sicotte, H., Li, Y., Eckel-Passow, J. E., Dasari, S., Vedell, P. T., Barman, P., Wang, L., Weinshiboum, R., Jen, J., Huang, H., Kohli, M. & Kocher, J. A. (2016a) Measure transcript integrity using RNA-seq data. *BMC Bioinformatics.* 17 (58). doi: 10.1186/s12859-016-0922-z.

Wang, L., Wang, S., & Li, W. (2012b) RSeQC: quality control of RNA-seq experiments. *Bioinformatics*. 28 (16), pp. 2184–2185. doi: 10.1093/bioinformatics/bts356.

Wang, M., C., Bohmann, D. & Jasper, H. (2005) JNK extends life span and limits growth by antagonising cellular and organism-wide responses to insulin signalling. *Cell.* 121 (1), pp. 115-125.

Wang, X. C., Liu, Z. & Jin, L. H. (2019) *Drosophila* jumu modulates apoptosis via a JNK-dependent pathway and is required for other processes in wing development. *Apoptosis*. 24 (5), pp. 465-477.

Wang, X., Hu, S. & Liu, L. (2017) Phosphorylation and acetylation modifications of FoxO3a: independently or synergistically? *Oncology Letters.* 13 (5), pp. 2867-2872.

Wang, Y., Zhou, Y. & Graves, D. T. (2014) FOXO transcription factors: their clinical significance and regulation. *BioMed Research International.* 925350. doi: 10.1155/2014/925350.

Wang, Z., Gerstein, M. & Snyder, M. (2009b) RNA-seq: a revolutionary tool for transcriptomics. *Nature Reviews Genetics.* 10 (1), pp. 57-63.

Wang, Z., Yu, T. & Huang, P. (2016b) Post-translational modifications of FoxO family proteins (review). *Molecular Medicine Reports.* 14 (6), pp. 4931-4941.

Warren, J. T., Petryk, A., Marqués, G., Jarcho, M., Parvy, J. P., Dauphin-Villemant, C., O'Connor, M. B., Gilbert, L. I. (2002) Molecular and biochemical characterization of two P450 enzymes in the ecdysteroidogenic pathway of *Drosophila melanogaster*. *Proceedings of the National Academy of Sciences of the United States of America.* 99 (17), pp. 11043-11048.

Warren, J. T., Petryk, A., Marqués, G., Parvy, J., Shinoda, T., Itoyama, K., Kobayashi, J., Jarcho, M., Li, Y., O'Connor, M. B., Dauphin-Villemant, C. & Gilbert, L. (2004) Phantom encodes the 25-hydroxylase of *Drosophila melanogaster* and *Bombyx mori*: a P450 enzyme critical in ecdysone biosynthesis. *Insect Biochemistry and Molecular Biology.* 34 (9), pp. 991-1010.

Wat, L. W., Chao, C., Bartlett, R., Buchanan, J. L., Millington, J. W., Chih, H. J., Chowdhury, Z. S., Biswas, P., Huang, V., Shin, L. J., Wang, L. C., Gauthier, M. L., Baron, M. C., Montooth, K. L., Welte, M. A. & Rideout, E. J. (2020) A role for triglyceride lipase brummer in the regulation of sex differences in *Drosophila* fat storage and breakdown. *PLoS Biology*. 18 (1), e3000595.

Watford, M. (2015) Starvation: metabolic changes. *eLS.* doi: 10.1002/9780470015902.a0000642.pub2.

Webb, A. E., Kundaje, A. & Brunet, A. (2016) Characterization of the direct targets of FOXO transcription factors throughout evolution. *Aging Cell.* 15, pp. 673-685.

Weigel, D., Jürgens, G., Küttner, F., Seifert, E. & Jäckle, H. (1989) The homeotic gene *fork head* encodes a nuclear protein and is expressed in the terminal regions of the *Drosophila* embryo. *Cell.* 57, pp. 645-658.

Wells, L., Whelan, S. A. & Hart, G. W. (2003) O-GlcNAc: a regulatory post-translational modification. *Biochemical and Biophysical Research Communications*. 302 (3), pp. 435-441.

Welte, M. A. (2015) As the fat flies: the dynamic lipid droplets of *Drosophila* embryos. *Biochimica et Biophysica Acta.* 1851 (9), pp. 1156-1185.

Whicher, C. A., O'Neill, S. & Holt, R. I. G. (2020) Diabetes in the UK: 2019. *Diabetic Medicine.* 37 (2), pp. 242-247.

White, M. A., Bonfini, A., Wolfner, M. F. & Buchon, N. (2021) *Drosophila melanogaster* sex peptide regulates mated female midgut morphology and physiology. *Proceedings of the National Academy of Sciences of the United States of America.* 118 (1), e2018112118.

Wilfling, F., Wang, H., Haas, J. T., Krahmer, N., Gould, T. J., Uchida, A., Cheng, J. X., Graham, M., Christiano, R., Fröhlich, F., Liu, X., Buhman, K. K., Coleman, R. A., Bewersdorf, J., Farese, R. V. & Walther, T. C. (2013) Triacylglycerol synthesis

enzymes mediate lipid droplet growth by relocalizing from the ER to lipid droplets. *Developmental Cell.* 24 (4), pp. 384-399.

Williamson, J. H., Krochko, D. & Bentley, M. M. (1980) Properties of *Drosophila* NADP+-isocitrate dehydrogenase purified on procion brilliant blue-sepharose-4B. *Comparative Biochemistry and Physiology Part B: Comparative Biochemistry*. 65 (2), pp. 339-343.

Wilson, D. F., Harrison, D. K. & Vinogradov, A. (1985) Mitochondrial cytochrome c oxidase and control of energy metabolism: measurements in suspensions of isolated mitochondria. *Journal of Applied Physiology*. 117 (12), pp. 1424-30. doi: 10.1152/japplphysiol.00736.2014.

Wu, Y., Pan, Q., Ya, H., Zhang, K., Guo, X., Xu, Z., Yang, W., Qi, Y., Guo, C., Hornsby, C., Zhang, L., Zhou, A., Li, L., Chen, Y., Zhang, W., Sun, Y., Zheng, H., Wondisford, F., He, L. & Guo, S. (2018) Novel mechanism of FoxO1 phosphorylation in glucagon signalling in control of glucose homeostasis. *Diabetes.* 67 (11), pp. 2167-2182.

Wullschleger, S., Loewith, R. & Hall, M. N. (2006) TOR signaling in growth and metabolism. *Cell.* 124 (3), pp. 471-484.

Xie, Q., Chen, J. & Yuan, Z. (2012a) Post-translational regulation of FoxO. *Acta Biochimica et Biophysica Sinica.* 44 (11), pp. 897-901.

Xie, Q., Hao, Y., Tao, L., Peng, S., Rao, C., Chen, H., You, H., Dong, M. & Yuan, Z. (2012b) Lysine methylation of FOXO3 regulates oxidative stress-induced neuronal cell death. *EMBO Reports.* 13 (4), pp. 371-377.

Xu, H., Jiang, Y., Miao, X., Tao, Y., Xie, L. & Li, Y. (2021) A model construction of starvation induces hepatic steatosis and transcriptome analysis in Zebrafish larvae. *Biology.* 10, 92.

Xu, J., Liu, L., Xu, L., Xing, Y. & Ye, S. (2020) Metformin alleviates renal injury in diabetic rats by inducing Sirt1/FoxO1 autophagic signal axis. *Clinical and Experimental Pharmacology and Physiology.* 47, pp. 599-608.

Xu, J., Sheng, Z. & Palli, S. R. (2013) Juvenile hormone and insulin regulate trehalose homeostasis in the red flour beetle, *Tribolium castaneum. PLoS Genetics*. 9 (6), pp. e1003535. doi: 10.1371/journal.pgen.1003535.

Xu, K., Diangelo, J.R., Hughes, M.E., Hogenesch, J.B. & Sehgal, A. (2011) The circadian clock interacts with metabolic physiology to influence reproductive fitness. *Cell Metabolism*. 13 (6), pp. 639-654.

Xu, P., Atkinson, R., Jones, D. N. M. & Smith, D. P. (2005) *Drosophila* OBP LUSH is required for activity of pheromone-sensitive neurons. *Neuron.* 45 (2), pp. 193-200.

Xu, X., Gopalacharyulu, P., Seppänen-Laakso, T., Ruskeepää, A.L., Aye, C.C., Carson, B.P., Mora, S., Orešič, M. & Teleman, A.A. (2012) Insulin signaling regulates fatty acid catabolism at the level of CoA activation. *PLoS Genetics*. 8 (1), pp. e1002478.

Yalley, A., Schill, D., Hatta, M., Johnson, N. & Cirillo, L. A. (2016) Loss of interdependent binding by the FoxO1 and FoxA1/A2 forkhead transcription factors culminates in perturbation of active chromatin marks and binding of transcriptional regulators at insulin-sensitive genes. *Journal of Biological Chemistry*. 291 (16), pp. 8848–8861.

Yamagata, K., Daiotku, H., Takahashi, Y., Mukai, H., Kasuya, Y. & Fukamizu, A. (2008) Arginine methylation of FOXO transcription factors inhibits their phosphorylation by Akt. *Molecular Cell.* 32 (2), pp. 221-231.

Yambire, K. F., Rostosky, C., Watanabe, T., Pacheu-Grau, D., Torres-Odio, S., Sanchez-Guerrero, A., Senderovich, O., Meyron-Holtz, E. G., Milosevic, I., Frahm, J., West, A. P. & Raimundo, N. (2019) Impaired lysosomal acidification triggers iron deficiency and inflammation in vivo. *eLife.* 8, e51031.

Yan Y., Wang H., Chen H., Lindström-Battle, A. & Jiao, R. (2015) Ecdysone and insulin signaling play essential roles in readjusting the altered body size caused by the dGPAT4 mutation in *Drosophila*. *Journal of Genetics and Genomics.* 42 (9), pp. 487-94.

Yanai, H. & Yoshida, H. (2019) Beneficial effects of adiponectin on glucose and lipid metabolism and atherosclerotic progression: Mechanisms and perspectives. *International Journal of Molecular Sciences*. 20 (5), 1190.

Yang, G., Lim, C. Y., Li, C. Xiao, X., Radda, G. K., Li, C., Cao, X. & Han, W. (2009a) FoxO1 inhibits leptin regulation of pro-opiomelanocortin promoter activity by blocking STAT3 interaction with specificity protein 1. *Journal of Biological Chemistry*. 284 (6), pp. 3719-3727.

Yang, J. Y., Chang, C. J., Xia, W., Wang, Y., Wong, K. K., Engelman, J. A., Andreeff, M., Hortobagyi, G. N. & Hung, M. C. (2010) Activation of FoxO3a is sufficient to reverse mitogen-activated protein/extracellular signal-regulated kinase kinase inhibitor chemoresistance in human cancer. *Cancer Research.* 70 (11). doi: 10.1158/0008-5472.CAN-09-4524.

Yang, J. Y., Zong, C. S., Xia, W., Yamaguchi, H., Ding, Q., Xie, X., Lang, J. Y., Lai, C. C., Chang, C. J., Huang, W. C., Huang, H., Kuo, H. P., Lee, D. F., Li, L. Y., Lien, H. C., Cheng, X., Chang, K. J., Hsiao, C. D., Tsai, F. J., Tsai, C. H., Sahin, A. A.,

Muller, W. J., Mills, G. B., Yu, D., Hortobagyi, G. N. & Hung, M. C. (2008) ERK promotes tumorigenesis by inhibiting FoxO3a via MDM2-mediated degradation. *Nature Cell Biology.* 10 (2), pp. 138-148.

Yang, Q., Inoki, K., Ikenoue, T. & Guan, K. L. (2006) Identification of Sin1 as an essential TORC2 component required for complex formation and kinase activity. *Genes & Development*. 20 (20), pp. 2820-2832.

Yang, Y., Zhao, Y., Liao, W., Yang, J., Wu, L., Zheng, Z., Yu, Y., Zhou, Li, L., Feng, J., Wang, H., Zhu, W. G. (2009b) Acetylation of FoxO1 activates Bim expression to induce apoptosis in response to histone deacetylase inhibitor depsipeptide treatment. *Neoplasia.* 11 (4), pp. 313-324.

Yao, Y., Li, X., Wang, W., Liu, Z., Chen, J., Ding, M. & Huang, X. (2018) MRT, functioning with NURF complex, regulates lipid droplet size. *Cell Reports*. 24 (11), pp. 2972-2984.

Ye, J., Coulouris, G., Zaretskaya, I., Cutcutache, I., Rozen, S. & Madden, T. L. (2012) Primer-BLAST: a tool to design target-specific primers for polymerase chain reaction. *BMC Bioinformatics*. 13 (1), pp. 1-11.

Young, M. D., Wakefield, M. J., Smyth, G. K., & Oshlack, A. (2010) Gene ontology analysis for RNA-seq: accounting for selection bias. *Genome Biology*. 11 (2), R14. doi: 10.1186/gb-2010-11-2-r14.

Yu, F., Wei, R., Yang, J., Liu, J., Yang, K., Wang, H., Mu, Y. & Hong, T. (2018) FoxO1 inhibition promotes differentiation of human embryonic stem cells into insulin producing cells. *Experimental Cell Research*. 362 (1), pp. 227-234.

Yu, G., Wang, L. G. & He, Q. Y. (2015) ChIPseeker: an R/Bioconductor package for ChIP peak annotation, comparison and visualization. *Bioinformatics*. 31 (14), pp. 2382-2383.

Yu, W., Wang, J., Ma, L., Tang, X., Qiao, Y., Pan, Q., Yu, Y. & Sun, F. (2014) CD166 plays a pro-carcinogenic role in liver cancer cells via inhibition of FOXO proteins through AKT. *Oncology Reports*. 32 (2), pp. 677-683.

Yuan Tang, H., Smith-Caldas, M. S. B., Driscoll, M. V., Salhadar, S. & Shingleton, A. W. (2011) FOXO regulates organ-specific phenotypic plasticity in *Drosophila. PLoS Genetics*. 7 (11). doi: 10.1371/journal.pgen.1002373.

Zandawala, M., Yurgel, M. E., Texada, M. J., Liao, S., Rewitz, K. F., Keene, A. C. & Nässel, D. R. (2018) Modulation of *Drosophila* post-feeding physiology and behavior by the neuropeptide leucokinin. *PLoS Genetics.* 14 (11), pp. e1007767.

Zeng, B., Huang, Y., Xu, J., Shiotsuki, T., Bai, H., Palli, S. R., Huang, Y. & Tan, A. (2017) The FOXO transcription factor controls insect growth and development by regulating juvenile hormone degradation in the silkworm, *Bombyx mori. Journal of Biological Chemistry.* 292 (28), pp. 11659-11669.

Zeng, J., Huynh, N., Phelps, B. & King-Jones, K. (2020) Snail synchronizes endocycling in a TOR-dependent manner to coordinate entry and escape from endoreplication pausing during the *Drosophila* critical weight checkpoint. *PLoS Biology.* 18 (2), e3000609.

Zeng, W., Ball, A. R. & Yokomori, K. (2010) HP1: heterochromatin binding proteins working the genome. *Epigenetics.* 5 (4), pp. 287-292.

Zhang, H., Guo, W., Zhang, F., Li, R., Zhou, Y., Shao, F., Feng, X., Tan, F., Wang, J., Gao, S., Gao, Y. & He, J. (2020a) Monoacylglycerol lipase knockdown inhibits cell proliferation and metastasis in lung adenocarcinoma. *Frontiers in Oncology.* 10, 559568.

Zhang, J., Liu, Y., Jiang, K. & Jia, J. (2020b) Hedgehog signalling promotes lipolysis in adipose tissue through directly regulating Bmm/ATGL lipase. *Developmental Biology.* 457 (1), pp. 128-139.

Zhang, S., Hulver, M. W., McMillan, R. P., Cline, M. A. & Gilbert, E. R. (2014a) The pivotal role of pyruvate dehydrogenase kinases in metabolic flexibility. *Nutrition and Metabolism.* 11 (10). doi: 10.1186/1743-7075-11-10.

Zhang, T., Liao, Y., Hsu, F.N., Zhang, R., Searle, J.S., Pei, X., Li, X., Ryoo, H.D., Ji, J.Y. & Du, W. (2014b) Hyperactivated Wnt signaling induces synthetic lethal interaction with Rb inactivation by elevating TORC1 activities. *PLoS Genetics*. 10 (5), pp. e1004357.

Zhang, W., Hietakangas, V., Wee, S., Lim, S. C., Gunaratne, J. & Cohen, S. M. (2013) ER stress potentiates insulin resistance through PERK-mediated FOXO phosphorylation. *Genes & Development*. 27 (4), pp. 441-449.

Zhang, W., Patil, S., Chauhan, B., Guo, S., Powell, D. R., Le, J., Klotsas, A., Matika, R., Xiao, X., Franks, R., Heidenreich, K. A., Sajan, M. P., Farese, R. V., Stolz, D. B., Tso, P., Koo, S. H., Montminy, M. & Unterman, T. G. (2006) FoxO1 regulates multiple metabolic pathways in the liver: effects on gluconeogenic, glycolytic, and lipogenic gene expression. *Journal of Biological Chemistry*. 281, pp. 10105–10117.

Zhang, X., Tang, N., Hadden, T. J. & Rishi, A. K. (2011) Akt, FOXO, and apoptosis. *Biochimica et Biophysica Acta (BBA) – Molecular Cell Research.* 1813 (11), pp. 1978-1986.

Zhang, X., Wei, L. H., Wang, Y., Xiao, Y., Liu, J., Zhang, W., Yan, N., Amu, G., Tang, X., Zhang, L. & Jia, G. (2019a) Structural insights into FTO's catalytic mechanism for the demethylation of multiple RNA substrates. *Proceedings of the National Academy of Sciences of the United States of America*. 116 (8), pp. 2919-2924.

Zhang, X., Yang, S., Chen, J., & Su, Z. (2019b) Unraveling the regulation of hepatic gluconeogenesis. *Frontiers in Endocrinology*. 9, 802.

Zhang, Y., Liu, T., Meyer, C. A., Eeckhoute, J., Johnson, D. S., Bernstein, B. E., Nusbaum, C., Myers, R. M., Brown, M., Li, W. & Liu, X. S. (2008) Model-based Analysis of ChIP-Seq (MACS). *Genome Biology*. 9 (9), R137. doi: 10.1186/gb-2008-9-9-r137.

Zhang, Y., Smallbone, L. A., Morton, R. & Finan, T. M. (2016) Loss of malic enzymes leads to metabolic imbalance and altered levels of trehalose and putrescine in the bacterium *Sinorhizobium meliloti*. *BMC Microbiology*. 16 (1), pp. 1-13.

Zhao, S., Fung-Leung, W., Bittner, A., Ngo, K. & Liu, X. (2014) Comparison of RNA-seq and microarray in transcriptome profiling of activated T cells. *PLoS One.* 9 (1), e78644.

Zhao, X., Li, G., & Liang, S. (2013) Several affinity tags commonly used in chromatographic purification. *Journal of Analytical Methods in Chemistry*. doi: 10.1155/2013/581093.

Zheng, W., Rus, F., Hernandez, A., Kang, P., Goldman, W., Silverman, N. & Tatar, M. (2018) Dehydration triggers ecdysone-mediated recognition-protein priming and elevated anti-bacterial immune responses in *Drosophila* Malpighian tubule renal cells. *BMC Biology*. 16 (1), pp. 1-14.

Zhou, F., Liu, Q., Zhang, L., Zhu, Q., Wang, S., Zhu, K., Deng, R., Liu, Y., Yuan, G., Wang, X. & Zhou, L. (2020) Selective inhibition of CBP/p300 HAT by A-485 results in suppression of lipogenesis and hepatic gluconeogenesis. *Cell Death & Disease.* 11 (745). doi: 10.1038/s41419-020-02960-6.

Zimmerman, J. E., Chan, M. T., Jackson, N., Maislin, G. & Pack, A. I. (2012) Genetic background has a major impact on differences in sleep resulting from environmental influences in *Drosophila. Sleep*. 35 (4), pp. 545-557.

Zou, P., Liu, L., Zheng, L., Liu, L., Stoneman, R.E., Cho, A., Emery, A., Gilbert, E. R. & Cheng, Z. (2014) Targeting FoxO1 with AS1842856 suppresses adipogenesis. *Cell Cycle*. 13 (23), pp. 3759-3767.

Appendix 1

APPENDIX 1

Table of reagents including catalogue numbers, manufacturers, and distributors.

Reagent	Catalogue number/product code	Manufacturer	Distributor
0.2 mL PCR strip tubes, clear	12179770	Fisher Scientific	Fisher Scientific
0.6 mL tubes, clear	11916955	Fisher Scientific	Fisher Scientific
1.5 mL Axygen™ Maxyclear Snaplock tubes, clear	525-0260	Corning	VWR
1.5 mL tubes, clear	11926955	Fisher Scientific	Fisher Scientific
25-gauge needle	12389169	BD	Fisher Scientific
2 mL screw cap tube, clear	E1420-2340	Starlab	Starlab
96-well clear flat-bottomed microplates	10216341	Corning	Fisher Scientific
Acetic Acid	10492411	Fisher Scientific	Fisher Scientific
Acrylamide / N,N'-Methylenebisacrylamide 37.5:1, 40% mix solution	10397511	Fisher Scientific	Fisher Scientific
Acrylamide (40%); bisacrylamide free	15484859	Fisher Scientific	Fisher Scientific
Active yeast	N/A	S. I. LeSaffre	Amazon
Agar	A7002-5KG	Merck	SLS
Agarose	10366603	Fisher Scientific	Fisher Scientific
Amersham™ Protran™ premium 0.45 µM nitrocellulose membrane	15269794	Cytiva	Fisher Scientific
Amyloglucosidase from *Aspergillus niger*, lyophilized powder	A7420-5MG	Merck	SLS
Autolysed yeast	02103304-CF	MP Biomedicals	MP Biomedicals
Extra Thick Blot Filter Paper, Precut, 7.5 x 10 cm	1703965	Biorad	Biorad
Brewer's yeast	290331225	MP Biomedicals	MP Biomedicals
Bright white real-time PCR 96-well plate for Roche Lightcycler 480	BW-96480	Primer Design	Primer Design
Brilliant Blue	08BLU00200-1KG	Fiorio Colori	Fast Colours
Bovine serum albumin (BSA)	12737119	Fisher Scientific	Fisher Scientific
Chloroform	15408689	Fisher Scientific	Fisher Scientific
Copper (II) sulphate pentahydrate	10604902	Fisher Scientific	Fisher Scientific
D-(+)-glucose anhydrous	10373242	Fisher Scientific	Fisher Scientific
D-(+)-trehalose dihydrate	T9531-25G	Merck	SLS
Dichlorodiphenyltrichloroethane	31041-100MG	Merck	Merck
Diethyl ether	11399047	Fisher Scientific	Fisher Scientific
DNA 1kb hyperladder	BIO33026	Meridian Bioscience	SLS
DNase-I	79254	QIAgen	QIAgen

DTT	10699530	Fisher Scientific	Fisher Scientific
EDTA	10182903	Fisher Scientific	Fisher Scientific
Ethanol	12347163	Fisher Scientific	Fisher Scientific
Formaldehyde, 16%	11586711	Fisher Scientific	Fisher Scientific
Free fatty acid quantification kit	ab65341	Abcam	Abcam
Glass beads	G8772-100G	Merck	SLS
Glycerol	G5516-100ML	Merck	Merck
Glycerol standard solution	G7793-5ML	Merck	SLS
Glycine	10061073	Fisher Scientific	Fisher Scientific
Glycogen from oyster	G8751-5G	Merck	SLS
Goat anti-mouse antibody (HRP)	ab6789	Abcam	Abcam
Goat anti-rabbit antibody (HRP)	ab6721	Abcam	Abcam
Granulated sugar	N/A	Tate & Lyle	Amazon
Hydrogen peroxide	10386643	Fisher Scientific	Fisher Scientific
Phosphoric acid	10763611	Fisher Scientific	Fisher Scientific
HEPES	10397023	Fisher Scientific	Fisher Scientific
Hexane	10147642	Fisher Scientific	Fisher Scientific
Infinity Glucose reagent	TR15421	Fisher Scientific	Fisher Scientific
Infinity Triglycerides reagent	TR22421	Fisher Scientific	Fisher Scientific
Invitrogen™ dNTP set	10083252	Fisher Scientific	Fisher Scientific
Invitrogen™ Dynabeads	10446293	Fisher Scientific	Fisher Scientific
Invitrogen™ DTT	10328062	Fisher Scientific	Fisher Scientific
Invitrogen™ first strand buffer	10328062	Fisher Scientific	Fisher Scientific
Invitrogen™ Oligo(dT)12-18 Primer	11513127	Fisher Scientific	Fisher Scientific
Invitrogen™ Platinum Hot Start Taq polymerase	15480584	Fisher Scientific	Fisher Scientific
Invitrogen™ RNaseOUT™ recombinant ribonuclease inhibitor	10154652	Fisher Scientific	Fisher Scientific
Invitrogen™ SuperScript™ II reverse transcriptase	10328062	Fisher Scientific	Fisher Scientific
Isopropanol	10378293	Fisher Scientific	Fisher Scientific
KCl	10735874	Fisher Scientific	Fisher Scientific
KOH	P0517.0500	Melford	Melford
Laemmli sodium dodecyl sulfate (SDS) sample buffer	15415809	Fisher Scientific	Fisher Scientific
LiCl	L45000-500.0	Melford	Melford
Merck Millipore Luminata Forte Western HRP substrate, 100mL	10394675	Merck Millipore	Fisher Scientific
Methanol	11367996	Fisher Scientific	Fisher Scientific
Methyl viologen dichloride hydrate (paraquat)	856177-1G	Merck	SLS
Midori green DNA stain	S6-0022	Geneflow	Geneflow
Mouse anti-FLAG antibody	F3165-1MG	Merck	Merck
Mouse anti-RNA polymerase II antibody	05-623-25UG	Merck	Merck
Na deoxycholate	15494689	Fisher Scientific	Fisher Scientific

Na acetate	11434584	Fisher Scientific	Fisher Scientific
Na_2CO_3	10577182	Fisher Scientific	Fisher Scientific
NaCl	10112640	Fisher Scientific	Fisher Scientific
Nonidet-P40	N59000-500.0	Melford	Melford
Oleic acid standard	75090	Merck	Merck
Orange G loading dye	10371691	Fisher Scientific	Fisher Scientific
PageRuler™ plus prestained protein ladder	11832124	Fisher Scientific	Fisher Scientific
Parafilm®	P7793-1EA	Merck	Merck
PBS	12821680	Fisher Scientific	Fisher Scientific
Pierce™ bovine serum albumin standard	10443834	Fisher Scientific	Fisher Scientific
Pierce™ ionic detergent compatibility reagent	10570044	Fisher Scientific	Fisher Scientific
Pierce protease and phosphatase inhibitor cocktail	16326532	Fisher Scientific	Fisher Scientific
Pierce™ 660 nm protein assay reagent	10177723	Fisher Scientific	Fisher Scientific
PMSF	P20270-5.0	Melford	Melford
Polymeric silica gel 60 matrix thin layer chromatography aluminium sheet	1.16484	Merck	Merck
PrecisionPLUS qPCR mastermix with SYBRgreen	PPLUSBLUE-SY-20ML	Primer Design	Primer Design
Pronase E	10372541	Merck	Fisher Scientific
Propionic acid	10193190	Fisher Scientific	Fisher Scientific
Proteinase K	10103533	Fisher Scientific	Fisher Scientific
QIAgen gel extraction kit	28704	QIAgen	QIAgen
QIAgen PCR purification kit	28104	QIAgen	QIAgen
Rabbit anti-FoxO antibody	N/A	Giannakou *et al.* 2007	Received as a gift from Dame Prof. Linda Partridge.
Rabbit anti-tubulin antibody	2148S	Cell Signalling Technologies	Cell Signalling Technologies
Red grape juice	N/A	Ritchies	Amazon
Ringcaps® graduated capillaries	Z611239-250EA	Hirschmann Laborgerate	SLS
RNase A	10753721	Fisher Scientific	Fisher Scientific
RNeasy mini kit	74104	QIAgen	QIAgen
SDS	15450685	Fisher Scientific	Fisher Scientific
Skimmed milk powder	70166-500g	Merck	Merck
StarSeal advanced polyolefin film	E2796-9795	Starlab	Starlab
Sterilin bijou bottles	11369123	Sterilin	Fisher Scientific
Tegosept	FLY1136	Apex Bioresearch Products	SLS
Trehalase	E-TREH	Megazyme	Megazyme
Trioleoylglycerol lipid standard	Y0001113	Merck	Merck
Tris base	10376743	Fisher Scientific	Fisher Scientific
Tris-HCl	10795104	Fisher Scientific	Fisher Scientific
Triton x100	T8787-50ML	Merck	Merck
TRIzol™	15596026	Fisher Scientific	Fisher Scientific
Tween-20	10485733	Fisher Scientific	Fisher Scientific